

Efficient Switching of RAFT to Hydroxyl Capped Polymers as a Versatile Scaffold for Block Copolymer Synthesis

**and their Characterization with Advanced Hyphenated
Techniques**

Zur Erlangung des akademischen Grades eines
DOKTORS DER NATURWISSENSCHAFTEN
(Dr. rer. nat.)

Fakultät für Chemie und Biowissenschaften
Karlsruher Institut für Technologie (KIT) - Universitätsbereich

genehmigte
DISSERTATION
von

Dipl.-Chem. Christina Maria Schmid

aus
Würzburg

Dekan: Prof. Dr. M. Bastmeyer

Referent: Prof. Dr. C. Barner-Kowollik

Korreferent: Prof. Dr. M. Wilhelm

Tag der mündlichen Prüfung: 20.07.2012

Die vorliegende Arbeit wurde von März 2009 bis Juni 2012 unter Anleitung von Prof. Dr. Christopher Barner-Kowollik am Karlsruher Institut für Technologie (KIT) – Universitätsbereich angefertigt.

Abstract

Reversible addition fragmentation chain transfer (RAFT) polymerization is a versatile technique to synthesize polymers with narrow polydispersity and high chain-end functionality. To enable a switch from RAFT to other polymerization protocols such as ring-opening polymerization (ROP), it is desirable to modify the thiocarbonyl thio moiety to generate a chemical anchor for polymer conjugation and chain extension.

The transformation of RAFT polymers was achieved via a novel end-group conversion of thiocarbonyl thio end-capped polymers yielding hydroxyl functional polymers. The end-group switch from RAFT to hydroxyl functional polymers involving THF/AIBN at 60 °C at ambient conditions was successfully demonstrated for a variety of polymer backbones and RAFT agents.

The procedure of the quantitative end-group conversion was subsequently employed to generate narrowly dispersed sulfur-free poly(styrene)-*block*-poly(ϵ -caprolactone), poly(acrylate)-*block*-poly(ϵ -caprolactone) as well as poly(methacrylate)-*block*-poly(ϵ -caprolactone) copolymers, demonstrating that the RAFT process can serve as a methodology for the generation of sulfur-free block copolymers. The ring opening polymerization of ϵ -caprolactone (ϵ -CL) was carried out either under organo-catalysis or metal catalysis. The same procedure involving a mechanistic switch from RAFT polymerization to ROP was applied to synthesize linear ABA poly(ϵ -caprolactone)-*block*-poly(styrene)-*block*-poly(ϵ -caprolactone) and star-shaped pS-*b*-pCL copolymers.

Further, the synthesis of multi-block copolymers poly(styrene)-*block*-poly(tetrahydrofuran) was enabled via the end-group switch forming dihydroxyl terminated poly(styrene), which subsequently reacted with a diisocyanate terminated polytetrahydrofuran based prepolymer to form multi-block copolymer structures.

The obtained complex polymers were thoroughly analyzed via a variety of state-of-the-art characterization techniques including hyphenated methods such as liquid chromatography under critical conditions coupled to size exclusion chromatography (LCCC-SEC), liquid-chromatography coupled to mass spectrometry (LC/MALDI-MS) as well as SEC coupled to infrared spectroscopy (SEC/FT-IR) to evidence the (multi-) block (star) copolymer structures and the efficiency of the synthetic processes.

Contents

1. Introduction	1
1.1. Motivation	1
1.2. Thesis Overview	4
2. Theory and Background	7
2.1. Controlled Radical Polymerization	7
2.1.1. Nitroxide-Mediated Polymerization (NMP)	9
2.1.2. Atom Transfer Radical Polymerization (ATRP)	10
2.1.3. Reversible Addition-Fragmentation Chain Transfer (RAFT) Polymerization	11
2.2. End-group Modification of RAFT Polymers	12
2.2.1. Thermolysis	13
2.2.2. Reactions with Nucleophiles	15
2.2.3. Radical-induced End-group Modification	16
2.2.4. End-group Modification via Oxidation and Irradiation	16
2.2.5. Concluding Remarks	17
2.3. Ring-Opening Polymerization (ROP)	18
2.3.1. General Aspects	18
2.3.2. Metal-catalyzed Ring-Opening Polymerization	19
2.3.3. Organo-catalyzed Ring-Opening Polymerization	20
2.4. Polyurethanes	23
2.4.1. General Aspects	23
2.4.2. Alternative Synthetic Pathways and Recent Developments in Polyurethane Chemistry Associated with Environmental Aspects	25
2.4.3. Polyurethanes in Combination with Radical Polymerization and their Applications	26
2.5. Liquid Chromatography of Polymers	27
2.5.1. General Aspects of Liquid Chromatography	27
2.5.2. Size-Exclusion Chromatography (SEC)	28
2.5.3. Liquid Chromatography at Critical Conditions (LCCC)	32

2.5.4. Gradient Elution Liquid Chromatography (GELC)	34
2.5.5. LCCC/GELC Coupled to SEC	34
2.5.6. Liquid Chromatography Coupled to Chemical Detectors	35
3. Materials and Characterization Techniques	41
3.1. Materials	41
3.1.1. Chemicals Used in Chapter 4	41
3.1.2. Chemicals Used in Chapter 5	41
3.1.3. Chemicals Used in Chapter 6	42
3.1.4. Chemicals Used in Chapter 7	43
3.2. Size-Exclusion Chromatography	43
3.2.1. Size-Exclusion Chromatography with Triple Detection	43
3.2.2. Size-Exclusion Chromatography Coupled to a Fraction Collector	44
3.3. Liquid Chromatography at Critical Conditions Coupled to Size-Exclusion Chromatography	44
3.4. Mass Spectrometry	46
3.4.1. Size-Exclusion Chromatography Coupled to Electrospray Ionization Mass Spectrometry	46
3.4.2. Matrix-Assisted Laser Desorption/Ionization-Time of Flight Mass Spectrometry	46
3.5. Fourier Transform Infrared Spectroscopy	47
3.6. Size-Exclusion Chromatography coupled to Fourier Transform Infrared Spectroscopy	47
3.7. Nuclear Magnetic Resonance Spectroscopy	49
4. Switching from RAFT to Hydroxyl-terminal Polymers	51
4.1. Introduction	51
4.1.1. Mechanism of the OH End-group Switch of Polymers Containing a Dithiobenzoate End-group	52
4.1.2. Mechanism of the OH End-group Switch of Symmetrical Trithiocarbonate Functional Polymers	54
4.2. Synthetic Procedures	57
4.3. Results and Discussion	60
4.4. Conclusions	73
5. Block Copolymers Generated via a Switch from RAFT Polymerization to ROP	75
5.1. Introduction to Block Copolymers	75
5.2. Poly(styrene)- <i>block</i> -poly(ϵ -caprolactone)	78
5.2.1. Introduction to pS- <i>b</i> -pCL Block Copolymers	78
5.2.2. Synthesis	79

5.2.3. Results and Discussion	82
5.2.4. Conclusions	95
5.3. Poly(acrylate)- <i>block</i> -poly(ϵ -caprolactone) and Poly(methacrylate)- <i>block</i> - poly(ϵ -caprolactone)	96
5.3.1. Introduction to pA- <i>b</i> -pCL and pMMA- <i>b</i> -pCL Block Copolymers	96
5.3.2. Synthesis	96
5.3.3. Results and Discussion	98
5.3.4. Conclusions	109
5.4. Poly(styrene)- <i>block</i> -poly(lactide)	111
5.4.1. Introduction to pS- <i>b</i> -pLA Block Copolymers	111
5.4.2. Synthesis	112
5.4.3. Results and Discussion	114
5.4.4. Conclusions	120
6. In-Depth LCCC-(GELC)-SEC Characterization of ABA (star) Block Copolymers	121
6.1. Introduction Including a Theoretical Background to Star RAFT Polymers	121
6.2. Synthesis	125
6.3. Results and Discussion	128
6.4. Conclusions	147
7. Multi-block Polyurethanes via RAFT End-group Switching	149
7.1. Introduction	149
7.2. Synthesis	151
7.3. Results and Discussion	153
7.4. Conclusions	167
8. Concluding Remarks and Outlook	169
8.1. Concluding Remarks	169
8.2. Outlook	171
Bibliography	173
A. Appendix	197
List of Abbreviations	205
Curriculum Vitae	209
List of Publications and Conference Contributions	211
Acknowledgements	213

1

Introduction

1.1. Motivation

The reversible addition-fragmentation chain transfer (RAFT) process^[1] is among the most versatile techniques to prepare polymers with pre-determined molecular weight and narrow polydispersity for a wide range of monomer systems, including those difficult to polymerize in a controlled fashion via alternative protocols (such as vinyl acetate-type monomers). While the RAFT process can be highly efficient – including for construction of complex macromolecular architectures – it is still hampered by the fact that many applications need to employ sulfur-free polymer materials, as the presence of sulfur in the polymeric material can lead to unpleasant odors or to a discoloration of the material. In the worst case, the thiocarbonyl thio end-group can be the starting point of degradation processes within the polymer. Over the past years, several end-group modification techniques for RAFT made polymers have been proposed,^[2] yet only few remove the sulfur completely from the polymer (the most popular method is aminolysis to the corresponding thiol) and those that do require either high reaction temperatures (*i.e.*, exceeding 100 °C) and do not progress to complete conversions or necessitate the use of large amounts of radical initiator to decouple the RAFT agent from the polymers (with the inevitable consequence that significant amounts of bimolecular coupling products are formed). Thus, no cost effective and efficient methodologies exist that can transform large quantities of thiocarbonyl thio functional polymers into sulfur-free materials that carry a benign

yet universally applicable chemical anchor (such as a hydroxyl function). Such a function can be employed for subsequent reactions, including as a initiator for block copolymer formation.

Block copolymers are among the most important polymeric entities in polymer science. There exists a great variety of synthetic approaches to generate well-defined (*i.e.*, featuring narrow polydispersity and a high degree of functionalization), block copolymers via polymerization processes such as anionic polymerization, ring opening metathesis polymerization (ROMP) as well as living/controlled free radical polymerization (often in a sequential synthetic approach, *i.e.*, chain extension). While anionic polymerization constitutes in many regards the ‘gold standard’ in block copolymer formation, it requires demanding reaction conditions. Controlled radical polymerization, on the other hand, can be employed to generate block copolymers in a more facile fashion, albeit with a certain loss of definition when compared to anionic polymerization.

A particularly important aspect of block copolymer formation is the transition from one polymerization methodology to another to combine polymer strands with very different properties. A transition which is of particular interest is from non-degradable vinylic polymers to macromolecules that feature a degradable backbone structure. Such partially degradable well-defined copolymers attract increasing interest due to their applications in biomedical and pharmacological areas as base materials for scaffolds, meshes or sutures as well as base materials for tissue engineering (wound patches) or as degradable surgical implants in procedures such as inguinal hernia repair. The preparation of such copolymers with degradable and non-degradable strands should be achievable in a facile manner if the resulting polymers are to be employed in biomedical contexts. More importantly, the preparation procedures for such polymers should be as free as possible of any harmful species such as transition metal catalysts and be as pure as possible. The requirements with regard to the polymer purity are highly stringent as approval for their use has to be obtained for a defined application for the respective controlling bodies (*e.g.*, the federal food and drug administration in the USA). Over the past decade living/controlled radical polymerization methods have been combined with ring opening polymerization (ROP) techniques^[3] via a sequential method for the preparation of linear block copolymers^[4,5] or miktoarm star copolymers,^[6,7] using heterofunctional initiators, as well as graft copolymers.^[8–12] In these approaches atom transfer radical polymerization (ATRP) as well as the reversible addition fragmentation chain transfer (RAFT) process has been employed, typically using an appropriately (*i.e.*, -OH) functionalized (multifunctional) initiator or mediating agent. The above approaches suffer the disadvantage that either transition metals have to be employed during the polymerization process (in the case of ATRP), that ATRP is not able to mediate the polymerization of all monomers (*e.g.*,

acrylic acid or vinyl acetate) or that specific RAFT agents carrying a primary or secondary -OH functionality (either in Z- or R- position) have to be synthesized. Disadvantages of current methodologies include the fact that the RAFT prepared block copolymers contain dithioester end-groups.

Thus – as pointed out above – it would be very desirable to have a process at hand, which allows for a simple transformation from a polymer prepared via the RAFT process (*i.e.*, featuring a thiocarbonyl thio end cap or mid chain function), to a polymer that has no thio components at all and instead features a hydroxyl function directly attached to the polymer backbone.

Polyurethanes find – due to their flexible construction options – a wide variety of applications such as foams, tissue engineering, coatings, and adhesives.^[13,14] Linear polyurethanes are commonly synthesized via polyaddition reactions of a diol and diisocyanate prepolymers.^[15] Due to the rigidity and H-bonding of the urethane linkages the polyurethane chains precipitate in many solvents and become insoluble with increasing chain length. Thus, macromolecular diols are often inserted in the polyaddition process to obtain a higher chain mobility due to less intermolecular H-bonding resulting in a better solubility of the polymer chains.^[16] Typical diols employed for polyurethane synthesis are polyether and polyester polyols, which are synthesized by anionic ring-opening polymerization of ethylene oxide, propylene oxide or by cationic ring-opening polymerization of tetrahydrofuran. Polymerization of vinyl monomers result in general not in hydroxy end-functional polymers. Consequently, the diol precursors are usually limited to polymers synthesized of cyclic monomers. The insertion of vinyl monomers in polyurethane structures resulted often in minor defined materials. However, improvement in mechanical properties and water resistance of polyurethane ionomers containing vinylic polymer strands have been identified. An alternative investigated method to generate more defined materials is starting from the polyurethane synthesis with subsequent attachment of the vinylic polymers, involving a high number synthetic steps. Using the RAFT process with subsequent end-group transformation for the formation of dihydroxyl terminated vinylic polymers would enable the generation of tailor-made polyurethanes with completely new material properties.

Inspection of the literature indicates that the most commonly employed approaches towards the characterization of block copolymers and higher architectures are via conventional SEC based on a linear calibration of the first block, via NMR, and – if appropriate – via mass spectrometry.^[17–19] Via SEC, the average molar masses and the polydispersity are determined but no composition (chemical) information may be obtained when classical RI detection is employed. NMR spectroscopy yields information on the chemical composition and functional groups, however, topological information of the generated macromolecules is difficult to ascertain. And mass spectrometry on

its own is problematic for samples with broad or multiple distributions and high molar masses.

Liquid chromatography at critical conditions (LCCC) enables the separation of block copolymer samples by their chemical heterogeneity in the absence of size exclusion effects of one block segment. Combining LCCC and SEC in a two dimensional chromatography set-up provides information about the chemical composition and the molecular masses of the synthesized sample, respectively. Alternatively, for obtaining informations about chemical composition and molar masses of complex structures, chromatographic systems can be combined to chemical detectors such as mass spectrometry (LC-MS) or infrared spectroscopy (LC/FT-IR). Such advanced hyphenated techniques are the todays best facilities for obtaining reliable and most detailed informations of block copolymers as well as complex structures. Consequently, these methods will be applied for the characterization of the synthesized block structures in the current thesis.

1.2. Thesis Overview

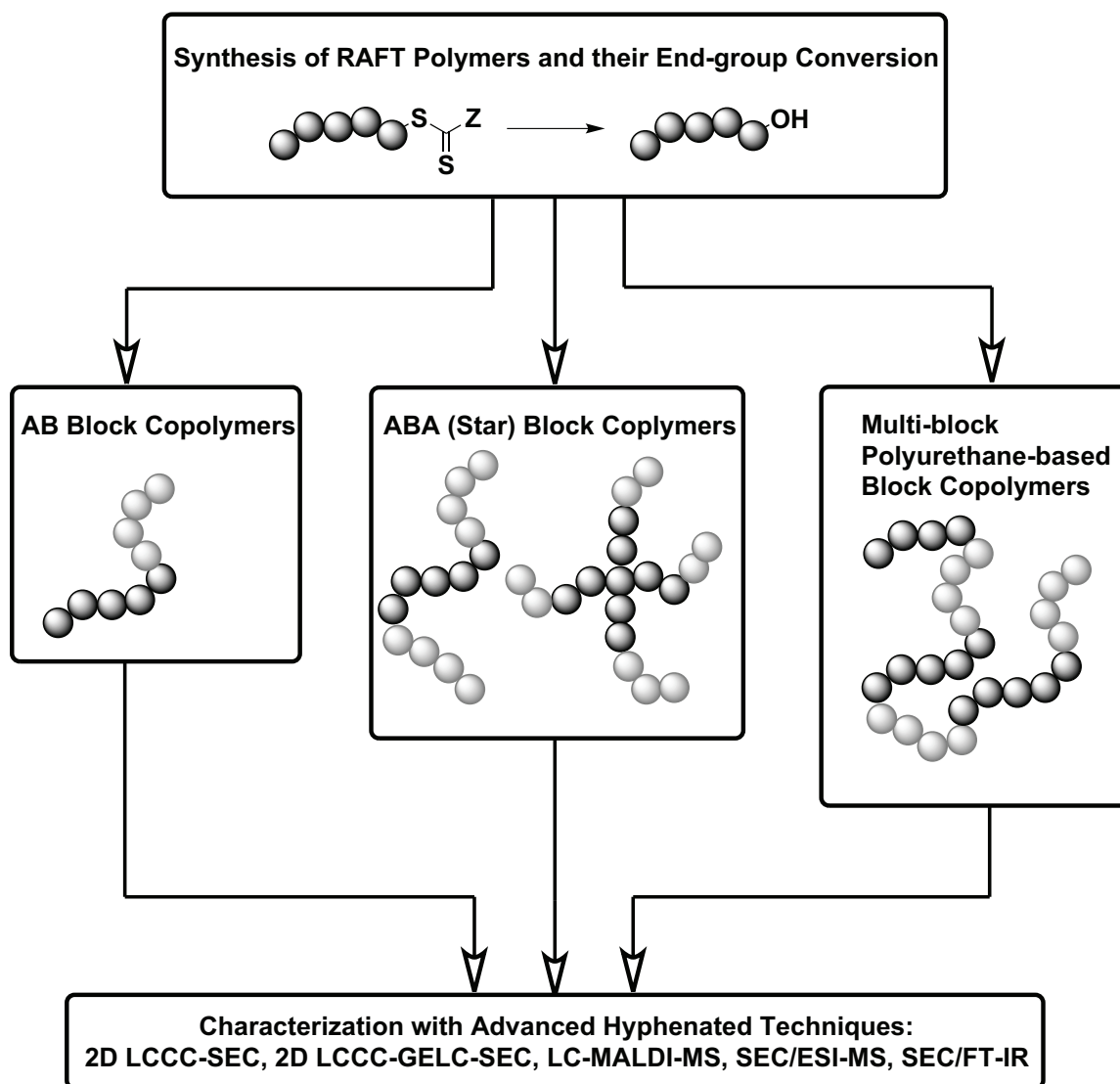
The present thesis investigations address the exploitation of a simple and fast reaction sequence that can turn narrow polydispersity polymers prepared via the RAFT process into sulfur-free hydroxyl terminal polymers, which can subsequently be employed for the generation of di-, tri- (star) block copolymers via ring opening polymerization (ROP) as well as multi-block structures via polyurethane synthesis. The transformation processes of the thiocarbonyl thio polymers into OH terminal moieties as well as the chemical and molecular weight constitution of the generated block copolymeric material will be - among other characterization techniques - assessed via size-exclusion chromatography coupled to electrospray ionization mass spectrometry (SEC/ESI-MS) as well as liquid chromatography at critical conditions coupled to SEC (LCCC-SEC).

Specifically, the investigations entail (see also Scheme 1.1):

1. The full establishment (including the conversion of larger quantities) of the recently introduced technique to convert RAFT polymers into sulfur-free hydroxyl functional polymers for a range of thiocarbonyl thio end caps as well as polymer backbones;
2. The use of the prepared hydroxyl functional polymers as initiators in the ROP (catalysed by both inorganic as well as organic initiators) for the preparation of block copolymers with degradable as well as non-degradable strands. The aim is to examine all OH terminated polymers towards their suitability to act as ROP macroinitiators, including those polymers that will feature tertiary alcohol chain ends.

3. The synthesis of RAFT difunctional and star polymers via the R-approach and subsequent end-group switch with subsequent chain extension via ROP to generate ABA (star-shaped) block copolymers.
4. Employing the dihydroxyl functional polymers as a synthetic scaffold for the preparation of multi-block polyurethanes via the reaction with isocyanate based prepolymers.
5. The detailed characterization of the prepared OH capped polymers and the derived block copolymers via hyphenated characterization techniques to arrive at a complete image of both the chemical and molecular weight homogeneity of the polymers.

The significance of the proposed investigations lies in the fact that for the first time a procedure is presented with which polymers prepared via a controlled radical polymerization technique (*i.e.*, RAFT) can be transformed under very mild conditions and in rapid reaction times into a pure OH end-functional polymer. The lack of simple conversion techniques of RAFT polymers into macromolecules that are free of sulfur – yet feature a useful synthetic handle – has long limited the large scale application of the RAFT process. To demonstrate the versatility of the OH capped polymers, the hydroxy functional polymers are employed in various approaches to prepare block copolymers.



Scheme 1.1 Thesis overview showing the individual aims of the investigations.

2

Theory and Background

In Chapter 1, an overview and the theoretical background of the employed techniques for the synthesis and the characterization used in this thesis are provided. The polymerization techniques applied for the synthesis of homopolymers as well as block-, star-, and multi-block-copolymers are described including controlled radical polymerization (CRP), ring-opening polymerization (ROP) as well as the polyaddition process operative during polyurethane synthesis. Furthermore, end-group modification methods of polymers obtained by the reversible addition-fragmentation chain transfer (RAFT) polymerization process, one version of CRP, are explained, since the main synthetic routes are based on a specific method to modify the terminal groups of RAFT polymers, as explained in the introduction. The theoretical chapter is concluding with the main analytical method utilized in the thesis, *i.e.*, liquid chromatography (LC) of polymers. An overview of this analytical method as well as associated coupled techniques will be presented.

2.1. Controlled Radical Polymerization

Today, approximately half of the commercially available man-made polymeric materials are synthesized via free radical polymerization (FRP).^[20] As a consequence, FRP has been one of the most applied polymerization processes in industry for the last 80 years and is highly significant. Thus, before discussing controlled radical polymerization, a short overview on FRP is provided.

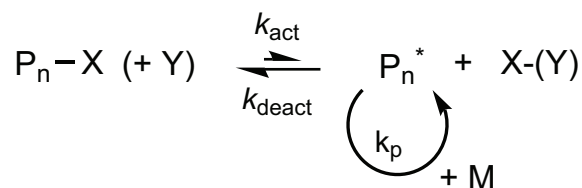
The mechanism of FRP can be divided into four relevant reactions involving free radicals.

1. Initiation: Generation of radicals from a non-radical starting molecule.
2. Propagation: Addition of the radical to an alkene.
3. Atom transfer and atom abstraction reactions (termination by disproportionation and chain transfer reactions).
4. Recombination of two radicals (termination process).

Due to its radical mechanism the polymerization process tolerates many other functionalities such as carboxylic acids or hydroxyl functions. Thus, a large variety of vinyl monomers can be polymerized under mild conditions. However, the FRP bears some disadvantages resulting from bimolecular termination and chain transfer processes. The degree of polymerization, the polydispersities, and the end-functionality of a chain are typically very poorly controlled.^[21]

With the discovery of ionic polymerization a higher control over the polymerization process was possible. A polymerization process such as anionic polymerization in which ideally no termination or chain transfer occurs, was defined by Szwarc as a ‘living’ polymerization.^[22] Drawbacks of the ionic polymerization are the limiting variety of monomers applicable for the polymerization, since many functional groups affect and inhibit the polymerization process. Further, especially anionic polymerization is very intolerant to impurities and proceeds only under the stringest conditions.

In radical polymerization, termination processes always occur due to coupling of two radicals. However, there are ways to minimize the termination reaction and to ‘control’ the polymerization in terms of polydispersity, degree of polymerization, and end-functionality.



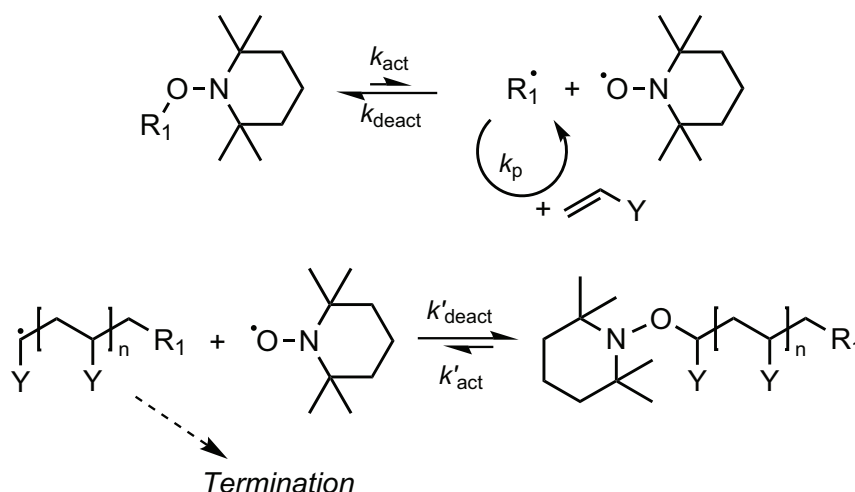
Scheme 2.1 General concept of controlled radical polymerization.

The key feature of CRP is reversible termination or reversible degenerative chain transfer. In Scheme 2.1, a very general concept of CRP is depicted. The radical species is reversibly trapped by a controlling agent forming the *dormant* species. The *dormant* species, however, can be re-activated by a catalyst or even spontaneously, *i.e.*, thermally. The exchange between *active* and *dormant* species enables a simultaneous chain growth with suppression of radical termination reactions.^[20]

The different types of CRP – including the Nitroxide-Mediated Radical Polymerization (NMP),^[23] the Atom Transfer Radical Polymerization (ATRP),^[24,25] and the Reversible Addition-Fragmentation Chain Transfer (RAFT) Polymerization^[26,27] – are described in more detail in the following sections.

2.1.1. Nitroxide-Mediated Polymerization (NMP)

For controlling the polymerization via the NMP process, stable nitroxide radicals are introduced into the polymerization.^[23] In Scheme 2.2 the mechanism exemplified on the nitroxide radical 2,2,6,6 - tetramethyl piperidin-N-oxyl (TEMPO), which is the most investigated nitroxide for NMP, is illustrated. The persistent nitroxide radical is utilized to reversibly terminate the propagating chains by forming an alkoxyamine.^[28] In this way, the radical concentration is limited and the termination reaction via recombination of two radicals can be suppressed to a certain extent. Due to the very stable alkoxyamine species the NMP process is conducted in bulk and at elevated temperatures, which allows to adjust the equilibrium of the *dormant* and *active* radical species.^[29]

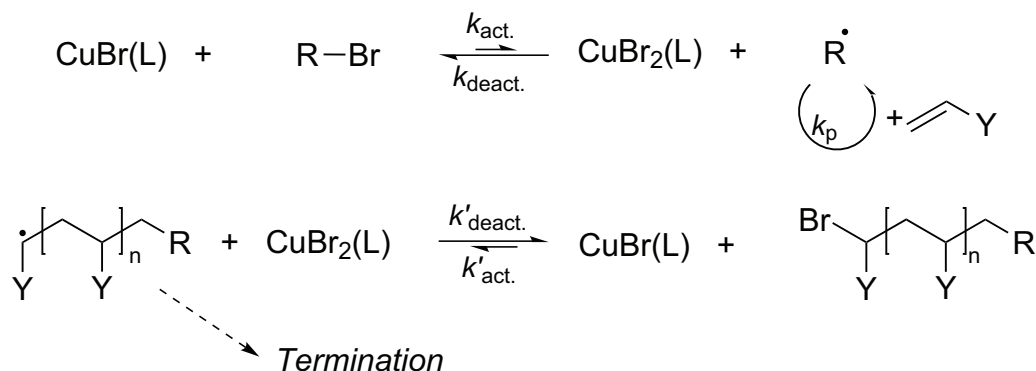


Scheme 2.2 Nitroxide-mediated polymerization with TEMPO.

For the nitroxide TEMPO depicted in Scheme 2.2 a conventional radical initiator such as 2,2'-azobis(isobutyronitrile) (AIBN) or benzoyl peroxide (PBO) is required. For more advanced NMP, low molecular alkoxyamines are utilized as initiators, which decompose at elevated temperatures to form the starting radicals for the chain growth and the stable nitroxide radical that can reversibly terminate the propagating species. More details as well as latest research themes concerning the NMP process are provided in the following reviews.^[23,30–33]

2.1.2. Atom Transfer Radical Polymerization (ATRP)

The ATRP is based on the same process as NMP: a reversible termination reaction. The equilibrium of *dormant* and *active* species is generated by employing a reversible redox system.^[24,25] Via a single electron transfer of the solubilized metal complex and the halide abstraction of an organic compound the initial radical is formed, which can propagate to form a polymer chain. The radical polymer chain can be deactivated by reacting with the oxidized metal complex in the solution to regenerate the transition metal complex. Due to this redox system an equilibrium between *dormant* (deactivated) species and *active* (radical) polymer chain is established.^[34] Effectively, the radical concentration is minimized and thus also termination via radical coupling is reduced, giving the polymerization a ‘living’ character.^[35,36] The most common system is the Cu(I)Br / Cu(II)Br₂. The basic mechanism of ATRP is presented in Scheme 2.3.

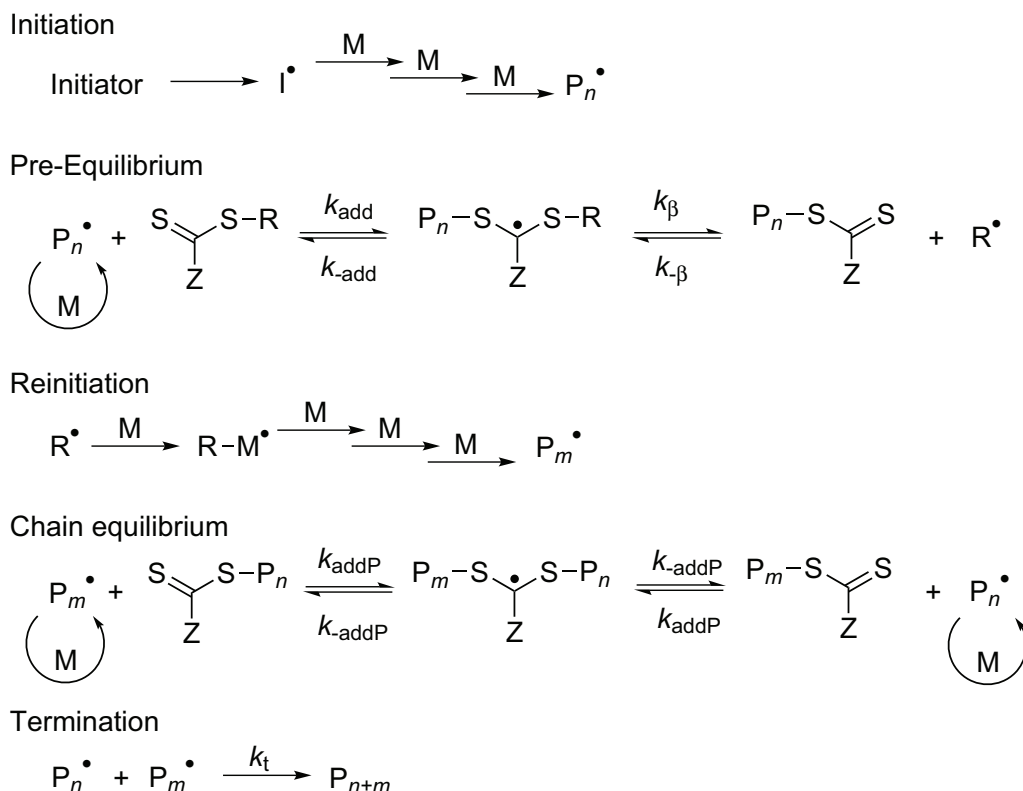


Scheme 2.3 Atom transfer radical polymerization employing the redox-system CuBr/CuBr₂.

Compared to NMP a higher variety of monomers can be applied to this polymerization process. In addition, milder conditions such as lower temperatures are tolerated. Disadvantages are the required purification steps to remove the metal catalysts. In addition, it should be considered that only polymers with conversion up to 40 % bear high enough end-functionality. To improve the ATRP process for specific applications and monomers, modifications of the original ATRP have been investigated. Modifications include ‘reverse’ ATRP,^[37] activator generated by electron transfer (AGET) ATRP,^[38–40] activator regenerated by electron transfer (ARGET) ATRP^[41,42] as well as initiators for continuous activator regeneration (ICAR) ATRP.^[43] For more insides into the ATRP process and its modifications, the reader is referred to the reviews from Matyjaszewski and coworkers.^[35,36,43,44]

2.1.3. Reversible Addition-Fragmentation Chain Transfer (RAFT) Polymerization

The RAFT process operates on a fundamentally different principle than the ATRP and NMP processes, mentioned above. The radical concentration is not reduced as in ATRP or NMP, in fact is almost equal to FRP. The control over the polymerization is provided by degenerative reversible chain transfer. In Scheme 2.4, the mechanism of the RAFT polymerization is provided.



Scheme 2.4 Basic reaction mechanism of reversible addition-fragmentation chain transfer polymerization.

Conventional initiators are utilized to start the reaction. The initial propagating radical adds to the sulfur center of the chain transfer agent (RAFT agent) to generate an intermediate radical. The intermediate species can undergo β -scission to release the R-group of the RAFT agent, which is subsequently the propagating species adding monomer units. With the main equilibrium in the RAFT process eventually a symmetrical equilibrium between propagating radical and *dormant* species is established. A macroRAFT agent reacts with a propagating radical chain to form the radical intermediate, which possesses two polymer chains. For the intermediate two possibilities exist to fragment – the back reaction and the reaction to form a new macroRAFT agent. In total, only an exchange of the *dormant* and the *active* chains takes place, which provides a chain length equilibrium.^[1,26,27]

The main part of the RAFT agent is the thiocarbonyl thio moiety. Common RAFT agents used are dithioesters and trithiocarbonates. Xanthates are applicable for monomers with low reactivity (*i.e.*, with high radical reactivity) and follow the same mechanism. It should be mentioned here that due to the invention history the polymerization process with xanthates is termed Macromolecular Design by Interchange of Xanthates (MADIX).^[45]

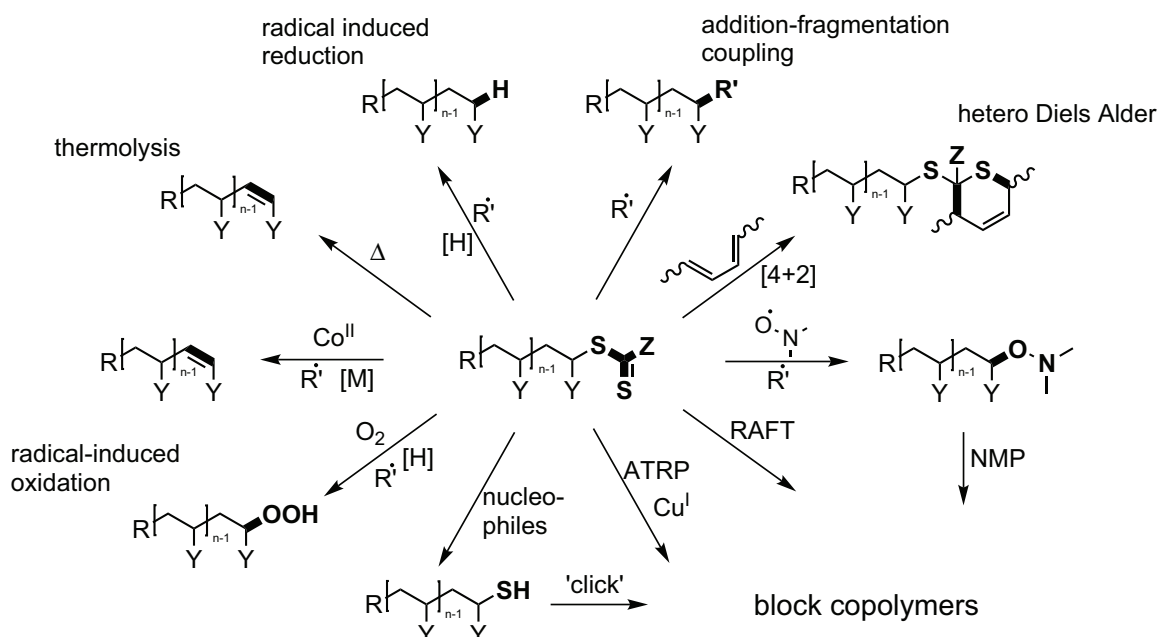
The groups attached to the thiocarbonyl thio moiety – the R- (which is connected directly to the sulfur atom) and the Z-group – fundamentally influence the polymerization process. The choice of the R- and the Z-groups depends highly on the reactivity of the monomer. The R-group acts as a leaving group in the pre-equilibrium and should favor the fragmentation reaction. The Z-group influences the stability of the intermediate. The Z-moiety should be chosen carefully in a way that the formation of the intermediate is favored, without creating a persistent species.^[46] Typically, a 10 fold excess of the RAFT agent compared to the initiator in the reaction provides the incorporation of the R-group to a very high extent and thus generates polymers with high end-functionality.

As mentioned above, the radical concentration is not suppressed by the presence of the RAFT agents. Thus, in theory the polymerization rate is not affected by the RAFT process.^[47] However, rate retardation can be observed, in particular when dithiobenzoates are utilized as RAFT agents. Explanations for this phenomena include radical coupling of the intermediate radical and the propagating radical chain end or a delayed/slow fragmentation of the intermediate in the main equilibrium step.^[48,49]

2.2. End-group Modification of RAFT Polymers

The polymer obtained at the conclusion of the RAFT polymerization bears the R-group at one chain end and the thiocarbonyl thio moiety with the Z-group at the other chain end. Visually, the presence of the thiocarbonyl thio moiety imparts color onto the polymer. Additionally, the polymer can release odor after some time due to abstraction of volatile sulfur-containing molecules. Thus, in some cases, especially in optoelectronic and biomedical applications, it is desirable that the end-group is removed.^[50–54] In other circumstances, it is expedient to transform the thiocarbonyl thio group to generate new functionalities at the polymer chain end. This is the case when the RAFT polymers are employed to construct more complex structures, *e.g.*, block and star polymers as well as functional nanoparticles.^[55–57] An overview over different processes for RAFT end-group transformation is provided in Scheme 2.5. Via thermolysis and radical-induced reactions complete desulfuration of the polymer

material is achieved. The reaction with nucleophiles typically generates polymers with thiol end-groups, which can subsequently be applied in 'click'-type reactions such as thiol-ene reactions and reactions with isocyanates.^[58,59] For other applications RAFT polymers can be introduced into ATRP and NMP processes, in many cases after modification of the thiocarbonyl thio moiety. Despite the variety of transformations depicted in Scheme 2.5, only a selection of transformation options will be presented in the following subsections. The transformation of the RAFT end-group with oxygen in THF to form peroxides will be described in more detail in Chapter 4. More information provide the review from Harvison *et al.* as well as O'Reilly and coworkers.^[60,61]

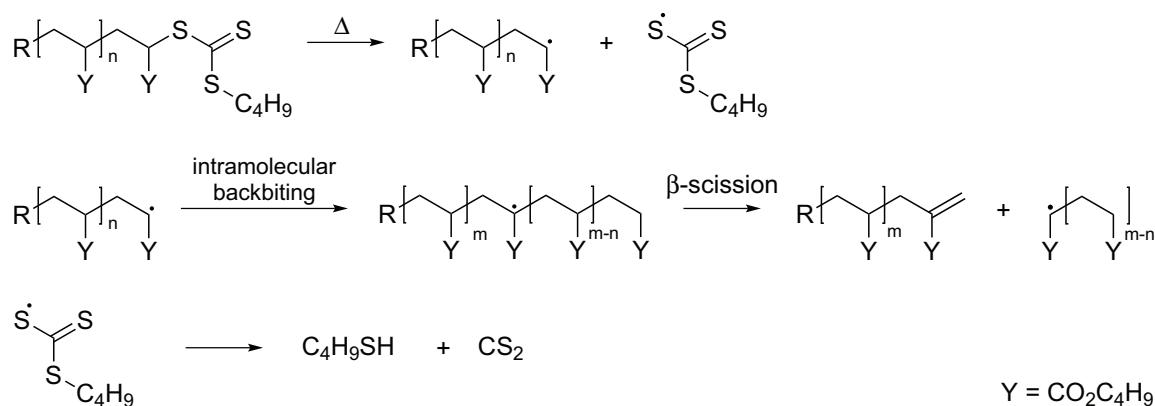


Scheme 2.5 Established modification reactions of a RAFT polymer bearing a thiocarbonyl thio moiety.

2.2.1. Thermolysis

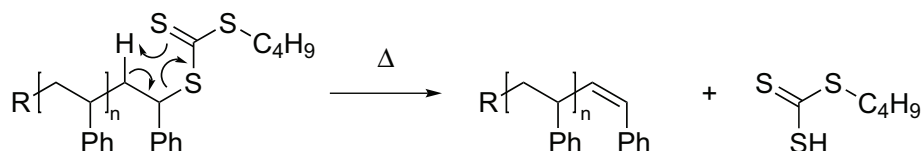
The thiocarbonyl thio end-group can be removed completely via thermal decomposition.^[62–66] The advantage of the thermolysis is that no chemicals are employed for the treatment. Due to the high temperatures the polymer itself, however, needs to be sufficiently stable. Commonly, the obtained polymer bears an unsaturated end-group, resulting from the homolytic scission of the C-S bond and subsequent disproportionation or elimination.^[2] The mechanism, the final product and the required temperature highly depends on the type of polymer and the Z-group attached to the thiocarbonyl thio moiety. For clarification, some examples are provided here. The thermal decomposition of poly(butyl acrylate) with a trithiocarbonate end-group requires temperatures of around 180 °C and absence of air leading to a macromonomer with an *exo*-methylene double bond. The double bond is generated via homolysis

of the C-S bond, followed by a backbiting reaction and a subsequent β -scission (see Scheme 2.6).^[67,68] 65-90% vinyl end-group functionality can be achieved via such a thermal end-group elimination.^[63]



Scheme 2.6 Thermolysis of poly(butyl acrylate) bearing a butyl trithiocarbonate end-group.

The thermal decomposition of poly(styrene) bearing a cumyl dithiobenzoate RAFT group starts above 120 °C yielding dithiobenzoic acid and α -methyl styrene.^[69] In the temperature range between 210 – 250 °C, the butyl trithiocarbonate end-group is removed from RAFT end capped polystyrene. The process of the cleavage is proposed to be a concerted Chugaev elimination (Scheme 2.7).^[70,71]



Scheme 2.7 Thermolysis of poly(styrene) bearing a butyl trithiocarbonate end-group.

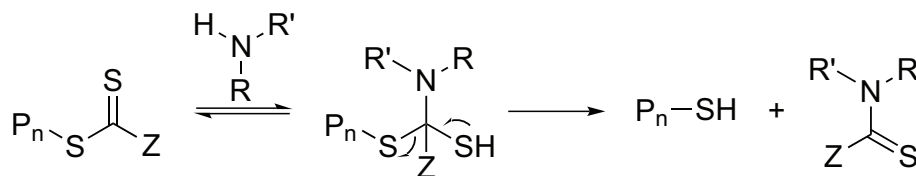
Poly(methyl methacrylate) is found to be thermally unstable and tends to degrade at elevated temperatures. However, thermal decomposition of poly(methyl methacrylate) possessing dithiobenzoate end-groups leads to less weight loss than thermolysis of polymers with no RAFT end-group.^[66] Here again, a concerted Chugaev elimination is responsible for the end-group removal.^[72,73] Additionally, it was observed that thiocarbonyl thio capped poly(methyl methacrylate) is less stable in the presence of impurities such as residual initiator and metal contamination in the sample.^[66]

Generally speaking, the order of the thermal stability concerning the Z-group was observed to be: dithiobenzoate > trithiocarbonates > xanthates.^[74] Additionally, it was found that the thermal stability is significantly improved by an aromatic Z-group compared to the linear alkane chains. Further, it should be noted that thermolysis can be conducted in presence of copper powder. Due to the catalytic effect of the metal, the temperature required for the thermal decomposition can be significantly decreased, *i.e.*, from 210 to 165 °C for the elimination of the end-group on a poly(styrene)

chain.^[64]

2.2.2. Reactions with Nucleophiles

The thiocarbonyl thio end-group can react with nucleophiles such as hydroxides, amines, and thiols to form polymers with a thiol end-group.^[75-77] The transformation of dithioesters to thiols via hydrolysis has been carried out under acidic and basic conditions,^[78,79] yet it was found that the rate coefficient for hydrolysis increases with increasing pH.^[80] Thus, common strong bases such as sodium hydroxide are employed for the hydrolysis.^[81-83] Due to many side reactions ranging from the formation of disulfide bridges to base-catalyzed elimination and cyclization the end-group fidelity is rather low.^[82] An alternative approach to obtain thiol end-capped polymers is the aminolysis with primary or secondary amines, employed as nucleophiles.^[62,72,73,75,84] The reaction is depicted in Scheme 2.8.



Scheme 2.8 Aminolysis of a dithioester end-group.

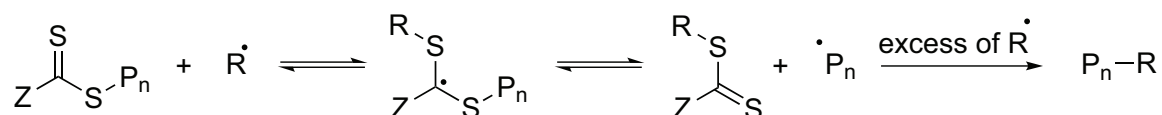
The main side reaction occurring during the aminolysis process is the coupling of thiols to generate disulfides, when traces of oxygen are present in the reaction flask. The formation of disulfides can be observed in the SEC elugrams, showing bimodal distributions or a shoulder at higher molar masses due to chain-chain coupling.^[85] Alternatively, the coupling reaction can be utilized as a tool for the formation of linear multi-block copolymers, provided that the aminolysis was applied on polymers synthesized via difunctional chain transfer agents.^[9] In most cases, however, the disulfide-bridge is not desirable and conditions can be identified where the coupling is avoided. Reducing agents such as sodium bisulfide, zinc/acetic acid, and tris(2-carboxyethyl)phosphine are found to prevent the oxidation of thiols.^[73,78,86] Ionic reducing agents, *e.g.*, boro hydrides, minimize the oxidation of thiols as well.^[87] It should also be mentioned that very little disulfide formation is obtained employing hydrazines as nucleophiles. This approach can even be carried out under ambient air.^[88] The obtained thiol end capped polymers can be employed for the stabilization of gold nanoparticles or for biopolymer conjugates,^[77,87,89,90] and can undergo further post-modification reactions. These reaction include thiol-ene reactions, reactions with α -bromoesters, isocyanates, and 2,2'-dithiodipyridines and can be summarized under the term thiol-click reactions.^[56,58,59,91,92] The reactions are applied for instance to generate biopolymer conjugates by disulfide exchange and to form cyclic poly-

mers.^[85,91] Polymer-polymer conjugation was obtained via radical thiol-ene process, which is, however, not considered as a click-reaction.^[93]

2.2.3. Radical-induced End-group Modification

Two processes are combined under the term radical-induced end-group removal – the radical-induced reduction and the radical-addition-fragmentation coupling. Via radical-induced reduction a complete removal of the thiocarbonyl thio end-group can be obtained. Free radicals react with the C=S double bond to generate a radical intermediate. The intermediate can subsequently fragment back or – alternatively – release the radical polymer chain, which terminates in the presence of a trapping agent. For this synthetic route a high excess of free radicals is required. If hydrogen donors are added, the thiocarbonyl thio end-group is replaced by a hydrogen atom. Tri-*n*-butylstannane or hypophosphite salts can be applied to obtain hydrogen terminated polymers.^[62,63,94,95]

The same initial process can be applied to obtain a radical induced ester exchange. In the presence of an excess of radical initiator the RAFT polymer is heated up to 60–90 °C. The generated macroradical recombines with one of the free radicals present in the solution. Thus, depending on the nature of the free radical, a new functionality can be introduced into the polymer chain (see Scheme 2.9). Furthermore, with this process the RAFT agent can be recovered.^[96] However, when the polymer bears a butyltrithiocarbonate end-group or a dithiobenzoate, incomplete transformation have been observed.^[64,97] Consequently, the radical-addition-fragmentation coupling process can not be applied to all types of RAFT polymers.

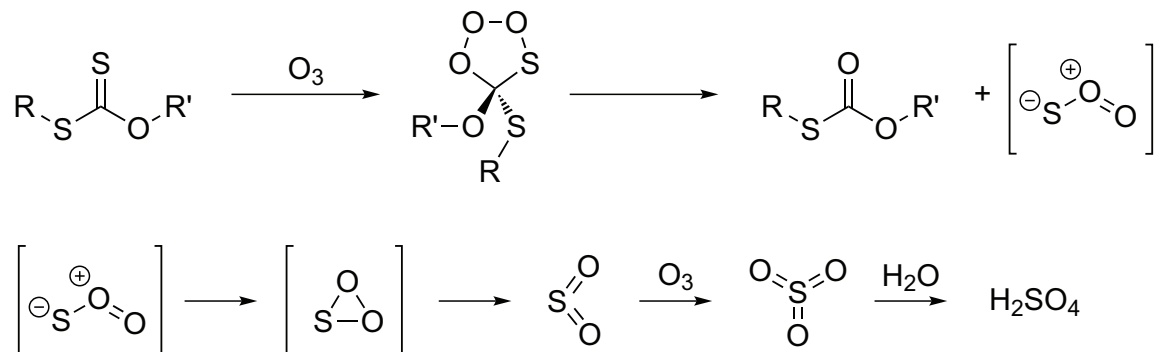


Scheme 2.9 Radical induced addition-fragmentation coupling.

2.2.4. End-group Modification via Oxidation and Irradiation

End-group modification of thiocarbonyl thio end-capped polymers also occurs when oxidizing agents such as ozone, hydrogen peroxide and peracids are present in the solution.^[98–100] Hydroperoxides such as *t*-butylhydroperoxide are applied to transform the dithioester to obtain a sulfine end-group. The success of the process was previously studied on small molecules.^[47,100,101] A transformation of the end-group of the poly(*N*-vinylpyrrolidone) was conducted with hydrogen peroxide at 60 °C to yield hydroxyl terminated polymer. A proposed mechanism consists of thermal generation of hydroxyl radicals with subsequent addition-fragmentation-coupling. However, ther-

mal homolysis of hydrogen peroxides requires high temperatures.^[99] An alternative method to transform the end-group via oxidation is the employment of ozone. Ozone reacts with xanthates to form thiocarbonate end-group and sulfuric acid as a side product. A possible mechanism is depicted in Scheme 2.10.^[98]



Scheme 2.10 Reaction with ozone forming a thiocarbonate.

Applying UV light to RAFT polymers in solution leads in some cases to removal of the thiocarbonyl thio group.^[102] The success of this reaction depends on the structure of the RAFT end-group. As reported in the study of Quinn *et al.*^[103] dithiobenzoates are among the most sensitive to UV irradiation. The cumyl dithiobenzoate and the 2-cyanopro-2-yl(4-fluoro)dithiobenzoate decompose at the UV light of their characteristic absorption wavelength.^[103–105] On the other hand, trithiocarbonates are relatively stable under UV irradiation.^[104]

2.2.5. Concluding Remarks

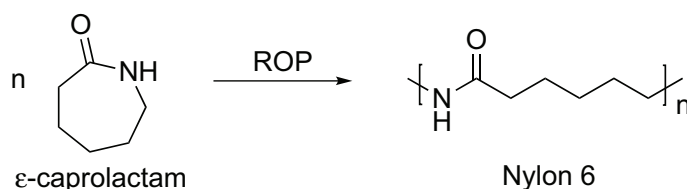
As described in the last sections, most of the modification techniques have some drawback concerning the yield of the reaction or the reaction conditions. Transforming the thiocarbonyl thio end-group to an hydroxyl function is an elegant method to provide a new functionality which enables further reactions. This new modification method will be introduced in Chapter 4.

2.3. Ring-Opening Polymerization (ROP)

2.3.1. General Aspects

In industry commodity polymers such as poly(styrene) or poly(methyl methacrylates) are synthesized by free radical polymerization on very large scales. Ring-opening polymerization (ROP) of cyclic monomers, in contrast, finds application for more specific and typically biomedical high performance materials. The production of those materials is in general of much smaller volumes.^[106]

A large variety of cyclic monomers, *e.g.*, lactams, lactones, cyclic ethers, and siloxanes can be polymerized via the ring-opening process. Prominent examples of ring-opening polymerization in industry are the generation of Nylon 6 synthesized from ϵ -caprolactam (see Scheme 2.11) and poly(ethylene oxide) (PEG) produced via ROP of ethylene oxide.^[21]



Scheme 2.11 Polymerization of ϵ -caprolactam, a prominent example for ring-opening polymerization.

The ability of cyclic monomers to form macromolecules by sequential ring-opening depends both on thermodynamic as well as kinetic aspects. The most important factors are the relative stabilities of the cyclic monomer and the linear polymer structure. For example, the Gibb's free energy of the conversion of cycloalkanes is negative for almost all ring sizes except for the 6-membered ring and thus, thermodynamically, the polymerization is favored in most cases.^[107,108] The thermodynamic feasibility is associated with bond angle strain, eclipsed conformational strain, and transannular strain of the cyclic monomers depending on the ring size. Since the entropy ΔS is negative for the polymerization process, higher temperatures lead to less negative values of the free energy. Although almost all cycloalkanes are thermodynamically able to undergo ring-opening polymerization, the polymerization process was only successful in very few cases such as for cyclopropane derivatives.^[21] Consequently, not only the thermodynamic factors are crucial, but also the kinetics play a major role.

For polymerization a bond which the initiator can attack is required in the monomer structure. This is achieved by incorporation of heteroatoms in the ring. Such monomers are more facile to be electrophilically or nucleophilically attacked by an initiator and can subsequently propagate to form a polymer chain.

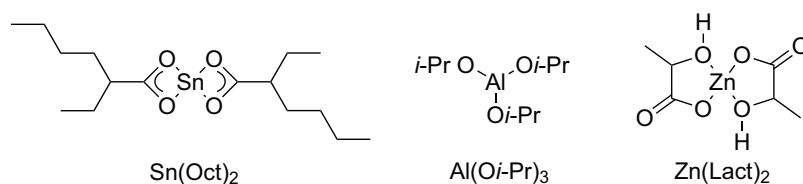
The ring-opening polymerization belongs to the chain-growth polymerization mech-

anism which includes initiation, propagation, and termination reactions. The specific mechanism of ring-opening polymerization highly depends on the initiator/catalyst system. The processes mostly employed are based on ionic, coordination, covalent, methathetic, radical, and enzymatic polymerization mechanisms.^[109–113] Many ring-opening processes can be regarded as polymerization techniques featuring living characteristics since in most cases the number-average molar mass increases linearly with monomer conversion. However, the comparison of anionic polymerization of vinyl monomers with anionic polymerization of cyclic ethers, shows that the propagation rate of the ROP is much slower and is more similar to a step-growth polymerization. The main reason for that is the equilibrium between polymerization and depolymerization, which plays a greater role in ROP than in chain polymerization of vinyl monomers.^[21]

In the following sections selected ring-opening polymerization processes for the formation of polylactones and polylactides are described.

2.3.2. Metal-catalyzed Ring-Opening Polymerization

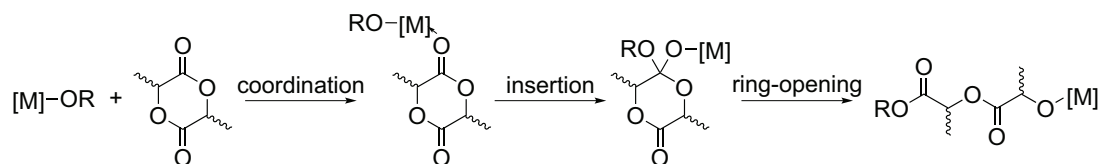
Metal complexes are very frequently employed as catalysts for ring-opening polymerization. Tin(II)bis(2-ethylhexanoate) ($\text{Sn}(\text{Oct})_2$) is the most prominent representative. This catalyst is soluble in many solvents, easy to handle, and high molar masses can be obtained in short times by polymerization of lactones and lactides.^[114–118] Beside tin, aluminum alkoxides, and zinc complexes can be applied. In Scheme 2.12 different catalysts are depicted. With aluminum alkoxides and zinc complexes as catalysts much longer reaction times are required to obtain polymer structures compared to the catalysis with $\text{Sn}(\text{Oct})_2$. However, zinc-based catalysts are preferred for some applications due to their non-toxicity.^[119–121]



Scheme 2.12 Main metal catalysts utilized for ROP of lactones and lactides.

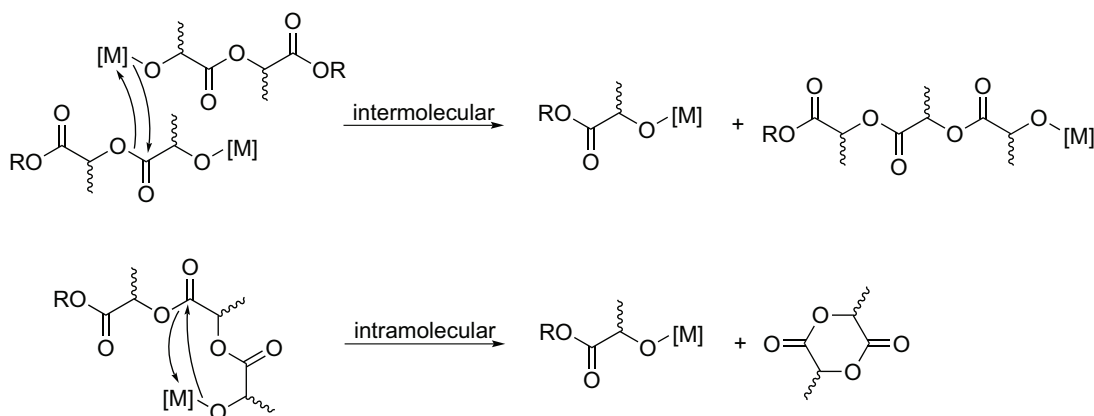
The mechanism of metal-catalyzed ring-opening polymerization includes three steps: coordination, insertion, and ring-opening of the cyclic monomer.^[122–124] An example for the ROP of a lactide catalyzed via a metal complex is given in Scheme 2.13. To terminate the reaction, the polymerization can be quenched by hydrolysis, releasing the metal complex from the chain end.

Polymers, synthesized via metal-catalyzed ring-opening polymerization are observed to possess broader mass distributions with increasing conversion (up to PDI s ~ 2).



Scheme 2.13 Coordination-insertion mechanism of a lactide employing metal catalysts.

This problem results from the susceptibility of the system to undergo side reactions. Especially when $\text{Sn}(\text{Oct})_2$ is employed, transesterification reactions can occur. The two possible transesterifications, *i.e.*, intermolecular and intramolecular, are depicted in Scheme 2.14. The intramolecular backbiting leads to monomer recovery and macrocycles, whereas the intermolecular reaction yields chain redistributions, resulting in higher *PDI*s of the obtained polymeric material.^[125–127]



Scheme 2.14 Main side reactions occurring in the ROP process via metal-catalysis.

For some biomedical applications metals and metal complexes are preferably excluded.^[128] Consequently, organo-catalysis is addressed with growing interest.

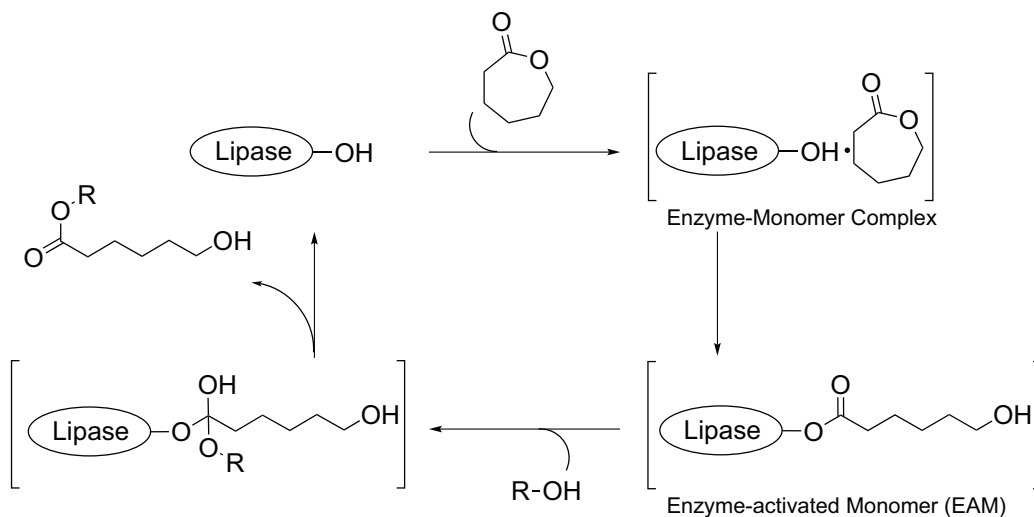
2.3.3. Organo-catalyzed Ring-Opening Polymerization

Organo-catalyzed ring-opening polymerization mainly includes enzymatic ROP, ROP with *N*-heterocyclic carbenes, pyridine- as well as amidine- and guanidine-based ring-opening polymerization. A very short overview is provided below for each metal-free catalytic system.

Enzyme-catalyzed Ring-Opening Polymerization

Enzyme catalysis for ring-opening polymerization was first developed by Knani and Kobayashi in 1993.^[129–131] In nature the lipases, a subgroup of the hydrolases, are involved in the hydrolysis of fatty acid esters. After extraction from living organisms, the lipases can be employed in synthetic processes such as the ring-opening polymer-

ization of cyclic esters. With enzyme catalysis high regio- and stereo-selectivity is provided and the reaction can be carried out under mild conditions. A commercially available enzyme is Novozym 435. This enzyme can be employed for variable cyclic esters except for lactides.^[132–134] The process involves a monomer-activated mechanism depicted in Scheme 2.15.



Scheme 2.15 Proposed mechanism for the ring-opening polymerization with lipase acting as catalyst.

The first step of the mechanism is a nucleophilic attack of a hydroxyl group attached to the lipase onto the ester group of the cyclic monomer. The so obtained acyl-enzyme intermediate releases the alkoxy group to form the enzyme-activated monomer (EAM). Via a nucleophilic attack of a hydroxy end functional species, the open chain is released and the enzyme is regenerated. Iterations of the cycle process finally form polymeric structures.^[106,135,136]

Organo-catalysis by Pyridines and *N*-Heterocyclic Carbenes

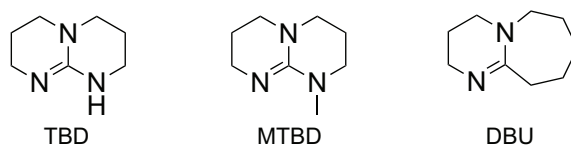
Nucleophilic catalysts such as pyridines and *N*-heterocyclic carbenes have been observed to promote ring-opening polymerization of cyclic esters.^[106] The first successful pyridine-catalyzed living ring-opening polymerization was achieved by Hedrick and coworkers in 2001.^[137] Employing 4-(dimethylamino)pyridine (DMAP) in combination with 4-pyrrolidinopyridine (PPY) at 35 °C, narrowly dispersed polylactide was obtained after 20 h. The mechanism is assumed to proceed by monomer-activation via nucleophilic attack by DMAP on the cyclic monomer.^[138,139] Further, it was observed that no increase in the polydispersity occurs with increasing molar masses, which implies that side reactions such as transesterification are minimized during the polymerization process.

N-heterocyclic carbenes have also been found to act as powerful catalysts for ring-

opening polymerization. In 2002, the first example was reported by Hedrick and coworkers.^[140] 1,3-Bis-(2,4,6-trimethylphenyl)imidazol-2-ylidene (IMes) was employed to promote the polymerization of lactides and lactones. Achieving polymers with high end-functionality and narrow polydispersity in a very short time (within 10 min), showed the high catalytic activity of the carbene.^[141] For the ROP of lactides a monomer-activated mechanism via nucleophilic attack of the carbene was proposed.^[142] In the absence of protic initiators, however, a zwitterionic mechanism is assumed.^[143] For more detailed information, the reader is advised to refer to the review of Hedrick.^[144]

Amidine- and Guanidine-based Ring-Opening Polymerization

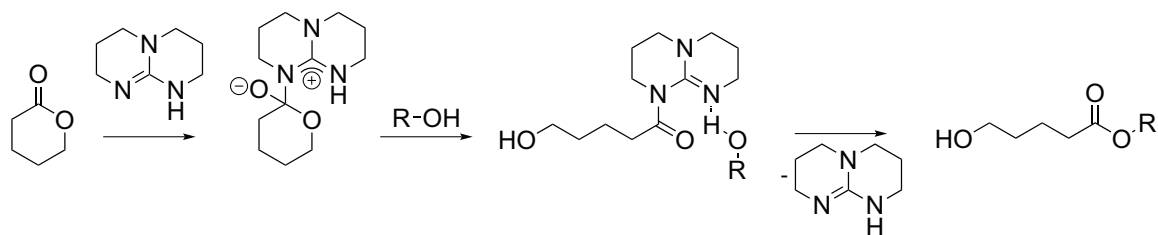
Strong basic species, so-called ‘superbases’, are known as transesterification catalyst for small molecules.^[145] In 2006, Waymouth and Hedrick employed the basic catalyst 1,5,7-triazabicyclo[4.4.0]dec-5-ene (TBD) for ring-opening polymerization successfully for the first time.^[146] Further investigated active basic catalysts are 1,8-diazabicycloundec-7-ene (DBU) and *N*-methyl TBD (MTBD) (see Scheme 2.16).^[147,148]



Scheme 2.16 Structures of the catalysts 1,5,7-triazabicyclo[4.4.0]dec-5-ene (TBD), *N*-methyl TBD (MTBD), and 1,8-diazabicycloundec-7-ene (DBU).

The basic catalysts, especially TBD, enable ultra-fast ring-opening polymerization with controlled character. It was reported that complete polymerization of lactide was realized in 1 min at ambient temperature.^[146] Only after significantly longer reaction times (5 h), broadening of the mass distribution due to transesterification reactions was observed, which can be prevented by quenching the solution with benzoic acid after a reasonable time. It is proposed that the ring-opening proceeds via a bifunctional mechanism. Corey and Grogan showed in a small molecule study that TBD can function as a bifunctional catalyst.^[149] The mechanism for the polymerization process is presented in Scheme 2.17. In the first stage the imine of TBD attacks the cyclic monomer. Secondly, after the ring-opening and proton transfer the alcohol moiety of the initiator is activated by the adjacent nitrogen and can attack the open chain.^[150,151]

MTBD and DBU are also very strong bases.^[152] However, they only possess one catalytic site. Ring-opening polymerization with these catalysts is assumed to proceed via a pseudo-anionic mechanism. For the ROP of ϵ -caprolactone and δ -valerolactone with MTBD and DBU additional co-catalysts such as thiourea are required.^[148]



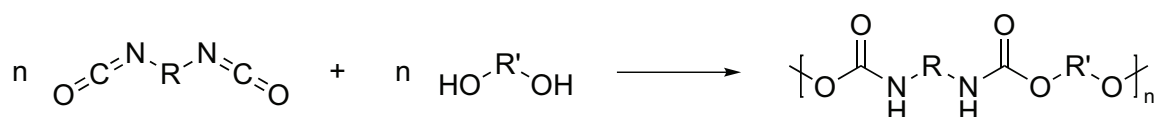
Scheme 2.17 Dual activation of the cyclic monomer and the alcohol by TBD.

2.4. Polyurethanes

2.4.1. General Aspects

Polyurethanes were first reported by Bayer in 1947 within a diisocyanate polyaddition procedure. He published results obtained 10 years before in 1937 on the polyaddition of 1,6-diisocyanatohexane and 1,4-butanediol.^[153] Since then polyurethanes have been established as industrial products, mainly in the form of elastomers and polyurethane foams. Presently, polyurethanes belong to the top five of the most industrially produced synthetic polymers.

Nowadays most commercially available polyurethanes are still based on the step-growth polymerization of diisocyanates and multi-functional polyols. The use of diol results in linear polyurethanes and with polyols at higher functionality cross-linked networks are obtained. The polyaddition process is depicted in Scheme 2.18. The polyurethane formation proceeds via a nucleophilic attack of the hydroxyl function onto the carbon atom of the isocyanate group and is in general promoted by basic or organo-metallic catalysts.



Scheme 2.18 Synthesis of polyurethanes via polyaddition of diisocyanates and diols.

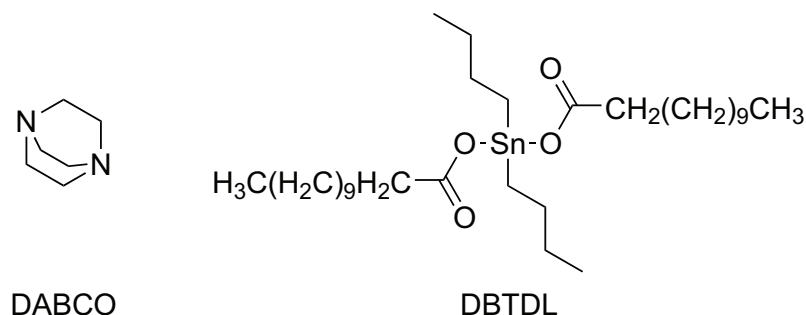
Due to the step-growth mechanism, the two components should be employed utmost exact stoichiometrically for the synthesis of high-molar-mass materials. A prevalent and more facile method to obtain polymers with high molar masses via the polyaddition process is the so-called prepolymer synthesis method, in which one of the components – generally the diisocyanate – is added in excess to the reaction. The resulting macromolecules with isocyanate end-groups are subsequently extended using small molecules possessing two hydroxy moieties, *e.g.*, 1,4-butanediol or diethylene glycol, for the final polymer formation.

Typically, isocyanates employed in the polyurethane synthesis are aliphatic isocyanates such as 1,6-diisocyanatohexane or isocyanates possessing an aromatic center,

e.g., 4,4'-methylene bis(phenyl isocyanate) (MDI) and toluene 2,4-diisocyanate (TDI). The industrial process for the generation of such isocyanates is the phosgenation of amines.^[154] Due to the extreme toxicity of phosgene, extensive research was applied towards alternative methods. Possible synthetic strategies are two step processes in which carbamates are first formed by an oxidative or a reductive carbonylation. In the second step thermal decomposition of the obtained carbamates generates the isocyanates.^[155–157]

Established polyols utilized for the polyurethane synthesis are polyether and polyester polyols. Polyethers are synthesized by anionic ring-opening polymerization of ethylene oxide, propylene oxide or by cationic ring-opening polymerization of tetrahydrofuran. Polyesters can also be obtained by ring-opening polymerization, for instance by ROP of ϵ -caprolactone with a dual hydroxy-functionalized initiator. Alternatively, polycondensation of dicarboxylic acids and dihydroxy functional molecules also results in polyester polyols such as polyadipates.

The polyaddition of diisocyanates and polyols is promoted by specific catalysts. Preferred systems are tertiary amines and organo-metallic complexes. The most frequently used metal-free catalyst is 1,4-diazabicyclo-[2.2.2]-octane (DABCO). The most widely employed metal catalyst is dibutyltin dilaurate (DBTDL) (Scheme 2.19).

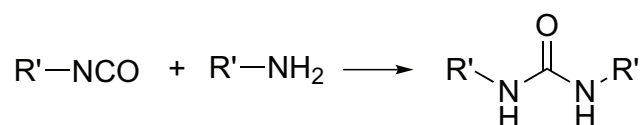
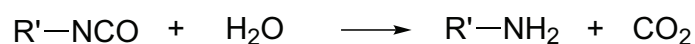


Scheme 2.19 Main catalysts employed for polyurethane synthesis.

Beside the liquid tin catalyst, iron, zirconium, and cobalt complexes can also be applied as catalysts depending on the applications. In industrial processes amine and tin catalysts are often employed synergistically to significantly accelerate the process.^[158–160]

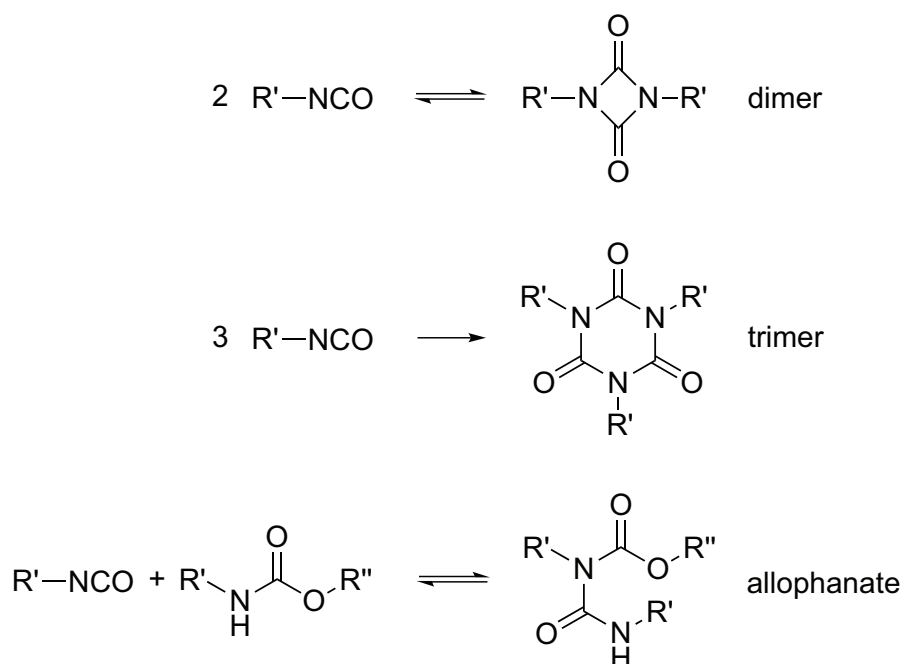
It should be noted that several side reactions can occur during the polymerization process. The reaction with water impurities results in the formation of urea groups (see Scheme 2.20). Therefore the polymerization is conventionally carried out under nitrogen atmosphere and exclusively dry solvents are utilized. However, especially for the formation of polyurethane foams, the reaction with water is indispensable due to the release of carbon dioxide, which causes the foam structure.

Other potential side reactions are dimerisation and trimerisation of the isocyanate moiety. The dimerisation is enhanced at temperatures above 43 °C, but dimers can



Scheme 2.20 Formation of urea bonds resulting from water traces.

be cleaved again elevating the temperature to at least 175 °C. By visual inspection, namely a yellow discoloration, the side reaction can be identified. The trimerisation of the isocyanates are promoted under alkaline conditions. The formation of six-membered rings is irreversible and stable up to 200 °C before it decomposes at temperatures above 200 °C. Further allophanate linkages are observed, resulting from the reaction of isocyanates with the urethane moiety. Thus, cross-linkages are generated, which can be desirable in the production of elastomeric materials. The reaction is favored under alkaline conditions at elevated temperatures. All the mentioned side reactions are collated in Scheme 2.21.^[161,162]

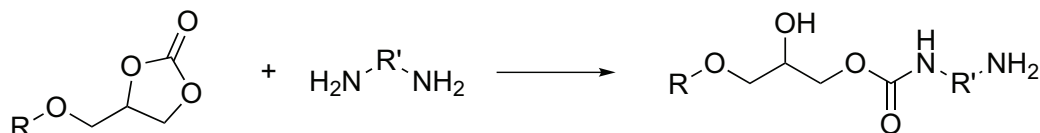


Scheme 2.21 Side reactions occurring during the polyurethane synthesis.

2.4.2. Alternative Synthetic Pathways and Recent Developments in Polyurethane Chemistry Associated with Environmental Aspects

Due to the environmental hazards of the isocyanate synthesis and the intolerance of the polyurethane reaction to water impurities, extensive investigations on isocyanate-free procedures have been carried out in the recent years. The non-isocyanate polyurethane

(NIPU) can be obtained by cationic ring-opening polymerization. Seven-membered rings with urethane moieties can undergo polymerization with initiators such as trifluoromethylsulfonate.^[163,164] An alternative synthetic route to provide NIPU is the reaction of diamines and bischloroformates. During the condensation reaction HCl is released.^[165,166] A more investigated pathway is the formation of urethane linkages via a reaction of cyclocarbonates with diamines (see Scheme 2.22).^[167–172]



Scheme 2.22 Isocyanate free procedure to obtain urethane linkages.

Compared to conventionally synthesized polyurethanes, NIPU shows higher chemical resistance, lower permeability, and improved thermal stability and water absorption. Typical applications for NIPU are foams, coatings, and sealants.^[173,174]

Environmental aspects also include the biodegradability of the synthesized material. For linear polyurethanes a great variety of natural products can be employed facilitating the recycling processes. Examples of natural products include castor oil, starch, cellulose as well as natural rubber.^[175–177] For more details the reader is encouraged to refer to the numerous reviews and books on this topic.^[178–182]

2.4.3. Polyurethanes in Combination with Radical Polymerization and their Applications

Polyurethanes are generally known to possess good water resistance and resistance to other atmospheric conditions as well as to oils and diluted acids. Furthermore, if no aromatic systems are present, they are resistant against photo-oxidative aging. As described in the previous section, the trend of polyurethane synthesis moves to biodegradable raw material. Of major interest today are waterborne polyurethanes or so-called polyurethane ionomers.^[183,184] However, the increased amount of hydrophilic groups can be detrimental to the performances, especially the resistance to water. For that reason, polyurethanes are often combined with polymers synthesized via radical polymerization of vinyl monomers. For instance, the combination with poly(vinyl acetate) or styrene to form interpenetrating networks or grafted block copolymers highly improved the resistance to water as well as the adhesion to metallic and ceramic substrates.^[185,186] Copolymers of polyurethane ionomers and polyacrylates find application in environmentally friendly laquers.^[16] Conventional polyurethane-co-poly(acrylate) copolymers have been investigated for applications such as contact lenses and dental materials.^[187,188] Further methods to combine polyurethanes and vinyl-based polymers to multi-block copolymers can be found in Chapter 7.

2.5. Liquid Chromatography of Polymers

The first use of a chromatographic setup was reported by Tswett in 1903-1906.^[189,190] In this publication the separation of colored plant pigments by chromatography was investigated. Tswett termed the separation by retardation of the substances ‘chromatographic method’ derived from the greek words ‘chromos’ = color and ‘graphe’ = to write.

Today a large variety of separation methods exist. Widely used chromatographic techniques include thin layer chromatography, gas chromatography, flash chromatography, high performance liquid chromatography as well as size-exclusion chromatography.^[191,192]

In general, the separation is conducted by a mobile phase and a stationary phase. The mobile phase, including the material which is to be separated, is transported over the stationary phase. During the movement of the mobile phase through the stationary phase the separation of the material into its components occurs.

Polymeric materials often show heterogeneity in more than one of the following aspects: chemical composition, molar masses, configuration and topology. As such different chromatographic techniques are applied concerning the different aspects.^[193,194]

Mostly relevant for macromolecules and polymer structures is liquid chromatography, including size-exclusion chromatography and liquid adsorption chromatography.

2.5.1. General Aspects of Liquid Chromatography

The liquid chromatographic technique is carried out with a liquid mobile phase and conventionally a solid stationary phase. Liquid chromatography can be separated into ion-exchange, adsorption, liquid-partition and size-exclusion chromatography. Thus, the retention in liquid chromatography can be caused by enthalpic and entropic interaction as well as adsorption or partition of the sample with the stationary phase.

In the chromatographic process the retention volume V_R can be expressed by

$$V_R = V_M + K_{LC} V_S \quad (2.1)$$

where V_M is the volume of the mobile phase, V_S is the equivalent liquid volume for the stationary phase and K_{LC} is a parameter which expresses the thermodynamic balance of the sample between the phases for a specific mobile phase and column packing. The equilibrium constant is related to the change in the Gibb’s free energy ΔG^0 . For the retention, both the change in entropy ΔS and in enthalpy ΔH contribute to the separation process. Consequently, the retention factor for conventional liquid

chromatography is given as

$$k' = \frac{V_R - V_M}{V_M} = K_{LC} \frac{V_S}{V_M} = \exp\left(-\frac{\Delta G_{LC}^0}{RT}\right) \frac{V_S}{V_M} \quad (2.2)$$

$$\ln k' = \frac{-\Delta H_{LC}^0}{RT} + \frac{\Delta S_{LC}^0}{R} + \ln \phi, \quad \ln \phi = \frac{V_S}{V_M} \quad (2.3)$$

with the temperature T and the gas constant R .^[195]

Due to the influence of entropic and enthalpic affects, polymer samples are separated according to their chemical composition and their molar masses. For a more facile assignment of the signals, however, it is preferred to mainly exclude one of the effects.

2.5.2. Size-Exclusion Chromatography (SEC)

In 1959 it was firstly reported that macromolecules can be separated by their size.^[196] In the publication the researchers from Sweden applied polydextran gels for the fractionation of water-soluble biomolecules. Synthetic polymers were firstly analyzed via a setup consisting of a stationary phase of cross-linked polystyrene gel in organic solvents.^[197] The term gel permeation chromatography (GPC) is derived from this kind of setup employing particles of lightly cross-linked organic-polymer networks for the separation. Today more rigid porous particles are utilized as column packing material for time-saving reasons. The lightly cross-linked networks were not stable to high pressures and fast flow rates, which elongated the separation experiments significantly. Further SEC is applied routinely today not to separate completely different structures, but to obtain the average molar masses and the molar mass distribution of synthetic polymers.^[198]

With SEC the polymer chains are separated via a partition equilibrium of the polymer chains between the solvent phase at the interstitial space and the solvent in the pores of the packing material. During the process the polymer chains permanently diffuse in and out of the pores. As such the concentration gradient between the interstitial and the space in the pores is the driving force of the fractionation process. Small polymer chains penetrate more into the pores of the column packing material than large molecules. Consequently, large polymers elute faster from the column than small chains.

The retention volume V_R for a sample in SEC can be expressed by the adduct of the volume in the interstitial space V_I and the internal pore volume V_P .

$$V_R = V_I + K_{SEC} V_P \quad (2.4)$$

The ratio of the average sample concentration inside and outside the pores of the

column packing material is expressed by the distribution coefficient K_{SEC} . In SEC, the enthalpic interaction between the polymer chains and the column packing material is minimized by employing an inert column packing and carefully choosing the mobile phase. Thus, under ideal conditions the enthalpic term of the Gibb's free energy can be neglected.

$$K_{\text{SEC}} = \exp\left(-\frac{\Delta G_{\text{SEC}}^0}{RT}\right) \cong \exp\left(\frac{\Delta S_{\text{SEC}}^0}{R}\right) \quad (2.5)$$

For a correct interpretation of a SEC experiment the 'local polydispersity' should be taken into account. Axial dispersion during the chromatographic process causes band broadening. Further, local dispersity can be observed in the analysis of complex polymer structures, for instance when the same retention volume is obtained for branched and star polymers although they vary in size.^[195] In this context it should be noted that the SEC separation depends on the molecular size in solution and not on the exact molar masses. A more accurate definition for size-exclusion chromatography is that SEC separates according to the hydrodynamic volume of a polymer chain rather than its actual chain length.^[195,198]

Beside the separation setup including the column packing material, an SEC system requires devices which can detect the eluting solvent containing the polymer sample. Detectors utilized for SEC include physical and chemical detectors. Chemical detectors involve detection via mass spectrometry, Fourier transform infrared spectroscopy, and nuclear magnetic resonance spectroscopy and involve in general cost-intensive setups. Physical detectors include concentration detectors such as the differential refractometers and UV/Vis detectors as well as light-scattering detectors and viscometric detection. A conventional SEC setup is typically equipped with a differential refractometer and a UV/Vis detector.

Calibration

The conventional SEC is a relative method which makes calibration of the setup essential for the determination of the desired values such as the average molar masses and the molar mass distribution of a polymeric sample. For a calibration a series of polymer standards such as polystyrene and poly(methyl methacrylate) with low polydispersity and known molar masses are measured with the specific setup. The calibration curve is subsequently established via a polynomial fit of the obtained elution time versus $\log M$ relation. The calibration can then be applied for analyzing the same or very similar polymer structures. However, when polymers with other structures are analyzed the obtained molar masses and molar mass distribution are no longer exact values.

With the Mark Houwink Kuhn Sakurada calibration, *i.e.*, the universal calibration, the standard calibration can be extended. An empirical relationship of the intrinsic viscosity $[\eta]$ with the molar mass of a polymer can be expressed by the Mark-Houwink equation.

$$[\eta] = KM^\alpha \quad (2.6)$$

K and α are constants specific for a polymer type, solvent and temperature. For conventional SEC, to which no viscometer is attached, the molar masses of a polymer structure can be calculated via the equation:

$$K_1M_1^{1+\alpha_1} = K_2M_2^{1+\alpha_2} \quad (2.7)$$

provided that the Mark-Houwink constants of the polymer are established values.^[199,200] This method can also be applied on the complete values of the calibration curve and the method is then denoted as the universal calibration procedure. The Mark-Houwink parameters of the polymer, which should be analyzed, are employed on the standard calibration giving a new calibration curve. Based on this calibration curve the molar masses and the polydispersity of the specific polymer can be identified.^[201] For more complex polymer structures, such as comb, block or multi-block structures with varying block ratios as well as polymers built up from new monomers the Mark-Houwink parameters are typically unavailable. If accurate values for these structures are required, setups with further detectors are utilized.

SEC with Triple Detection

An SEC system equipped with differential refractometry, differential viscometry and right-angle light scattering detectors is known by the term SEC³.^[202,203] With this system the molar mass of unknown polymer structures is obtained. To understand how these detectors work in synergism, a short outline of the methods of each detector is provided. The *differential refractometer* is a concentration-sensitive detector. A typical refractometer operates in the deflection mode. The light beam passes through the flow cell – possessing a sample and a reference side – is reflected by a mirror and again passing the flow cell, before being detected by a photosensor. The photosensor detects a signal, when the sample and the reference side have different refractive indices. The concentration of a polymer sample in the eluent correlates with the refractive indices of the solution n , of the polymer sample n_p and the pure solvent n_0 in the following form.

$$c \propto \frac{n - n_0}{n_p - n_0} \quad (2.8)$$

The signal intensity does not only depend on the solvent concentration, but also depends on the nature and the chemical composition of the analyzed polymer sample. The dependency is described by the refractive index increment $\delta n/\delta c$.

The *differential viscometric detector* measures the differential pressure ΔP , resulting from two flow systems, one with pure solvent and one with the solution containing the polymer sample. The viscosity can be determined based on the proportionality to the differential pressure given by the Hagen-Poiseuille equation

$$\Delta P = \frac{8L\eta Q}{\pi r^4} \quad (2.9)$$

with L , r and Q being the length, the radius and the volumetric flow rate of the tube, respectively.

A more important quantity is the intrinsic viscosity $[\eta]$, which is the degree for the hydrodynamic effective volume of the polymer sample in infinite dilution.

$$[\eta] = \lim_{c \rightarrow \infty} \left(\frac{\eta_{sp}}{c} \right); \eta_{sp} = \frac{\eta}{\eta_0} - 1 \quad (2.10)$$

For a first approximation, the Solomon and Situa equation can be employed:

$$[\eta] = \frac{\sqrt{2[\eta_{sp} - \ln \eta_{rel}]}}{c} \quad (2.11)$$

The intrinsic viscosity $[\eta]$ is then applied for instance for the determination of the Mark-Houwink parameters, see Section 2.5.2.

In a *light-scattering setup* the excess Rayleigh ratio at a specific angle $R(\theta)$ is measured, by detecting the amount of light scattered by the solution containing the polymer sample and comparing the amount with the pure solvent.

$$R(\theta) = \frac{I_\theta r^2}{I_0} \quad (2.12)$$

I_θ represents the corrected scattered intensity, I_0 the incident emitted light by the light source and r is the distance of the flow cell to the detector. The correlation between the excess Rayleigh ratio and the weight-average molar mass M_w is given by the Rayleigh-Gans-Debye approximation

$$\frac{K^* c}{R(\theta)} = \frac{1}{P(\theta)} \left(\frac{1}{M_w} + 2A_2 c + 3A_3 c^2 + \dots \right) \quad (2.13)$$

with

$$K^* = \frac{4\pi^2 n_0^2 (\delta n/\delta c)^2}{\lambda_0^4 N_A} \quad (2.14)$$

in which n_0 represents the refractive index of the pure eluent, c the polymer concentration, λ_0 the wavelength of the incident light beam, $P(\theta)$ a form factor, which describes the intramolecular interference, and the $\delta n/\delta c$ the specific refractive index increment. Consequently, the absolute M_w for each elution volume can be determined by equation (1.13) due to the direct proportionality of the Rayleigh ratio with the product of the molar mass and the concentration of the solution.^[204]

Analyzing a polymer with a setup of the three detectors in a sequence features the possibility to obtain the Mark-Houwink parameters and the absolute average molar masses of an unknown or complex polymer sample. However, not only the size of complex polymer structures is of interest. In many cases also the chemical composition is a matter of investigations.

2.5.3. Liquid Chromatography at Critical Conditions (LCCC)

Beside size-exclusion chromatography, further chromatography techniques for the separation of polymer structures are established. Figure 2.1 visualizes the differentiation of the three modes of chromatography, which can be applied for the separation of polymeric materials.^[205,206]

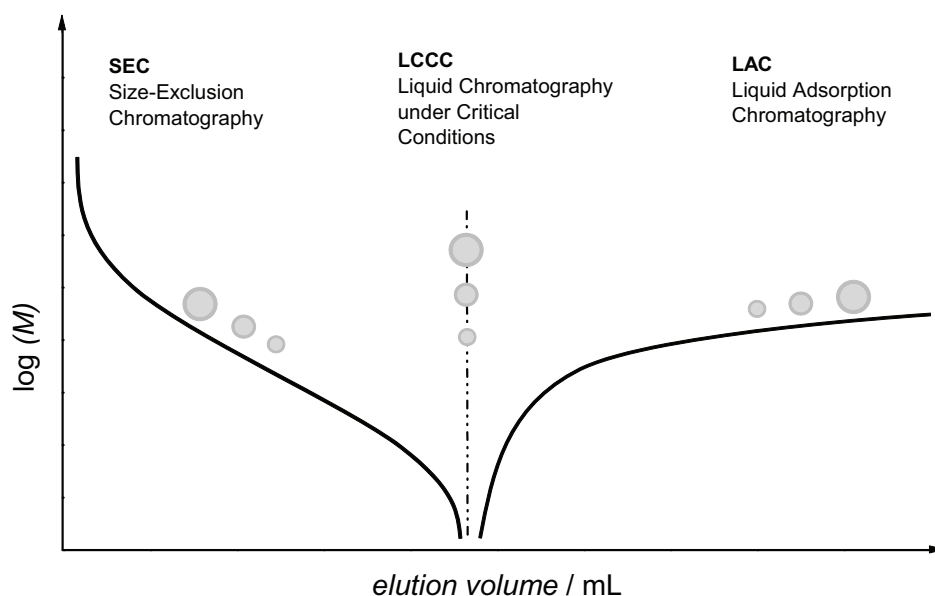


Figure 2.1. Different modes utilized in the separation of polymer structures.

The elution volume is plotted in dependency of the molar mass for the different modes. In the SEC mode, as already mentioned above, polymer samples with high

molar masses elute first, while small molecules elute later. In the adsorption mode the polymer samples elute in the opposite order – first samples containing small molecules elute and with higher elution volume the polymer samples with high molar masses elute. In the critical condition mode, the polymer samples of the same structure, yet with different molar masses, elute at the same elution volume. With liquid chromatography under critical conditions, a polymer sample can be separated according to its chemical heterogeneity, *e.g.*, the composition and end-functionality of the polymer chains, independent of the size of the polymer structures.

This special method – liquid chromatography at critical conditions (LCCC) or alternatively named LC at the exclusion adsorption point – was established by Belenky *et al.*,^[207] who investigated narrow dispersed polystyrenes of different molar masses with thin layer chromatography. Later Pasch and colleagues published a detailed description of the theory as well as the experimental approaches of the critical conditions mode.^[208]

Critical conditions for a polymer are established when the entropic and the enthalpic contribution to the retention volume compensate (see equation in 2.3). Consequently, the critical behavior of a polymer depends on a variety of conditions – the mobile phase composition, the temperature, and the stationary phase.^[209] Commonly, the critical conditions of a polymer are adjusted by varying the composition of a mixture of two solvents, a good and a poor solvent for the specific polymer sample. Further, the eluent strength has to be adjusted to the column packing material.^[191] Alternatively to varying the solvent composition, LCCC can also be adjusted by alternating the temperature.^[210] It should be noted that the LCCC method is a very sensitive method. Small variation in solvent composition or temperature can readily change the elution pattern. The LCCC method has been applied for the separation of numerous complex polymer samples. Examples include block and graft polymers, polymer blends, functional polymers, linear and cyclic polymers.^[211–213]

A typical separation process with LCCC is explained on block copolymers. For the separation of a block copolymer containing block A and block B, the critical conditions of polymer A are established. While polymer A elutes at the critical point and thus becomes ‘chromatographically invisible’, polymer B elutes either in the SEC modus or in the adsorption modus, depending on the conditions. Secondly, the critical conditions are evaluated for the polymer B and thus the retention only depends on the block length of polymer A. Consequently, homopolymer residues can be detected. Furthermore, the chain length of the block, which elutes not under CC, can be evaluated. The method can subsequently be applied as the first dimension in two-dimensional chromatography (2D LC). With this setup, the fractions of the first dimension can further be separated with the second dimension, which is commonly a SEC device. More information to 2D-LC is provided in the Section 2.5.5.

2.5.4. Gradient Elution Liquid Chromatography (GELC)

Gradient elution liquid chromatography on macromolecules was first reported by Porath, who separated proteins by zone precipitation.^[214] Synthetic polymers were investigated later with the same system by Ingagaki and Belenky.^[215,216] Commonly, the separation procedure starts with the injection of the sample into a setup, for which the conditions are established in the way that adsorption of the sample onto the stationary phase is highly favored. Subsequently, the solvent composition is changed to increase the solvent content, which promotes the elution of the sample. The sample finally elutes after desorption from the stationary phase. Consequently, the sample is separated dependent on its affinity towards the column packing material. In early reports this setup is also termed precipitation-dissolution process. It should be noted that no complete sample recovery was observed for some GELC systems, which implies that part of the sample was adsorbed on the stationary phase.^[217]

2.5.5. LCCC/GELC Coupled to SEC

Combining LC systems such as LCCC and GELC with SEC to two dimensional chromatography yields information about the chemical composition in the first dimension and additionally the molar masses of the separated compounds in the second dimension. The complete setup is shown in Figure 2.2.

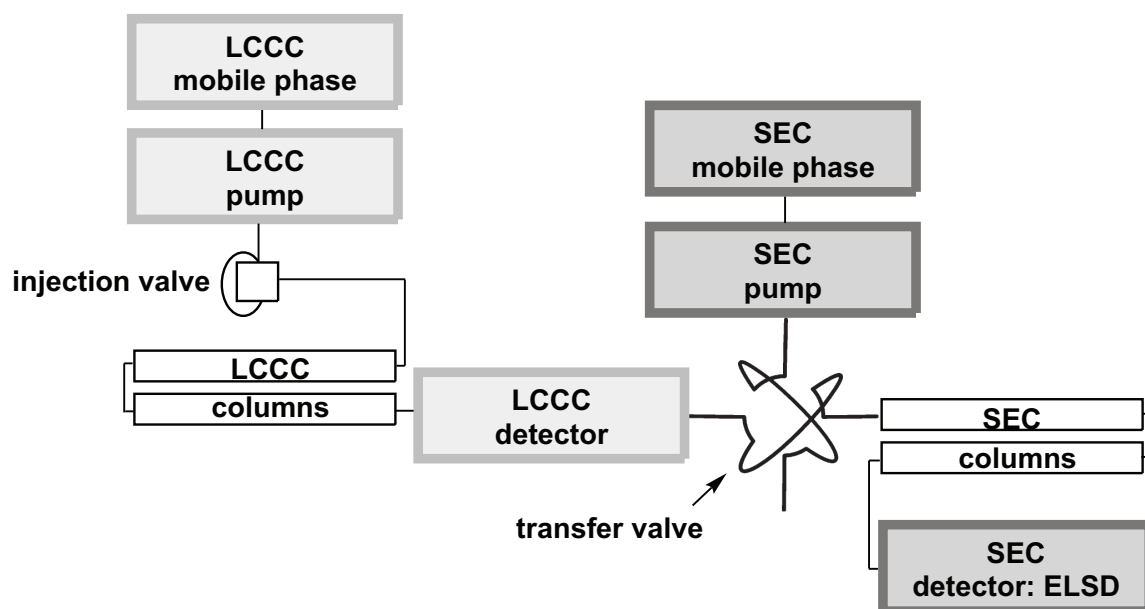


Figure 2.2. Setup of two dimensional chromatography with LCCC in the first dimension and SEC in the second dimension.

In early stages the system was used in off-line mode. The fractions were collected with a fraction collector or by hand and subsequently injected in the second dimension. This revealed to be very time-consuming. A fully automated system was devel-

oped by Kilz.^[218,219] The two dimensions are connected via a switching/transfer valve, equipped with two injection valves. The polymer sample is injected into the LCCC system, passing through the columns and a detector. Slices of the eluent from the LCCC system are subsequently transferred via the switching valve into the SEC system, where they pass through the SEC columns and are detected. The flow rate has to be adjusted properly to ensure a complete transfer of the analyte into the second dimension. For obtaining high resolution, very low flow rates in the first dimension and very fast flowrates in the second dimension are commonly selected.

As a final detector no detector that is sensitive to solvent variation should be chosen. An evaporative light-scattering detector (ELSD) is favored for such a setup. The detector only detects analytes which are less volatile than the solvent. In the detector an aerosol is formed by nebulizing the eluting solvent from the chromatographic setup. In a heated drift tube the solvent is evaporated and the analyte is subsequently detected in an optical cell via light-scattering. Due to the evaporation of the solvent, the detector can handle gradient elution chromatography as well as 2D LC.

A wide variety of examples exists, in which this 2D LC system was successfully applied.^[193,205,218,220–225] In Chapter 5 and 6 more examples are provided.

2.5.6. Liquid Chromatography Coupled to Chemical Detectors

Variable chemical detectors can be coupled to liquid chromatography systems. The detection of chemical compositions via spectroscopic and spectrometric techniques will be discussed below.

Liquid Chromatography Coupled to Mass Spectrometry

Mass detectors for macromolecules include matrix-assisted laser desorption/ionization time-of-flight (MALDI-ToF), electrospray ionization (ESI) and inductively coupled plasma (ICP) mass spectrometry. ICP is preferably used for the detection of environmental and biological molecules, whereas MALDI-ToF and ESI-MS are employed for the characterization of synthetic polymers. These two methods – MALDI-ToF-MS and ESI-MS – allow the analysis of the large molecules via ionization with no or only little fragmentation occurring.

LC/ESI-MS

Electrospray ionization mass spectrometry (ESI-MS) was established by Dole as well as Fenn and coworkers.^[226–230] An ESI mass spectrometer basically consists of an ion source, a mass analyzer such as a quadrupole-ion trap or a time-of-flight analyzer and a detector.

In the ion-source setup a potential between the electrospray capillary tip, at which the eluent emerges, and the counterelectrode is established. When an electric field is applied, charges in the eluent are drawn to the counterelectrode. At the onset potential, which highly depends on the solvent and the radius of the capillary as well as the distance between the tip and the counterelectrode, charged droplets leave the capillary tip in the direction of the counterelectrode. The solvent in the droplet is evaporated, enhanced by a coaxial flow of nitrogen or a heated transfer capillary, generating smaller droplets. When the repulsive Coulomb forces in the droplet exceed the surface tension, the droplet splits into even smaller droplets. This process is repeated until minute charged droplets are formed, which contain only several molecules in the solvent enclosure. Eventually gas-phase ions are generated from the small charged droplets. For this mechanism two models are proposed, the *charged residue model* (CRM) and the *ion evaporation model* (IEM).^[226,231,232] The CRM model is based on the assumption that the charge of the analyte-ion originates from the droplet surface, whereas the IEM model predicts a process in which ion emission from the droplets occurs. However, for large molecules such as macromolecules the analyte-ions are assumed to be generated according to CRM.^[233]

The generated ions are transferred through a small opening in the counter electrode into the mass analyzer. The mass analyzer filters the ions according to their size and charging envelope, the m/z values. The choice of the mass analyzer depends on the resolution and accuracy required. Existing systems include quadrupole mass filters, quadrupole ion traps, time-of-flight mass analyzers as well as orbitrap and Fourier transform ion cyclotron resonance analyzers. For example, in a time-of-flight analyzer the ions are accelerated in an electric field and detected according to the time they require to pass a certain distance. A quadrupole mass filter consists of four rod-like electrodes, on which different voltages are applied and overlaid by a radio frequency field. Depending on the applied voltage the ions follow stable or unstable trajectories. The ions on stable trajectories eventually reach the detector. Further information to mass analyzers can be found for example in reference^[234].

With ESI-MS not only single charged, yet also multiple charged ions occur in the final spectrum, depending on the nature of the analyte. Since the single charged and the multiple charged distributions are superimposed upon each other, a quite complex spectrum maybe obtained. Coupling ESI-MS to SEC separates the charged envelopes and facilitates the assignment of the peaks.

First attempts to couple liquid chromatography to ESI-MS was reported in 1993 and 1995 by Prokai and Simonsick, respectively.^[235,236] They coupled an SEC setup to ESI-MS to analyze oligomers and acrylic macromonomers. Other liquid chromatography modes coupled to ESI-MS were investigated Nielen and Buijtenhuis.^[237,238] For the setup, the solvent and the flow rate must be adjusted to the mass spectrometer. Thus,

in general, a eluent splitter is introduced, highly reducing the flow rate for the ESI-MS instrument. Further a source of alkali metal ions, which enhance the ionization, can be provided with post-column addition. Size-exclusion chromatography coupled to ESI-MS is often utilized for the end-group determination of a synthesized polymer.

By a combination of SEC with ESI-MS as well as refractive index detection, accurate molar mass distributions (*MMD*'s) can be obtained when employing a specific method invented by Gründling *et al.* For processing the data from the two detectors, a computational algorithm based on the maximum entropy principle is utilized, yielding in accurate *MMD*'s, corrected for chromatographic band broadening. The procedure can be applied to various polymers without the necessity of an external calibration.^[239,240]

An example of liquid chromatography coupled to ESI-MS was recently reported by Falkenhagen.^[241] In here, ultra performance liquid chromatography was coupled to an ESI-ToF instrument to characterize poly(ethylene oxide) (pEO) and poly(propylene oxides). In Figure 2.3, the determination of the critical conditions of pEO via mass detection is displayed. The advantage is that only one polymer sample is required for determining the critical conditions and no polymer standards are needed.

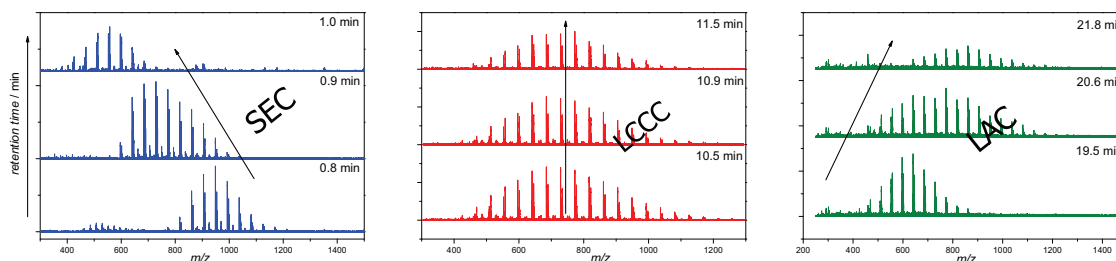


Figure 2.3. SEC (left), LCCC (center), and LAC (right) mode of one poly(ethylene oxide) sample. Adapted with permission from Falkenhagen, J. and Weidner, S. *Analytical Chemistry*.^[241] Copyright (2009) American Chemical Society.

Examples for SEC coupled to ESI-MS can be found in the Chapters 4 and 6.

LC/MALDI-ToF

Only a few years after the invention of the laser, first experiments on the generation of ions via laser radiation were performed. The spectra of organic molecules were recorded with a ToF mass analyzer.^[242,243] The principle of matrix-assisted laser desorption/ionization (MALDI) was later reported in 1984 by Karas *et al.*^[244,245] While Karas investigated biopolymers such as proteins, Tanaka was first reporting synthetic polymer mass spectra.^[246] The core principle of MALDI is the employment of a matrix surrounding the polymer sample, consisting of small molecules, which can readily absorb at the energy of the laser. In a MALDI setup, the matrix, which is utilized

in high excess compared to the analyte, transfers the energy from the laser to the analyte in a controlled manner. Subsequently, the analyte is desorbed and ionized into the gas phase. It is assumed that the ionization of the analyte takes place due to collisions with charge carriers and the excited matrix molecules. Basically the matrix has the following functions: Enhancing the desorption of the non-volatile analyte from the surface and thus increasing the ion yield as well as preventing the polymer from decomposing due to too high energy absorption and inhibiting cluster formation of the analyte. Thus, the matrix selection highly depends on the polymer sample which is analyzed. Many structures have been investigated as potential matrices for MALDI and have been collected for instance in a review written by Nielen.^[247]

Typically MALDI is conducted in combination with a ToF mass analyzer. They are preferably used in this combination due to the possibility of recording all ions from one ionization event and offering a higher sensitivity and greater mass range than scanning technologies.^[248]

With MALDI-ToF multiple charging is commonly not registered in the obtained spectra, which facilitates the ion-assignment. The analysis of broad polymer structures or structures with many different end-group functionalities, however, lacks in resolution of the individual signals. Further, the weight-average molar mass of polymers with high polydispersity, determined with MALDI often differs from the SEC results.

The analysis of polymer samples with high *PDI*s benefits from coupling size-exclusion chromatography to MALDI-ToF. The fractionation results in ‘eluent slices’ containing polymer fractions of low polydispersity, which enhances the resolution of the MALDI spectra, giving M_w values in good agreement to the SEC measurements.^[249,250] Coupling other liquid chromatography techniques such as LCCC to MALDI-ToF, is offering the possibility to identify polymers with different end-functionalities and separate and detect polymer blends.

LC coupled to MALDI-ToF proceeds usually in a continuous off-line mode. The eluent is sprayed onto a moving target, which is subsequently introduced into the MALDI-ToF instrument. Initially, the target was precoated with the appropriate matrix.^[252] With the new setup depicted in Figure 2.4, the matrix solution can be added simultaneously.^[251] With the electrospray deposition (ESD) interface the eluent is sprayed onto the target from the capillary to which a high voltage is applied. Heated gas which enters through a series of holes enhances the evaporation of the solvent. Adding a T-piece to the eluent line enables the continuous addition of matrix solution employing a microsyringe pump.

Liquid chromatography coupled to MALDI-ToF is applied for identifying polymer structures in the Chapter 6.

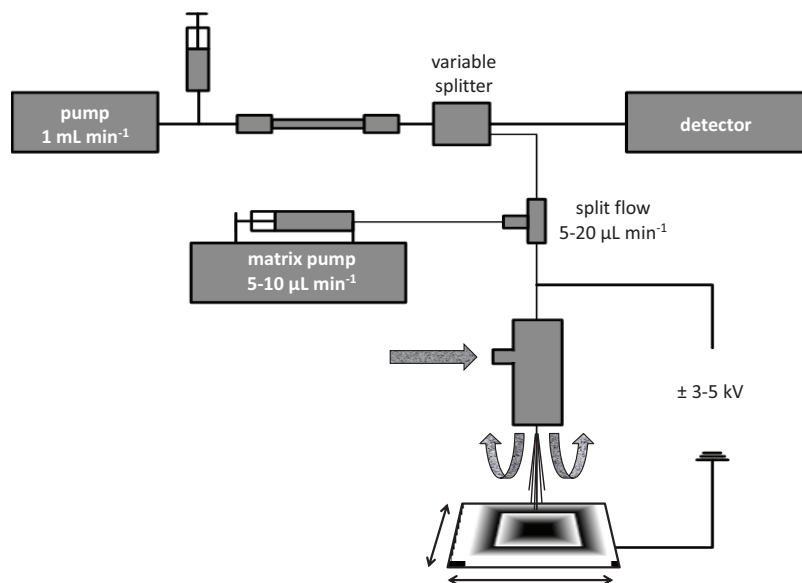


Figure 2.4. Setup of the electrospray deposition interface used for continuous transfer of the chromatographic samples onto the MALDI target. Adapted from Weidner, S. M. and Falkenhagen, J. *Analytical Chemistry*.^[251]

Liquid Chromatography Coupled to Fourier Transform Infrared Spectroscopy

Liquid chromatography coupled to Fourier transform infrared spectroscopy (LC/FT-IR) can be performed in an on-line and an off-line approach. In the off-line mode, the solvent deriving from the LC is removed before analyzing the sample in the FT-IR instrument; in the on-line modus, the eluent of the LC is directed through a FT-IR flow-cell.

In the off-line approach the eluent of the LC system is sprayed on an interface and the solvent is evaporated instantaneously. The evaporation is carried out with a heated nebulizer in combination with a nebulizer gas. Thus, only the analyte is deposited on the target plate. The interface or target is usually an infrared-transparent substrate such as ZnSe, Ge or CaF₂. Subsequently, the circle plate – serving as target – is positioned in an FT-IR device for detection.^[253] Advantages of the off-line setup are the possibility to increase the scanning time to obtain a better signal-to-noise ratio as well as the absence of absorbing bands from the eluent, which can interfere with the signals of the analyte. Thus, for qualitative analysis the off-line mode appears to be very attractive, quantitative analysis of individual components in the analyte, however, can be rather challenging. During the depositing process of the analyte to the plate, crystallization or oxidation of the analyte can occur.^[254,255]

The detection mode of FT-IR coupled on-line to LC can be via reflection, transmission or attenuated total reflection.^[256–258] Problems concerning the on-line setup up to now are the background absorption of the eluent utilized in the LC system and

the low sensitivity due to the high eluent to analyte ratio. Preferable eluents, which exhibit low IR-absorbance, are chosen for the setup. Highly chlorinated solvents show only low amount of absorbing bands.^[259-261] Another approach is the employment of expensive deuterated solvents.^[262] These solvent limitations can be circumvented with the aid of specialized mathematical solvent suppression techniques. This coupled measuring technique is being currently developed, basic ideas and first results have been reported by Beskers *et al.*^[263]

3

Materials and Characterization Techniques

3.1. Materials

3.1.1. Chemicals Used in Chapter 4

Styrene (99% extra pure, stabilized, Acros Organics) was freed from inhibitor by percolating through a column of basic alumina prior to use. Isobornyl acrylate was purified by vacuum distillation. 2,2'-Azobis(isobutyronitrile) (98%, Sigma Aldrich) was recrystallized twice from ethanol prior to use. 2[(Dodecylsulfanyl) carbonothioyl]-sulfanyl propanoic acid (DoPAT, Orica Pty Ltd., Melbourne, Australia), propanediol (Sigma Aldrich), ethylene glycol (Sigma Aldrich), 4-dimethylamino pyridine (DMAP, ABCR), *N,N'*-dicyclohexylcarbodiimid (DCC, Alfa Aesar), 2,2'-azobis(2,4-dimethylvaleronitrile) (V65, Wako), 2,2'-azobis(4-methoxy-2,4-dimethyl valeronitrile) (V70, Wako), tetrahydrofuran (multisolv, 250 ppm BHT, Scharlau), tetrahydrofuran (inhibitor-free, Bernd Kraft), triphenylphosphine (PPh₃, Merck), dimethyl sulfide (Merck), triethylamine (min. 99% Sigma Aldrich) and methanol (chromasolv, Sigma Aldrich) were used as received.

3.1.2. Chemicals Used in Chapter 5

Styrene (99% extra pure, stabilized, Acros Organics), methyl methacrylate (99%, Sigma Aldrich), methyl acrylate (99%, Acros Organics), and isobornyl acrylate (tech-

nical grade, Sigma Aldrich) were freed from inhibitor by percolating through a column of basic alumina prior to use. The RAFT agents dibenzyl trithiocarbonate (DBTC) and 2-(2-cyanopropyl) dithiobenzoate (CPDB) were synthesized according to literature procedures and their structures were confirmed by $^1\text{H-NMR}$ spectroscopy.^[264–266] 2,2'-Azobis(isobutyronitrile) (98%, Sigma Aldrich) was recrystallized twice from ethanol prior to use. ϵ -Caprolactone was distilled from CaH_2 and kept over molecular sieve. 1,5,7-triazabicyclo[4.4.0]dec-5-ene (TBD, Sigma Aldrich), toluene (extra dry, water < 30 ppm, Acros Organics), *t*-butanol (Merck), triphenylphosphine (PPh_3 , Merck), acetic acid glacial (rotipuran, 100% p.a., Roth) benzoic acid (99,5%, Sigma Aldrich), hydrochloric acid (37%, Roth), *trans,trans*-2,4-hexadien-ol (99%, stabilized, Acros Organics), trifluoroacetic acid (HPLC grade, Fisher Scientific), sodium iodide (puriss. p.a., Fluka), tetrahydrofuran (multisolvant, 250 ppm BHT, Scharlau), tetrahydrofuran (inhibitor-free, Bernd Kraft) and methanol (chromasolv, Sigma Aldrich) were used as received. Further, D,L-lactide (LA, Purac, stored under argon at 4 °C), 4,4-dimethylaminopyridine (DMAP, 99%, Acros Organics), styrylmercaptan (1-phenylethyl mercaptan 98%, Alfa Aesar), styrene (Reagent Plus, >99%, Aldrich) and ethylenediamine (99% GC, Aldrich), tetrahydrofuran (THF, Fisher) and *N,N'*-Dimethylformamide (DMF, Fisher Scientific, 99,9%) were used as received without further purification.

3.1.3. Chemicals Used in Chapter 6

Styrene (99% extra pure, stabilized, Acros Organics) was purified by percolating through a column of basic alumina prior to use. The 4-arm (non rate-retardant) RAFT agent 1,2,4,5-tetrakis(phenylthioacetylthiomethyl)benzene (see Scheme 6.2 and Scheme 6.3) was synthesized according to a literature procedure with its purity being confirmed by $^1\text{H-NMR}$ spectroscopy.^[267] 2,2'-Azobis(isobutyronitrile) (98%, Sigma Aldrich) was recrystallized twice from ethanol prior to use. ϵ -Caprolactone was distilled from CaH_2 and kept over molecular sieves. 1,5,7-triazabicyclo[4.4.0]dec-5-ene (TBD, Sigma Aldrich), toluene (extra dry, water < 30 ppm, Acros Organics), triphenylphosphine (PPh_3 , Merck), glacial acetic acid (Rotipuran, 100% p.a., Roth), benzoic acid (99,5%, Sigma Aldrich), hydrochloric acid (37%, Roth), sodium iodide (puriss. p.a., Fluka), tetrahydrofuran (multisolvant, 250 ppm BHT, Scharlau), carbon disulfide (Aldrich), benzylchloride (Alfa Aesar), α,α' -dibromo-*p*-xylene (Aldrich), 2-butanol (Fluka) and methanol (chromasolv, Sigma Aldrich) were used as received.

3.1.4. Chemicals Used in Chapter 7

Styrene (99% extra pure, stabilized, Acros Organics) was purified by percolating through a column of basic alumina. 2,2'-Azobis(isobutyronitrile) (98%, Sigma Aldrich) was recrystallized twice from ethanol prior to use. Triphenylphosphine (PPh₃, Merck), tetrahydrofuran (multisolvant, 250 ppm BHT, Scharlau), tetrahydrofuran (inhibitor-free, Bernd Kraft), 2,2,4-trimethylhexane-1,6-diisocyanate (TMDI, Evonik), poly(tetrahydrofuran) ($M_n \sim 1000 \text{ g mol}^{-1}$, Sigma Aldrich), 2[(dodecylsulfanyl) carbonothioyl]-sulfanyl propanoic acid (DoPAT, Orica Pty Ltd., Melbourne, Australia), di-*n*-butyltin-dilaurate (DBTDL, Alfa Aesar), 4-dimethylamino pyridine (DMAP, ABCR), *N,N'*-dicyclohexylcarbodiimid (DCC, Alfa Aesar), 1,3-propanediol (Sigma Aldrich) and *N,N'*-dimethylacetamide (DMAc, Acros Organics) were used as received.

3.2. Size-Exclusion Chromatography

For the determination of molar mass distributions (MMD) an SEC system (Polymer Laboratories PL-GPC 50 Plus) comprising an auto injector, a guard column (PLgel Mixed C, 50 × 7.5 mm) followed by three linear columns (PLgel Mixed C, 300 × 7.5 mm, 5 μm bead-size) and a differential refractive index detector was employed. THF was used with a flow rate of 1 mL min⁻¹, the column temperature was set to 30 °C. The SEC system was calibrated using narrow polystyrene standards ranging from 160 to 6 · 10⁶ g mol⁻¹ (Polymer Standard Service GmbH, Mainz). The resulting molar mass distributions were reassessed by universal calibration using Mark-Houwink parameters for pCL ($K = 13.95 \times 10^5 \text{ dL g}^{-1}$ and $\alpha = 0.786$)^[268], piBoA ($K = 5.00 \cdot 10^{-5} \text{ dL g}^{-1}$, $\alpha = 0.745$)^[269] pMA ($K = 19.5 \cdot 10^5 \text{ dL g}^{-1}$ and $\alpha = 0.66$)^[270] pBA ($K = 12.2 \cdot 10^{-5} \text{ dL g}^{-1}$, $\alpha = 0.70$)^[271] pMMA ($K = 7.56 \cdot 10^{-5} \text{ dL g}^{-1}$, $\alpha = 0.731$)^[272] and for pS ($K = 14.1 \cdot 10^5 \text{ dL g}^{-1}$ and $\alpha = 0.70$)^[273] For (star) block copolymers pS-*b*-pCl and the multi-block copolymer pS-*b*-pTHF the Mark-Houwink parameters for polystyrene were used. For the other block copolymers always the Mark-Houwink parameters of the first block were employed.

3.2.1. Size-Exclusion Chromatography with Triple Detection

The triple-detection chromatographic setup used for the determination of the exact weight-average molar mass of the multi-block copolymers consisted of a modular system (Polymer Standard Service, PSS, Mainz/Agilent 1200 series) incorporating an ETA2010 viscometer (WGE Dr. Bures) and a multi-angle light-scattering unit (PSS SLD7000/BI-MwA, Brookhaven Instruments). Sample separation is achieved via two linear columns provided by PSS (SDVLux-1000 Å and 105 Å, 5 μm) with THF as

the eluent at 35 °C with a flow rate of 1 mL min⁻¹. The exact M_w is determined measuring light scattering at an angle of 90° and utilizing the method ‘factor times concentration’ for data analysis. The factor for the concentration detector was determined by measuring a narrow dispersed polystyrene standard of 120 000 g mol⁻¹ of a known concentration.

3.2.2. Size-Exclusion Chromatography Coupled to a Fraction Collector

For fractionation of the samples an SEC system equipped with a high speed column (SDV, linear M) was connected to a fraction collector (Super Fraction Collector CHF122SC, Advantec, Japan). The concentration of the samples was 10 g L⁻¹. At a flow rate of 1 mL min⁻¹ fractions were collected every 20 s. Fractionation was repeated 10 times. The fractions from 6.65 - 9.95 mL were combined and dried for further analysis.

3.3. Liquid Chromatography at Critical Conditions Coupled to Size-Exclusion Chromatography

Liquid Chromatography at Critical Conditions (LCCC) and Concomitant Gradient Liquid Elution Chromatography (GELC): The measurements were carried out on a Hewlett Packard (HP1090) HPLC system using a diode array UV detector and an evaporative light scattering detector (ELSD) (SEDEX 45, ERC). The flow rate was 0.5 mL min⁻¹; 25 µL of close to 2 wt-% polymer solutions were injected. For the critical conditions of polystyrene a reversed phase system was employed: YMC-ODSA column (250 × 3 mm inner diameter), 300 Å pore size, 5 µm average particle size. The eluent was a mixture of tetrahydrofuran and water. The critical solvent compositions contain 88.4 % (v/v) THF for poly(styrene). Premixing of the mobile phase by weight is necessary for a constant and exact composition. 0.1 vol-% acetic acid was added to the system. For the measurements at the critical conditions of poly(ε-caprolactone) an alternative reversed phase system was employed: PLRP-S column (250 × 4.6 mm), 100 Å pore size, 5 µm average particle size. The starting eluent composition contained 30 % (v/v) of THF and 70 % (v/v) of Methanol. The gradient ended in a 80/20 % (v/v) mixture of THF and MeOH. The samples were dissolved in 40 % THF / 60% MeOH. The critical conditions of pMA were conducted on a Discovery Cyano-column (250 × 4.6 mm, 300 Å pore size, 5 µm average particle size). The solvent composition consisted of 62 % (v/v) THF and 38 % (v/v) *n*-Hexane.

Alternatively, in case of the analysis of pS-*b*-pLA, the LCCC experiments were performed on a Varian PL-GPC 120 apparatus, which was composed of an Agilent

1100 series pump, a degasser and a RI detector. The injection loop, the columns, and the RI detector were in the same thermostated oven. In the pS case, the following columns were used: Macherey and Nagel 250 mm \times 4.6 mm Nucleodur C18 Gravity, pore diameter 110 Å, particle size 3 μm and Macherey and Nagel 250 mm \times 4.6 mm Nucleodur C18 Gravity (reverse phase), pore diameter 110 Å, particle size 5 μm . The eluent was dimethylformamide, filtered over a 0.2 μm Nylon Alltech membrane. The samples were dissolved in dimethylformamide (DMF) at 0.25 wt% before being filtered through a 0.2 μm Nylon Macherey and Nagel filter. The flow rate was fixed at 0.8 mL min⁻¹ and the oven temperature was 80 °C. In the pLA case, the following columns were used: VWR 250 \times 4.6 mm Nucleosil, pore diameter 300 Å, particle size 7 μm and Macherey and Nagel 250 \times 4.6 mm Nucleosil, pore diameter 100 Å, particle size 7 μm . The eluent was a mixture of acetone (62.7 wt%) and n-hexane (37.3 wt%) both filtered through a 0.2 μm PTFE Alltech membrane. The pLA critical conditions have here been determined experimentally by testing different ratios of acetone/hexane. The samples were dissolved in the same acetone / n-hexane mixture as the eluent at 0.25 wt% before being filtered through a 0.2 μm PTFE Macherey and Nagel filter. The flow rate was fixed at 0.7 mL min⁻¹ and the oven temperature was 40 °C.

Size-Exclusion Chromatography (SEC): The SEC experiments were performed on a Hewlett Packard (HP1050) HPLC modular system, including a Mistral column oven (SunChrom). For detection an evaporative light scattering detector (ELDS) (SEDEX 45, ERC) and additionally a variable wavelength UV-detector ($\lambda = 230$ nm) were employed. The flow rate was 3.0 mL min⁻¹. One high speed column, a SDV-gel column (PSS GmbH Mainz), 5 μm average particle size (20 mm \times 50 mm) and tetrahydrofuran as mobile phase were used. 100 μL of a 1 wt-% polymer solution were injected. Calibration was performed using poly(styrene) standards (ranging from 760 to 1 10⁶ g mol⁻¹). Detection proceeds via the ELSD.

Two-dimensional Chromatography (LCCC-(GELC)-SEC): The crossover of LCCC fractions to SEC was performed by two combined electrical Rheodyne six-port switching transfer valves. While the first valve is filled with the eluent of the first dimension, the content of the second valve is analyzed in the second chromatographic system (SEC). The measurements were evaluated by using the PSS WinGPC (Unity) and PSS 2D Software. The LCCC dimension in 2D mode was operated with a flow rate of 0.02 mL min⁻¹.

3.4. Mass Spectrometry

3.4.1. Size-Exclusion Chromatography Coupled to Electrospray Ionization Mass Spectrometry

Spectra were recorded on an LXQ mass spectrometer (ThermoFisher Scientific, San Jose, CA, USA) equipped with an atmospheric pressure ionization source operating in the nebulizer assisted electrospray mode. The instrument was calibrated in the m/z range 195-1822 using a standard containing caffeine, Met-Arg-Phe-Ala acetate (MRFA) and a mixture of fluorinated phosphazenes (Ultramark 1621) (all from Aldrich). A constant spray voltage of 4.5 kV and a dimensionless sweep gas flow rate of 2 and a dimensionless sheath gas flow-rate of 12 were applied. The capillary voltage, the tube lens offset voltage and the capillary temperature were set to 60V, 110V and 275 °C respectively. The LXQ was coupled to a Series 1200 HPLC-system (Agilent, Santa Clara, CA, USA) consisting of a solvent degasser (G1322A), a binary pump (G1312A), a high-performance autosampler (G1367B), followed by a thermostat-controlled column compartment (G1316A). Separation was performed on two mixed bed size-exclusion chromatography columns (Polymer Laboratories, Mesopore 250 × 4.6 mm, particle dia. 3 μm) with pre-column (Mesopore 50 × 4.6 mm) operating at 30 °C. THF at a flow rate of 0.30 mL min⁻¹ was used as eluent. The mass spectrometer was coupled to the column in parallel to a RI-detector (G1362A with SS420x A/D) in a setup described previously.^[240] 0.27 mL min⁻¹ of the eluent were directed through the RI detector and 30 μL min⁻¹ infused into the electrospray source after post-column addition of a 100 μL solution of sodium iodide in methanol at 20 μL min⁻¹ by a micro-flow HPLC syringe pump (Teledyne ISCO, Model 100DM). 20 μL of a polymer solution with a concentration of approximately 3 mg mL⁻¹ were injected onto the HPLC system. Measurements can also be conducted via direct infusion ESI-MS. However, pre-separation via SEC provides an improved ionization due to the absence of low molar mass impurities and the slice by slice ionization of the investigated polymers.

3.4.2. Matrix-Assisted Laser Desorption/Ionization-Time of Flight Mass Spectrometry

An Autoflex III MALDI-TOF mass spectrometer (Bruker Daltonic, Germany) was employed. The system was equipped with a Smartbeam™ laser working at 356 nm with a frequency of 200 Hz. 2000 laser shots were accumulated for one spectrum. 2-[(2 E)-3-(4-*tert*-Butylphenyl)-2-methylprop-2-enylidene]malononitrile (DCTB) or dithranole (THAC) (10 mg mL⁻¹ in THF) were used as matrix. Depending on the polymer

structure, 2 μL of a silver trifluoroacetate (AgTFAc) solution ($c = 2 \text{ mg mL}^{-1}$) for the ionization of poly(styrene)s or a potassium trifluoroacetate (KTFAc) solution ($c = 5 \text{ mg mL}^{-1}$) for poly(ϵ -caprolactone)s and copolymers were added to the matrix solution. For the sample preparation, a volume of 20 μL of polymer solution was mixed with 50 μL of matrix solution; subsequently, 1 μL was deposited on the MALDI target employing an Eppendorf pipette.

Coupling of LC with MALDI-ToF MS: The electrospray deposition interface consists of a Teflon x-y table, which was adapted to the size of conventional 384 MALDI target plates. A small contact was connected to enable contact of the target plate with the ground potential. The spray capillary (stainless steel, 0.1 mm inner diameter) was fixed in a Teflon block. The distance between the target plate and the capillary could be varied from 0.5 to 3 cm. High voltage (3-5 kV) was generated by a DC power supply (FuG Elektronik GmbH, Rosenheim, Germany) and applied to the capillary. Additionally, heated gas could be applied through a series of concentric holes around the capillary to enable a better evaporation of solvents. The deposition flow could be varied from 5 to 30 $\mu\text{L min}^{-1}$ by means of an adjustable flow splitter (ASI-QuickSplit, Analytic Scientific Instruments, Richmond, CA). The matrix solution (5-10 $\mu\text{L min}^{-1}$) was added via a T-piece to the eluent line using a micro syringe pump (Harvard Apparatus, Holliston, MA). The schematic setup can be found in Figure 2.4.

3.5. Fourier Transform Infrared Spectroscopy

Infrared spectra were obtained from a Bruker Vertex 80 FT-IR/NIR spectrometer possessing a standard DTGS detector and a KBr beam splitter, a sample holder, as well as an attenuated total reflection (ATR) unit. The parameters employed for the collection of each spectrum were a resolution of 4 cm^{-1} , 128 background scans, and 64 sample scans.

3.6. Size-Exclusion Chromatography coupled to Fourier Transform Infrared Spectroscopy

For the detection of the SEC elugrams via online IR spectroscopy a modular system (Polymer Standard Service, PSS, Mainz/Agilent 1200 series) was coupled to a Vertex 70 FT-IR spectrometer (Bruker Optics, Ettlingen). A SDV semi-preparative column linear M (PSS) was utilized for the separation of the samples. A concentration of 10–15 g L^{-1} was prepared for the injected volume (100 μL) of the samples. The sample cell of the IR spectrometer was a self-designed flow-cell, based on a six reflexions

ATR unit (Gateway, Specac, Cranston, RI, USA). The eluent was THF, the flow rate 1 mL min⁻¹. IR spectra were taken every 5 seconds and 50 scans were co-added. Further mathematical solvent suppression and data treatment were performed with an in-house written MATLAB routine.^[263]

Calibration of the SEC/FT-IR

For the calibration of the SEC/FT-IR setup, blends of pS ($M_n = 3280$ g mol⁻¹) and pTHF ($M_n = 990$ g mol⁻¹) with a known concentration were injected to the SEC system. The measured integral intensities and the injected mass can be found in Table 3.1. The signals intensities at 1493 cm⁻¹ and 1110 cm⁻¹ for pS and pTHF, respectively, were used for the integration.

Table 3.1. Collation of data for the calibration of the online SEC/FT-IR measurements. The integrals of the intensities at 1493 cm⁻¹ for the calibration of pS and 1110 cm⁻¹ for the calibration of pTHF were utilized.

Polymer	Integral of Intensity / a.u.	Injected mass / mg
pS	0.01215254	1.8820
pS	0.00568553	1.0374
pS	10.00405891	0.5187
pTHF	0.05845686	2.1320
pTHF	0.02855431	1.1439
pTHF	0.01786355	0.5719

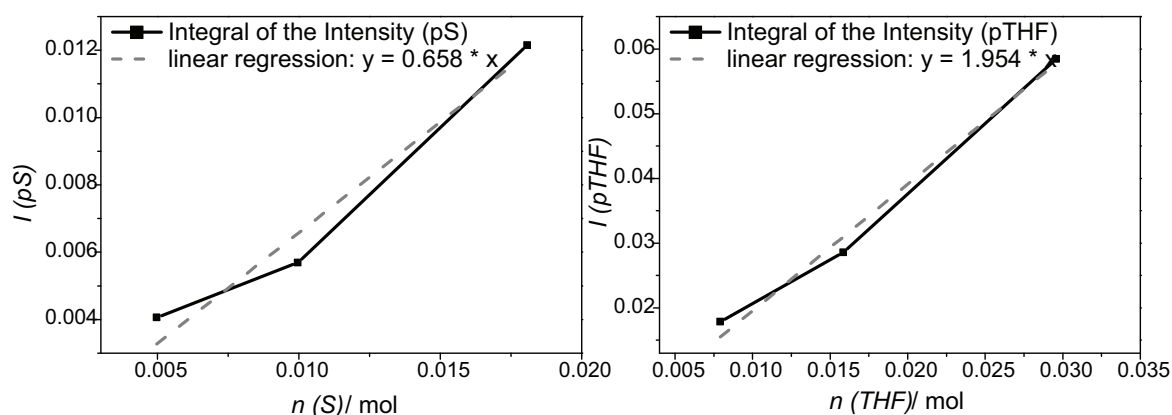


Figure 3.1. Calibration of SEC/FT-IR. Three concentrations of each homopolymer were used to obtain three signal intensities. Linear regression is applied to the values to obtain the slope.

Via the linear regression the value of the slope is obtained, which can subsequently be applied to the signals intensities of the multi-block copolymers to obtain the exact block fractions (see Chapter 7).

3.7. Nuclear Magnetic Resonance Spectroscopy

^1H -NMR spectroscopy was carried out on a Bruker AM 400 MHz as well as a Bruker AM 250 MHz spectrometer. All samples were dissolved in CDCl_3 .

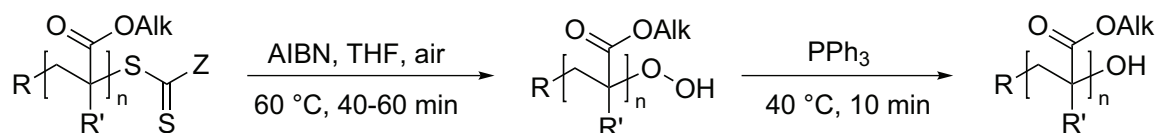
4

Switching from RAFT to Hydroxyl-terminal Polymers

4.1. Introduction

As described in the background section addressing end-group modifications of RAFT polymers, the thiocarbonyl thio end-group derived from the RAFT process is in some cases undesirable due to various causes (see Chapter 2.2). Consequently, the development of efficient transformations of the thiocarbonyl thio end-group is a matter of priority. One method, which was established in our laboratories, involves the transformation of the thiocarbonyl thio end-capped polymer into a peroxide terminal polymer, which can subsequently be reduced to a hydroxyl functional polymer. The degradation of dithiobenzoate capped poly(methyl methacrylate) in peroxide-containing tetrahydrofuran (THF) was observed based on a sample discoloration and analyzed via SEC/ESI-MS.^[274] The main product of the transformation was not the oxidized species of the thiocarbonyl thio group, namely the formation of thioesters or sulfines, yet a hydroperoxide functional polymer. The modification can be performed in a one-pot procedure under ambient conditions in THF with addition of 2,2'-azobis(isobutyronitrile) (AIBN). Subsequently, the hydroperoxide functionality at the polymer chain end is reduced with triphenylphosphine to a hydroxyl function. Scheme 4.1 depicts the general synthetic strategy on the example of RAFT based poly(acrylate)s.

4. Switching from RAFT to Hydroxyl-terminal Polymers



R' = H, Me

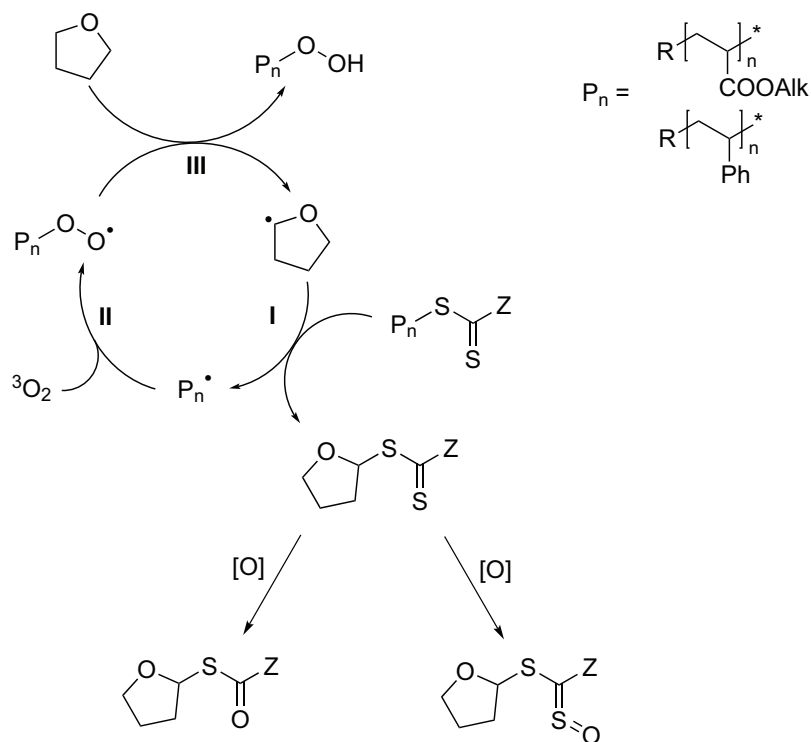
Scheme 4.1 Overall reaction scheme for the switch of a thiocarbonyl thio end-group of RAFT into hydroxyl terminal polymers.

The advantage of the modification is the generation of a versatile functional end-group in a facile fashion, which can be employed for further reactions including polymerizations.

In the following section the mechanism of the thiocarbonyl thio to OH transformation will be discussed.

4.1.1. Mechanism of the OH End-group Switch of Polymers Containing a Dithiobenzoate End-group

A radical oxidation cycle, including an intermediate chain transfer step, is proposed as a possible mechanism. Based on SEC/ESI-MS studies during the modification of dithiobenzoate terminal poly(acrylate)s, this mechanistic suggestion emerged. In Scheme 4.2 the pathway for the transformation is depicted.

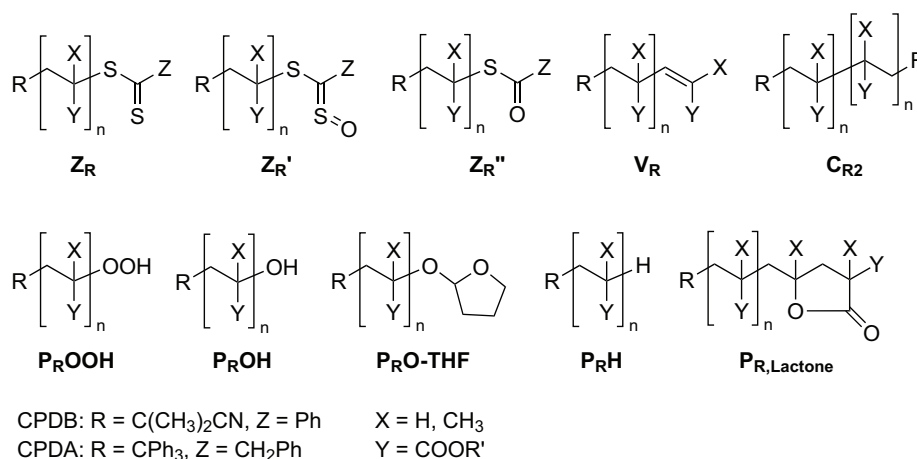


Scheme 4.2 Proposed mechanism of the transformation of dithiobenzoate terminal into hydroxyl end-capped polymers.

A tetrahydrofuranyl radical cleaves the dithiobenzoate group of the polymer, forming a polymerradical \mathbf{P}_n^\bullet and the tetrahydrofuranyl dithioester (**I**). Molecular oxygen present in the solution adds to the macroradical \mathbf{P}_n^\bullet in the subsequent step (**II**). By radical chain transfer to a tetrahydrofuran molecule the hydroperoxide terminated polymer is generated (**III**). The tetrahydrofuranyl dithioester is oxidized during the process after some time to a sulfine or a thioester in the THF solution. These molecules have been identified after the transformation in the solution by SEC/ESI-MS detection.^[275]

The ability of a RAFT end-group to be transformed via the above mechanism is dependent on the stability of the formed macroradical \mathbf{P}_n^\bullet . The stability of the macroradical depends on the monomer class utilized in the polymerization process. Thus, macroradicals consisting of the monomer units styrene, acrylate or methacrylate may undergo this mechanism, while polymer radicals of highly active monomers are less likely to be formed via the transformation procedure,^[276] as they represent poor leaving groups.

The various species which can be present in the reaction mixture of a modification reaction are shown in Scheme 4.3. Beside the structures formed via the mechanism of the transformation to hydroperoxide terminal polymers, oxidation or cyclization can also occur. To visualize the modification, one example of SEC/ESI-MS spectra, obtained before and after the end-group conversion of poly(methyl acrylate), is depicted in Figure 4.1.



Scheme 4.3 Possible structures formed during the transformation reaction of thiocarbonyl thio end-capped poly(acrylate)s.

Before the transformation, only the starting material (in addition to some unavoidable termination products), the RAFT polymer \mathbf{Z}_R , is observed via SEC/ESI-MS (refer to the spectrum in Figure 4.1 at the top). After 60 min, the transformation to the peroxide terminal polymers has proceeded (see spectrum in the center). Beside the peroxide end-capped polymer \mathbf{P}_{ROOH} , polymer with the oxidized thiocarbonyl

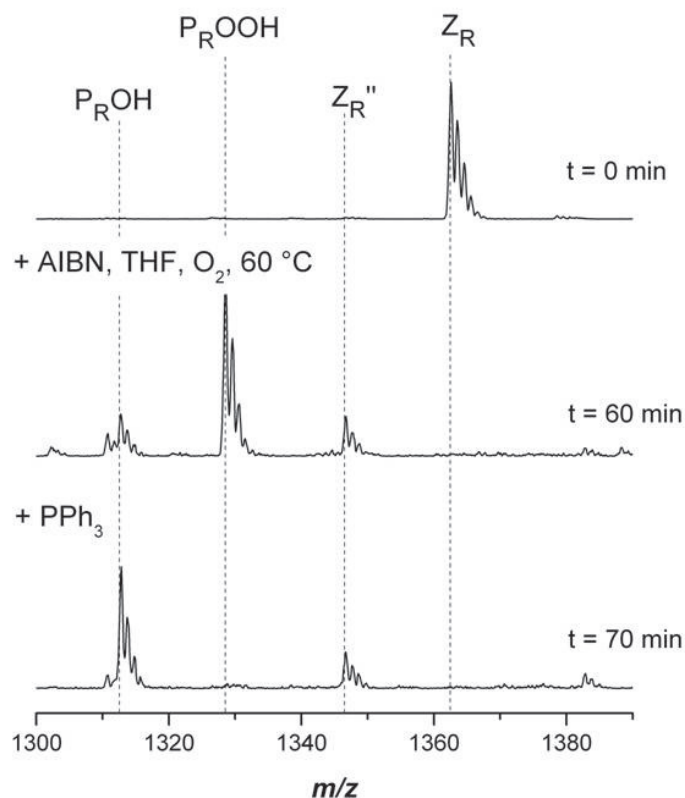


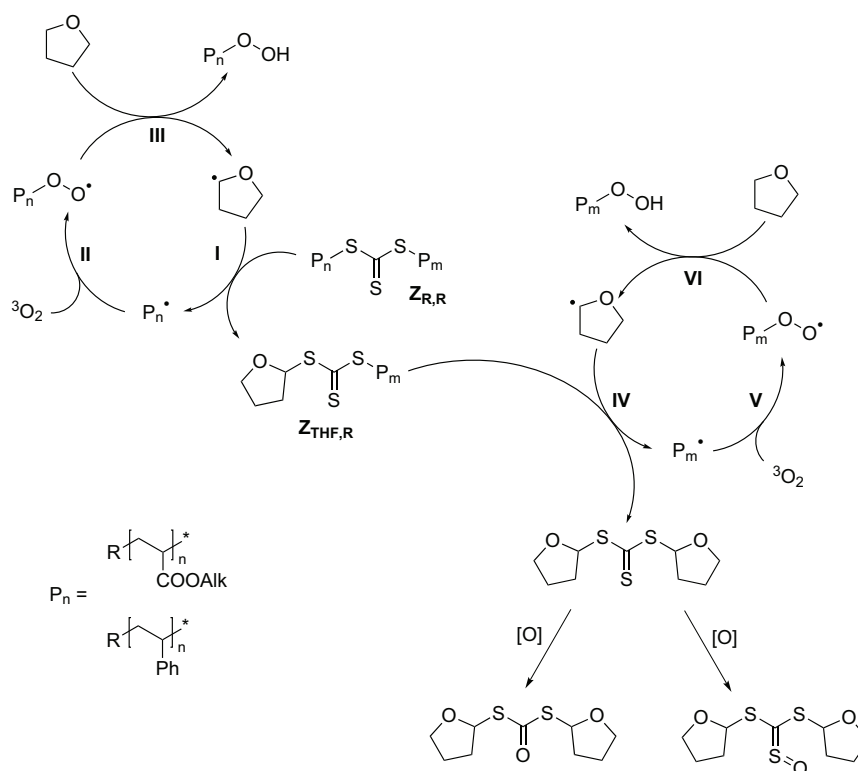
Figure 4.1. Electrospray ionization mass spectra of the end-group transformation of poly(methyl acrylate) carrying a dithiobenzoate end-group into hydroxyl functional pMA in the charge state $z = 1$. The reagents AIBN/THF and PPh_3 were added sequentially at $t = 0$ and 60 min. Full conversion was reached after 70 min.

thio group Z_R'' is also observed in minor amounts as well as small traces of polymer, where the hydroperoxide group has already been reduced to the hydroxyl end functionality P_ROH . Adding the triphenylphosphine to the reaction mixture results in the complete conversion of the hydroperoxide to the hydroxyl moiety (refer to the spectrum at the bottom of Figure 4.1). Only very small amounts of polymer bearing other functional end-groups can be identified.

4.1.2. Mechanism of the OH End-group Switch of Symmetrical Trithiocarbonate Functional Polymers

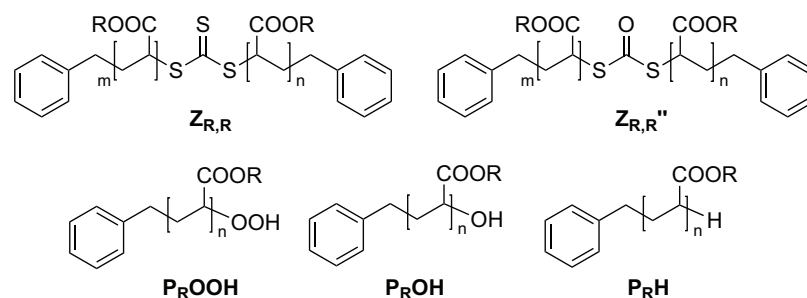
The mechanism associated with the transformation of RAFT polymers bearing a trithiocarbonate moiety is similar to the mechanism introduced in the precedent section. The poly(acrylate)s with a symmetrical trithiocarbonate moiety are synthesized via a RAFT polymerization with dibenzyltrithiocarbonate (DBTC) as the chain transfer agent. The polymer chains are formed on both sides of the trithiocarbonate group. Thus, the trithiocarbonate moiety is positioned in the middle of the polymer structure.

In Scheme 4.4 the pathway, which symmetrical trithiocarbonate groups follow dur-



Scheme 4.4 Proposed mechanism for the transformation of RAFT polymers containing a trithiocarbonate moiety.

ing the transformation process in THF, is depicted. Initially the polymer chain is cleaved from the trithiocarbonate group by a tetrahydrofuran radical, forming the polymer radical P_n^\bullet and a tetrahydrofurantrithio functional polymer $Z_{THF,R}$ (I). The macroradical P_n^\bullet follows the oxidation cycle in an identical fashion as described in the previous mechanism of dithiobenzoate end-capped polymers (II/III). $Z_{THF,R}$, however, reacts again with a tetrahydrofuran radical generating another macroradical P_m^\bullet and a ditetrahydrofurantrithiocarbonate (IV). The macroradicals again react with oxygen to the hydroperoxide end-capped poly(acrylate)s (V/VI) and the ditetrahydrofurantrithiocarbonate is oxidized in the reaction mixture. The structures associated with the mechanism depicted in Scheme 4.4 are presented in Scheme 4.5. The mechanism is underpinned by the measurement of SEC and SEC/ESI-MS of the solution. SEC traces were detected after specific time intervals during the end-group modification and can be found in the publication of Dietrich *et al.*^[276] A shift to higher retention volume is observed after 30 min. The M_n after the transformation compared to the M_n before the modification of the poly(acrylate)s is almost halved, caused by the trithiocarbonate group which is positioned in the middle of the polymer chain. Cleaving the group, two polymer chains with halve of the M_n are generated. Consequently, the obtained SEC traces further substantiate the proposed mechanism.



Scheme 4.5 Possible structures formed during the transformation reaction of poly(acrylate)s containing a symmetrical trithiocarbonate moiety.

Furthermore, SEC/ESI-MS experiments were conducted to follow the transformation reaction. The spectrum before the transformation shows only features the RAFT polymer. After 5 min reaction time, the signals of the hydroperoxide terminated poly(acrylate) $\mathbf{P}_{\mathbf{R}}\mathbf{OOH}$ as well as the tetrahydrofuranlytrithio functional polymer $\mathbf{Z}_{\mathbf{THF},\mathbf{R}}$ are observed. Within 45 min the $\mathbf{Z}_{\mathbf{THF},\mathbf{R}}$ is completely converted to $\mathbf{P}_{\mathbf{R}}\mathbf{OOH}$. After adding the triphenylphosphine, the signal of $\mathbf{P}_{\mathbf{R}}\mathbf{OOH}$ shifts to the m/z ratios of the hydroxyl terminated polymer. To prove the formation of the tetrahydrofuranlytrithio functional polymer, $\mathbf{Z}_{\mathbf{THF},\mathbf{R}}$, collision induced dissociation electrospray ionization mass spectra (CID-ESI-MS) were additionally recorded. They verify the proposed intermediate structure.^[276]

In the current chapter a selection of further end-group conversion reactions of RAFT polymers are presented in the Results and Discussion section to extend the library of polymers capable of undergoing the transition containing thiocarbonyl thio end-groups. More over, the transformation reactions were realized in some cases on a preparative scale in a reaction flask, and not only on an analytical scale. Further transformation reactions can be found in the subsequent chapters. A table collating all the transformation reactions performed so far will be presented at the end of the chapter.

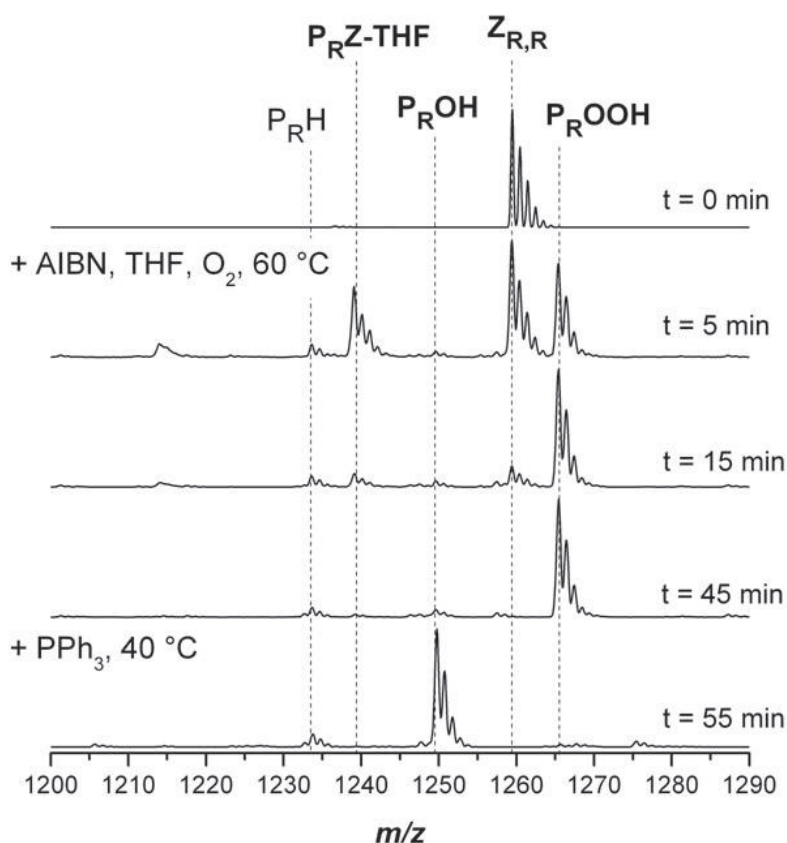


Figure 4.2. Tracing the RAFT to OH transformation via SEC/ESI-MS spectra of poly(methyl acrylate) containing a symmetrical trithiocarbonate moiety.

4.2. Synthetic Procedures

The specifications of the materials used in this synthesis section are provided in Chapter 3.

Synthesis of the RAFT Agent Ethane-1,3-diyl

bis(2-(((dodecylthio)carbonothioyl)thio)propanoate), 2-arm DoPAT

The RAFT agent was synthesized via a Steglich esterification of the acid group of 2[(dodecylsulfanyl) carbonothioyl]sulfanyl propanoic acid (DoPAT). 2 g of DoPAT (5.7 mmol), 0.176 g of ethyleneglycol (2.85 mmol) and 0.14 g of DMAP (1.1 mmol) were dissolved in 10 mL of dry dichloromethane and cooled with ice. A solution of *N,N'*-dicyclohexylcarbodiimide (1.18 g, 5.70 mmol) in dry dichloromethane (2 mL) was slowly added, the cooling bath was removed, and the mixture was stirred overnight at ambient temperature. The white precipitate was filtered off and the solution was extracted with 0.5 N hydrochloric acid (2×50 mL) and washed with saturated NaHCO_3

solution (50 mL). The organic solution was dried over MgSO_4 and concentrated under reduced pressure. The crude product was purified via column chromatography on silica gel with hexane/ethyl acetate (10 : 1, v/v, R_f : 0.5) as the eluent and dried under high vacuum to yield the RAFT agent (1.4 g, 67 %) as a yellow solid. $^1\text{H-NMR}$ (250 MHz, CDCl_3) δ / ppm: 0.81 (t, 6H, $-\text{CH}_3$), 1.10-1.22 (m, 36H, $-\text{CH}_2$), 1.58 (d, 6H, $-\text{CH}_3$), 1.59-1.74 (m, 4H, $-\text{CH}_2$), 1.78-1.90 (m, 4H, $-\text{CH}_2$), 3.43 (t, 4H, $-\text{CH}_2\text{S}$), 4.28 (t, 4H, $-\text{OCH}_2$), 4.85 (q, 2H, $-\text{CH}$).

For propane-1,3-diyl bis(2-(((dodecylthio)carbonothioyl)thio)propanoate) the same synthetic procedure is used. Instead of ethyleneglycol, 1,3-propanediol is employed. Both synthesis result in a 2-arm RAFT agent. The first is employed in the polymerization of *i*BoA in the RAFT process, the latter in the polymerization of styrene.

Synthesis of the RAFT Agent 3-Hydroxypropyl 2-(((dodecylthio)carbonothioyl)thio)propanoate, DoPAT-OH

6.33g of DoPAT (18.1 mmol), 5.66 g of propanediol (74.4 mmol) and 0.45 g of DMAP (3.7 mmol) were dissolved in 40 mL of dry dichloromethane and cooled with ice. A solution of *N,N'*-dicyclohexylcarbodiimide (5.70 g, 27.6 mmol) in dry dichloromethane (10 mL) was slowly added, the cooling bath was removed and the mixture was stirred overnight at ambient temperature. The white precipitate was filtered off and the solution was extracted with 0.5 N hydrochloric acid (2×50 mL) and washed with saturated NaHCO_3 solution (50 mL). The organic solution was dried over MgSO_4 and concentrated under reduced pressure. The crude product was purified via column chromatography on silica gel with hexane/ethyl acetate (10 : 1, v/v, R_f : 0.2) as the eluent and dried under high vacuum to yield the RAFT agent (3.39 g, 46 %) as a yellow solid. $^1\text{H-NMR}$ (400 MHz, CDCl_3) δ / ppm: 0.81 (t, 3H, $-\text{CH}_3$), 1.09-1.26 (m, 18H, $-\text{CH}_2$), 1.58 (d, 3H, $-\text{CH}_3$), 1.60-1.68 (m, 2H, $-\text{CH}_2$), 1.79-1.87 (m, 2H, $-\text{CH}_2$), 3.29 (t, 2H, $-\text{CH}_2\text{S}$), 3.63 (t, 2H, $-\text{OCH}_2$), 4.18-1.30 (m, 2H, $-\text{CH}_2\text{O}-$), 4.48 (q, 1H, $-\text{CH}$).

Polymerizations of Isobornyl Acrylate and Styrene Using DoPAT and DoPAT Derivatives

A solution of RAFT agent and 2,2'-azobis(iso-butyronitrile) in monomer (50 mL) was degassed by purging with nitrogen for 20 min. The solution was heated to 60 °C for a pre-set period of time, after which the reaction was stopped by cooling in liquid nitrogen. The residual monomer was removed under vacuum and the polymers precipitated in cold methanol. The concentrations utilized in the synthesis and the number molar mass average are collated in Table 4.1.

Table 4.1. Reaction conditions for the polymerization of isobornyl acrylate (*i*BoA) and styrene (Sty) with DoPAT and its derivatives. c_{RAFT}^0 and c_{AIBN}^0 are the initial concentrations of the RAFT agent and AIBN, respectively.

Monomer	RAFT agent	c_{RAFT}^0 / mmol L ⁻¹	c_{AIBN}^0 / mmol L ⁻¹	time / min	M_n / g mol ⁻¹	PDI
<i>i</i> BoA	DoPAT	41.78	1.52	52	4 100	1.2
<i>i</i> BoA	2-arm DoPAT	12.29	3.19	40	7 500	1.1
<i>i</i> BoA	DoPAT-OH	23.71	3.04	10	5 900	1.2
Sty	DoPAT	52.00	3.67	990	4 300	1.1
Sty	2-arm DoPAT	24.86	3.16	300	1 500	1.1
Sty	2-arm DoPAT	24.86	3.26	840	6 900	1.1

Analytical (Small Scale) End-group Conversion

A solution of 2,2'-azobis(isobutyronitrile) (30 mmol L⁻¹) in 2 mL of THF was heated to 60 °C in the presence of ambient air. The RAFT-polymer (5 – 10 mmol L⁻¹ based on M_n) was added to the solution into the vial. After discoloration of the solution indicated full conversion or after max. 45 min, respectively, the temperature was reduced to 40 °C and 3 eq. triphenylphosphine were added.

Preparative (Large Scale) End-group Conversion

A solution of 2,2'-azobis(isobutyronitrile) (50 mmol L⁻¹) in THF was heated to 60 °C for 60 min under ambient air. A solution of 500 mg RAFT-polymer in the pre-treated THF (10 mmol L⁻¹ based on M_n) was prepared in a 100 mL round flask under ambient atmosphere. The flask was heated to 60 °C under vigorous stirring. After 40 min, the temperature was reduced to 40 °C and 3 equiv. triphenylphosphine were added. After 10 min the solvent was evaporated and the polymer was precipitated in cold methanol.

Long-term End-group Conversion

A solution of 2,2'-azobis(isobutyronitrile) (30 mmol L⁻¹) in 2 mL of THF was heated to 60 °C in the presence of ambient air. The RAFT polymer (5 – 10 mmol L⁻¹ based on M_n) was added to the solution in the vial. After certain time intervals, samples were taken from the solution. The reaction was stopped after 170 min.

End-group Conversion with V65 and V70

The reaction was conducted similar to the analytical end-group conversion. Instead of AIBN, the azo-initiators 2,2'-azobis(2,4-dimethyl valeronitrile) (V65) and

2,2'-azobis(4-methoxy-2,4-dimethyl valeronitrile) (V70) were employed. The reaction was conducted at 40 °C and ambient temperature, respectively. After 30 min reaction time, 3 equiv. of triphenylphosphine were added and the solution was allowed to react for another 10 min.

End-group Conversion using Alternative Reducing Agents

The modification reaction proceeded in analytical scale. Instead of PPh₃, 3 equiv. of dimethyl sulfide (Me₂S) or triethylamine (NEt₃) were added to the reaction mixture. The solution was allowed to react for 30 min at 50 °C.

End-group Conversion with UV Irradiation

A solution of 2,2'-azobis(isobutyronitrile) (30 mmol L⁻¹) and 0.77 g of RAFT-polymer in 50 mL of THF was positioned in a custom built photo reactor. The flasks were irradiated by a compact low-pressure fluorescent lamp (Arimed B6, Cosmedico GmbH, Stuttgart, Germany) emitting at 320 nm (± 30 nm) at a distance of 40-50 mm. The solution was allowed to react for 1 hour. 3 equiv. of triphenylphosphine were added and the reaction was stirred for 30 min. The solvent was evaporated and the polymer was precipitated in cold methanol.

Cleavage of the formed Ether End functionality

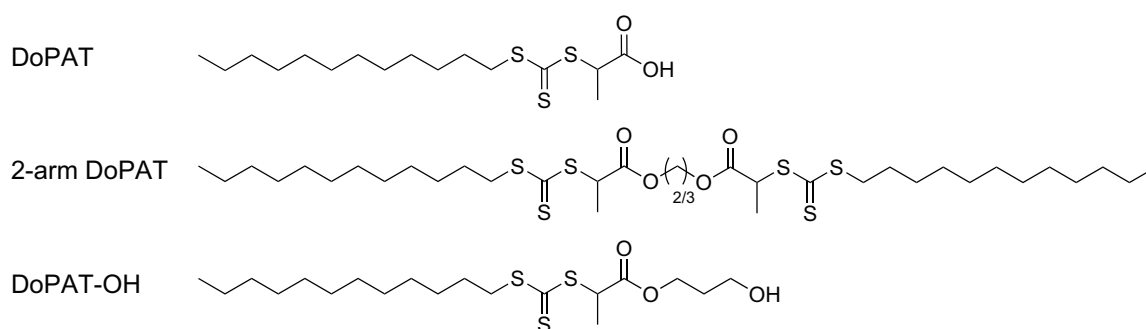
A solution of MeOH, 0.1 mL of HCl and the RAFT polymer, dissolved in THF, was stirred for 120 min at ambient temperature. The solvent was evaporated and the polymer was precipitated in cold methanol.

4.3. Results and Discussion

In here, the investigation of a selection of end-group conversion reactions are presented. The transformations described in the introduction are generally performed for very low amounts of material (20 mg of polymer). If the transformation is utilized to obtain a polymer, which can subsequently be introduced to further reactions as described in the subsequent chapters, higher amounts of material are required. Thus, the reactions are additionally performed in a large scale and compared with the results obtained via small scale modifications.

Beside the conventional established transformation, slight modifications of the reactions have been investigated including the use of alternative azo-initiators, change in temperature, other solvents and the employment of other reducing agents. Furthermore, the transformation of polymers bearing two thiocarbonyl thio end-groups will

be presented. The modification reactions described in the present chapter are based on polymers, which are synthesized with the RAFT agents depicted in Scheme 4.6. The RAFT agents employed for the synthesis of poly(styrene) (pS) and poly(isobornyl acrylate) (piBoA) are the 2[(dodecylsulfanyl) carbonothioyl]-sulfanyl propanoic acid (DoPAT) and derivatives of DoPAT (2-arm DoPAT, DoPAT-OH). The modifications of DoPAT were achieved via a Steglich esterification with 1,3-propanediol or ethylene-glycol, respectively, employing *N,N'*-dicyclohexylcarbodiimide (DCC) as a coupling agent. The reason for preparing the modifications of DoPAT will be explained later in the section.



Scheme 4.6 DoPAT and modified DoPAT employed in the polymerization process of isobornyl acrylate and styrene.

Transformations based on piBOA

piBoA synthesized with the RAFT agent DoPAT

Firstly, the modification reactions of piBoA, possessing one thiocarbonyl thio end-group on the chain end, are described. The polymer was synthesized employing DoPAT as a RAFT agent, resulting in a poly(isobornyl acrylate) bearing a dodecyl trithiocarbonate end-group with an M_n of 4100 g mol⁻¹ and a *PDI* of 1.2. The transformation reaction was conducted on a small as well as on a large scale and the resulting intermediates and products were detected after preset time intervals via SEC/ESI-MS. The left side of Figure 4.3 depicts SEC/ESI-MS spectra obtained during the transformation on an analytical scale. The theoretical and the measured m/z ratios of the observed species during the process are depicted in Table 4.2. Before the transformation only the m/z signal from the RAFT polymer Z_R is visible. Already after 9 min more than 50% of the trithiocarbonate terminated polymer is transformed into polymer bearing a hydroperoxide ($P_{R}OOH$) or a hydroxyl ($P_{R}OH$) functionality at the chain end. H-terminated polymer $P_{R}H$ is also present in the reaction mixture. Further, a signal, which can be assigned to an epoxide terminated piBoA V_{R+O} , is detected. It is possible that an elimination via a side reaction occurs to form the vinyl terminated polymer, which can subsequently be oxidized to an epox-

ide. After 36 min the transformation to the hydroperoxide end functional polymer is completed. The signal from the epoxide functionalized polymer has almost fully disappeared, leading to the assumption that the epoxide was oxidized to the hydroperoxide functionality. Adding PPh_3 to the reaction mixture results in the reduction of the hydroperoxide functionality to the hydroxyl terminated polymer. The final product consists of hydroxyl functionalized polymer and a small amount of H-terminated material. On the right side of Figure 4.3 the SEC/ESI-MS spectra obtained during and after the transformation reaction on the preparative scale are depicted. After 40 min, the RAFT polymer is converted into hydroperoxide terminated polymer. Adding PPh_3 reduces the hydroperoxide to a hydroxyl functionality. Here, comparing the spectra after 40 min and the spectra after adding the PPh_3 , a slightly higher amount of H-terminated material is found after the reduction process. Furthermore, the reduction is not completed after 10 min. A small signal from the hydroperoxide terminated polymer remains in the sample.

Comparing the results obtained on the analytical scale with the ones obtained on the preparative scale, only small differences are observed. The undesired H-terminated polymer is present in both reactions, however, after the reduction process on the preparative scale, more H-terminated polymer was observed.

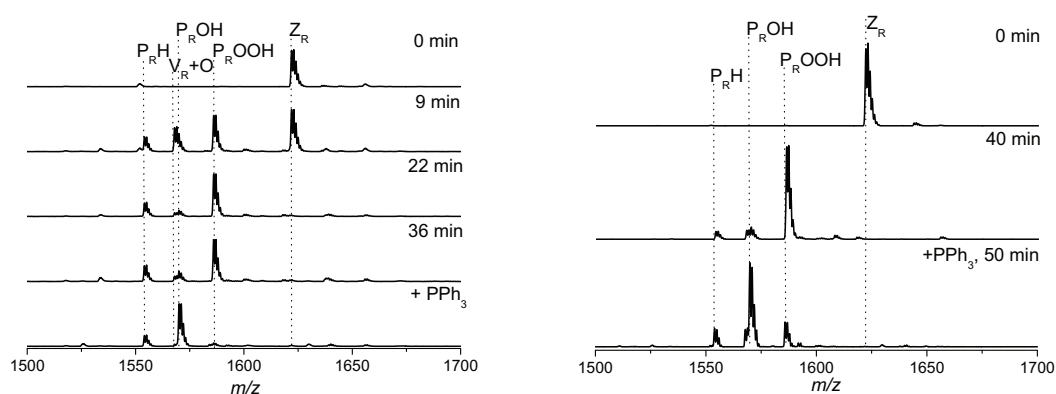


Figure 4.3. Electrospray ionization mass spectra at specific time intervals during the transformation of poly(isobornyl acrylate) bearing one trithiocarbonate group on the chain end. The transformation was conducted in small scale (left) and preparative scale (right).

In the articles which were published concerning the end-group conversion, the modification reaction was always performed until discoloration of the solution was observed.^[276] Referring to the mechanism of the transformation reaction in Scheme 4.2, discoloration takes not place when the thiocarbonyl thio end-group is cleaved from the polymer, but results from the oxidation of the tetrafuranyl thiocarbonyl thio molecule, which takes place as a side reaction after the formation of the tetrafuranyl thiocarbonyl thio molecule. Consequently, the completion of the reaction is not necessarily

Table 4.2. Theoretical and measured m/z ratios of the main species in the transformation process of dodecyl trithiocarbonate terminated *pi*BoA.

Structure	[M + Na] ⁺		
	m/z^{theo}	m/z^{exp}	$\Delta m/z$
Z_R	1622.03	1622.00	0.03
P_ROOH	1586.07	1586.16	0.09
P_ROH	1570.07	1570.00	0.07
V_R+O	1568.05	1568.08	0.03
P_RH	1554.07	1554.08	0.01
?	-	1655.91	-

indicated by a discoloration. Especially reaction solutions on the preparative scale were observed to keep their color over days. However, in some cases, the reaction was found to be complete, although the solution stayed colored. Further, in other cases, when the reaction proceeded until discoloration, side products were found in the reaction mixture.

Long-term studies have been carried out to define after which reaction time side reactions affecting the reactive hydroperoxide functionalized polymer start to occur. In Figure 4.4 SEC/ESI-MS spectra during the transformation reaction, evolving longer reaction times, are depicted. After 45 min the main signal can be assigned to the hydroperoxide functional polymer. In addition to the **P_ROOH**, small signals corresponding to hydroxyl and H-terminated polymer are present. After 65 min, the signal from the H-terminated polymer chain increased whereas the signal corresponding to the **P_ROOH** strongly decreased. Additionally, a new signal at $m/z = 1655.91$ is observed, which cannot be assigned to any possible structure. The unknown structure is stable over the next 105 min. After a total of 170 min, the signal from the hydroperoxide terminated polymer has almost completely disappeared, thus suggesting that the reaction time should not exceed more than 45 min, independent of whether discoloration is observed. If the reaction time is extended, undesired side reaction can occur.

In Figure 4.3, depicting the SEC/ESI-MS spectra of the conventional transformation (end-group conversion employing AIBN/THF at 60 °C and PPh₃ as reducing agent), H-terminated polymer as a minor side product was observed. The occurrence of **P_RH** is even in small amounts undesired due to the fact that it is dead polymer bearing no functionality, which cannot subsequently be employed in other reactions. To minimize this side reaction, slight modifications of the transformation process were investigated. One strategy to obtain less side products is reducing the temperature. Since AIBN is less reactive at lower temperatures, alternative azo-initiators were

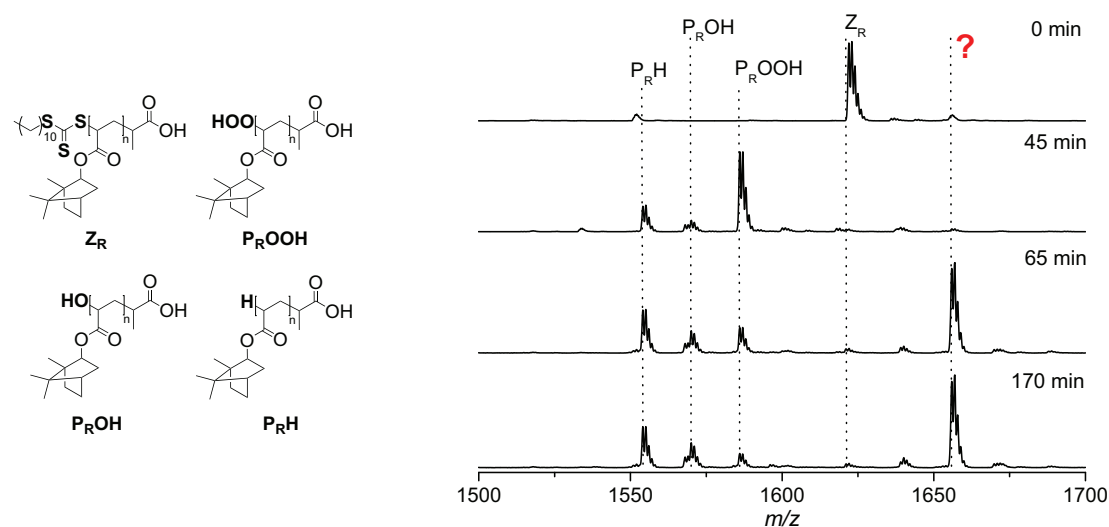


Figure 4.4. Electrospray ionization mass spectra at specific time intervals during the transformation of poly(isobornyl acrylate) bearing one trithiocarbonate group on the chain end. The long term study of the transformation was conducted on a small scale. On the left hand side the associated structures are depicted.

employed. 2,2'-Azobis(2,4-dimethyl- valeronitrile) (V65) and 2,2'-azobis(4-methoxy-2,4-dimethyl valeronitrile) (V70) with a 10 hour half-life decomposition temperature of 51 °C and 30 °C (in toluene), respectively, can operate sufficiently at lower temperatures compared to AIBN. The SEC/ESI-MS spectra depicted in Figure 4.5 are taken after specific time intervals from the end-group conversions conducted at 40 °C and ambient temperature, respectively. The transformation reaction with the azo-initiator V65 and the subsequent reduction is completed after 51 min (see Figure 4.5 on the left hand side). The main signal corresponds to the hydroxyl terminated polymer. No signals are observed which can be assigned to the H-terminated material, yet a minor signal corresponding to the oxidized RAFT polymer (Z_R) is visible. As soon as the RAFT agent is oxidized, it cannot react in the radical oxidation process to form the hydroperoxide terminated polymer and is thus also undesired dead polymer. The SEC/ESI-MS spectra obtained from the transformation process at ambient temperature employing V70 are depicted on the right hand side of Figure 4.5. After 10 min the signal corresponding to the RAFT polymer has disappeared and the main signal is assigned to the hydroperoxide terminated polymer. Side products include H-terminated polymer and the oxidized species of the RAFT polymer. Reducing the reaction with PPh_3 for 10 min results not in complete conversion from the $P_R OOH$ to the $P_R OH$. This circumstance can be explained by the fact that also the reduction reaction was conducted at ambient temperature leading to a slower reduction process.

As an overall result for the transformation with V65 and V70, it can be stated that

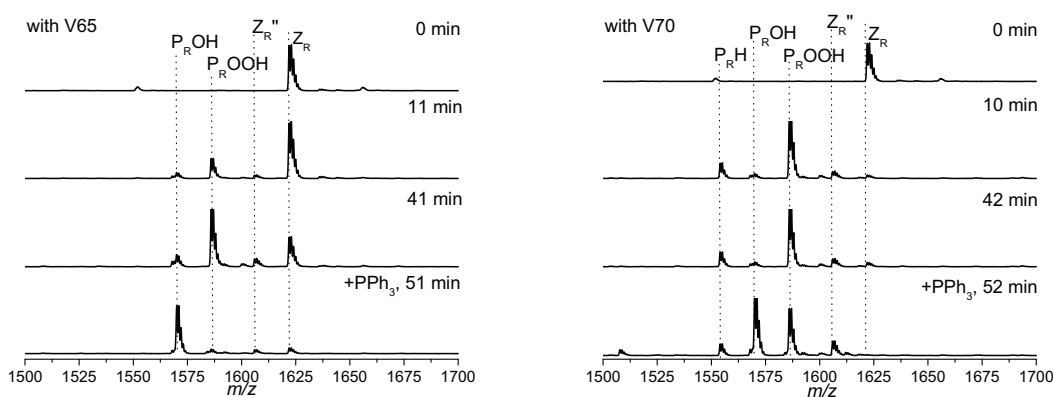


Figure 4.5. Electrospray ionization mass spectra at specific time intervals during the transformation of poly(isobornyl acrylate) bearing one trithiocarbonate group on the chain end. The transformation was conducted on a small scale and instead of AIBN, the azo-initiators V65 (40 °C) and V70 (ambient temperature) were employed, respectively.

the end-group conversion can also be conducted at lower temperatures. This can be advantageous when thermally unstable groups are present in the polymer structure. However, minor side reactions occur to the same extent as in the reaction employing AIBN leading to no major improvement of the end-group conversion.

As observed in Figure 4.3 an increase in H-terminated polymer during the subsequent reduction with PPh_3 can occur in some cases. Beside PPh_3 , further reducing agents were tested. The reduction with Mg/MeOH and with Zn/HOAc was found to be inefficient. Additionally, triethylamine and dimethyl sulfide were investigated. The SEC/ESI-MS spectra obtained during the end-group conversion and the subsequent reduction with NEt_3 and Me_2S , respectively, are presented in Figure 4.6. The reducing agents were allowed to operate for 30 min. The left mass spectra in Figure 4.6 show the effect of the reduction with triethylamine. The signals after the reduction can be assigned to hydroxyl and the epoxide terminated polymer. Consequently, the reaction is not selective, however, the material is completely functionalized and can be employed in subsequent reactions. The reduction with dimethyl sulfide is depicted at the right hand side in Figure 4.6. After 30 min the polymer is completely transformed into hydroxyl terminated material, evidencing that Me_2S is an efficient and selective reducing agent for the transformation of hydroperoxide into hydroxyl terminated polymer. Thus, dimethyl sulfide can also be employed as reducing agent for the end-group conversion of RAFT polymers.

Additional experiments were conducted to investigate the selectivity and the efficiency of the end-group conversion under similar reaction conditions. Trioxane and dioxane were tested in the radical oxidation cycle as chemical substitutes for THF. The employment of these chemicals results not in the desired hydroperoxide terminal polymer.

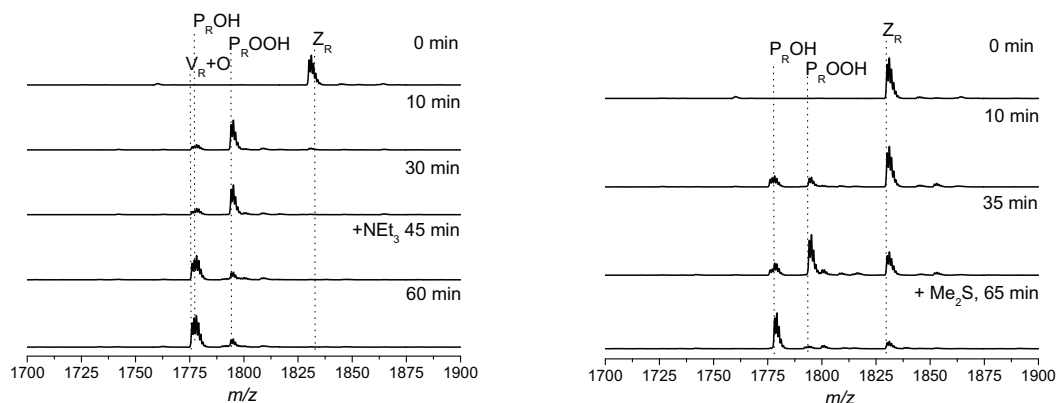


Figure 4.6. Electrospray ionization mass spectra at specific time intervals during the transformation of poly(isobornyl acrylate) bearing one trithiocarbonate group on the chain end. The transformation was conducted on small scale and instead of PPh_3 , the reducing agents Me_2S and NEt_3 were employed, respectively.

It was further investigated if bubbling oxygen through the reaction mixture using an oxygen gas bottle would abbreviate the reaction time. However, no significant change in reaction time was observed.

piBoA synthesized with the difunctional RAFT agent 2-arm DoPAT

In the next step the end-group conversion was carried out on RAFT polymers possessing two trithiocarbonate moieties on the chain ends. In many cases, especially for the formation of more complex polymer structures, it is mandatory to have reactive functionalities on both chain ends. The RAFT agent 2-arm DoPAT (see Scheme 4.6 for the structure) was employed in the polymerization of *iBoA* to obtain a polymer structure onto which trithiocarbonate moieties are attached on both chain ends ($M_n = 7500 \text{ g mol}^{-1}$, $PDI = 1.1$). The end-group conversion was performed in the first instance on the analytical and on the preparative scale. The corresponding SEC/ESI-MS mass spectra are depicted in Figure 4.7 and the theoretical as well as the experimental m/z ratios are listed in Table 4.3. Due to the molar mass of the polymer, signals with m/z ratios with $z = 2$ are obtained. The mass spectra during the transformation on the analytical scale are presented on the left hand side in Figure 4.7. After 10 min the signal corresponding to the RAFT polymer has almost disappeared. The signals can be assigned to polymer on which one trithiocarbonate group is converted to a hydroperoxide moiety, Z_ROOH , to the dihydroperoxide terminated polymer $\text{P}_R(\text{OOH})_2$ and to the dihydroxyl end-functional polymer $\text{P}_R(\text{OH})_2$. After 37 min, after the monofunctionalized polymer Z_ROOH has disappeared, PPh_3 was added to the reaction mixture to reduce the dihydroperoxide end-functional polymer. In the mass spectrum of the final product the main signals correspond to

the dihydroxyl functional polymer. Two side products of only slightly less intensity are observed, the $\mathbf{P}_R\text{OOH}/\text{OH}$ and the $\mathbf{P}_R\text{OH}/\text{H}$. The end-group conversion on the preparative scale (see mass spectra in the right figure) exhibits similar results. The signal corresponding to $\mathbf{P}_R\text{OOH}/\text{OH}$ in the mass spectrum of the final product, however is much less intense, when compared with the product of the analytical scale end-group conversion. However, an additional signal of minor intensity, which can be assigned to the fully H-terminated polymer $\mathbf{P}_R(\text{H})_2$, indicates the presence of dead polymer in the final product.

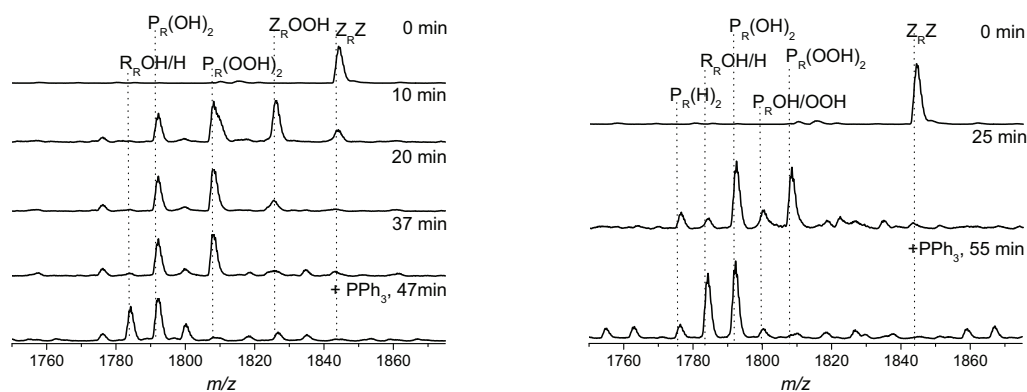


Figure 4.7. Double charged electrospray ionization mass spectra at specific time intervals during the transformation of poly(isobornyl acrylate) bearing trithiocarbonate groups on both chain ends. The transformation was conducted on the analytical (left) as well as on the preparative scale (right).

Table 4.3. Theoretical and measured m/z ratios (with $z = 2$) of the main species in the transformation process of *pi*BoA possessing trithiocarbonate end functionalities on both chain ends.

Structure	$[\text{M} + \text{Na}]^+$		
	m/z^{theo}	m/z^{exp}	$\Delta m/z$
$\mathbf{Z}_R\mathbf{Z}$	1843.18	1843.25	0.07
$\mathbf{Z}_R\text{OOH}$	1825.21	1825.25	0.04
$\mathbf{P}_R(\text{OOH})_2$	1807.22	1807.16	0.06
$\mathbf{P}_R\text{OOH}/\text{OH}$	1799.22	1799.25	0.03
$\mathbf{P}_R(\text{OH})_2$	1791.22	1791.17	0.05
$\mathbf{P}_R\text{OH}/\text{H}$	1783.22	1783.25	0.03
$\mathbf{P}_R(\text{H})_2$	1775.23	1775.33	0.10

The end-group conversion of RAFT polymer possessing two trithiocarbonate moieties can thus be regarded as successful before adding the reducing agent. After reaction with the reducing agent, H-terminated $\mathbf{P}_R(\text{H})_2$ or partially H-terminated polymer $\mathbf{P}_R\text{OH}/\text{H}$ is present. Experiments to improve the selectivity of the reduc-

tion using other reducing agents – as performed for the monofunctional polymer – have been conducted. These experiments, however, did not lead to a lower amount of H-terminated polymer. An explanation for the high amount of dead chains, when compared with the monofunctional polymer, could not be derived from the obtained data. It is assumed that the polymer chain ends interact in the way that the hydroperoxide functionality is cleaved.

piBoA synthesized with the RAFT agent DoPAT-OH

The third polymerization of *piBoA* was performed with the RAFT agent DoPAT-OH (for the structure see Scheme 4.6). On the one hand, it is feasible when one chain end is already equipped with a appropriate functionality. On the other hand, it should be investigated, if increased H-termination during the end-group conversion of the difunctional polymer is influenced by interactions of the functional chain ends.

On the left hand side in Figure 4.8 the mass spectra, obtained after preset time intervals during the end-group conversion on the preparative scale, are presented. For the theoretical and experimental m/z ratios, the reader is referred to Table 4.4. The

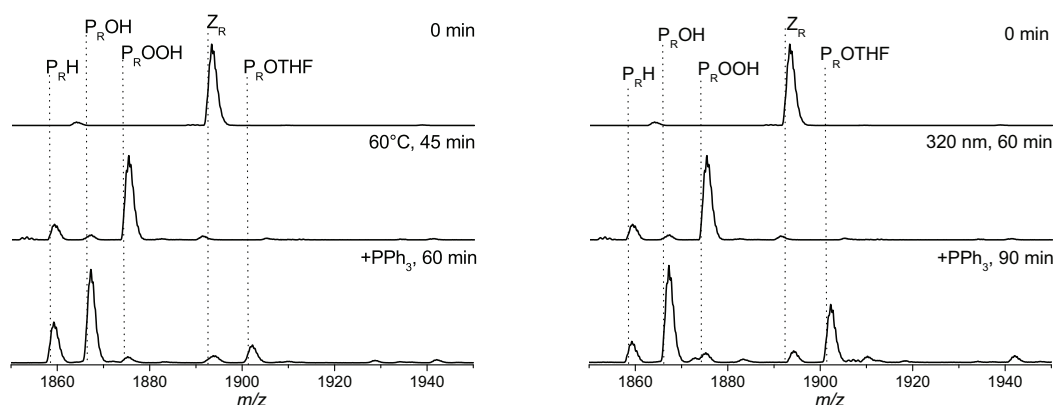


Figure 4.8. Electrospray ionization mass spectra with $z = 2$ at specific time intervals during the transformation of poly(isobornyl acrylate) bearing the DoPAT-OH on the chain ends. The transformation was conducted on a large scale under conventional conditions (left) and at ambient temperature under UV radiation (right figure).

transformation to the hydroperoxide functional polymer is completed after 45 min. Upon reduction of $\mathbf{P}_R\text{OOH}$, the main product is hydroxyl terminated polymer. H-terminated polymer is present in the reaction mixture as well and an additional signal in the mass spectrum, which is assigned to polymer possessing a tetrahydrofuranyl ether moiety on the chain end $\mathbf{P}_R\text{OTfH}$, is observed. To decrease the amount of non-functional polymer chains, the experiments with different azo-initiators and other reducing agents, mentioned above, were performed, leading to no improvement of the resulting product selectivity. Thus, a new method was assessed, using UV irradiation for the end-group transformation. The reaction was conducted at ambient

temperature on the preparative scale and a UV lamp emitting irradiation of 320 nm was employed. The mass spectra of the transformation reaction are depicted on the right hand side of Figure 4.8. After 60 min complete conversion to the hydroperoxide functional polymer is observed. The reduction with PPh_3 for 30 min yields three signals in one repeat unit in the mass spectrum. The main signal is assigned to the hydroxyl functional polymer. Signals associated with P_ROTHF with a relatively high intensity and P_RH with a low intensity are visible as well. Comparing only the signals from the dead polymer chains, P_RH , the transformation of the RAFT polymer with UV irradiation led to less amount of undesired side products.

Table 4.4. Theoretical and measured m/z ratios (with $z = 2$) of the main species in the transformation process on the preparative scale of piBoA possessing the modified DoPAT-OH on the chain ends.

Structure	$[\text{M} + \text{Na}]^+$		
	m/z^{theo}	m/z^{exp}	$\Delta m/z$
Z_R	1892.27	1892.33	0.06
P_ROOH	1874.29	1874.32	0.03
P_ROH	1866.29	1866.16	0.07
P_RH	1858.30	1858.25	0.05
P_ROTHF	1901.32	1901.25	0.07

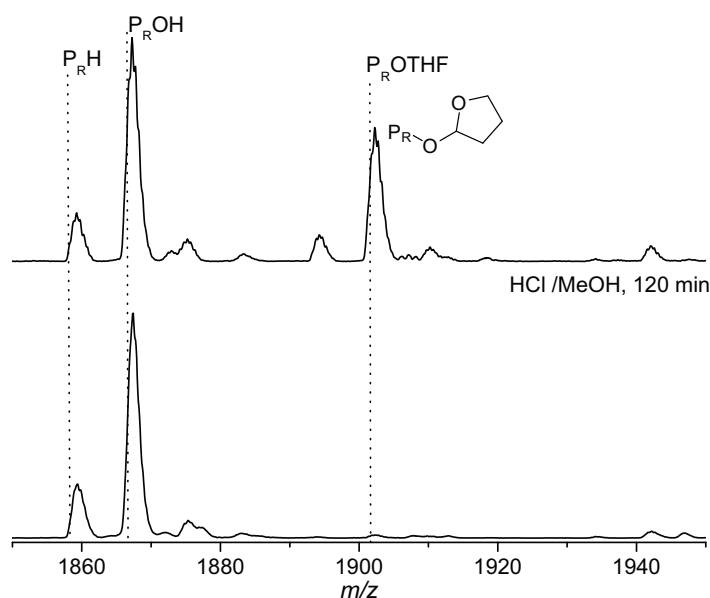


Figure 4.9. Electrospray ionization mass spectra before and after the ether cleavage. The spectrum at the top show the product mixture obtained via the end-group conversion. The lower spectrum is obtained after cleaving the tetrahydrofuranyl ether under acidic conditions.

The tetrahydrofuranyl ether moiety at the polymer chain end can be cleaved under

acidic conditions. In Figure 4.9 the mass spectra before and after the cleavage are depicted.

The signal of **P_ROTHF** has completely disappeared after 120 min reaction time. The H-terminated polymer did not significantly increase during the process. Thus, the tetrahydrofuranyl ether functional polymer is fully converted into hydroxyl terminated polymer.

In conclusion, the transformation with UV irradiation leads to less dead polymer than the thermal conversion at 60 °C, however, an additional step for the cleavage of the ether formation is required to obtain the desired product.

Transformations based on pS

Beside isobornyl acrylate, styrene was polymerized with DoPAT, the modified DoPAT possessing a hydroxyl function and the 2-arm DoPAT (see Scheme 4.6). The obtained polymers were converted by the standard procedure for large scales for end-group modification and characterized after precipitation in methanol with MALDI-ToF MS and SEC. The synthesis and the characterization of the poly(styrene) with DoPAT-OH and its transformation will be described in Chapter 7.

pS synthesized with the RAFT agent DoPAT

Firstly, styrene was polymerized with the RAFT agent DoPAT. The resulting polymer was analyzed via SEC ($M_n = 4300 \text{ g mol}^{-1}$, $PDI = 1.1$). Due to the acidic end-group and the molar mass, the polymer cannot be analyzed with standard SEC/ESI-MS conditions and in MALDI-ToF-MS measurements the trithiocarbonate end-group would decompose resulting in a mass distribution where the trithiocarbonate functionality is cleaved. However, the characterization of the polymer after transformation proofs that the RAFT polymerization process was successful.

The transformation of poly(styrene) equipped with one dodecyl trithiocarbonate end-group from the DoPAT RAFT agent proceeds in the conventional conversion process. After modification the polymer is precipitated and dried. The MALDI-TOF mass spectrum of the sample is depicted in Figure 4.10. The inset in the figure displays the comparison of one repeat unit of the obtained spectra with a simulated isotopic pattern of the expected structure **P_ROH**. The isotopic pattern was simulated with a resolution of 0.3 Dalton. The isotopic structure cannot be observed in the experimentally obtained spectrum due to its low resolution. However, the values for the m/z ratios correspond very well with the expected data. Since no further signals are observed in the spectra, the reaction is considered as successful, *i.e.*, no side reactions occurred and full conversion was achieved.

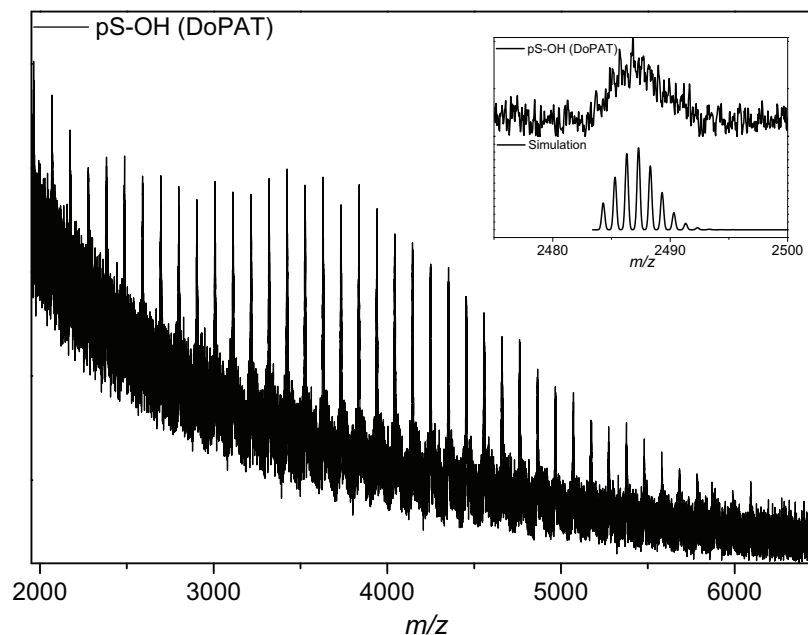


Figure 4.10. MALDI ToF mass spectrum of the transformed poly(styrene) bearing end-groups from DoPAT RAFT agent. The inset depicts the comparison of the measured spectrum to a simulated isotopic pattern of $\mathbf{P_R(OH)}$ (resolution: 0.3 Da).

pS synthesized with the RAFT agent 2-arm DoPAT

The difunctional RAFT agent (2-arm DoPAT) was also employed for the polymerization of styrene yielding a pS with for instance $M_n = 6900 \text{ g mol}^{-1}$, $PDI = 1.1$ or $M_n = 1500 \text{ g mol}^{-1}$, $PDI = 1.1$. The SEC/ESI-MS spectrum of pS with the low molar mass is presented in Figure 4.11.

The end-group conversion of the two trithiocarbonate moieties was conducted under the same conditions as mentioned above, by simply halving the concentration of the polymer to adapt the procedure to two trithiocarbonate moieties. The MALDI-ToF mass spectrum of the obtained polymer is given in Figure 4.12. In the inset a zoom-in into three repeating units is depicted. The main product can be assigned to the dihydroxyl terminated polymer $\mathbf{P_R(OH)_2}$. However, additional signals of minor intensity are observed. The MALDI mass spectrum exhibits signals that fit to the dihydroperoxide terminated polymer $\mathbf{P_R(OOH)_2}$ as well as signals which can be assigned to the H-terminated polymer $\mathbf{P_R(H)_2}$. Repeating and varying the synthesis was not improving the resulting MALDI-ToF mass spectrum. The side reactions to H-terminal polymers possibly occur due to the circumstance that two end-groups on the same polymer chain are involved in the modification process. The two end-groups probably interact in a specific way leading to partially H-terminated polymers. Since the so-terminated polymers can not be involved in further reaction steps, they are

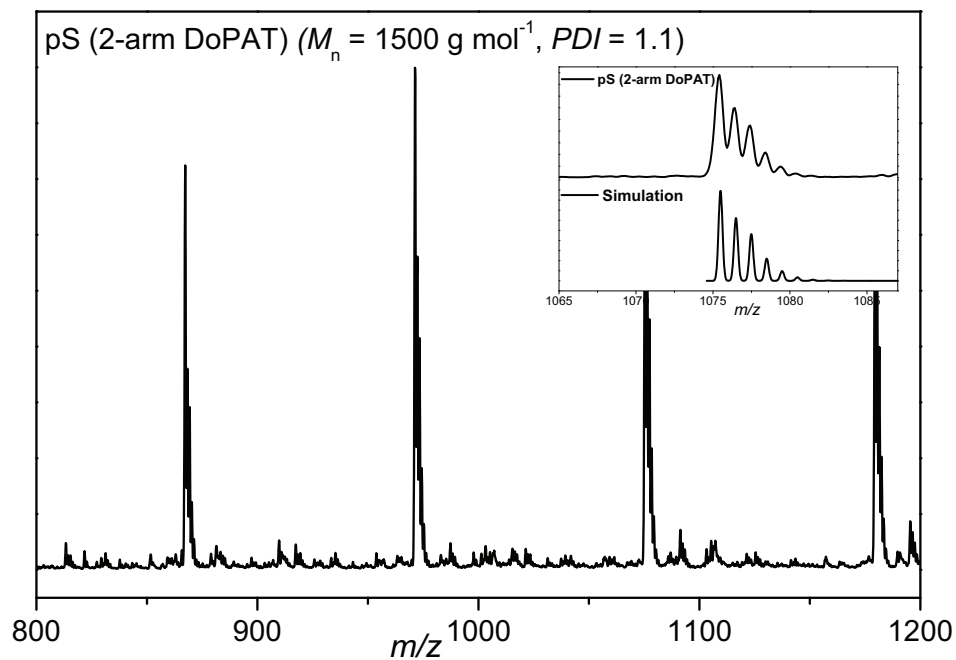


Figure 4.11. Electrospray ionization mass spectrum of poly(styrene) bearing trithiocarbonate groups on both chain ends. The inset shows the simulated isotopic pattern in comparison with the experimental data. The experimental values m/z^{exp} (1075.41) correspond perfectly to the simulated m/z^{theo} value (1075.49).

undesired side products. As similar results are obtained with the *p*iBoA with the 2-arm RAFT agent, it is clear that the reason for the increased content of side products results from the circumstance that two trithiocarbonate moieties on the same polymer chain are involved in the end-group conversion.

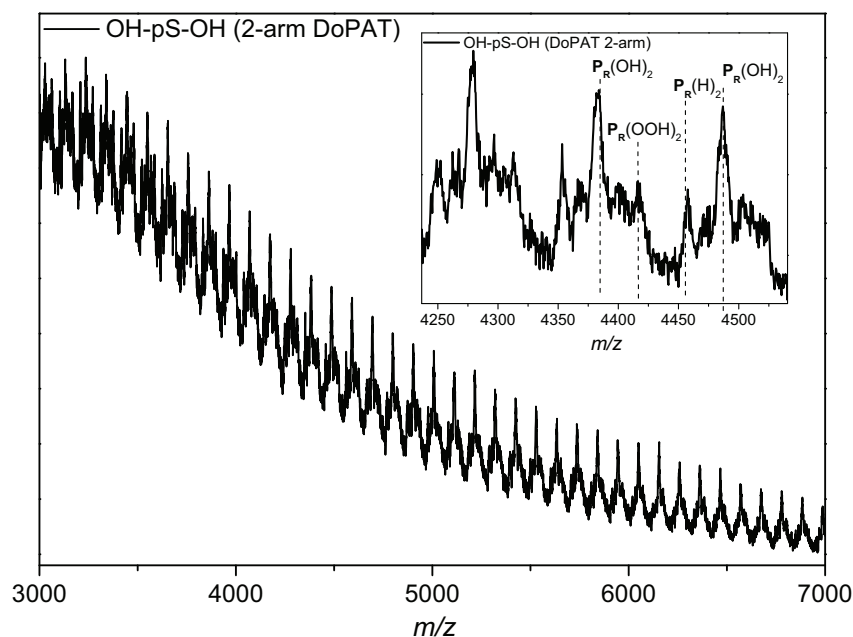


Figure 4.12. MALDI ToF mass spectrum of the transformed poly(styrene) bearing trithiocarbonate groups on both chain ends.

4.4. Conclusions

In the majority of cases, the thiocarbonyl thio to OH transformation is successful. The end-group conversion of polymer equipped with one thiocarbonyl thio moiety results in less side reactions than the transformation of polymer featuring two thiocarbonyl thio groups. Furthermore, the transformation reaction of one trithiocarbonyl group seems to proceed more selectively and leads to less side products on poly(styrene) than on poly(isobornyl acrylate). Emphasis should be set on the fact that the reaction should not necessarily proceed until the color has disappeared and not exceed 45 min reaction time, as side reactions are likely to occur at elongated reaction times. It should be additionally noted that the end-group transformation can also be slightly modified, employing other azo-initiators and/or reducing agents. The conversion applying UV irradiation instead of heat is also a successful way to obtain hydroxyl terminated polymers.

Not all transformation reactions could be discussed here in this chapter. However, a collation of all data obtained so far from the modification of different polymer/RAFT agent systems is given in Table 4.5.

4. Switching from RAFT to Hydroxyl-terminal Polymers

Table 4.5. Collation of all transformation reactions on different polymer/RAFT agent systems reported in the literature so far as well as in the present thesis.

Monomer	RAFT agent	analytical scale	preparative scale ^a	presented in ^b
pMA	CPDB ^c	✓	–	Dietrich <i>et al.</i> ^[276]
pMA	CPDA ^d	✓	–	Dietrich <i>et al.</i>
pMA	DBTC ^e	✓	✓	Dietrich <i>et al.</i>
pMMA	CPDB	✓	✓	Gründling <i>et al.</i> ^[275]
pMMA	CPDA	✓	✓	Gründling <i>et al.</i> ^[274]
pBA	CPDB	✓	–	Dietrich <i>et al.</i>
pBA	CPDA	✓	–	Dietrich <i>et al.</i>
pBA	DBTC	✓	–	Dietrich <i>et al.</i>
ptBA	DBTC	✓	–	Dietrich <i>et al.</i>
p <i>i</i> BoA	CPDB	✓	✓	Dietrich <i>et al.</i>
p <i>i</i> BoA	DBTC	✓	✓	Dietrich <i>et al.</i>
p <i>i</i> BoA	BPDF ^f	✓	✓	Gründling <i>et al.</i>
p <i>i</i> BoA	DoPAT	✓	✓	this work
p <i>i</i> BoA	2-arm DoPAT	✓	✓	this work
p <i>i</i> BoA	DoPAT-OH	✓	✓	this work
pS	CPDA	✓	✓	Gründling <i>et al.</i>
pS	DBTC	✓	✓	this work
pS	2-arm star ^g	✓	✓	this work
pS	4-arm star ^h	✓	✓	this work
pS	DoPAT	✓	✓	this work
pS	2-arm DoPAT	✓	✓	this work
pS	DoPAT-OH	✓	✓	this work
pNiPAAM	DoPAT	✓	✓	PhD thesis of Nicolas Zydziak

^a Transformations on the preparative scale were all firstly conducted during this work (partly not discussed in the thesis) except for the polymer/RAFT systems pMA/DBTC and pNiPAAM/DoPAT.

^b References for transformations on the analytical scale.

^c Cyanoisopropyl dithiobenzoate.

^d Cumylphenyl dithiobenzoate.

^e Dibenzyl trithiocarbonate.

^f Benzyl-2-dithiopicolate.

^g 1,4-Dis(phenylthioacetylthiomethyl)benzene.

^h 1,2,4,5-Tetrakis(phenylthioacetylthiomethyl)benzene.

5

Block Copolymers Generated via a Switch from RAFT Polymerization to ROP

5.1. Introduction to Block Copolymers

The provision of efficient avenues for block copolymer synthesis is one of the most important contemporary research themes, as such structures find wide applications in the generation of self-organizing systems, polymer based therapeutics and optoelectronics.^[277,278] For the generation of block copolymers two pathways are feasible: the formation by sequential addition of two types of monomers or the coupling of two polymer chains, which possess the appropriate end functionalities. If the block copolymer formation is performed via sequential addition, the macromonomer obtained via the polymerization of the first monomer initiates the polymerization of the second monomer, which involves basic considerations concerning the order of the monomer types. For the coupling of two polymer types, high end-functionality of the polymer strands and accurate stoichiometry in the coupling reactions are fundamentally. In both cases the synthesis of well-defined block copolymers requires polymerization techniques with living or/and controlled character.

Anionic living polymerization has been employed in the past decades for block copolymer formation. More recent examples can be retrieved from the references provided here.^[279-282] Due to the intolerance to many functionalities, however, the process can be applied only to specific monomer structures and block copolymer

compositions.

The generation of block copolymers has been greatly simplified and its variability has significantly enlarged via the introduction of reversible activation/deactivation radical polymerization protocols such as nitroxide-mediated polymerization (NMP),^[283] atom transfer radical polymerization (ATRP)^[284,285] as well as the reversible addition-fragmentation chain transfer (RAFT) process.^[286–290] Basic information about the individual processes are described in Chapter 2.1. One recently published example of the synthesis via sequential CRP is the formation of double hydrophilic pentablock copolymers, which show both, pH and thermo-response.^[291] Further, Pang *et al.* used sequential ATRP to generate amphiphilic multi-arm poly(acrylic acid)-*b*-poly(styrene) block copolymers. Sequential RAFT polymerization was employed by Chen and coworkers to synthesize water-soluble stimuli responsive block copolymers.^[292]

A particular interesting area due to specific applications such as drug delivery is the switching from one polymerization technique to another during the synthetic process.^[293,294] This provides the possibility to use different types of monomers, for instance vinyl and cyclic monomers. Importantly, the generation of block copolymers with degradable and non-degradable strands requires the preparation of one block via a living/controlled radical polymerization process, while the second block is generated via ring-opening polymerization (ROP).^[4,5,295]

For the synthesis of block copolymers via a combination of RAFT and ROP techniques, several synthetic methods have been reported. One of the most frequently employed method is based on a dual initiator, *i.e.*, a RAFT agent bearing a hydroxyl function in either the Z- or R-position, which is capable to initiate the ROP of a lactide.^[1] For example, Alexander and co-workers^[296] employed 2-(benzylsulfanylthiocarbonylsulfanyl)ethanol (BSTSE) as RAFT agent and tin(II) 2-ethylhexanoate (Sn(Oct)₂) as ROP catalyst to synthesize poly(lactic acid-*co*-glycolid acid)-*co*-poly(ethyleneglycol methacrylate) (pLGA-*co*-pEGMA) block copolymers. Furthermore, Hedrick and colleagues^[146] synthesized several hydroxyl-functionalized macroinitiators (pMMA-OH, pDMAEMA-OH, p(MMA-*co*-HEMA)-OH, pMMA-*b*-pS-OH and p2VP-OH) employing 4-cyano-4-((thiobenzoyl)sulfanyl)-pentan-1-ol as RAFT agent and subsequently used them to initiate the ROP of lactides with a thiourea-amine catalyst system. In addition, Pan and co-workers^[4] synthesized pLA-*b*-pNIPAM-*b*-pLA triblock copolymers by using a symmetrical RAFT agent with two terminal hydroxyl groups. Alternative strategies, yet not including a dual initiator, have been developed as well. Li *et al.*^[297] introduced the RAFT agent after the ROP of the lactide to produce star-block amphiphilic copolymers via attaching 3-benzylsulfanylthiocarbonylthiocarbonylsulfanylpropionic acid (BSPA) to the hydroxyl terminated macro-star molecule. Transforming the hydroxyl function of the polymer synthesized via ROP has also been successfully investigated by several other research groups. Studies via such an approach to block

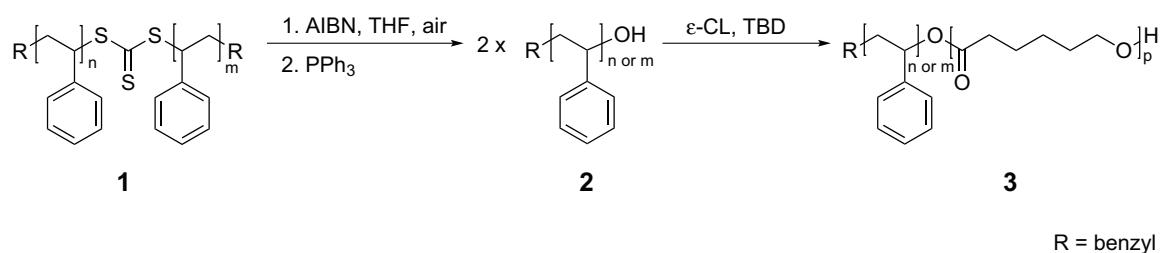
copolymer formation can be found by researchers including Zhang *et al.*, Mishra *et al.*, Bian *et al.* as well as Riess and coworkers.^[17,298–300] Starting from a RAFT polymer, Perrier and colleagues^[301] synthesized star-shaped copolymers by initiating a bifunctional thiourea organocatalyzed ROP of lactide from the hydroxyl function of the monomer (hydroxyethyl acrylate) previously polymerized by RAFT. Barner-Kowollik and colleagues^[302] combined simultaneous RAFT and ROP with Sn(Oct)₂ as catalyst to produce poly(2-hydroxyethyl methacrylate)-*g*-poly(ϵ -caprolactone) grafted copolymers. An alternative approach to block copolymer formation is via orthogonal modular ligation (*'click'* chemistry).^[303–305] For such an approach two homopolymers synthesized via RAFT and ROP are equipped with specific end functionalities, which react via for instance [2+3] or [2+4] cycloadditions to connect the homopolymers, forming a block copolymer.^[299,306–308]

In the following sections, novel avenues to block copolymer formation via a switch from RAFT polymerization to ROP are presented. The switch is generated either by the transformation reaction of the thiocarbonyl thio to hydroxyl functionalities, which was discussed in the previous chapter or by aminolysis of the RAFT end-group to obtain thiol terminated polymers, which subsequently can be employed as an initiator in the ROP process.

5.2. Poly(styrene)-*block*-poly(ϵ -caprolactone)

5.2.1. Introduction to pS-*b*-pCL Block Copolymers

The approaches mentioned above yield the desired block copolymer, however, the generated material contains the chemical functionality of the controlling agent, *e.g.*, a thiocarbonyl thio moiety of the employed RAFT agent. Thus, employing the RAFT process, it is difficult to generate sulfur-free block copolymers. To address this shortcoming, the method described in the previous chapter for quantitatively switching RAFT prepared polymers into hydroxyl terminal macromolecules that contain no sulfur and merely consist of the backbone monomer repeat units with a terminal OH function can be introduced.^[275,276] In this case, narrowly dispersed poly(styrene) (pS) were prepared via the RAFT process (employing the RAFT agent dibenzyltrithiocarbonate (DBTC)). Subsequently the thiocarbonyl thio groups were replaced by hydroxyl groups and the gained pS-OH was employed as macroinitiator in the ROP of ϵ -caprolactone (ϵ -CL), producing variable molar mass, sulfur-free narrow polydispersity pS-*b*-pCL block copolymers. PS was chosen as the radically prepared polymer due to its considerable polarity difference to pCL, which allows for a more facile chromatographic separation in two dimensional liquid chromatography than if for instance poly(methyl acrylate) or poly(methyl methacrylate) would have been employed as the first block. In addition, the ω -hydroxylation produces shelf-stable polymers without the possibility of intramolecular transesterification reactions occurring. The ROP process in the current study was organo-catalyzed (with 1,5,7-triazabicyclo[4.4.0]dec-5-ene (TBD)).^[148] The entire reaction sequence is depicted in Scheme 5.1.



Scheme 5.1 Reaction sequence depicting the generation of poly(styrene)-*block*-poly(ϵ -caprolactone) copolymers **3** from a narrowly dispersed RAFT precursor **1**, which is quantitatively transformed into a hydroxyl-terminal ROP initiator **2**.

Each step of the synthetic process is carefully monitored via (multi-dimensional) chromatographic techniques to prove the efficacy of the transformations. Inspection of the literature indicates that the most commonly employed approach towards the characterization of block copolymers prepared via living polymerization/ROP is via conventional SEC based on a linear calibration of the first block.^[18,19,309] However, via conventional SEC techniques – at best – only the (absolute) molar mass of the re-

spective block copolymer can be determined. In addition, conventional SEC typically provides only limited information on the chemical composition of a polymer sample, if not interfaced with chemically sensitive detectors such as NMR^[310,311] or mass spectrometry.^[312–314] An alternative technique that can provide chemical information when hyphenated with SEC is liquid chromatography at critical conditions (LCCC), which enables the separation of block copolymer samples by their chemical heterogeneity in the absence of size-exclusion effects of one block segment. The method is described in Chapter 2.5.3. Thus, this powerful tool can be used for instance to separate the block copolymer from homopolymer residues. Combining LCCC and SEC in a two dimensional chromatography set-up provides information about the chemical composition and the molar masses of the synthesized sample, respectively. To name but a few examples, Matyjaszewski and colleagues employed the LCCC technique to characterize linear and star shaped block copolymers synthesized via ATRP polymerization^[315]. Variable length block copolymers of poly(methyl methacrylate)-*block*-poly(*tert*-butyl methacrylate) formed via living anionic polymerization were analyzed via two dimensional chromatography by Falkenhagen and Müller.^[205] Further Pasch and colleagues employed LCCC-SEC to study block copolymers that were synthesized by coupling two homopolymers.^[208] For key references on LCCC-SEC coupling as well as its application and development, the reader is referred to Chapter 2.5.5. The characterization of the poly(styrene)-*block*-poly(ϵ -caprolactone) polymers prepared in the current chapter is also carried out via LCCC-SEC (besides several other characterization techniques) to establish their structure as exactly as possible. Thus, the key aim of this chapter is to evidence that the ω -functionality switch of RAFT prepared polymers to a hydroxyl-terminal function can be efficiently employed for a switch in polymerization mechanism enabling the generation of well-defined block-copolymers.

5.2.2. Synthesis

The materials and the characterization methods used in this chapter can be found in Chapter 3.

Preparation of the RAFT Polymer pS **1**

A solution of dibenzyltrithiocarbonate (DBTC) (10.27 mmol L⁻¹) and 2,2'-azobis(isobutyronitrile) (4.36 mmol L⁻¹) in styrene (50 mL) was degassed by purging with nitrogen for 15 min. The solution was heated to 60 °C for 540 min, after which the reaction was stopped by cooling in liquid nitrogen. The residual monomer was removed under vacuum and the polymers precipitated in cold methanol. The number-average molar mass was determined via SEC after precipitation ($M_n = 10500$ g mol⁻¹, $PDI = 1.3$).

End-group Switching (Synthesis of Species **2**)^[276]

A solution of 2,2'-azobis(isobutyronitrile) (10 mmol L^{-1}) in THF was heated to $60 \text{ }^\circ\text{C}$ for 120 min under ambient air. 500 mg RAFT-polymer (10 mmol L^{-1} based on its M_n) were dissolved in the pre-treated THF in ambient atmosphere. The filled flask was heated to $60 \text{ }^\circ\text{C}$ under vigorous stirring. After a discoloration of the solution indicated full conversion, the temperature was reduced to $40 \text{ }^\circ\text{C}$ and 3 equiv. triphenylphosphine were added. After 60 min the polymer was precipitated in cold methanol. The average molar mass was determined by SEC after precipitation ($M_n = 6500 \text{ g mol}^{-1}$, $PDI = 1.2$). A MALDI-TOF mass spectrum of **2** can be found in Figure 5.2.

Ring-Opening Polymerization (Synthesis of Species **3**)

The ring-opening polymerization was performed in an inert gas atmosphere (argon) inside a glove box to rigorously exclude water from the reaction system. ϵ -CL was added to a solution of TBD and pS-OH in toluene. The solution was stirred for 5 h and subsequently quenched by addition of benzoic acid. The polymer was precipitated in cold methanol. The concentrations of the reacting agents and the resulting molar masses of the block copolymers are collated in Table 5.1.

Table 5.1. Reaction conditions and number-average molar masses, M_n , of the ring-opening polymerizations to generate poly(styrene)-*block*-(ϵ -caprolactone) polymers. $c_{\text{pS-OH}}^0$ and c_{TBD}^0 are the initial concentrations of the macroinitiator and the organo-catalyst, respectively.

$c_{\text{pS-OH}}^0$ / mmol L^{-1}	c_{TBD}^0 / mmol L^{-1}	M_n / g mol^{-1}	<i>PDI</i>
10.3	2.6	26000	1.3
8.8	2.2	37000	1.1
7.6	1.9	44000	1.1
6.8	1.7	45000	1.1

Hydrolysis of pS-*b*-pCL **4**

The block copolymer (0.1 g) was dissolved in tetrahydrofuran and hydrochloric acid ($c = 0.002 \text{ mol L}^{-1}$) was added. The solution was stirred for 74 h at ambient temperature. The solvent was removed and the polymer was precipitated in cold methanol. The resulting molar masses of the hydrolyzed polymer are summarized in Table 5.4.

Ring-Opening Polymerization with 2-Butanol as the ROP Initiator

The ring-opening polymerization was performed in an inert gas atmosphere (argon) inside a glovebox to rigorously exclude water from the reaction system. ϵ -CL (0.226 g, 2.0 mmol) was added to a solution of TBD (1.4 mg, 10 μ mol) and 2-butanol (2.3 mg, 40 μ mol) in toluene. The solution was stirred for 5 h and subsequently quenched via the addition of benzoic acid. The polymer was precipitated in cold hexane : diethyl ether (1:1) mixture. The average molar mass was determined by SEC after precipitation ($M_n = 8400 \text{ g mol}^{-1}$, $PDI = 1.4$). To obtain the lower molar mass of $M_n = 5500 \text{ g mol}^{-1}$, the amount of initiator and catalyst was doubled.

Synthesis of pS for the Subsequent Orthogonal Conjugation Block Copolymer Formation (Synthesis of Species 5)

A solution of pyridine-2-ylidithioformate (BPDF) (0.397 g, 1.62 mmol) and AIBN (0.043 g, 0.27 mmol) in styrene (80 mL, 0.7 mol) was degassed by purging with nitrogen for 30 min. The solution was heated to 60 °C for 660 min, after which the reaction was stopped by cooling in liquid nitrogen. The residual monomer was removed under vacuum and the polymers precipitated in cold methanol. The number-average molar mass was determined via SEC after precipitation ($M_n = 3600 \text{ g mol}^{-1}$, $PDI = 1.1$).

Synthesis of pCL for the Subsequent Orthogonal Conjugation Block Copolymer Formation (Synthesis of Species 6)

The ring-opening polymerization was performed in an inert gas atmosphere (argon) inside a glovebox to rigorously exclude water from the reaction system. ϵ -CL (226 mg, 2.0 mmol) was added to a solution of TBD (1.4 mg, 10 μ mol) and trans,trans-2,4-hexadien-1-ol (8 mg, 40 μ mol) in toluene. The solution was stirred for 5 h and subsequently quenched by addition of benzoic acid. The polymer was precipitated in cold methanol. The number-average molar mass was determined via SEC after precipitation ($M_n = 4100 \text{ g mol}^{-1}$, $PDI = 1.3$).

Synthesis of the pS-*b*-pCL Block Copolymer (Synthesis of Species 7)

Hetero Diels-Alder cycloaddition between pyridine-2-ylidithioformate terminated pS and hexadienoyl terminated poly(ϵ -caprolactone):

A solution of pS ($M_n = 3600 \text{ g mol}^{-1}$, 17 μ mol), pCL ($M_n = 4100 \text{ g mol}^{-1}$, 17 μ mol) and 1.1 eq TFA (2 μ L, 19 μ mol) in chloroform was kept at 50 °C for 2 hours. The polymer was isolated by removing the solvent in vacuo. GPC (THF): $M_n = 7000 \text{ g mol}^{-1}$, $PDI = 1.3$.

Preparation of the RAFT Polymer pS **8**

A solution of dibenzyltrithiocarbonate (DBTC) ($10.27 \text{ mmol L}^{-1}$) and 2,2'-azobis(isobutyronitrile) (4.36 mmol L^{-1}) in styrene (50 mL) was degassed by purging with nitrogen for 15 min. The solution was heated to $60 \text{ }^\circ\text{C}$ for 660 min, after which the reaction was stopped by cooling in liquid nitrogen. The residual monomer was removed under vacuum and the polymers precipitated in cold methanol. The number-average molar mass was determined via SEC after precipitation ($M_n = 13000 \text{ g mol}^{-1}$, $PDI = 1.3$).

End-group Switching (Synthesis of Species **9**)

A solution of 2,2'-azobis(isobutyronitrile) (10 mmol L^{-1}) in THF was heated to $60 \text{ }^\circ\text{C}$ for 120 min under ambient air. 500 mg RAFT-polymer (10 mmol L^{-1} based on its M_n) were dissolved in the pre-treated THF in ambient atmosphere. The filled flask was heated to $60 \text{ }^\circ\text{C}$ under vigorous stirring. After a discoloration of the solution indicated full conversion, the temperature was reduced to $40 \text{ }^\circ\text{C}$ and 3 equiv. triphenylphosphine were added. After 60 min the polymer was precipitated in cold methanol. The number-average molar mass was determined by SEC after precipitation ($M_n = 9100 \text{ g mol}^{-1}$, $PDI = 1.3$).

Ring-Opening Polymerization (Synthesis of Species **10**)

The ring-opening polymerization was performed in an inert gas atmosphere (argon) inside a glove box. ϵ -CL was added to a solution of TBD ($c_{\text{TBD}}^0 = 5 \text{ mmol L}^{-1}$) and pS-OH ($M_n = 9100 \text{ g mol}^{-1}$, $PDI = 1.3$; $c_{\text{pS-OH}}^0 = 20 \text{ mmol L}^{-1}$) in toluene. The solution was stirred for 5 h and subsequently quenched by addition of benzoic acid. The polymer was precipitated in cold methanol. The number-average molar mass was determined by SEC after precipitation ($M_n = 12000 \text{ g mol}^{-1}$, $PDI = 1.2$).

5.2.3. Results and Discussion

The initial step in the generation of sulfur free poly(styrene)-*block*-poly(ϵ -caprolactone) polymers is the quantitative conversion of the thiocarbonyl thio end-groups into terminal hydroxyl functionalities (see Scheme 5.1). The reaction sequence employed for this purpose - alongside its exact mechanism - has been previously described in detail and exemplified on a series of RAFT made polymers with a wide variety of monomers and initial RAFT agents (see Chapter 4).^[276] The importance of the above efficient functionality switching lies in the fact that a polymer synthesized via RAFT polymerization can be quantitatively transformed into a sulfur free polymer with a well-defined

hydroxyl end-group. Moreover, the converted (former thiocarbonyl thio capped) polymer can be employed as ROP macroinitiator due to its OH end-group functionality. In the present case poly(styrene), synthesized via RAFT polymerization employing a symmetrical trithiocarbonate as mediating agent, was used for the modification. Since the trithiocarbonate group is located (when considering an average over all chains) in the middle of the polymer, the resulting OH-terminal macromolecules will be divided into two polymer segments during the modification.

In Figure 5.1, the SEC traces of the trithiocarbonate functional and the switched polymers are depicted. Inspection of the figure indicates a clear shift in molar mass.

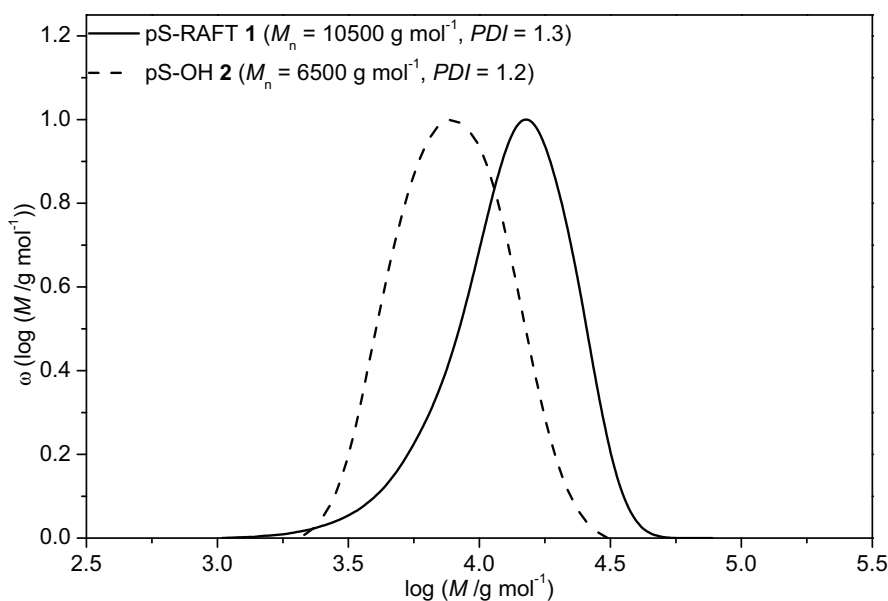


Figure 5.1. SEC traces of poly(styrene) with a trithiocarbonate moiety in the middle of the chain (pS-RAFT **1**) and the same poly(styrene) after the end-group switching (pS-OH **2**).

Although the molar mass is not exactly halved (decreasing from 10500 to 6500 g mol⁻¹), the end-group conversion has functioned as desired as the inspection of the MALDI-TOF spectra (see Figure 5.2) attests. No starting thiocarbonyl thio compound can be discerned and the agreement between the experimentally observed and the theoretically expected molar masses is excellent.

As can be seen in Scheme 5.1, the resulting poly(styrene) pS-OH **2** possesses a secondary alcohol function. In the following, the alcohol functionality was employed as a macroinitiator to commence the ring-opening polymerization. ϵ -Caprolactone was selected as the monomer for the subsequent ring-opening polymerization under conditions of organo-catalysis employing 1,5,7-triazabicyclo[4.4.0]dec-5-ene (TBD). The choice of ϵ -caprolactone as the monomer for the block formation is based on its relatively high hydrolytic stability compared for instance to lactides,^[316] thus avoiding

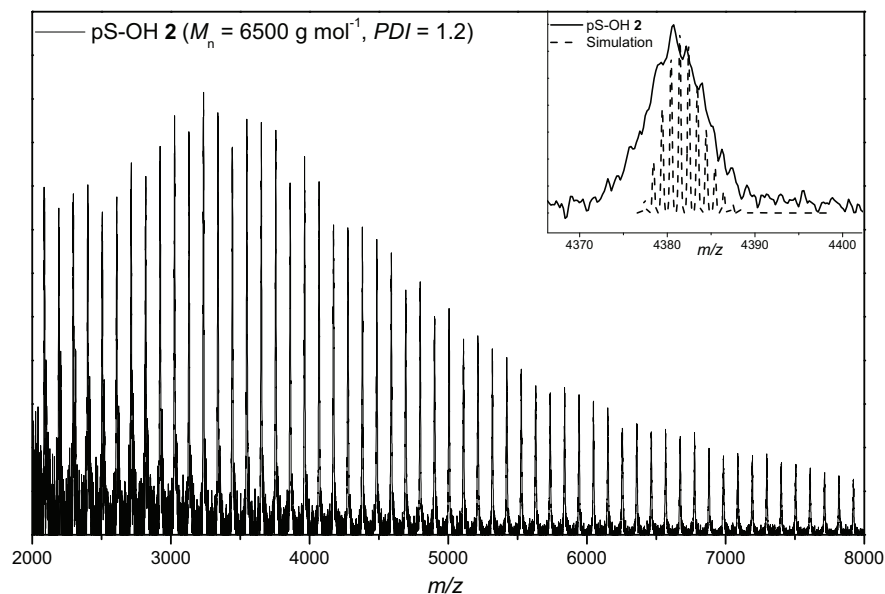


Figure 5.2. MALDI-TOF-MS of pS-OH **2** ($P_{R,40}$ OH; $[M + Ag]^+ : m/z^{\text{theo}} = 4381 \cdot 46$; $m/z^{\text{exp}} = 4380 \cdot 68$; $\Delta m/z = 0.78$). The inset depicts a zoom into a single repeat unit and the associated simulated isotopic pattern. Note that due to the higher masses, the isotopic resolution is limited.

polymer degradation problems during storage and the chromatographic analytical procedures. To ensure that secondary alcohols can indeed efficiently commence ring-opening polymerizations, a series of trial reactions employing 2-butanol as the ROP initiator were performed, indicating an efficiently operating ROP. The corresponding SEC elugrams and the SEC/ESI-MS spectrum of the pCL's initiated with 2-butanol are depicted in Figure 5.3. In Table 5.2 the theoretical and measured m/z ratios of the main species obtained via ESI-MS are collated.

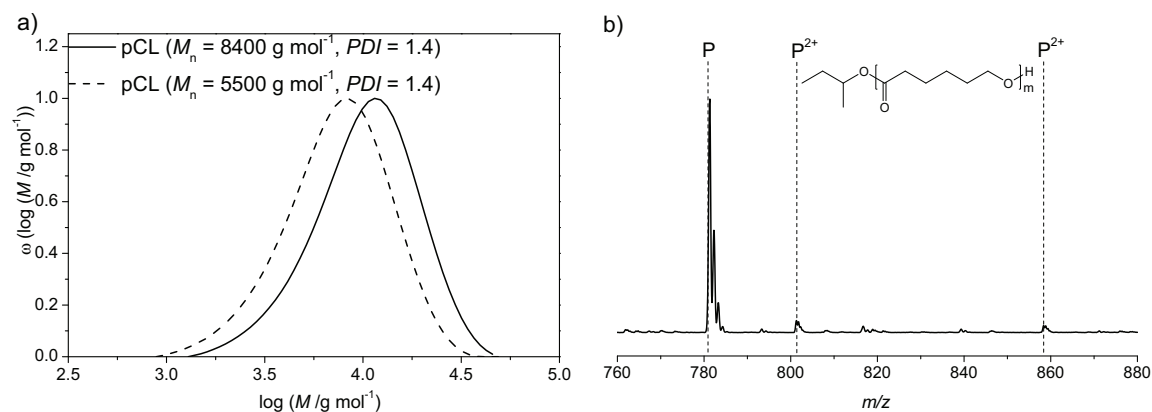
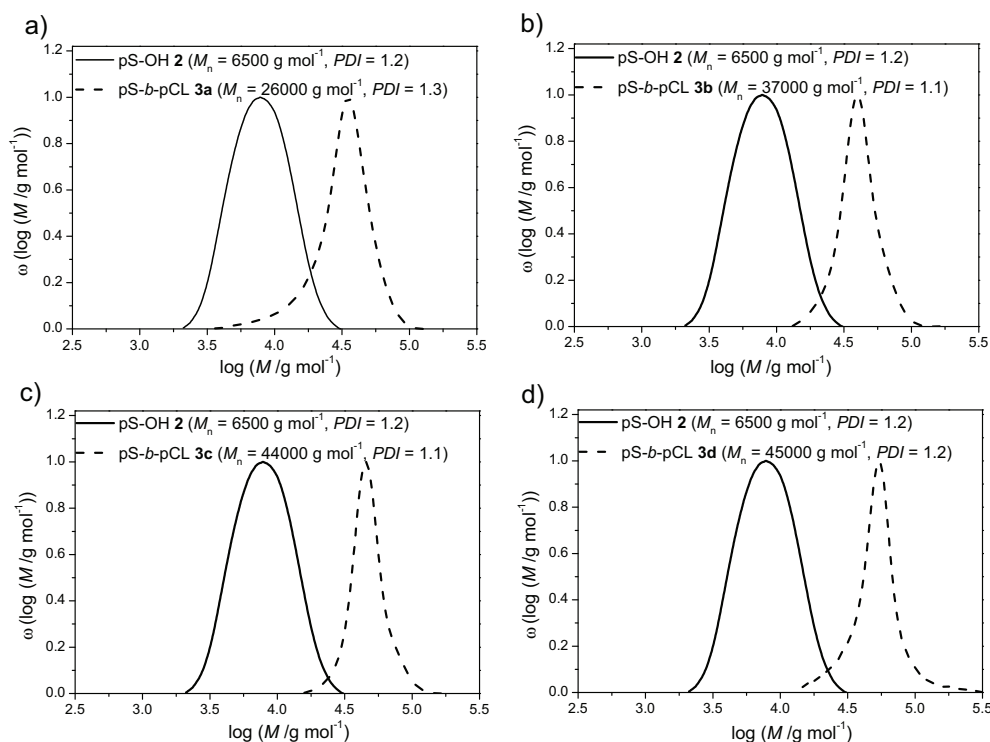


Figure 5.3. a) SEC of poly(ϵ -caprolactone) initiated by the secondary alcohol 2-butanol. b) Zoom of the electrospray ionization mass spectrum of pCL **P** with 2-butanol as the ROP initiator.

Table 5.2. Theoretical and measured m/z ratios of the main species of the pCL initiated with 2-butanol.

Structure	$[M + Na]^+$		
	m/z^{theo}	m/z^{exp}	$\Delta m/z$
P	781.67	781.52	0.15
P²⁺	801.50	801.58	0.08
P²⁺	858.53	858.67	0.14

**Figure 5.4.** SEC traces of the block copolymers (pS-*b*-pCL, **3a-d**) synthesized via chain extension employing pS-OH **2** as a macroinitiator and ϵ -CL as a monomer. The individual molar masses and polydispersities of the block copolymers are provided within each sub-figure.

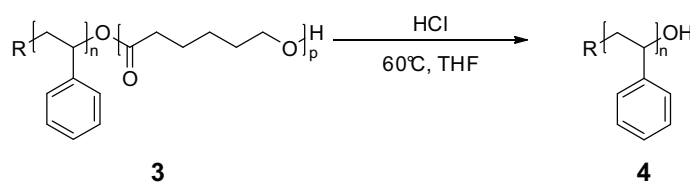
In Figure 5.4, the SEC traces of the block copolymers **3** based on the macroinitiator pS-OH **2** ($M_n = 6500 \text{ g mol}^{-1}$) are depicted. To obtain block copolymers with varying molar masses (*i.e.*, a varying length of the poly(ϵ -caprolactone) block), the ratio between macroinitiator and monomer was systematically varied. The reactants concentrations' data associated with the synthesized block polymers are collated in Table 5.1, whereas the individual number-average molar masses for each generated block copolymer, alongside its polydispersity, have been collated in Table 5.3. The obtained block copolymers vary in number-average molar mass between 26000 and

45000 g mol⁻¹ (relative to poly(styrene) standards). As expected, a significant shift in molar mass from the OH-terminal poly(styrene) macroinitiator to the various block copolymers can be observed. Visual inspection of the obtained block copolymer weight distributions suggests that – at least in Figure 5.4 – no significant amount of the initiator pS-OH **2** seems to remain in the final block copolymers. Taking Figure 5.4c as an example, it can be clearly observed that only minimal overlap between the molar mass distribution of the macroinitiator and the generated block copolymer exists.

Table 5.3. Collation of the number-average molar mass, M_n , and the peak molar mass, M_p , as well as the *PDI* of the precursor polymers **1** and **2**, as well as of the ROP generated block copolymers **3a-d**.

Sample	Polymer	M_n	M_p	<i>PDI</i>
		/ g mol ⁻¹	/ g mol ⁻¹	
1	pS-RAFT	10500	15500	1.3
2	pS-OH	6500	7800	1.2
3a	pS- <i>b</i> -pCL	26000	35000	1.3
3b	pS- <i>b</i> -pCL	37000	40000	1.1
3c	pS- <i>b</i> -pCL	44000	49000	1.1
3d	pS- <i>b</i> -pCL	45000	49000	1.2

While Figure 5.4 provides evidence for the formation of the desired poly(styrene)-*block*-poly(ϵ -caprolactone) polymers, further analysis is required to substantiate their structure. Thus, to further underpin the existence of the block copolymers, it seems a logical next step to remove the poly(ϵ -caprolactone) block under acid catalyzed conditions (see Scheme 5.2).^[317] If a block copolymer was formed, only the poly(styrene)



Scheme 5.2 Acid catalysed hydrolysis of the poly(ϵ -caprolactone) block **3**, reforming the original poly(styrene) block **4**.

block **4** should remain. Figure 5.5 depicts the SEC traces of the initial macroinitiator **2**, the block copolymer **3** and the re-generated macroinitiator after being hydrolyzed **4**. Inspection of Figure 5.5 reveals a clear shift between block copolymer **3** and the hydrolyzed polymer **4**. Importantly, the reformed macroinitiator **4** features nearly the same molar mass distributions and molar mass as the initial macroinitiator **2**. The slight deviations in the molar mass distribution between **2** and **4** lie within the accuracy of an SEC experiment and/or – considerably less likely – that one (or at most two) CL units closest to the poly(styrene) block were not completely hydrolyzed. The

hydrolysis results of samples **3a** to **3d** are collated in Table 5.4.

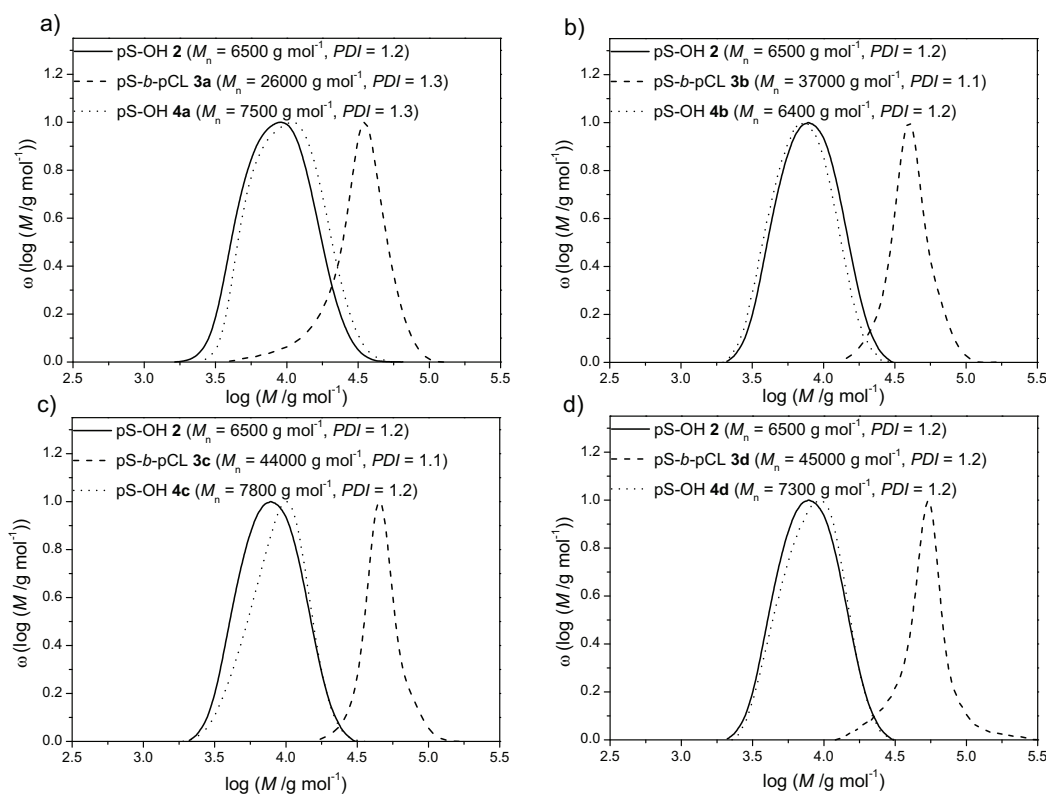


Figure 5.5. SEC traces of the initial macroinitiator poly(styrene) **2**, the block copolymer **3a-d**, and the polymer after being hydrolyzed **4a-d**.

Table 5.4. Collation of the results (number-average molar mass, M_n , and polydispersity, PDI) from the hydrolysis experiments subjecting **3a** to **3d** to the procedure depicted in Scheme 5.2.

sample	M_n^{block} / g mol ⁻¹	M_n^{hydro} / g mol ⁻¹	PDI^{hydro}
4a	26000	7500	1.3
4b	37000	6400	1.2
4c	44000	7800	1.2
4d	45000	7300	1.2

It is gratifying to note that the above hydrolysis reaction sequence seems to support the block copolymer hypothesis. However, a confirmation on a molecular level is nevertheless required. Consequently, the (quantitative) removal of the poly(ϵ -caprolactone) block is additionally evidenced via ¹H-NMR spectroscopy. Figure 5.6 depicts the proton resonance spectra of block copolymer **3a** ($M_n = 26000$ g mol⁻¹) as well as of the polymeric material **4a** after the hydrolysis reaction sequence ($M_n = 7500$ g mol⁻¹). The ¹H-NMR spectrum of the block copolymer **3a** is depicted by the solid line, whereas the dashed line represents the ¹H-NMR spectrum of the hydrolyzed polymer **4a**. Ev-

ery resonance is labeled with a character signifying the chemical shift of the different protons of the individual polymers: a, b and c represent the resonances of the poly(styrene) block, while d-h are associated with the poly(ϵ -caprolactone) block (the detailed assignments are provided within the figure). Comparing the two spectra it can clearly be observed that the resonances resulting from the poly(ϵ -caprolactone) block are only observed in the spectrum of the block copolymer **3** and are completely absent in the spectrum of the hydrolyzed polymer **4**; in the spectrum of the hydrolyzed polymer only the characteristic resonances of poly(styrene) remain. The NMR spectra of the block copolymers allow for the calculation of the length of each individual block via a comparison of the proton resonance h' with the resonances of protons associated with pS and pCL, respectively. For **3a**, integration via the above procedure

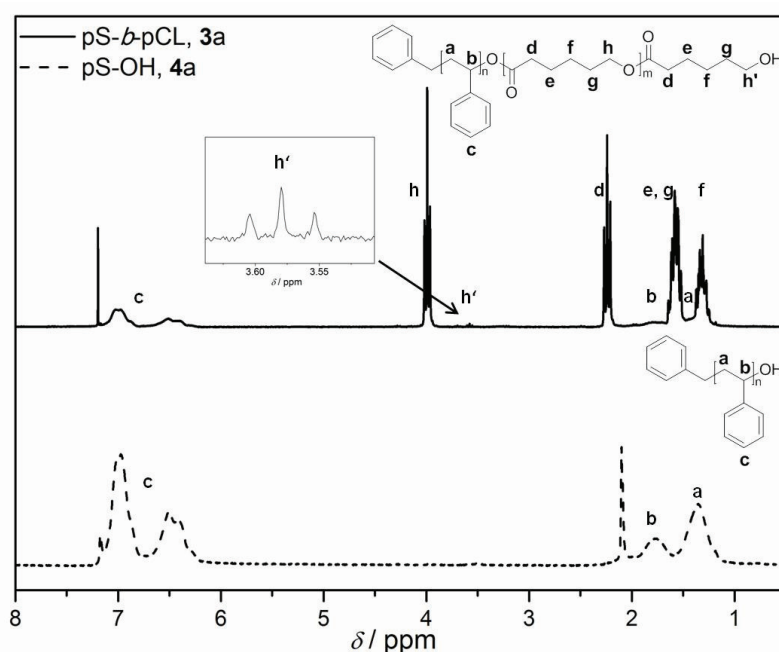


Figure 5.6. ^1H -NMR spectra in CDCl_3 of the block copolymer **3a** (26000 g mol^{-1}) and the poly(styrene) block **4a** (7500 g mol^{-1}) after the acid-catalyzed hydrolysis on the example of sample **3a** (see Table 5.4). The shift at 2.1 ppm is due to acetone residue.

yields a pS block length of 6500 g mol^{-1} , while the corresponding length for pCL reads 15500 g mol^{-1} , giving a total block copolymer molar mass of 22000 g mol^{-1} . It should be noted that the NMR determined block length of **2** is in excellent agreement with its SEC determined length ($M_n^{\text{SEC}} = 6500 \text{ g mol}^{-1}$). In addition, the block copolymer mass of **3a** determined via NMR is in equally good agreement with that determined via SEC ($M_n^{\text{SEC}} = 26000 \text{ g mol}^{-1}$), considering that the molar mass of **3a** is reported relative to poly(styrene) equivalents. For the highest molar mass block copolymer **3d**, the situation is equally satisfying: $M_n^{2,\text{NMR}} = 7100 \text{ g mol}^{-1}$ vs $M_n^{2,\text{SEC}} = 6500 \text{ g mol}^{-1}$, $M_n^{\text{pCL,NMR}} = 33000 \text{ g mol}^{-1}$, $M_n^{3d,\text{NMR}} = 40100 \text{ g mol}^{-1}$ vs $M_n^{3d,\text{SEC}} = 45000 \text{ g mol}^{-1}$. Note that the block length of **2** is determined via the (overall) pCL end-group h' in

good agreement with its SEC value. Such a situation can only occur if a true block copolymer has formed. Thus, the block copolymer nature of **3** has been established with high certainty.

In the above section, it was the aim to evidence that the transformation sequence depicted in Scheme 5.1 is truly operational and that indeed the block copolymer **3** is generated. In the following, a more thorough chromatographic analysis of **3** will be presented – employing LCCC coupled to SEC – to assess in detail if residues of **2** are found in **3**. In the first dimension (LCCC) the polymer is separated (ideally) only with respect to the block length of one block whereas the other block behaves ‘critical’ (*i.e.*, under CC of pS without size-exclusion effects), elutes independently from its molar mass and may be termed ‘invisible’. Thus a distinction between remaining traces of **2** in **3** should be achievable. To record a complete LCCC-SEC image of a polymer, liquid chromatography at critical conditions is typically performed in the first dimension. Therefore, knowledge of the critical conditions of both or at least one homopolymer constituting the block copolymer, *i.e.*, poly(styrene) and/or poly(ϵ -caprolactone), are required. At the critical point of adsorption, polymers with identical monomer units, the same structure and the same end-group yet with different molar masses elute at the same time. To achieve critical conditions, a binary solvent mixture was employed. In Figure 5.7, the elugrams of variable molar mass pS-OH’s at their critical conditions are depicted. As the solubility of **3** under the critical conditions of pS is excellent, the corresponding solubility under CC of pCL is poor and the ensuing chromatographic analysis is thus complex. It is for this reason that in the current contribution the critical conditions of pS are employed. Inspection of Figure 5.7 clearly indicates that the elution times for each polymer are invariant to the molar mass; critical conditions have thus been established. The critical conditions for the poly(styrene)s **2** were established on a silica based reversed phase column (RP18) with an eluent mixture of THF (88.4 % (v/v)) and water (11.6 % (v/v)). The applied solvent combination THF/H₂O is beside THF/ACN a common solvent mixture for LCCC of poly(styrene) and was used (amongst others) by Philipsen et al.^[318] as well as Beaudoin et al.^[319]

Subsequently, the established critical conditions of pS were employed to subject the block copolymers **3** to LCCC-SEC. Figure 5.8 depicts the elugrams of the block copolymers (identical to those shown in Figure 5.4) under critical conditions of the homopolymer pS. At the critical conditions (CC) of poly(styrene), the block copolymers elute in the SEC mode (*i.e.*, retention time/volume inversely proportional to their individual hydrodynamic volume). Thus, copolymers with a higher fraction of poly(ϵ -caprolactone) elute at lower elution volumes than with a lower fraction; this notion can be confirmed via inspection of Figure 5.8, where the highest pCL containing polymers elute at the lowest retention time (**3d**), whereas the polymers with the lowest fraction of pCL elute at the highest retention times (**3a** and **7**), see below for

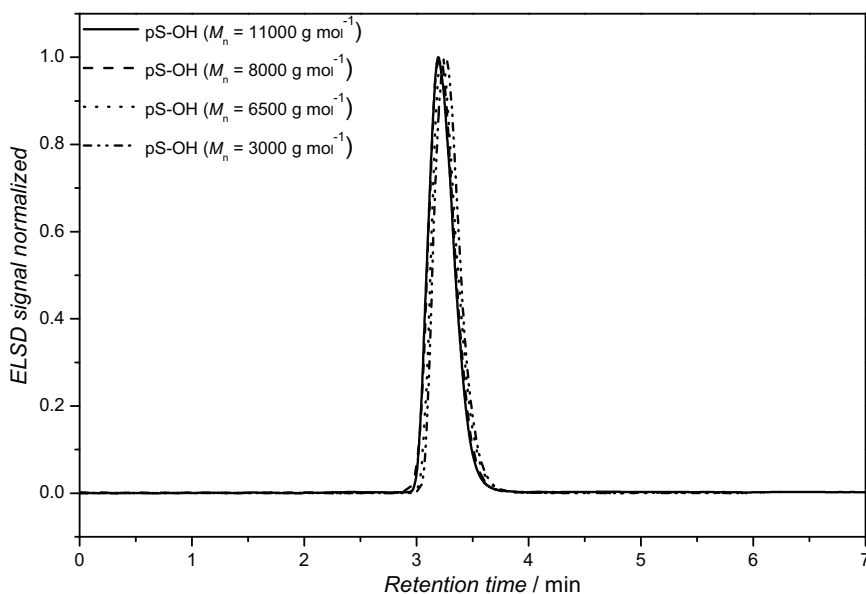


Figure 5.7. Critical conditions of variable pS-OH **2**. To obtain critical conditions a RP18 column with a solvent mixture of THF : H₂O = 88.4 : 11.6 % (v/v) with addition of 0.1 vol-% acetic acid was employed.

a discussion on the nature of polymer **7**.

Further inspection of Figure 5.8 indicates that the elugrams of the copolymers under the CC of pS possess a slight shoulder (tailing) in the region of the poly(styrene) elution time. Such an observation may be indicative of a small amount of pS homopolymer within the copolymer samples. Indeed, the potential amount of homopolymer pS within the sample is best visible in the 26000 g mol⁻¹ material (**3a**, dashed line in Figure 5.8). To underpin the analytical efforts, it would be desirable to have a poly(styrene)-*block*-poly(ϵ -caprolactone) polymer, where the reaction sequence leaves no other outcome as the formation of the block structure. Such a situation can be achieved when the block copolymer is prepared via a modular reaction pathway, which has been recently described in the literature based on a combination of RAFT and hetero Diels-Alder chemistry (RAFT-HDA),^[55] and was consequently employed to prepare a model pS-*b*-pCL polymer **7** for the present study. The characterization of the block copolymer **7** ($M_n = 7000$ g mol⁻¹, $PDI = 1.3$) via one-dimensional SEC can be found in Figure 5.9 and a schematic representation of the RAFT-HDA synthetic pathway is depicted in Scheme 5.3.

The LCCC elugram of the modularly constructed block copolymer **7** is shown in Figure 5.8 alongside the block copolymers **3a-d** prepared via sequential design. As block copolymer **7** only contains a pCL block length of 4100 g mol⁻¹, it is in elution volume close to the homopolymer pS. The reason for constructing **7** with smaller individual block lengths is to ensure that the modular ligation reaction proceeds to high

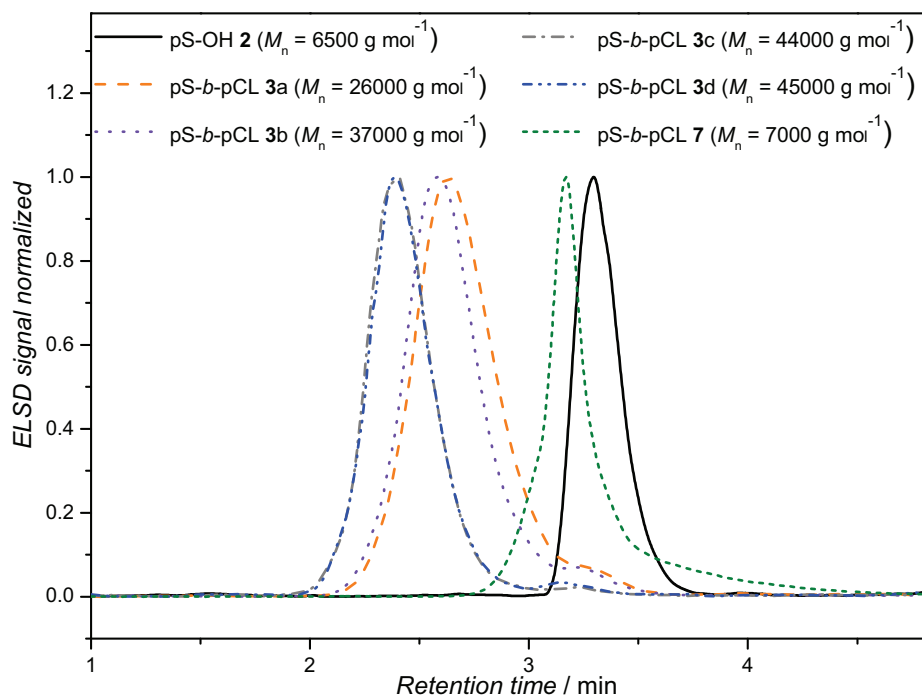


Figure 5.8. LCCC elugrams of pS-*b*-pCL block copolymers **3a-d** and **7** at the critical conditions of pS-OH **2** (THF:H₂O = 88.4 : 11.6 % (v/v) with addition of 0.1 vol-% acetic acid).

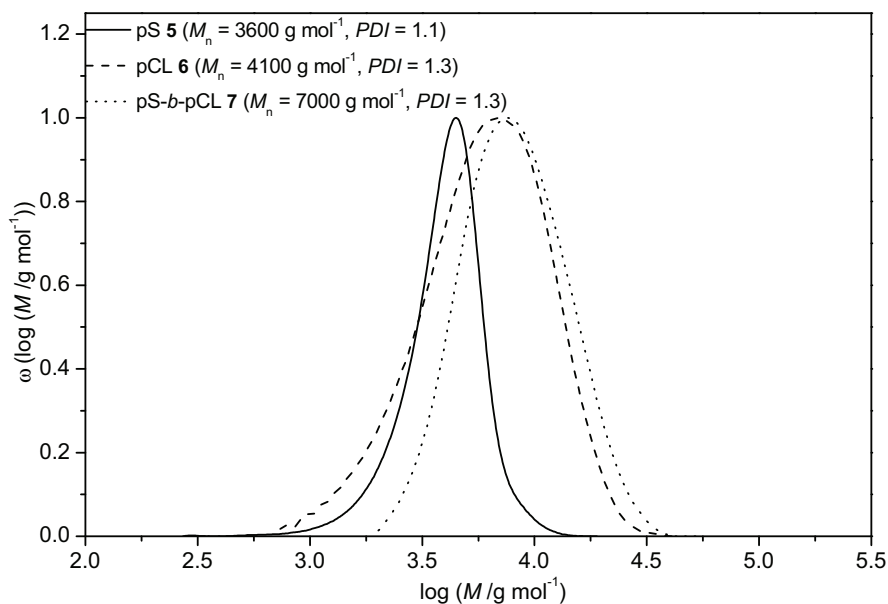
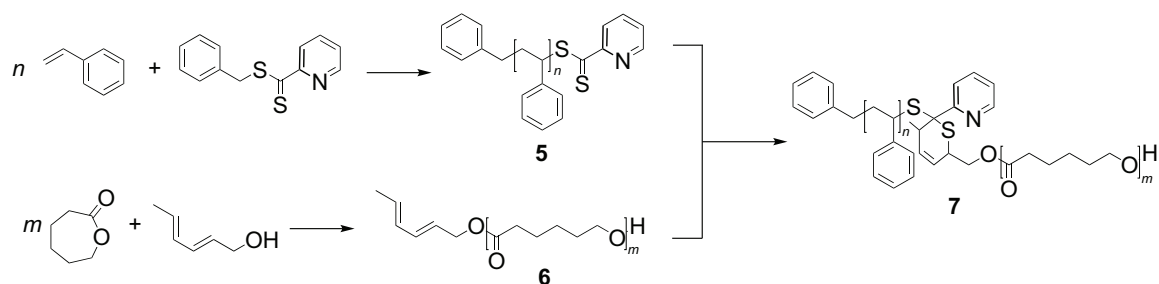


Figure 5.9. SEC trace of the block copolymer pS-*b*-pCL synthesized via modular hetero Diels-Alder chemistry, compared with the SEC traces of the starting material pS and pCL.



Scheme 5.3 Orthogonal modular construction of pS-*b*-pCL **7** copolymer via hetero Diels-Alder chemistry from a diene functional pCL **6** and a thiocarbonyl thio functional pS **5** precursor.

conversions and is not hampered by chain length effects. In order to obtain an initial image of a LCCC-SEC chromatogram of poly(styrene)-*block*-poly(ϵ -caprolactone) copolymers, a 2D chromatographic analysis of **7** was carried out, which is depicted in Figure 5.10. In such 2D plots, the x-axes depict the SEC trace, the y-axes the LCCC trace and the z-axes the intensity of the ELS detector signal. One broad spot can be observed, which features a diagonal shape due to the SEC mode, in which the block copolymer elutes due to the presence of pCL. Initially, the higher molar masses elute, whereas at higher retention times the lower molar masses of the block copolymer elute. Inspection of the 2D image thus indicates that the block copolymer **7** has formed in high yields, yet that also a small amount of homopolymer pS (eluting at LCCC elution volumes of close to 1.6 mL) may be present in the sample. A quantification of these amounts of pS is challenging due to the similar elution volumes of **2** and **7** in the LCCC dimension.

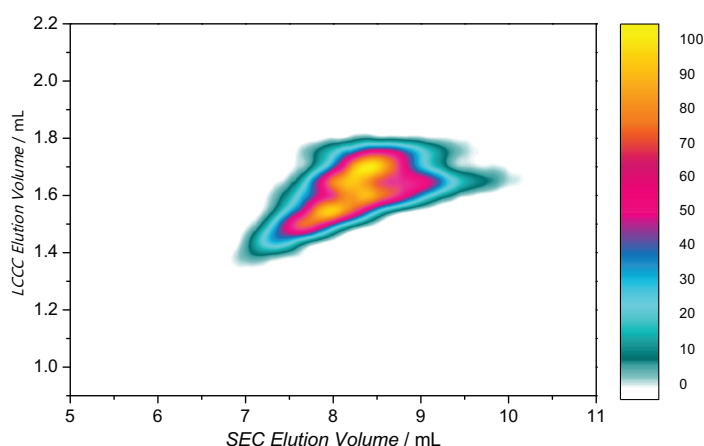


Figure 5.10. 2D LCCC-SEC analysis of the block copolymer pS-*b*-pCL **7** ($M_n = 7000 \text{ g mol}^{-1}$, $PDI = 1.3$) synthesized via a hetero Diels-Alder cycloaddition (see Scheme 5.3 for the representation of the synthetic pathway) at the critical conditions of pS (THF (88.4 % (v/v)) and H_2O (11.6 % (v/v))).

Two dimensional chromatography was subsequently performed on the block copolymers synthesized via RAFT/ROP **3**. The LCCC-SEC plot of two of the block copolymer samples (**3a** and **b**) is shown in Figure 5.11. The LCCC of the two dimensional chromatography was performed at the critical conditions of poly(styrene) **2**. Inspection of Figure 5.11 – depicting the 2D plots – clearly indicates that no or only little residual amount of **2** is visible and that the 2D chromatograms compare favorably with that of **7** (see Figure 5.10). Such an observation implies that the percentage of remaining **2** in Figure 5.11b (copolymer **3b**) – which was speculated upon during the discussion of Figure 5.8 above – within the block copolymer material **3** is likely lower than 5% (see the scaling of the color coded legend in Figure 5.11). In the case of copolymer **3a** (Figure 5.11a), some residual **2** (elution volume close to 1.6 mL) can be discerned in agreement with the observations in Figure 5.8. The amount of residual **2** in **3a** is estimated to be in slight excess of 5% (around 7 to 8%). It can further be observed that the spots are not round circles but diagonal shapes, mainly caused by the fact that the block copolymer elutes in SEC mode due to the present pCL as also discussed above for Figure 5.10.

Finally, it would be instructive to assess how a LCCC-SEC chromatogram appears, when the synthetic sequence was not as successful as in the above cases. The associated synthesis of the synthesized block copolymer with conventional SEC can be found in the Synthesis section (species **9** (pS-OH, $M_n = 9100 \text{ g mol}^{-1}$, and poly(styrene)-*block*-poly(ϵ -caprolactone) **10**, $M_n = 12000 \text{ g mol}^{-1}$). For this purpose, an example of a block copolymer sample is analyzed and discussed below, where **9** and poly(ϵ -caprolactone) initiated by for instance residues of water, is present. In Figure 5.12, the LCCC elugram (a) at critical conditions of poly(styrene) and a 2D plot (b) of the block copolymer **10** are depicted. The LCCC elugram displays a multi-modal structure with three clearly discernible species' contributions. Such a result implies that the sample is not homogeneous, but rather contains three types of polymer structures. The shoulder towards higher retention time is observed to overlap with the signal of the poly(styrene) **9** that was employed as the macroinitiator. The occurrence of **9** in **10** indicates that the starting material was not completely consumed during the reaction. As such, proof of remaining **9** was obtained by performing a two dimensional chromatographic analysis (see Figure 5.12). Three (well) separated spots can be observed: Spot (I) is assigned to the block copolymer since it features the typical diagonal shape observed for **3** (see Figure 5.10 and Figure 5.11) due to the fact that the block copolymer elutes in the SEC mode. The macroinitiator poly(styrene) is allocated to spot (III), since it emerges exactly at the critical point of pS-OH. A third spot (II) appears, which is most probably associated with poly(ϵ -caprolactone) that was initiated by water residues present in the reaction mixture.

Variable reasons for the incomplete conversion of the chain extension reaction in this

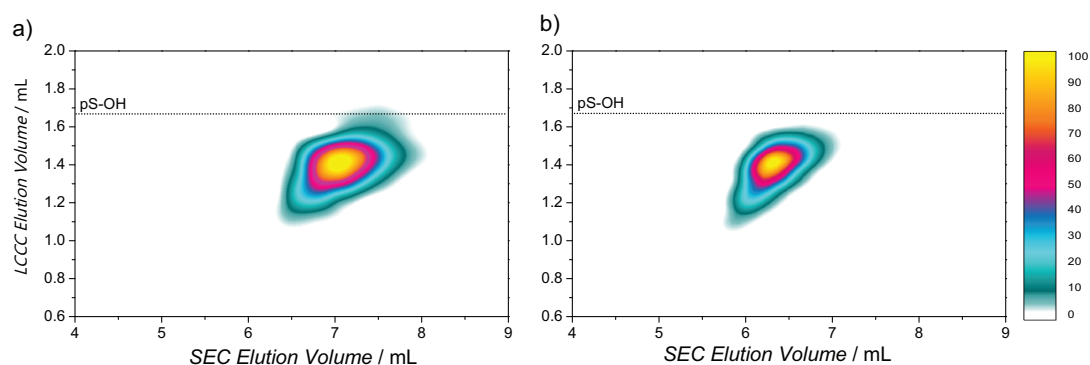


Figure 5.11. 2D plots of the block copolymers pS-*b*-pCL a) **3a** (pS-*b*-pCL, $M_n = 26000 \text{ g mol}^{-1}$, $PDI = 1.3$) and b) **3b** (pS-*b*-pCL, $M_n = 37000 \text{ g mol}^{-1}$, $PDI = 1.1$) under critical conditions of poly(styrene) (THF (88.4 % (v/v)) and H₂O (11.6 % (v/v))). The dotted line represents the peak maximum of the poly(styrene)-OH under critical conditions.

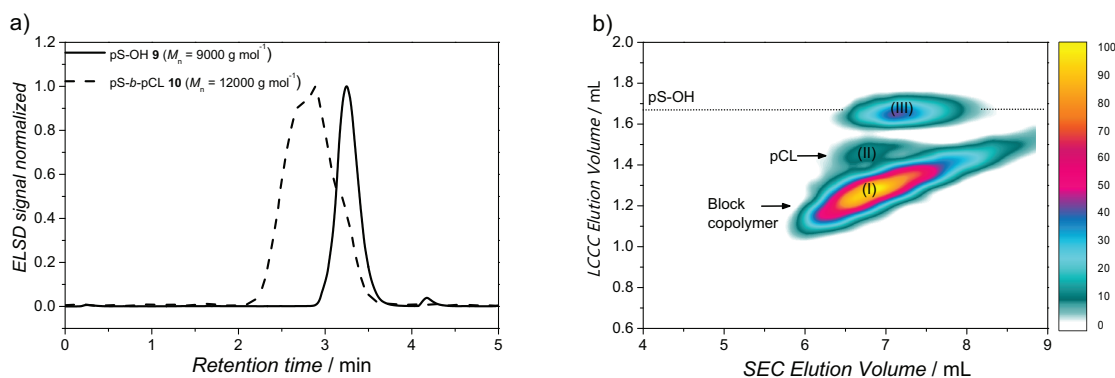


Figure 5.12. a) HPLC elugram and b) 2D plot of a block copolymer **10** with homopolymer residue under critical conditions of poly(styrene) (THF (88.4 % (v/v)) and H₂O (11.6 % (v/v))). The dotted line represents the peak maximum of the poly(styrene)-OH under critical conditions.

special case can be envisioned. The residual pCL species was most likely generated via traces of water present in the reaction mixture. Residues of non-chain extended **9** were most probably caused by a higher fraction of poly(styrene) chains that did not carry the appropriate OH terminus. Two conclusions can be drawn from the data depicted in Figure 5.12: Firstly, it is paramount to carefully assess each copolymer prepared via (any) chain extension process by LCCC-SEC techniques to ensure their structural homogeneity. Secondly, the data instills confidence into the successful preparation of reasonably well-defined poly(styrene)-*block*-poly(ϵ -caprolactone)s **3** discussed above, evidencing the functionality switch driven preparation of sulfur free block copolymers via RAFT technology as a highly efficient technique. Investigations, presented in the next chapter, will not only focus on the preparation of more complex macromolecular

architectures via the presented synthetic technique, but also entail the rather complex chromatographic analysis under the critical conditions of pCL (see Chapter 6).

5.2.4. Conclusions

The method of switching well-defined thiocarbonyl thio capped (RAFT) polymers into hydroxyl terminated species was employed to generate narrowly dispersed sulfur-free poly(styrene)-*block*-poly(ϵ -caprolactone) polymers by chain extension using ring-opening polymerization. The obtained block copolymers were carefully analyzed via SEC, NMR as well as LCCC-SEC to assess the block copolymer structure and the efficiency of the synthetic process. The current section demonstrated that the RAFT process can serve as a methodology for the generation of sulfur-free pS-*b*-pCL block copolymers via an efficient end-group switch.

5.3. Poly(acrylate)-*block*-poly(ϵ -caprolactone) and Poly(methacrylate)-*block*-poly(ϵ -caprolactone)

5.3.1. Introduction to pA-*b*-pCL and pMMA-*b*-pCL Block Copolymers

Beside poly(styrene), poly(acrylate)s and a poly(methacrylate) have been investigated as well for the formation of block copolymers to a certain extent. Poly(methyl acrylate) (pMA), poly(isobornyl acrylate) (p*i*BoA), and poly(methyl methacrylate) (pMMA) were polymerized via the RAFT process and transformed into hydroxyl functional polymers, which are subsequently applied as macroinitiators for ring-opening polymerization.

5.3.2. Synthesis

The materials used for the synthesis are provided in the Chapter 3.

Polymerization of Methyl Acrylate with DBTC

Solutions of dibenzyltrithiocarbonate (DBTC) ($c_{\text{DBTC}} = 29.52 \text{ mmol L}^{-1}$) and 2,2'-azobis(isobutyronitrile) ($c_{\text{AIBN}} = 3.65 \text{ mmol L}^{-1}$) in methyl acrylate (10 mL) were degassed by purging with nitrogen for 15 min. The solutions were heated to 60 °C for 40 and 35 min, respectively. The reaction was then stopped by cooling in liquid nitrogen. The residual monomer was removed under vacuum and the polymer precipitated in cold methanol. Average molar masses were determined by SEC after precipitation ($M_n = 3100 \text{ g mol}^{-1}$, $PDI = 1.2$ and $M_n = 3400 \text{ g mol}^{-1}$, $PDI = 1.1$, respectively).

Polymerization of Isobornyl Acrylate with DoPAT Derivatives

The synthesis of the RAFT agents 2-arm DoPAT and DoPAT-OH and the polymerization of isobornyl acrylate can be found in Chapter 4.

Polymerization of Methyl Methacrylate with CPDB

A solution of 2-(2-cyanopropyl) dithiobenzoate (CPDB) ($c_{\text{CPDB}} = 45.48 \text{ mmol L}^{-1}$) and 2,2'-azobis(isobutyronitrile) ($c_{\text{AIBN}} = 9.60 \text{ mmol L}^{-1}$) in methyl methacrylate (50 mL) was degassed by purging with nitrogen for 15 min. The solutions were heated to 60 °C for 120 min. Subsequently, the reaction was stopped by cooling in liquid nitrogen. The residual monomer was removed under vacuum and the polymer precipitated in cold methanol. Average molar masses were determined by SEC after precipitation ($M_n = 3000 \text{ g mol}^{-1}$, $PDI = 1.2$).

Analytical (Small Scale) End-group Conversion

A solution of 2,2'-azobis(isobutyronitrile) (30 mmol L^{-1}) in 2 mL of BHT-free THF was heated to $60 \text{ }^\circ\text{C}$ in the presence of ambient air. The RAFT-polymer ($5 - 10 \text{ mmol L}^{-1}$ based on M_n) was added to the solution in the vial. After a discoloration of the solution indicated full conversion, the temperature was reduced to $40 \text{ }^\circ\text{C}$ and 3 eq. triphenylphosphine were added. The reader is cautioned that - although triphenylphosphine acts as a quenching agent - formation of small amounts of potentially explosive THF-peroxides during the reaction is possible and liquid solvent waste should be tested and treated accordingly. The analytical scale end-group conversion is applied, when testing a new polymer/RAFT-agent combination on its efficiency towards the conversion process.

Large Scale End-group Conversion

A solution of 2,2'-azobis(isobutyronitrile) (50 mmol L^{-1}) in BHT-free THF was heated to $60 \text{ }^\circ\text{C}$ for 60 min under ambient air. A solution of 500 mg RAFT-polymer in the pre-treated THF (10 mmol L^{-1} based on M_n) was prepared in a 100 mL round flask under ambient atmosphere. The flask was heated to $60 \text{ }^\circ\text{C}$ under vigorous stirring. After 40 min, the temperature was reduced to $40 \text{ }^\circ\text{C}$ and 3 equiv. triphenylphosphine were added. After 10 min the solvent was evaporated and the polymer was precipitated in cold methanol. The large scale conversion is applied, when the obtained polymer is employed to further reactions such as chain extension with ϵ -CL.

Ring-Opening Polymerization with $\text{Sn}(\text{Oct})_2$ for the Generation of pMA-*b*-pCL

The ring-opening polymerization was performed in an inert gas atmosphere to rigorously exclude water from the reaction system. ϵ -CL was added to a solution of $\text{Sn}(\text{Oct})_2$ and the poly(methyl acrylate) macro-initiator in $\sim 1 \text{ mL}$ of toluene. The solution was stirred at $100 \text{ }^\circ\text{C}$ for 2.5 h. The reaction was stopped by cooling in liquid nitrogen. The polymer precipitated in cold hexane : diethylether = 1 : 1. The amount of the reacting reagents and the resulting average molar masses of the block copolymer samples are collated in Table 5.5.

Table 5.5. Reaction conditions and number-average molar masses, M_n , of the ring-opening polymerizations to generate poly(methyl acrylate)-*block*-poly(ϵ -caprolactone) polymers.

Structure	$n_{\epsilon\text{-CL}}$ / mmol	$n_{\text{Sn}(\text{Oct})_2}$ / μmol	n_{pA} / μmol	M_n / g mol^{-1}	<i>PDI</i>
pMA- <i>b</i> -pCL	0.66	14.8	9.66	9 100	1.2
pMA- <i>b</i> -pCL	3.51	16.8	13.71	17 400	1.3

Ring-Opening Polymerization with TBD (Synthesis of Block Copolymers)

The ring-opening polymerization was performed in an inert gas atmosphere (argon) inside a glove box to rigorously exclude water from the reaction system. ϵ -CL was added to a solution of TBD and the poly(acrylate)/poly(methacrylate) macro-initiator in 2 mL of toluene. The solution was stirred for 5 h and subsequently quenched by addition of benzoic acid. The amount of the reacting reagents and the resulting average molar masses of the block copolymer samples are collated in Table 5.6.

Table 5.6. Reaction conditions and number average molar masses, M_n , of the ring-opening polymerizations to generate poly(acrylate)-*block*-poly(ϵ -caprolactone) as well as poly(methacrylate)-*block*-poly(ϵ -caprolactone) polymers.

Structure	$n_{\epsilon\text{-CL}}$ / mmol	n_{TBD} / μmol	$n_{\text{pA/pMMA}}$ / μmol	time / h	M_n / g mol^{-1}	PDI
pMA- <i>b</i> -pCL	2.01	7.21	30.3	5	4 200	1.5
pMA- <i>b</i> -pCL	2.01	10.7	10.3	5	6 600	1.6
p <i>i</i> BoA- <i>b</i> -pCL	1.00	43.10	1.66	5	17 000	1.4
p <i>i</i> BoA- <i>b</i> -pCL	2.63	86.20	6.66	14	49 000	1.5
pMMA- <i>b</i> -pCL	1.98	10.1	9.80	5	3 100	1.4
pMMA- <i>b</i> -pCL	2.29	10.1	15.4	26	30 300	1.3

Ring-Opening Polymerization with *tert*-Butanol as Initiator

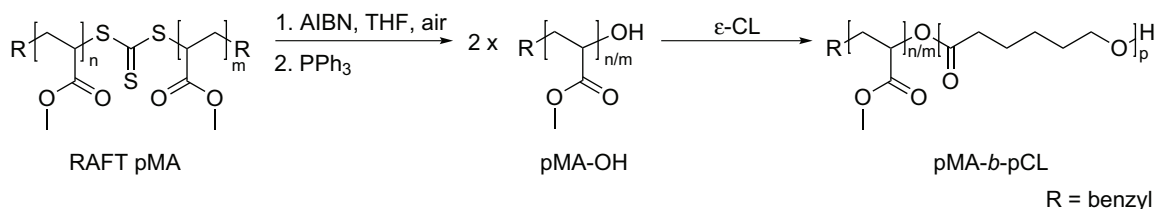
The ring-opening polymerization was performed in an inert gas atmosphere (argon) inside a glove box to rigorously exclude water from the reaction system. ϵ -CL (1.14 mg, 1 mmol) was added to a solution of TBD (5 μmol) and *tert*-butanol (0.4 mmol / 0.8 mmol / 1.2 mmol) in 2 mL of toluene. The solution was stirred for 5 h and subsequently quenched by addition of benzoic acid. The polymer precipitated in cold hexane : diethylether = 1 : 1. The resulting average molar masses of the obtained pCLs are: 6400 g mol^{-1} , 4200 g mol^{-1} , and 3000 g mol^{-1} , respectively, depending on the employed amount of initiator (*tert*-butanol).

5.3.3. Results and Discussion

pMA-*b*-pCL Block Copolymers

The synthesis of the first block was achieved by polymerization of methyl acrylate with DBTC as chain transfer agent. Subsequently, the trithiocarbonate moiety was transformed to generate hydroxyl terminated polymer chains. The transformation reaction for this specific polymer/CTA combination has been described previously in the Introduction section of Chapter 4. The procedure for the polymerization and the

end-group conversion is provided in the Synthesis section. After the transformation, the hydroxyl terminated poly(methyl acrylate) is introduced as an initiator for the ring-opening polymerization. The exact synthetic pathway is depicted in Scheme 5.4. The ring-opening polymerization was carried out under $\text{Sn}(\text{Oct})_2$ catalysis as well as under organo-catalysis involving 1,5,7-triazabicyclo[4.4.0]dec-5-ene (TBD).



Scheme 5.4 Synthetic strategy for the synthesis of pMA-*b*-pCL diblock copolymers.

Figure 5.13 shows the SEC elugrams of the chain extension of a RAFT-prepared poly(methyl acrylate) after its quantitative conversion into a hydroxyl terminal polymer and its subsequent use as a macroinitiator in the ROP of ϵ -caprolactone. $\text{Sn}(\text{Oct})_2$ is used as a catalyst. Inspection of Figure 5.13 clearly demonstrates that the chain extension appears to have properly functioned, as the molar mass increases and a clear shift in the molar mass distribution is observed. In addition, the system reacts in the expected fashion to a variation of the initiator concentration, *i.e.*, when the initiator concentration is decreased, the final molar mass increases ($M_n = 9100 \text{ g mol}^{-1}$ versus 17400 g mol^{-1}).

Additionally, the chain extension with ϵ -CL was conducted under organo-catalysis. While the reaction with $\text{Sn}(\text{Oct})_2$ proceeds at $100 \text{ }^\circ\text{C}$, the employment of TBD as a catalyst allows the reaction to proceed at ambient temperature. Figure 5.14 depicts the SEC elugrams of the block copolymers pMA-*b*-pCL generated with TBD as catalyst in comparison with the starting material pMA-OH. The molar masses of the block copolymer clearly are increased compared to the homopolymer pMA-OH. Here again it is observed that with decreasing amount of initiator the molar masses of the block copolymer increases ($M_n = 4200 \text{ g mol}^{-1}$ versus 6600 g mol^{-1}). It should be noted that the elugrams of the block copolymers overlap to a certain extent with the one of the macroinitiator pMA-OH. Thus, no exact statement can be made whether all chains of the macroinitiator started the ring-opening polymerization. Possible side reactions include transesterification, which can not only occur on the pCL chains but also on the poly(methyl acrylate) block, leading to side chains at the pMA polymer.

Beside SEC, the pMA-*b*-pCL block copolymers were characterized via $^1\text{H-NMR}$. One spectrum of block copolymer with a M_n of 17400 g mol^{-1} is displayed in Figure 5.15. The resonances are assigned to the polymer chains of pMA and pCL. The intensity of the pCL signals are much more intense than the resonance intensity of pMA. This circumstance is in-line with the SEC measurements. When the block

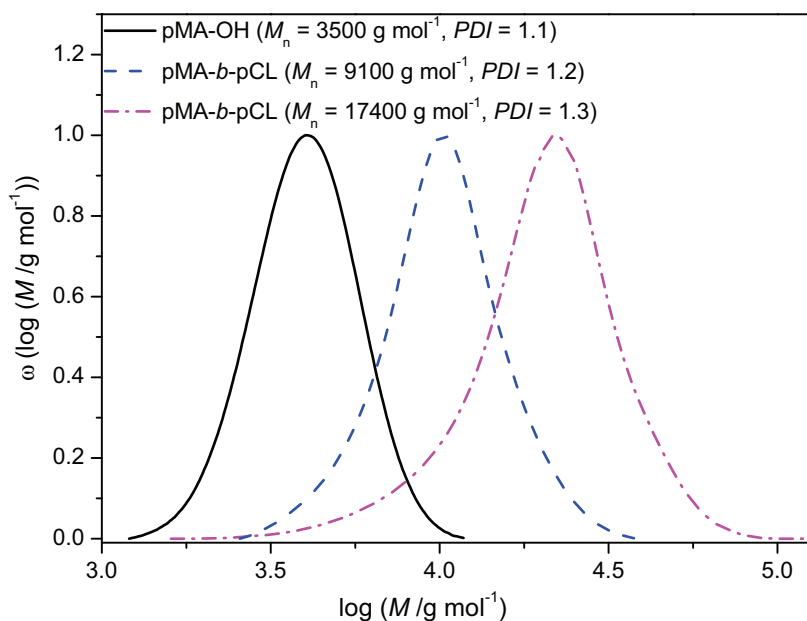


Figure 5.13. SEC traces of block copolymers pMA-*b*-pCL synthesized via chain extension employing pMA-OH as a macroinitiator and ϵ -CL as a monomer using $\text{Sn}(\text{Oct})_2$ as a catalyst. The individual molar masses and dispersities of the block copolymers are provided within the figure.

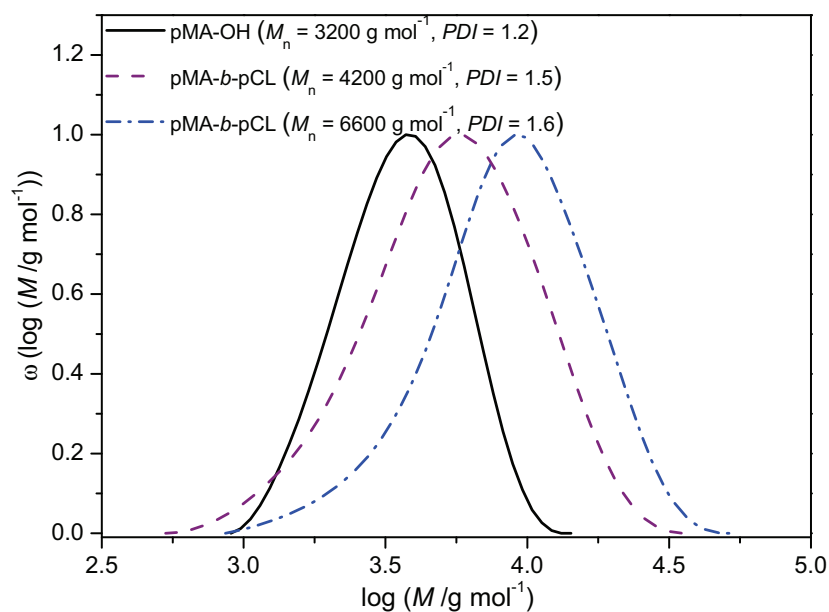


Figure 5.14. SEC traces of block copolymers pMA-*b*-pCL synthesized via chain extension employing pMA-OH as a macroinitiator and ϵ -CL as a monomer using TBD as a catalyst. The individual molar masses and dispersities of the block copolymers are provided within the figure.

copolymer possesses a M_n of 17400 g mol^{-1} and the macroinitiator pMMA has a molar mass of 3500 g mol^{-1} , the pCL part possesses a molar mass of 13900 g mol^{-1} . The amount of pCL in the block copolymer sample is thus higher than the pMMA content. Integrating the resonances in the NMR spectrum, however, results in an even higher ratio between pCL and pMA. (7.62 : 1). The difference in the values obtained via NMR and SEC could possibly be associated with the inaccuracy of SEC analysis. Due to the block structure, no exact calibration curve can be applied on the SEC traces. Another reason are the transesterification reactions as side reactions or initiation with water residues, which both result in homopolymer pCL. However, it is hardly possible to distinguish homopolymer pCL and the pCL block fraction in the copolymer with $^1\text{H-NMR}$ spectroscopy.

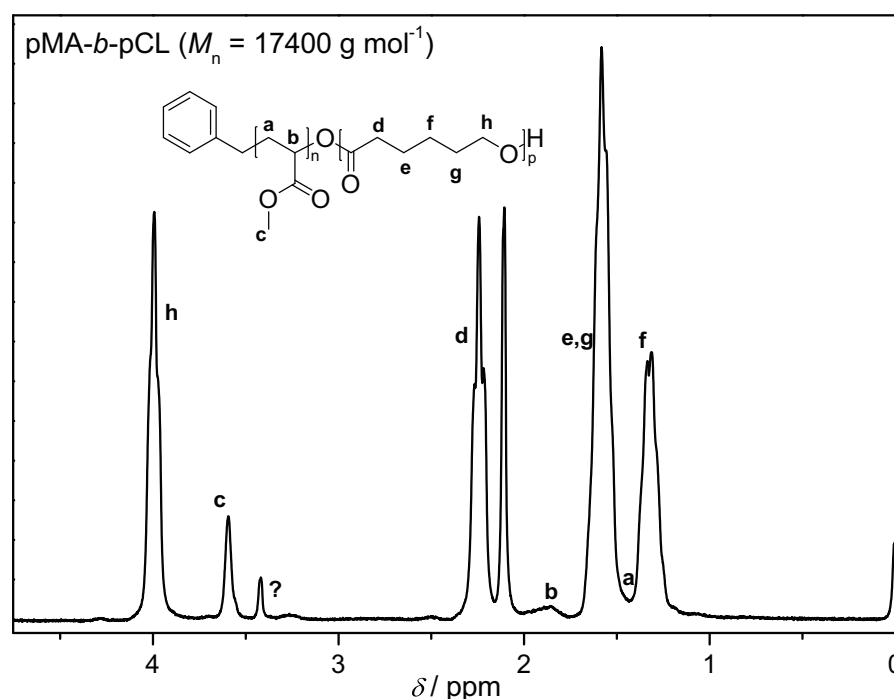


Figure 5.15. $^1\text{H-NMR}$ of the block copolymer pMA-*b*-pCL ($M_n = 17400 \text{ g mol}^{-1}$) synthesized via chain extension employing pMA-OH as a macroinitiator and ϵ -CL as a monomer.

However, the further investigation with more advanced techniques such as liquid chromatography under critical conditions to obtain more details about the block copolymer sample – especially the content of remaining homopolymer – revealed to be very complex due to the high similarity in polarity and chemical composition of pCL and pMA. For instance, the critical conditions of pMA were established on a Discovery Cyano-column with a solvent composition of 62 % (v/v) THF and 38 % (v/v) *n*-hexane (see Figure 5.16). However, almost no shift between the retention volume of pMA homopolymers and pMA-*b*-pCL block copolymers could be observed at the critical conditions of pMA. Consequently, the structure was not analyzed to

such a detailed extent as described for pS-*b*-pCL in the previous chapter.

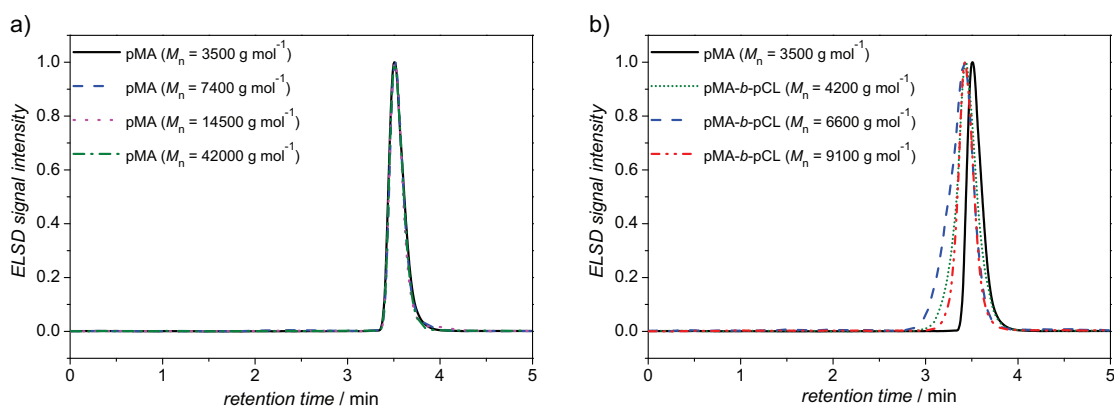
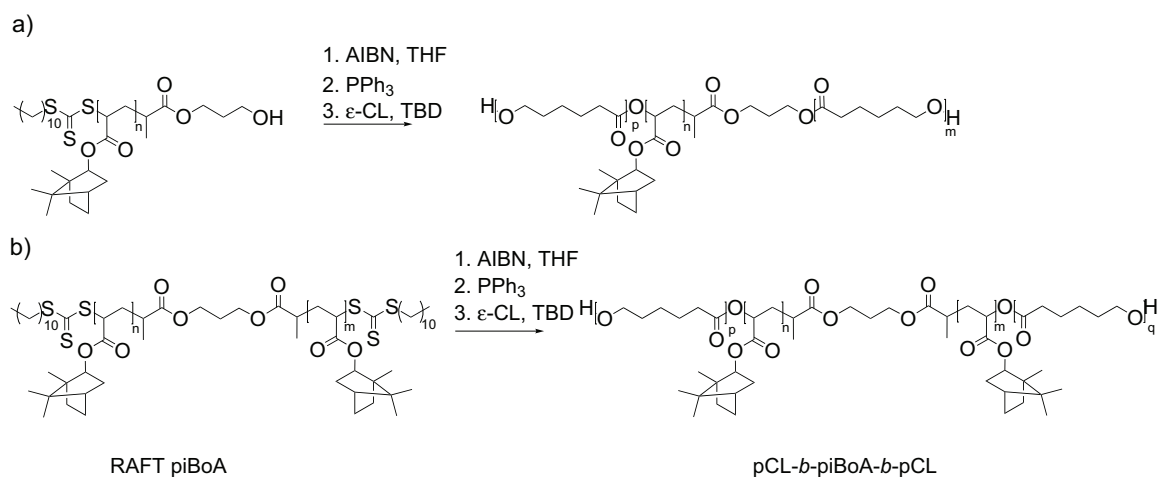


Figure 5.16. a) LCCC elugrams of pMA homopolymers for the setup of the critical conditions of pMA and b) LCCC elugrams of the synthesized block copolymers pMA-*b*-pCL. The LCCC was conducted employing a Discovery Cyano-column and using a solvent composition of 62 % and 38 % (v/v) *n*-hexane.

piBoA-*b*-pCL Block Copolymers

Block copolymer formation has also been investigated utilizing RAFT derived hydroxyl functionalized poly(isobornyl acrylate) as starting material. For this purpose isobornyl acrylate was polymerized in the presence of the RAFT agent 2-arm DoPAT and DoPAT-OH (for structures see Scheme 4.6). The polymer was subsequently converted via the transformation reaction in THF, leading to polymer chains with OH functionalities on both chain ends. The procedure especially for this polymer/CTA combination has been described in detail in Chapter 4. In the following the chain extension is presented (see Scheme 5.5).



Scheme 5.5 Synthetic strategy for the synthesis of piBoA-*b*-pCL block copolymers starting from a) DoPAT-OH and b) 2-arm DoPAT RAFT polymers.

The chain extension with ε-CL was conducted under organo-catalysis employing

TBD. Figure 5.17 depicts the SEC traces of the obtained block copolymers. Figure 5.17a displays additionally the elugram of the macroinitiator *pi*BoA, which possesses one hydroxyl function at each end of the polymer chain. Since the chain extension can proceed on each end of the *pi*BoA chain, an ABA block structure can be generated. The elugram of the obtained block copolymer is clearly shifted to higher molar masses when compared to the elugram of the starting material. Consequently, the chain extension was likely successful. A closer survey reveals that the elugram of the block copolymer exhibits a shoulder to higher molar masses. Additionally, the polydispersity index for the chain extended sample has increased. A possible explanation is the co-existence of a diblock structure beside an ABA triblock copolymer structure. The chain extension was additionally conducted on the transformed *pi*BoA derived from the polymerization with the 2-arm DoPAT chain transfer agent. The transformation described in Chapter 4 did not result in a polymer bearing only the two hydroxy functionalities at the chain end, but also a minor content of H-terminated and small amounts of hydroperoxide terminated polymer structures. Still, as it is depicted in Figure 5.17b, the chain extension proceeded, leading to polymer structures with high molar masses. For the ROP, the reaction time was elongated to 14 h since after 5 h the SEC traces showed exclusively starting material. After 14 h, however, a clear shift in the SEC elugrams of starting material to the block copolymer is observed. Almost no overlap of the SEC elugram of the generated block structure with the elugram of the *pi*BoA macroinitiator is observed. The obtained SEC elugram possesses a shoulder to lower molar masses, which can be explained by the same hypothesis given for the elugram block structure in Figure 5.17a. Additionally, due to the elongated reaction time, transesterification reactions are likely to occur.

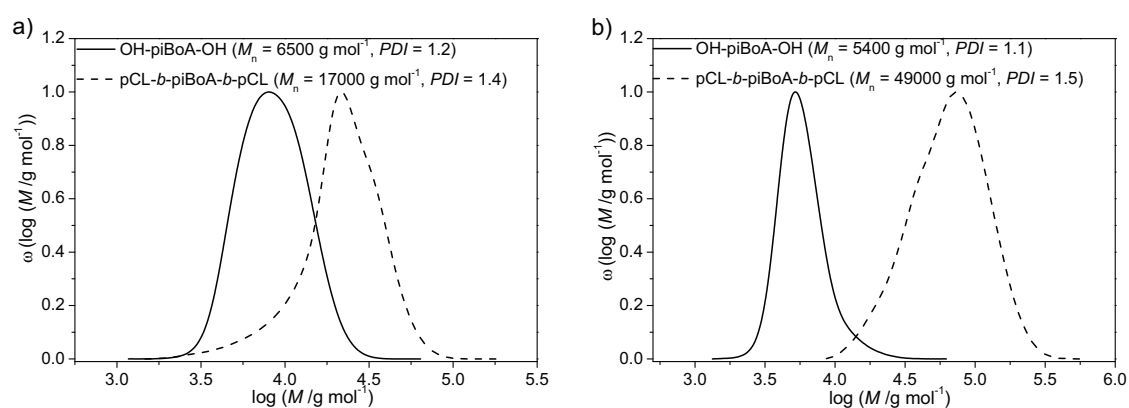


Figure 5.17. SEC elugrams of the synthesized block copolymers generated via chain extension of the hydroxyl terminated *pi*BoA macroinitiators, which were obtained via the polymerization with a) DoPAT-OH and b) 2-arm DopAT.

For further analysis $^1\text{H-NMR}$ was carried out. The spectrum of one of the block copolymers *pi*BoA-*b-p*CL with an M_n of 17000 g mol^{-1} is depicted in Figure 5.18.

The signals can be assigned to the polymeric structures *pi*BoA and pCL. Assuming that the M_n of the *pi*BoA block is 6500 g mol^{-1} , as obtained from the SEC data, the molar mass of the pCL block is calculated by integrating and comparing the resonances *c* associated with *pi*BoA and *i* associated with pCL. A block length for pCL of 6000 g mol^{-1} is obtained, which departs from the data obtained from the SEC ($M_n^{\text{pCL}} = M_n^{\text{block}} - M_n^{\text{piBoA}} = 10500 \text{ g mol}^{-1}$). However, due to the block structure the SEC data should be treated with care, since no Mark Houwink parameters are available for the block copolymers *pi*BoA-*b*-pCL. Thus, the calibration curve was adjusted with the parameters of *pi*BoA, leading to slightly inaccurate molar masses of the block copolymer. The $^1\text{H-NMR}$ -spectrum of the block copolymer with an M_n^{SEC}

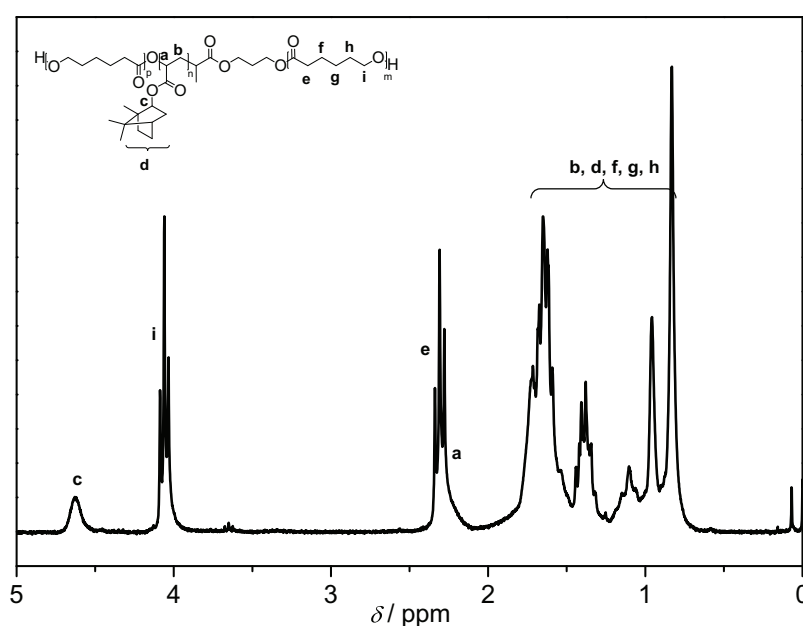
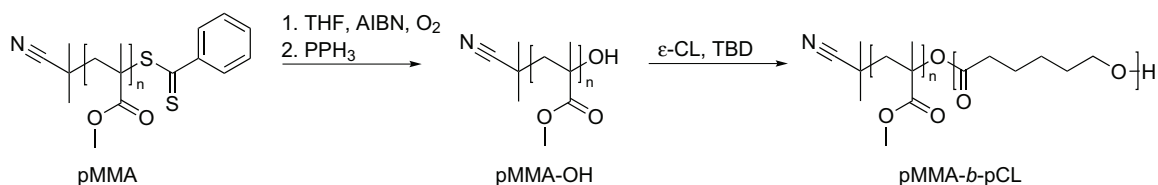


Figure 5.18. $^1\text{H-NMR}$ of the block copolymer *pi*BoA-*b*-pCL ($M_n = 17000 \text{ g mol}^{-1}$) synthesized via chain extension employing OH-*pi*BoA-OH as a macroinitiator and ϵ -CL as a monomer using TBD as a catalyst.

of 49000 g mol^{-1} shows results with the same trends. The block pCL calculated via the same procedure explained above, possesses an $M_n^{\text{pCL,NMR}}$ of 41800 g mol^{-1} resulting from NMR data and $M_n^{\text{pCL,SEC}}$ of 43600 g mol^{-1} calculated from the SEC data. Thus, the values obtained from the SEC data are in both cases higher than the results obtained from the NMR spectra. As mentioned above, the molar masses obtained via SEC measurements of block copolymer structures should be treated with care. The data obtained from NMR are of higher accuracy. For more detailed analysis with hyphenated techniques of ABA block copolymer structures in general, the reader is referred to Chapter 6.

pMMA-*b*-pCL Block Copolymers

Beside the poly(acrylate)s pMA and p*i*BoA, pMMA was selected for chain extension with ϵ -CL. The synthesis strategy for the block copolymer formation pMMA-*b*-pCL is depicted in Scheme 5.6. Methyl methacrylate was polymerized in the presence of cyanoisopropyl dithiobenzoate (CPDB) as a RAFT agent. The final polymer was characterized via SEC and SEC/ESI-MS.



Scheme 5.6 Synthetic strategy for the synthesis of pMMA-*b*-pCL diblock copolymers.

The transformation of the dithiobenzoate endcapped pMMA to hydroxyl functional polymer was previously investigated by Gründling *et al.*^[275] on a small scale at 60 °C. In Figure 5.19, SEC/ESI-MS spectra of the transformation after specific time intervals are depicted. The corresponding structures can be found in Chapter 4. After 10 min half of the dithiobenzoate terminated pMMA is transformed into hydroperoxide end capped polymer. After 20 min the reaction is completed and triphenylphosphine is added. Finally an ESI-MS spectrum is obtained, in which almost exclusively hydroxyl terminated pMMA is present.

Repeating the transformation reaction especially on a larger scale – moving from mg to g – often results in a polymer sample with non-uniform end-functionality. A commonly observed side reaction is the formation of a lactone ring at the end of the chain. In Figure 5.20, a spectrum often observed of the converted pMMA is presented and compared with the initial spectrum of the RAFT polymer. In Figure 5.20a the signal observed correspond to the thiocarbonyl thio containing polymer. In the spectrum in Figure 5.20b the signals of the material after the transformation proceeded are visible. The signals at $m/z = 708.33$ and 807.33 can be assigned to the hydroxyl terminated pMMA **P_ROH**. The signal at $m/z = 776.41$ correspond to the polymer possessing a lactone ring at the chain end **P_RLactone**. Beside the lactone formation also minor amounts of H-terminated polymer can be found in the sample. The corresponding theoretical values compared with the experimental data are given in Table 5.7.

Referring to Scheme 5.6 it can be noticed that the terminal functionality attached to the pMMA polymer is a tertiary end-group due to the additional methyl group within the monomer unit. Thus, before synthesizing the block copolymer, ROP pre-experiments were conducted with a small molecule initiator possessing a tertiary hydroxyl function. *tert*-Butanol was employed to initiate ϵ -CL in the ROP process. The

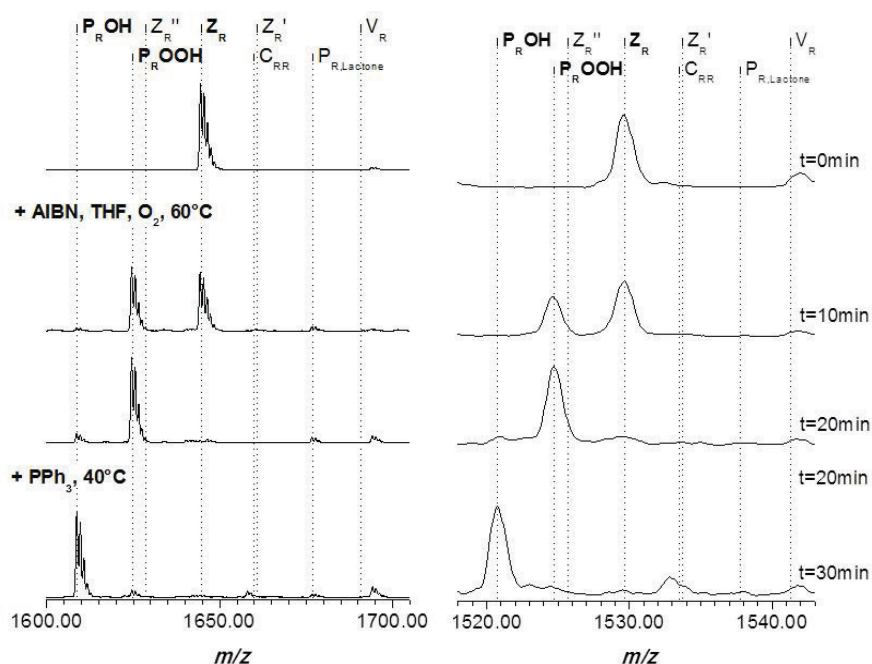


Figure 5.19. SEC/ESI MS recorded at variable reaction times, in the charge states $z=1$ (left) and $z=4$ (right). The reagents AIBN/THF and PPh_3 were added sequentially at $t=0$ and 20 min to the THF solution containing the dithiobenzoate terminated pMMA. Full conversion was reached after 30 min. Adapted with permission from Gründling, T., Dietrich, C. and Barner-Kowollik, C. Australian Journal of Chemistry, Copyright (2009) CSIRO PUBLISHING. [275]

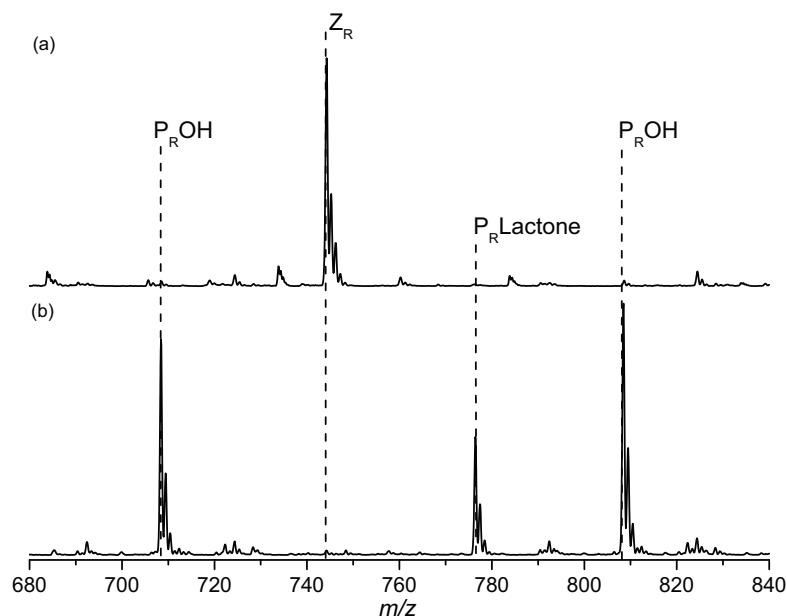
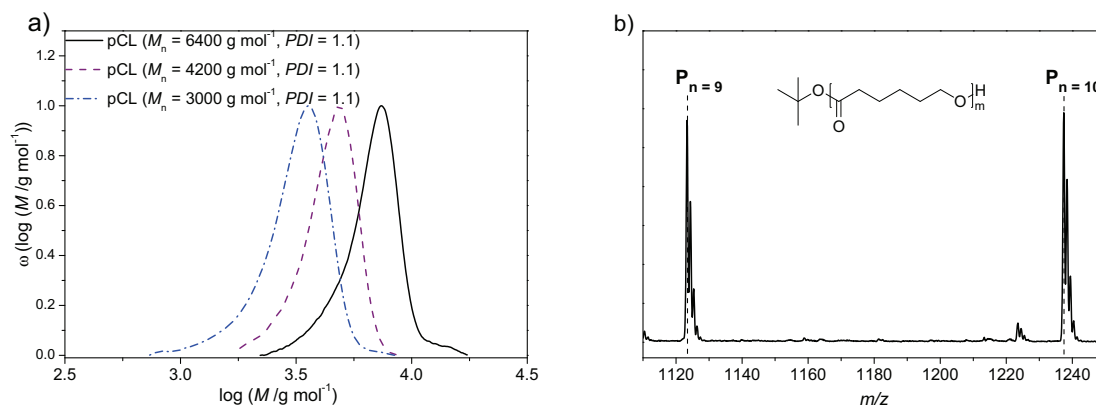


Figure 5.20. a) Electrospray ionization mass spectrum of one repeat unit of the dithiobenzoate end functional pMMA. b) A typical ESI-MS spectrum obtained after the transformation of dithiobenzoate capped pMMA.

Table 5.7. Theoretical and measured m/z ratios of the main species observed before and after the transformation of dithiobenzoate capped pMMA.

Structure	[M + Na] ⁺		
	m/z^{theo}	m/z^{exp}	$\Delta m/z$
Z_R	744.28	744.33	0.05
P_ROH	708.35	708.33	0.02
P_RLactone	776.38	776.41	0.03
P_ROH	808.35	808.33	0.02

SEC elugrams of the obtained polymers are depicted in Figure 5.21a. Decreasing the initiator concentration leads to an increase in molar mass of the polymer. Further SEC/ESI-MS measurements were conducted on the pCL with the lowest molar masses. A zoom into one repeating unit with signals at charge states $z = 1$ is depicted in Figure 5.21b. The signals are assigned to pCL with 9 and 10 monomer units, possessing a *tert*-butoxy moiety at the end of the chain (see Table 5.8). One additional small signal can be observed at $m/z = 1223.41$, which could not be assigned to any possible polymer structure. However, beside this signal no further impurities are observed. Consequently, the ring-opening polymerization with a tertiary hydroxyl function is successfully realized and can further be applied for the formation of block copolymers.

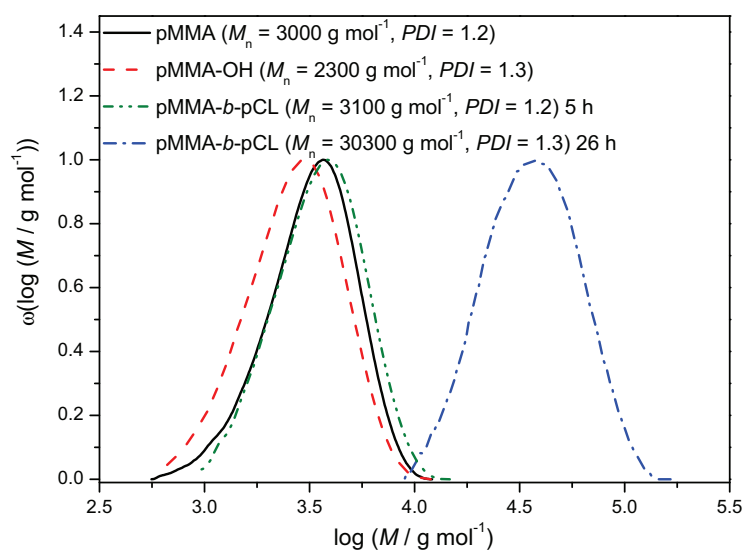
**Figure 5.21.** a) SEC traces of several pCL homopolymers initiated with a tertiary hydroxyl function and catalyzed with TBD. b) One repeat unit of pCL polymer recorded via SEC/ESI-MS.

The chain extension of pMMA-OH was conducted under organo-catalysis via ring-opening polymerization of ϵ -CL. The final polymer sample was measured with SEC and compared to the initial material. In Figure 5.22, the SEC elugrams of the RAFT pMMA, the hydroxyl terminated pMMA and the block copolymer sample pMMA-*b*-pCL after 5 h and after 26 h reaction time together with the determined molar

Table 5.8. Theoretical and measured m/z ratios of the main species of the pCL initiated with *tert*-butanol.

Structure	[M + Na] ⁺		
	m/z^{theo}	m/z^{exp}	$\Delta m/z$
P (n = 9)	1123.67	1123.67	0
P (n = 10)	1237.74	1237.75	0.01

masses are depicted. After 5 h the sample exhibits only a slight shift to higher molar masses. After 26 h, however, a clear shift to lower retention volume is observed. No overlap of the chromatogram of the macroinitiator and the one of the block copolymer can be identified. Furthermore, no significant shoulder or signal is observed in the molar mass range of the starting material. In general, the ROP employing TBD as a catalyst is completed after 5 h. The longer reaction time is associated with the application of a tertiary hydroxyl function as an initiator. The tertiary alcohol is less reactive than the secondary hydroxyl function applied in the synthesis of the other block copolymers presented earlier.

**Figure 5.22.** SEC traces of block copolymers pMMA-*b*-pCL synthesized via chain extension employing pMMA-OH as a macroinitiator and ϵ -CL as a monomer using TBD as a catalyst. The individual molar masses and dispersities of the block copolymers are provided within the figure.

The chain extension was investigated via ¹H-NMR. The spectrum of the block copolymer pMMA-*b*-pCL ($M_n = 30300 \text{ g mol}^{-1}$) is depicted in Figure 5.23. The resonances can be assigned to the polymers pMMA and pCL. However, due to the difference in chain length, the resonance intensities of pMMA are much lower than

the signals of pCL. Integrating and comparing the signal of pCL *i* with one of the resonances of pMMA *d* leads to a ratio of ϵ -CL: MA = 13.8 : 1. Calculating the molar mass of the pCL by subtracting the molar mass of pMMA obtained via SEC from the M_n of the block copolymer sample results in a molar mass of 28000 g mol⁻¹. Thus, the ratio between ϵ -CL and MMA is 10.6 : 1 calculated via SEC. The difference between the SEC and the NMR data result probably due to the long reaction time, in which side reactions occurred resulting in additional homopolymer pCL. Further, as mentioned above, the SEC data obtained via conventional SEC are inaccurate and should be treated with care. Two dimensional chromatography and other hyphenated

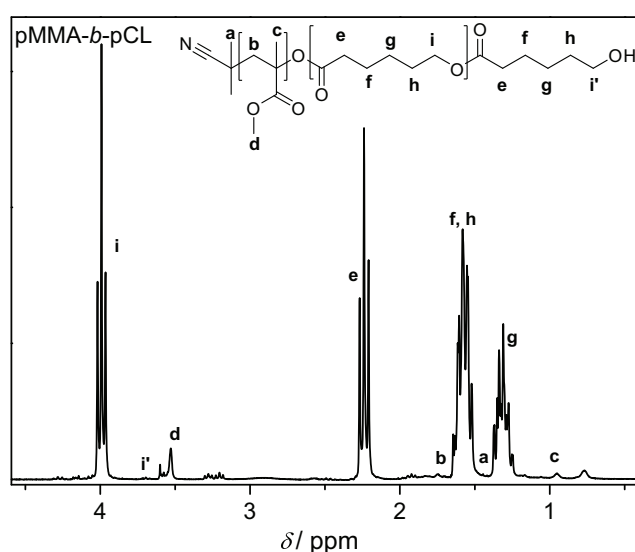


Figure 5.23. ¹H-NMR of the block copolymer pMMA-*b*-pCL ($M_n = 30300$ g mol⁻¹) synthesized via chain extension employing pMMA-OH as a macroinitiator and ϵ -CL as a monomer using TBD as a catalyst.

techniques were not conducted in the case for the block copolymer sample pMMA-*b*-pCL due to the high experimental effort.

5.3.4. Conclusions

The ring-opening polymerization of ϵ -CL with hydroxyl terminated poly(acrylate) as well as poly(methacrylate) as macroinitiators – generated from RAFT polymers – can be identified as a successful strategy to synthesize pA-*b*-pCL and pMMA-*b*-pCL block copolymers. The SEC traces of the block copolymers are always shifted to higher molar masses, when compared with the macroinitiator. Due to the nature of poly(acrylate)s and poly(methacrylate)s transesterification reactions can occur during the ROP process resulting in the observed broader polydispersity index. Beside SEC, NMR spectroscopy was utilized to clearly identify that pCL was formed during

the chain extension. The obtained ratios and molar masses of the block fractions via NMR vary slightly from the ones resulting from SEC measurements. Reasons for the variation are of analytical nature, since no Mark Houwink parameters of the block copolymers exist for an accurate calibration curve for SEC, or the circumstance that homopolymer structures which can occur due to side reactions, cannot be distinguished from block copolymer structures in NMR spectra. Attempts to characterize pA-*b*-pCL's with LCCC resulted in no further detailed information. With LCCC of pMA no significant separation between block copolymer and homopolymer pMA was observed. Thus, in-depth characterization via two dimensional chromatography has not been carried out for the pA-*b*-pCL block copolymers.

5.4. Poly(styrene)-*block*-poly(lactide)¹

5.4.1. Introduction to pS-*b*-pLA Block Copolymers

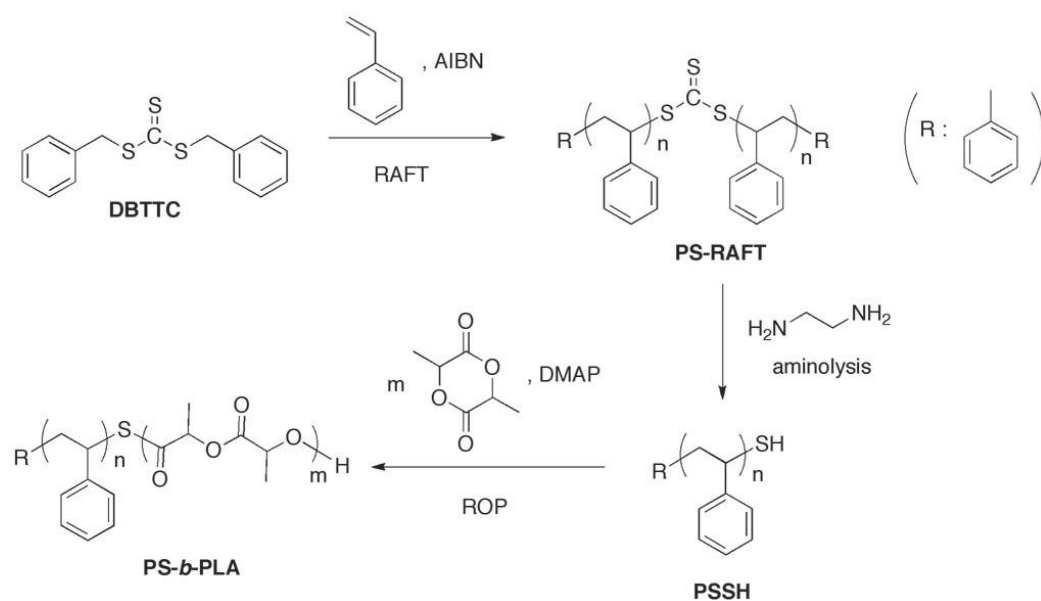
Poly(lactide) (pLA) is a biodegradable and biocompatible, thermoplastic aliphatic polyester derived from renewable resources. Due to these remarkable features, poly(lactide) is one of the most studied polymers for biomedical applications (*e.g.*, drug delivery devices or tissue engineering applications) but also as an alternative for petroleum based materials.^[125,320–323] However, depending on the targeted applications, poly(lactide)s homopolymer can be rather brittle and are – on their own – ill-equipped to serve as processable materials.^[324,325] To improve their mechanical properties, strategies have focused on the synthesis of pLA-based block copolymers. Among the various potential architectures (*e.g.*, block star, grafted or copolymers), diblock copolymers have been particularly intensively studied. More specifically, diblock copolymers with a degradable block of pLA synthesized via ring-opening polymerization (ROP) and a second block prepared via living/controlled radical polymerization (CRP) methods are an attractive option. The main CRP techniques, namely NMP,^[23] ATRP^[34,326], and the RAFT^[26,286,287,327] processes allow the preparation of well-defined polymers in terms of both molar mass and architecture in a convenient manner. Among these methods, the RAFT process is probably the most versatile due to the large range of (functional) monomers that can be polymerized.^[290]

This section details the efforts in preparing diblock copolymers based on pLA and a synthetic polymer (pS), where the two blocks are linked by a covalent sulfur bond. The key idea is to transform the dithioester/trithiocarbonate end-group into a thiol function by aminolysis and to subsequently use it as the initiator of the ROP of lactide. Thus, the efforts to employ RAFT polymers for subsequent ROP concentrate on both a P-SH (described herein) and a P-OH initiation system (described above). The use of a thiol function as initiator of ROP has not received detailed attention in the literature. Interestingly, the octadecylmercaptan has been briefly studied for the ROP of lactide with a thiourea organocatalyst.^[146] These authors obtained 80% conversion in 20 h with a M_n value of 7800 g mol⁻¹ and a *PDI* value of 1.06. More recently, Robin and colleagues^[328] employed a thiol-terminated macroinitiator obtained via RAFT polymerization to initiate the ROP of *N*-carboxyanhydride (NCA) for the generation of diblock copolymers based on peptides. It is worth noting that NCAs are usually initiated by an amino-terminated polymer chain, different to the case of lactides.

¹ The analysis described in this section was carried out to a large extent at the UMR 6264 Laboratoire Chimie Provence, Université de Provence, in France by the collaboration partner C. Lefay.

pLAs have thus never been synthesized by a ROP process initiated by a thiol-ended polymer chain derived from a terminal trithiocarbonate.

In the current chapter, a model study employing styrylmercaptan as initiator for the ROP of lactides to prove the ability of thiols to ring open the lactide in the presence of 4,4-dimethylaminopyridine as organocatalyst is initially conducted before the synthesis of several pS-*b*-pLA copolymers with various pS/pLA length ratios is presented. The entire synthetic strategy is depicted in Scheme 5.7. To characterize the prepared block copolymers, advanced characterization methods, such as liquid chromatography at critical conditions, have been employed to evaluate the purity of the diblock copolymers and to assess the proportion of residual homopolymers (pLA and/or pS).



Scheme 5.7 Synthetic strategy employed in the present contribution for the synthesis of pS-*b*-pLA diblock copolymers.

5.4.2. Synthesis

Polymerization of Styrene via the RAFT Process with the DBTC as Control Agent

The polymerizations were performed in bulk for 1 h at 80 °C under argon, with a molar ratio DBTC/AIBN of 10 : 1 as reported before (see Chapter 5).^[329] The poly(styrene)-DBTC was recovered by precipitation in cold methanol and subsequently dried under vacuum.

Aminolysis of the Trithiocarbonate Capped Poly(styrene)s

A solution of pS-RAFT ($2 \cdot 10^{-2}$ mol L⁻¹) was prepared in THF and degassed via percolating the solution with argon for 10 min. After the addition of 15 mol equivalents

of ethylenediamine, the solution was stored under argon and in the dark for one night. PS-SH was recovered by precipitation in cold methanol and subsequently dried under vacuum.

Ring-Opening Polymerization (ROP) of D,L-LA Initiated by Styrylmercaptan (SM)

In a typical recipe with the styrylmercaptan as initiator targeting a DP_n (pLA) of 122, the initiator ($1.7 \cdot 10^{-4}$ mol) in solution (5 mL) of toluene was degassed separately from the DMAP (0.08 g, 4 mol equivalents relative to the initiator) and LA (3 g, 0.02 mol) which were dried under vacuum at 40 °C. After 1 h of degassing by argon percolation, the initiator solution was added via a canula to the monomer. After 24 h of polymerization time, the pLA was isolated by precipitation in cold methanol and dried under vacuum.

Ring-Opening Polymerization (ROP) of D,L-LA Initiated via a Macromercaptan Based on Poly(styrene) (pS-SH)

The polymerizations were carried out in freshly distilled toluene at 100 °C under argon and the ROP of LA was performed according to the following method. In the case of an initial pS-SH of 1900 g mol^{-1} and targeting a DP_n (pLA) of 120, pS-SH (0.2 g, $1 \cdot 10^{-4}$ mol), DMAP (0.103 g, 8 mol equivalents relative to pS-SH), and LA (1.85 g, $[LA]_0/[pS-SH]_0 = 120$) were dried at 40 °C under vacuum for 1 h. 2 mL of toluene were subsequently added under argon and the temperature was increased to 100 °C. In the case of the same initial pS-SH (1900 g mol^{-1}) and targeting a DP_n (pLA) of 200, the synthesis method was similar yet employing 0.122 g of pS-SH ($6 \cdot 10^{-5}$ mol), 0.063 g of DMAP ($5 \cdot 10^{-4}$ mol), 1.85 g of LA ($[LA]_0/[pS-SH]_0 = 200$) and 2 mL of toluene. After 24 h or 48 h polymerization under argon and stirring, depending on the targeted DP_n (pLA), respectively 120 or 200, the pS-*b*-pLA diblock copolymers were recovered by precipitation in cold methanol. The reaction time was increased from 24 h to 48 h as the reaction rate is generally reduced when increasing the targeted DP_n from 120 to 200. The copolymers were subsequently dried under vacuum and analyzed as described below. A collation of the SEC analysis results of the pS-*b*-pLA copolymers can be found in Table 5.9.

Ring-Opening polymerization (ROP) of D,L-LA Initiated by Methanol or Water

The polymerizations were carried out in freshly distilled toluene at 100 °C under argon. In the case of employing methanol or water as initiators (liquid initiators), the ROP of LA was performed according to the following method. Targeting a DP_n (pLA) of 122, DMAP (0.103 g, 8 mol equivalents relative to initiators), and LA (1.85 g, $[LA]_0/[I]_0 = 122$) were dried at 40 °C under vacuum for 1 h. 2 mL of toluene with

methanol (0.005 g, $1 \cdot 10^{-4}$ mol) or water (0.003 g, $1 \cdot 10^{-4}$ mol) were subsequently added under argon and the temperature was increased to 100 °C. After 24 h of polymerization time under argon and stirring, the pLA polymers were recovered by precipitation in cold methanol. The polymers were subsequently dried under vacuum and analyzed as described below. The M_n (SEC) in pS equivalents and PDI values of pLA initiated by methanol and water, respectively, read 17700 g mol⁻¹ ($PDI = 1.46$) and 27200 g mol⁻¹ ($PDI = 1.39$).

5.4.3. Results and Discussion

Before exploring the block copolymer formation initiated by macromercaptans derived from RAFT made polymers, we investigated if thiol functionalized molecules are capable of efficiently initiating the ROP of lactides. Styrylmercaptan (SM) was chosen to mimic the behaviour of a thiol end capped poly(styrene) chain and further used to establish the proper experimental conditions for an efficient ROP of lactide. The ROPs of LA have been performed in distilled toluene at 100 °C for 24 h, targeting a degree of polymerization of 120. In the present section, the number average degree of polymerization always relates to the number of lactide units ($M = 144$ g mol⁻¹) within a polymer structure.

When analyzing the results of the styrylmercaptan initiated ROP of LA, a relatively monomodal molar mass distribution was obtained when using 4 mol equivalents of DMAP relative to the styrylmercaptan. The high conversion of 96 % obtained in 24 h (determined via ¹H NMR, see experimental section) provided an M_n of 15500 g mol⁻¹ ($PDI = 1.25$ (RI trace)) determined via SEC (relative to pS equivalents). On the basis of the result from this above model study, the synthesis of a pS-*b*-pLA diblock copolymer, *i.e.*, on the basis of a macromercaptan, was addressed in a subsequent step.

After demonstrating the ability of styrylmercaptan to initiate the ROP of LA, several pS-*b*-pLA diblock copolymers with various pS/pLA length ratios were synthesized. For this purpose, three poly(styrene)s with variable molar mass were prepared by RAFT polymerization employing DBTC as control agent. After aminolysis (see Scheme 5.7 and Figure 5.24), the obtained poly(styrene)s (here termed pS 1900, pS 3600 and pS 6100) presented a M_n of 1900, 3600 and 6100 g mol⁻¹, respectively, and PDI values between 1.14 and 1.23. Due to the symmetric nature of the RAFT agent, the thiocarbonyl thio moiety is in a mid-chain position. Thus, after aminolysis, the molar mass of the resulting thiol-terminal entities should be approximately half of that of the RAFT material. Figure 5.24 clearly indicates the net shift toward lower molar masses of the RI/SEC trace after aminolysis attesting the effective reduction of the RAFT agent and the formation of pS-SH chains (see Table 5.9 for the number-

average molar masses of the thiocarbonyl thio polymers as well as the resulting thiol terminal entities). It is worth noticing that concerning the smaller pS, the M_n values before and after aminolysis are quite similar because the samples are very close to the lower pS standard used for the calibration curve ($M_n = 1180 \text{ g mol}^{-1}$) and an increased error in molar mass cannot be excluded.

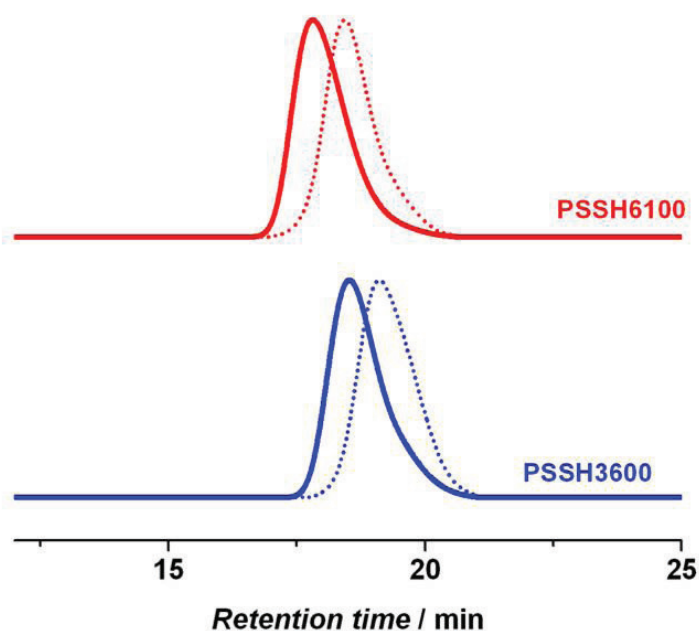


Figure 5.24. Typical RI/SEC traces of the variable molar mass RAFT precursor poly(styrene) chains before (bold line) and after (dotted line) aminolysis into the thiolmercaptan macroinitiators pS-SH 3600 ($M_n = 3600 \text{ g mol}^{-1}$) and pS-SH 6100 ($M_n = 6100 \text{ g mol}^{-1}$).

As already reported in the literature, macrothiol compounds are very sensitive to oxygen and temperature and may be readily oxidized to disulfur compounds.^[9,62] In the present case, the presence of such subsequent side reactions implies that generated pS-SH must be immediately employed after aminolysis. If stored for a few days before use – even at 5°C and under argon – the SEC analysis revealed bimodal molar mass distributions, caused by chain coupling via the formation of S-S bonds. For each of the three pS-SH, two lengths of pLA were targeted, *i.e.*, a DP_n of 120 or 200. The M_n , PDI and LA conversion values obtained for the six block copolymers are summarized in Table 5.9. Inspection of Table 5.9 clearly indicates that an efficient chain extension took place in all cases. To illustrate that the systems respond effectively to a change in the poly(lactide) block lengths, the parameter F is introduced. It gives the ratio of the expected block length increase ratio and the found block length increase ratio (for a mathematical formula refer to the bottom of Table 5.9). Ideally, F should be unity,

as in this case the expected increase in length of the poly(lactide) block conforms with the experimentally found increase in its length. It is pleasing to note that all values for Γ are – independent of the length of the initial poly(styrene) thiol – reasonably close to one, between 1.05 and 1.35, with no dependence on the number-average molar mass of the macromercaptane. Such a result is especially acceptable if one notes that the provided number-average molar masses are based on a poly(styrene) SEC calibration. It can thus be concluded that indeed block copolymers are generated via macrothiol initiation, however, a more through analysis is required and will be presented below.

Table 5.9. M_n , PDI , block length increase ratio and LA conversion values relating to the synthesis of pS-*b*-pLA diblock copolymers based on pS-SH precursors derived from trithiocarbonate capped macromolecules.

Sample	M_n (pS RAFT) ^a / g mol ⁻¹	M_n (pS-SH) ^b / g mol ⁻¹	DP_n (pLA) ^c targeted	M_n / g mol ⁻¹	PDI	Γ^d	Conv. ^e (LA)
blank	–	none	–	17,000	1.62	–	0.94
(pS- <i>b</i> -pLA)1	2100	1900	120	15,000	1.60		0.98
(pS- <i>b</i> -pLA)2	2100	1900	200	24,900	1.20	0.95	0.95
(pS- <i>b</i> -pLA)3	5300	3600	120	16,100	1.46		0.98
(pS- <i>b</i> -pLA)4	5300	3600	200	19,000	1.38	1.35	0.96
(pS- <i>b</i> -pLA)5	9500	6100	120	13,300	1.43		0.95
(pS- <i>b</i> -pLA)6	9500	6100	200	16,800	1.46	1.12	0.96

a M_n by RI/SEC are given in pS equivalents.

b Same as *a*.

c Targeted DP_n at 100 % conversion.

d $\Gamma = ((M_n(\text{pS-}i\text{b-pLA}(120)) - M_n(\text{pS-SH})) / (M_n(\text{pS-textitb-pLA}(200)) - M_n(\text{pS-SH}))) / (120/200)$.
Note that Γ should (in the ideal case) be unity.

e Conversion of lactide measured by ¹H NMR.

The aim of the current chapter is first to initiate pLA chains from a thiol terminal polymeric macroinitiator and secondly to prove the formation of these diblock copolymers. One of the major difficulties when synthesizing diblock copolymers is to be certain to produce the desired block copolymer structure and not two homopolymers. In the current study, the results of conventional SEC equipped with refractive index (RI) and UV detection as well as liquid chromatography under critical conditions at pS and pLA critical conditions were employed to assess the presence of diblock copolymer chain. These techniques can be used to estimate the proportion of diblock versus potentially remaining homopolymers chains. Specifically, LCCC is based on the controlled coupling of entropic and enthalpic retention mechanisms. Under critical conditions, the entropic and enthalpic effects compensate and macromolecules with different molar masses elute at the same elution time/volume. In the present chapter, LCCC under variable solvent conditions is employed, *i.e.*, as a single eluent

system (used in-here for LCCC at pS CC) and in mixed solvents (used in-here for the LCCC at pLA CC). Recently the former technique was successfully employed to determine the end functionality of pS chains^[330] as well as to separate pS from pS-*b*-pMMA chains,^[331] the single eluent LCCC method is nevertheless less developed than the mixed solvents one. It is indeed usually difficult to find a single solvent, which at a temperature below its boiling point, will play the role of both adsorli and desorli for a given (co)polymer. Yet, contrary to the mixed solvent method whose mobile phase composition evolves with the preferential evaporation of one of the mixture component, the single eluent technique allows for a better reproducibility of the results.^[332]

The first assessment of the structure of the generated polymeric material is carried out via conventional SEC equipped with RI and UV detectors. Figure 5.25 indicates that irrespective of the copolymer composition (refer to Table 5.9 for the employed notation), the RI and UV ($\lambda = 254$ nm) detector SEC traces overlap to a high degree, providing a strong indication that almost all the pLA chains were initiated by the pS-SH macroinitiator. (Note that a certain degree of disparity between RI and UV

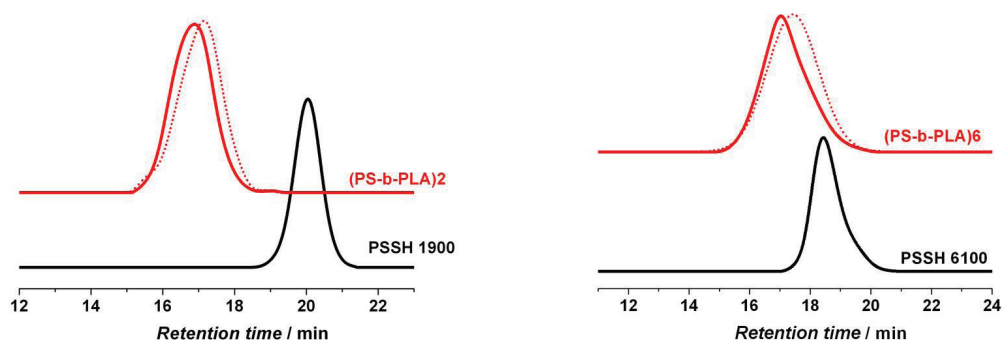


Figure 5.25. RI (bold line) and UV ($\lambda = 254$ nm) (dotted line) SEC traces of several poly(styrene)-*block*-poly(lactide) copolymers and their corresponding pS macroinitiator (see Table 5.9 for the number-average molar masses of the analyzed polymers).

trace is to be expected - even in relatively narrow polydispersity samples - due to the disparity in M_w and M_n (see above for a more detailed discussion)). In addition, the LCCC analysis at poly(styrene) critical conditions proves that almost all the pS-SH macroinitiators chains have been consumed and transformed into a new polymeric entity (most probably the desired pS-*b*-pLA chains) (see Figure 5.26), indicated by a clear shift of the polymer peak to lower retention volume compared to the pS-SH peak. The presence of some pS homopolymer chains observed at close to 450 s retention time can be explained either by pS-SH chains that did not initiate the ROP of LA (*i.e.*, not 100 % initiation efficiency) or - more likely - by dead (*i.e.*, not thiocarbonyl thio group terminal) pS chains produced during the RAFT process.

It is worth noting that the single eluent method, even though relatively facile to apply in the current case, does not allow for the separation of the various pS-*b*-pLA diblock copolymers according to their (pLA) block length as all the copolymers elute at the same time (and identical to the pLA homopolymer). The difference to the pLA homopolymer trace (black elugram, see Figure 5.25) is the broadening of the block copolymer traces to higher elution volumes - a phenomenon that has been previously observed in poly(styrene)-*b*-poly(ϵ -caprolactone) copolymers. According to Chang and colleagues,^[333] the elution mode is influenced by the solvent strength for the 'visible' block and can vary from the exclusion to the interaction mode. The very low shift of the copolymer traces with their pLA length are thus probably originating from the solvent strength. Nevertheless, as already mentioned, the aim of this chapter is above all to prove the presence of diblock copolymers.

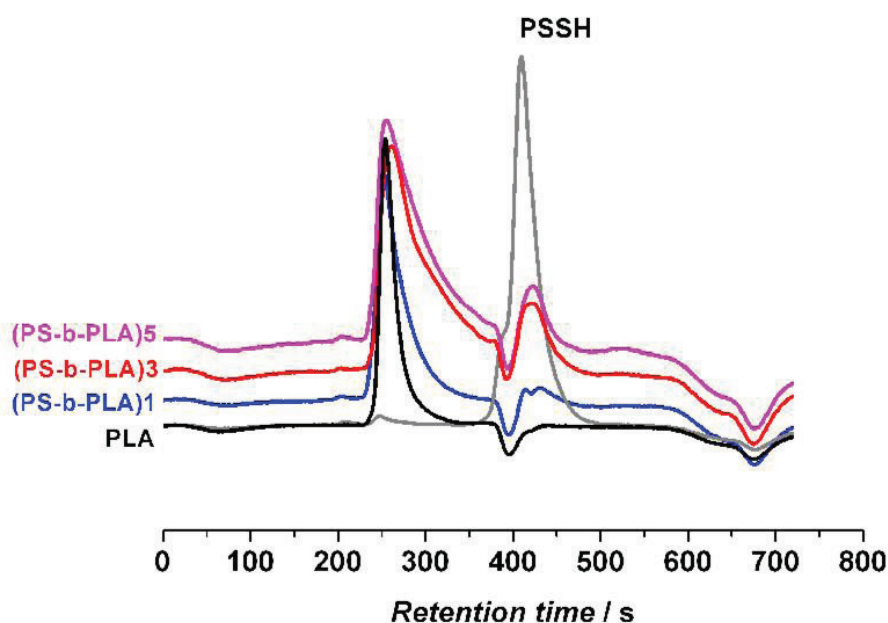


Figure 5.26. LC at CC of pS (single solvent method employing DMF) of an initial pS-SH ($M_n = 3600 \text{ g mol}^{-1}$), a model pLA ($M_n = 13300 \text{ g mol}^{-1}$) and several pS-*b*-pLA diblock copolymers (see Table 5.9).

While the analysis under critical conditions of pS give an indication that a transformation has taken place, an analysis via LC at CC of pLA (see Figure 5.27) confirms the conclusion obtained via dual detector SEC and LC at CC of pS, namely the synthesis of pS-*b*-pLA diblock copolymer chains (peaks around 600 s retention time in blue, red and purple, corresponding to the block copolymer pS-*b*-pLA 1, 3 and 5 and shifting to lower retention times with decreasing amounts of pLA present in the block copolymer). As one may expect, pLA homopolymer chains are formed in very low amounts (small peaks close to 700 s retention time) due to impurities present in the media (reagents, solvents) that initiate the LA ROP in parallel to pS-SH. The

formation of free pLA homopolymer chains is indeed very difficult to avoid, as a test performed without any initiator (Table 5.9, blank) proved that after 24 h at 100 °C in toluene and in the presence of $1 \cdot 10^{-3}$ mol of DMAP and $1.4 \cdot 10^{-2}$ mol of LA, pLA chains of 17000 g mol^{-1} (pS equivalents) were formed for an LA conversion of 94 %. Nevertheless, it is important to note here that the amount of free pLA homopolymer chains is relatively low compared to free pS homopolymer chains.

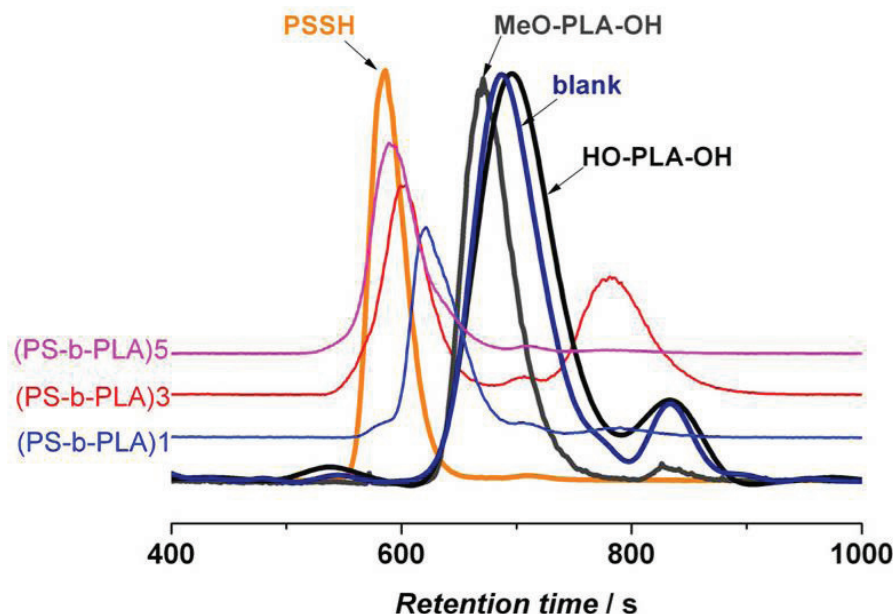


Figure 5.27. LC at CC of pLA of an initial pS-SH (3600 g mol^{-1}), various pLA initiated by water (HO-pLA-OH), methanol (MeO-pLA-OH) or by impurities of DMAP (blank) and several pS-*b*-pLA diblock copolymers (see Table 5.9) with increasing amounts of pS going from (pS-*b*-pLA)1 to 5. Note that with decreasing amounts of pLA in the block copolymer, the block copolymer peak shifts to lower retention times, attesting the variation in the block length ratio. The critical solvent mixture was acetone (62.7 wt%) and *n*-hexane (37.3 wt%).

In addition, it is worth noting that LCCC at pLA critical conditions allows for the separation of pLA initiated by methanol and water. As inspection of Figure 5.27 reveals, it seems that the major impurity of DMAP initiating the ROP of LA is water as the peaks corresponding of the blank experiment (without additional initiator) and the experiment with water as initiator overlap (peaks at close to 700 seconds retention time). The main issue when working with DMAP to avoid parasite initiation is thus to very carefully dry the catalyst before use. As observed in Figure 5.27 in the case of (pS-*b*-pLA)3, HO-pLA-OH, MeO-pLA-OH, and the blank experiment, an additional peak is observed after 800 s retention time. As already observed by Macko *et al.*^[332] and Srbek *et al.*^[334] when using mixed mobile phases, these additional peaks are most likely due to a preferential solvation of dissolved macromolecules or a preferential

adsorption of mobile phase components on the column surface. These peaks that are known to appear/disappear and move on the chromatograms and are thus inherent to the chromatographic system, coming from specific interactions between the stationary and mobile phases. Consequently, they were not taken into account when analyzing the pS-*b*-pLA and the pLA (co)polymer samples.

In conclusion, dual SEC, LCCC at both pS and pLA critical conditions provide substantial evidence for the presence of pS-*b*-pLA diblock copolymers chains. Nevertheless, it seems that the presence of residual free pS and/or pLA homopolymer chains are intrinsic to the polymerization system as pS homopolymer chains are certainly caused by thiocarbonyl thio non-functional material formed during the RAFT process and pLA homopolymer chains may eventuate from parasite initiation from media impurities. Even though the proportion of residual homopolymer chains cannot be quantified, the LCCC analysis and the comparison of the peak areas of homo and copolymer chains clearly indicate that homopolymer chains are in a net smaller quantity than diblock copolymer chains.

5.4.4. Conclusions

The preparation of block copolymers featuring a degradable poly(lactide) and a non-degradable poly(styrene) strand is possible via the use of macrothiols prepared from thiocarbonyl thio capped precursors prepared via the RAFT process, employing the thiol termini as macroinitiators in a ring-opening polymerization. The analyses of the polymeric material via multiple detector SEC and liquid chromatography under critical conditions evidences the formation of the desired block copolymer structures alongside residual macrothiol and homopoly(lactide) in minor quantities. The current section has demonstrated that it is indeed possible to employ RAFT derived macrothiols as initiating species in the organo-catalyzed ROP of lactides, thus providing an alternative platform for the generation of block copolymers with degradable and non-degradable strands.

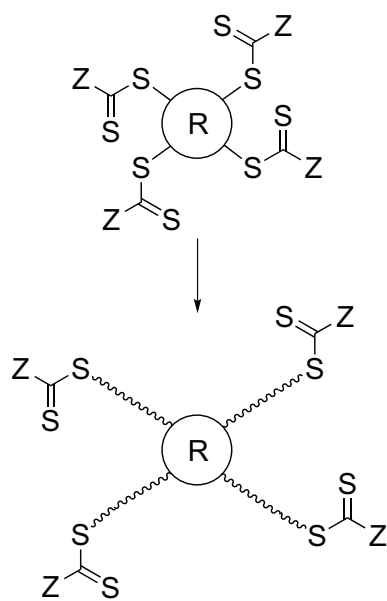
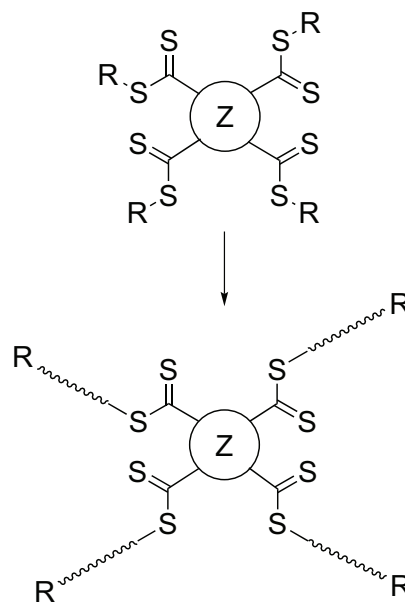
6

In-Depth LCCC-(GELC)-SEC Characterization of ABA (star) Block Copolymers

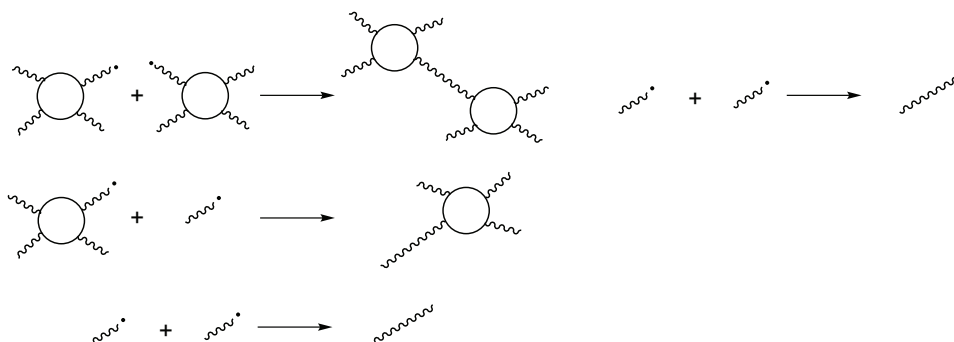
6.1. Introduction Including a Theoretical Background to Star RAFT Polymers

In Chapter 4, a facile method to alter the end-group functionality of RAFT generated polymers to obtain hydroxyl terminal macromolecules was reported. The method was applied to variable polymers and a variety of macroRAFT agents.^[274–276] The advantage of the above strategy is the generation of sulfur-free narrowly dispersed polymers that are equipped with a versatile synthetic handle. In the preceding Chapter 5, it was successfully demonstrated that the OH functional polymer can subsequently be employed as a macro-initiator for ROP. For the synthetic approach of the current chapter, the above-named end-group conversion is applied to obtain more complex and demanding polymer architectures such as ABA block copolymers and star block copolymers. Such an approach is possible by employing multi-functional RAFT agents for the preparation of ω -functional entities which can be transformed into multi-functional terminal alcohols.

For the formation of star polymers via the RAFT process two approaches can gen-

RAFT star *via* a R-group approach*via* a Z-group approach

Termination reactions:



Scheme 6.1 The core first technique for the synthesis of RAFT star polymers is subdivided in the Z- and the R-group approach. The possible termination reactions for the R- and the Z-group approach are included in the scheme.

erally be applied, *i.e.*, the Z- and the R-group approach (see Scheme 6.1). For the Z-group approach the thiocarbonyl thio groups are connected to the core via the Z-group, while in the R-group approach the thio entity is connected to the core via the R-group. By virtue of the RAFT process the propagating radicals are located either in the solution around the star core on the growing polymer chains (Z-group approach) or the radical is located at the core itself during the polymerization (R-approach). In Scheme 6.1, the possible termination reactions of the Z- and R-group approach are additionally depicted. When utilizing the R-group approach, three possible termination reactions can occur due to the RAFT process, *i.e.*, star-star coupling, star-chain coupling and the coupling of two propagating chains. Since no radical is located at the core during the polymerization utilizing the Z-approach, no star coupling occurs.

A higher control over the polymerization is obtained via the Z-group approach since less termination reactions take place.

Consequently, the Z-group approach is preferred to the R-approach in many cases. However, with the Z-approach the thiocarbonyl thio groups of the synthesized star polymers are directly attached to the core and not on the chain end.^[335] Transforming the thiocarbonyl thio groups into hydroxyl functions of star polymers synthesized via the Z-approach would lead to a destruction of the star (and to linear chains) and not to the desired star macro-initiators. Utilizing the R-approach for the star polymerization, the final product possesses thiocarbonyl end-groups at the chain end. Thus, the R-approach is utilized for the RAFT polymerization in the current study. By transformation of the dithioester groups, multifunctional polymers with OH groups at the chain end are obtained. The ω -hydroxylated star polymers were subsequently employed as macro-initiators for the ring-opening polymerization of ϵ -caprolactone catalyzed by (1,5,7-triazabicyclo[4.4.0]dec-5-ene (TBD)) (see also Scheme 5.1 in Chapter 5).

The resulting copolymers are characterized via spectroscopic, spectrometric and chromatographic methods. In general, block copolymers and higher architectures are analyzed via SEC, ¹H-NMR and – if appropriate – with mass spectrometry.^[17–19] Via SEC, the average molar masses and the polydispersity are determined but no composition (chemical) information may be obtained when classical RI detection is employed. NMR spectroscopy yields information on the chemical composition and functional groups, however, topological information of the generated macromolecules is difficult to ascertain. Mass spectrometry is problematic for samples with broad or multiple distributions and high molar masses.

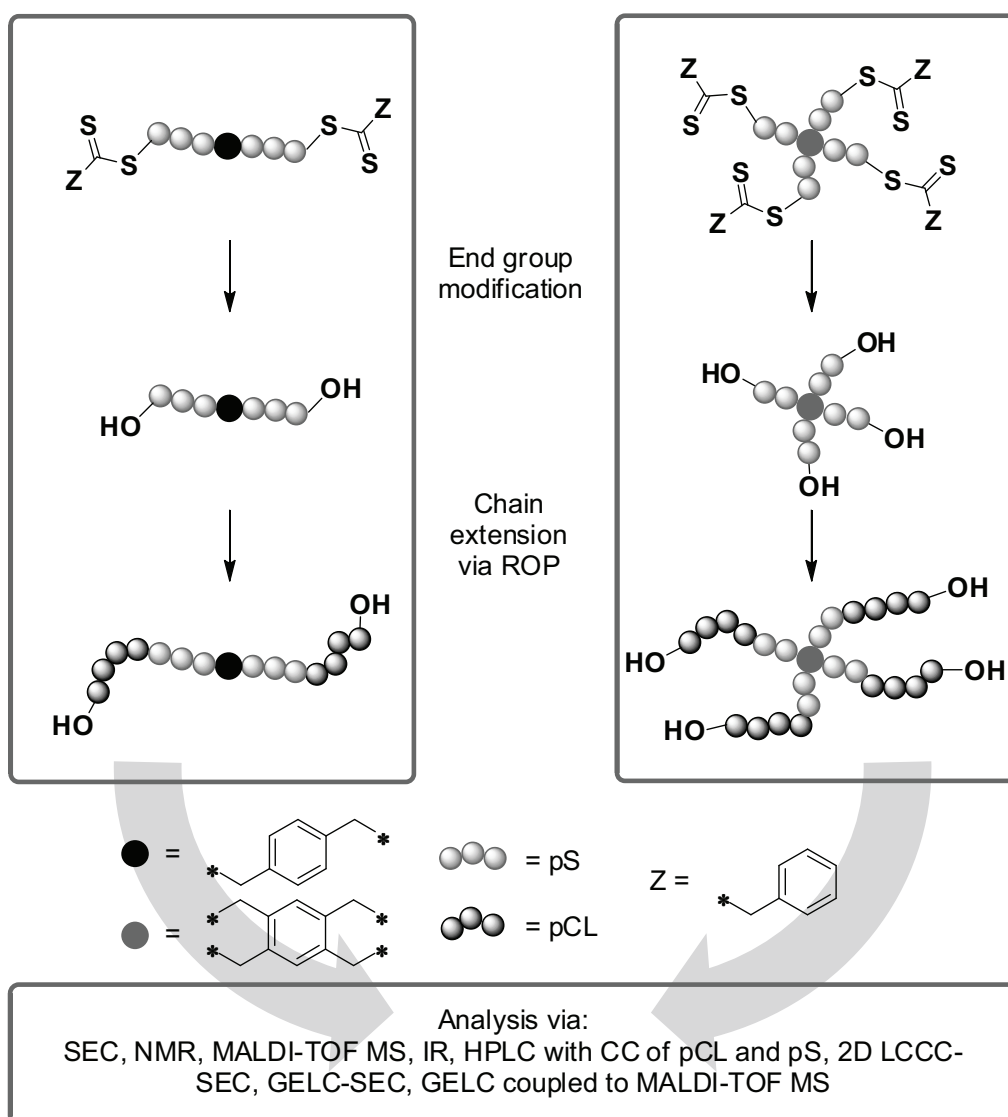
Thus, it is aimed here at employing hyphenated chromatographic techniques to elucidate the polymer structure, specifically aiming at identifying conditions under which poly(ϵ -caprolactone) (pCL) can be separated from true (star) block copolymer structures. A powerful method - liquid chromatography under critical conditions (LCCC) - features the ability to separate homopolymers from block copolymers. For a detailed description of chromatographic method the reader is referred to Chapter 2.5.3.

In the previous Chapter 5, the critical conditions of poly(styrene) (pS) have been applied on a LC system to separate poly(styrene) homopolymer from the AB block copolymers of the type poly(styrene)-*b*-poly(ϵ -caprolactone). The previously reported method will also be used in the current chapter to investigate ABA (star) block copolymers.

Additionally, a new method is introduced to separate (potential) residual poly(ϵ -caprolactone) (pCL) homopolymer from the generated block copolymer structures. The liquid adsorption chromatography is performed under critical conditions of poly(ϵ -

caprolactone). However, under the critical conditions of pCL the interactions between the stationary phase and the ABA (star) block copolymers are strong and thus the retention is too high, leading to permanent adsorption of the polymers on the column.^[336] Thus, the CC of pCL are combined with a solvent gradient, leading to a LCCC-gradient elution liquid chromatography (GELC) system. Via such an approach the separation of pCL homopolymer, block copolymers, and even the separation of pS homopolymer is feasible, as will be described below.

It is alternatively possible to hyphenate HPLC with further characterization systems such as ESI mass spectrometry.^[241] In the current study fractions eluting off an HPLC system are collected and characterized with IR spectroscopy. Additional structural information is provided by MALDI-TOF mass spectrometry. For this purpose, a newly designed electrospray deposition interface was used to fractionate and deposit samples onto MALDI targets. In summary, in the current chapter the extensive characterization of ABA (star) sulfur-free block copolymers synthesized via the RAFT/ROP technique (refer to Chapter 5), utilizing advanced multidimensional characterization techniques is reported (see Scheme 6.2).



Scheme 6.2 Synthetic concept to obtain ABA (star) block copolymers via RAFT/ROP and a summary of the utilized characterization techniques. Note that the depicted four armed star block copolymer represents the target structure only (for details see text).

6.2. Synthesis

Synthesis of 1,4-Di(phenylthioacetylthiomethyl)benzene (2-armed RAFT Agent) **2**

To a Grignard solution of 1.94 g magnesium metal (0.08 mol) in 10 mL of diethylether, 9.21 mL benzylchloride (0.07 mol) in 30 mL diethylether were added slowly under a nitrogen gas stream. After refluxing the solution for 1 h, the reaction mixture was cooled with ice. The subsequent addition of 4.82 mL carbondisulfide (0.05 mol) in 20 mL diethylether was performed at 0 °C and the reaction mixture was stirred for an additional hour. The mixture was poured into ice-cold water, the aqueous phase was washed two times with diethylether and acidified with HCl. The compound was ex-

tracted with diethylether and the solvent was removed under reduced pressure. 1.00 g potassium hydroxide was dissolved in 1 mL of water and mixed with the obtained compound. After drying the mixture under reduced pressure, it was dissolved in 20 mL of dry tetrahydrofuran and 2.15 g of α,α' -dibromo-p-xylene were added. The reaction mixture was refluxed for 1 h. Subsequently, water was added and the product was extracted twice with toluene. The product 1,4-dis(phenylthioacetylthiomethyl)benzene was obtained after evaporating the solvent and recrystallization from ethanol / chloroform (1/1). $^1\text{H-NMR}$ (250 MHz, CDCl_3): δ / ppm = 4.25 (s, 4H, $\text{CH}_2\text{-S}$), 4.3 (s, 4H, $\text{CH}_2\text{-CS}$), 7.15 (s, 4H, Ar-H), 7.15-7.30 (m, 10H, Ar-H).

2- and 4-armed Thiocarbonyl Thio Terminal Poly(styrene)s **3**, **4**

A solution of RAFT agent (**1**, **2**) and 2,2'-azobis(isobutyronitrile) in 100 mL styrene was freed from oxygen by purging with nitrogen for 20 min. The solution was heated to 60 °C for 180 min. The reaction was stopped by cooling with liquid nitrogen and the polymer was precipitated in cold methanol. The average molar mass and the polydispersity were determined via SEC and the corresponding ESI mass spectra combined with the corresponding isotopic pattern simulation can be found in Figure 6.1). The amount of the reagents and the resulting average molar masses of the poly(styrene) samples are collated in Table 6.1.

Table 6.1. Reaction conditions of the polymerization with 2-armed linear and 4-armed star RAFT agents **1** and **2**. c_{RAFT}^0 and c_{AIBN}^0 are the initial concentrations of the RAFT agent and AIBN, respectively. The molecular structures associated with the listed compounds can be found in Scheme 6.3.

Structure	RAFT agent	c_{RAFT}^0 / mmol L ⁻¹	c_{AIBN}^0 / mmol L ⁻¹	M_n / g mol ⁻¹	<i>PDI</i>
3	1 (2-armed)	10.4	0.06	3 400	1.3
4	2 (4-armed)	5.3	0.15	4 200	1.1

End-group Switching (Synthesis of Species **5**, **6**)

A solution of 2,2'-azobis(isobutyronitrile) (50 mmol L⁻¹) in THF was heated to 60 °C for 120 min under ambient air. 500 mg RAFT-polymer (**3**, **4**) (10 g mmol⁻¹ based on its M_n) were dissolved in the pre-treated THF/AIBN solution. The solution was heated subsequently to 60 °C under vigorous stirring. After 40 min, the temperature was reduced to 40 °C and 3 equiv. triphenylphosphine are added. After 20 min the solution was concentrated under reduced pressure with subsequent precipitation of the polymer in cold methanol. The resulting average molar masses and the *PDI*s are collated in Table 6.2. The SEC traces and a typical MALDI-TOF spectrum of **5** can

be found in Figure 6.2.

Table 6.2. Number-average molar mass, M_n , and polydispersity indices, PDI s, of the poly(styrene) samples after transformation of the end-group. The molecular structures associated with the listed compounds can be found in Scheme 6.3.

Structure	RAFT polymer	M_n / g mol ⁻¹	PDI
5	3 (2-armed)	3 900	1.2
6	4 (4-armed)	4 400	1.1

Ring-Opening Polymerization (Synthesis of Species **7,8**)

The ring-opening polymerization was performed in an inert gas atmosphere (argon) inside a glove box to rigorously exclude water from the reaction system. ϵ -CL was added to a solution of TBD and the poly(styrene) macro-initiator in 2 mL of toluene. The solution was stirred for 5 h and subsequently quenched by addition of benzoic acid. The polymer was precipitated in cold methanol. The concentrations of the reacting agents and the resulting average molar masses of the block copolymer samples are collated in Table 6.3.

Table 6.3. Reaction conditions and number-average molar mass, M_n , of the ring-opening polymerizations to generate ABA (star) poly(styrene)-*block*-(ϵ -caprolactone) polymers. The molecular structures associated with the listed compounds can be found in Scheme 6.3.

Structure	$n_{\epsilon\text{-CL}}$ / mmol	n_{TBD} / μmol	n_{pS} / μmol	M_n / g mol ⁻¹	PDI
7a	1.05	5.75	7.7	12 500	1.5
7b	2.63	5.75	12.8	33 000	1.3
7c	1.40	3.59	6.10	32 000	1.2
8	2.63	7.10	11.4	36 000	1.4

Ring-Opening Polymerization (PCL homopolymer for Determination of CC of pCL)

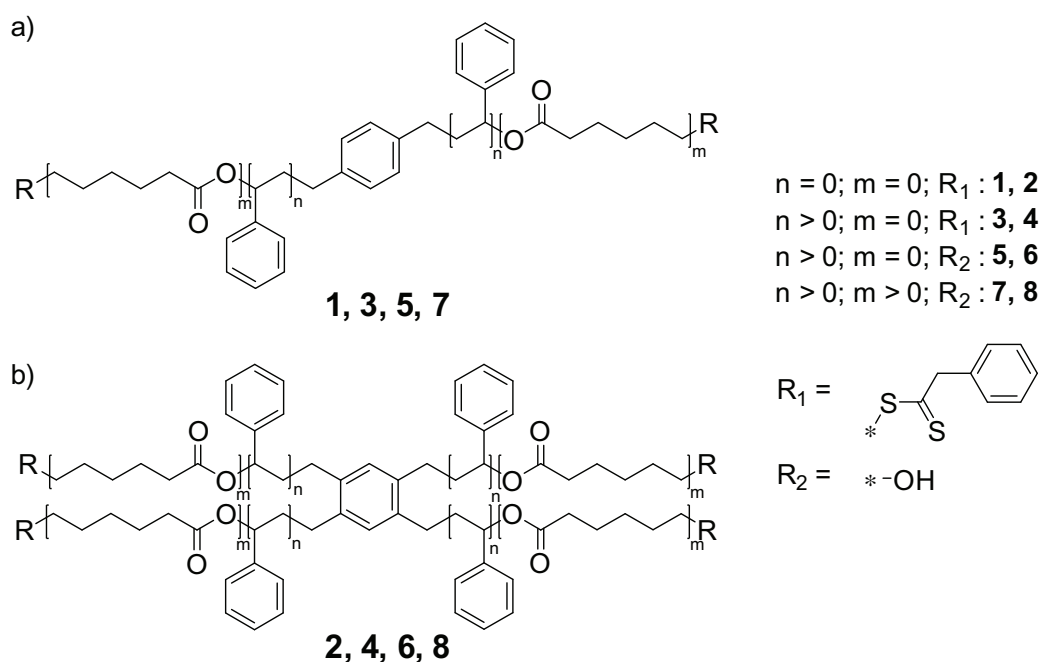
The ring-opening polymerization was performed in an inert gas atmosphere (argon) inside a glove box to rigorously exclude water from the reaction system. ϵ -CL was added to a solution of TBD and 2-butanol in 2 mL of toluene. The solution was stirred for 5 h and subsequently quenched via the addition of benzoic acid. The polymer was precipitated in a cold mixture of hexane : diethyl ether (1:1). The average molar mass was determined by SEC after precipitation. The amount of the reacting agent and the resulting molar mass of the poly(ϵ -caprolactone) samples are collated in Table 6.4.

Table 6.4. Reaction conditions and number-average molar mass, M_n , of the ring-opening polymerizations to generate poly(ϵ -caprolactone) homopolymer for the identification of critical conditions.

$n_{\epsilon\text{-CL}}$ / mmol	n_{TBD} / μmol	$n_{2\text{-butanol}}$ / μmol	M_n / g mol^{-1}	<i>PDI</i>
2.00	30.0	120	2 900	1.4
2.00	15.0	60	6 100	1.1
4.00	5.00	20	25 000	1.2

6.3. Results and Discussion

In the current chapter – as detailed in the introduction – the mechanistic switch from RAFT to ROP via a modification of the thiocarbonyl thio group to an OH end functionality is applied for the generation of ABA linear and star block copolymers (*i.e.*, by using 2-arm and 4-arm thiocarbonyl thio precursors) followed and intertwined with their in depth characterization (see Scheme 6.2).



Scheme 6.3 Overview of the target structures prepared in the current contribution. a) shows the linear and b) star structures.

In the initial step, styrene is polymerized utilizing the RAFT agents illustrated in Scheme 6.3. The thiocarbonyl thio groups are attached to the core via the R-group of the chain transfer molecule and the Z-group is located at the periphery, which is necessary for the subsequent end-group modification. The challenge of the reaction is to obtain polymer with a low *PDI* and high end-group fidelity, which can be hampered

by the side reactions occurring in an R-group approach polymerization, *i.e.*, star-star and chain-star coupling. However, side reactions can be reduced by minimizing the radical supply to the system, thus decreasing biradical termination and linear chain contamination.^[1,267,335] For the characterization, SEC traces and ESI mass spectra of the linear and 4-arm star RAFT polymers were recorded (refer to Table 6.1 and to Figure 6.1). The obtained ESI mass spectra were compared with the simulated isotopic patterns confirming the end-group functionality and the purity of the RAFT polymers.

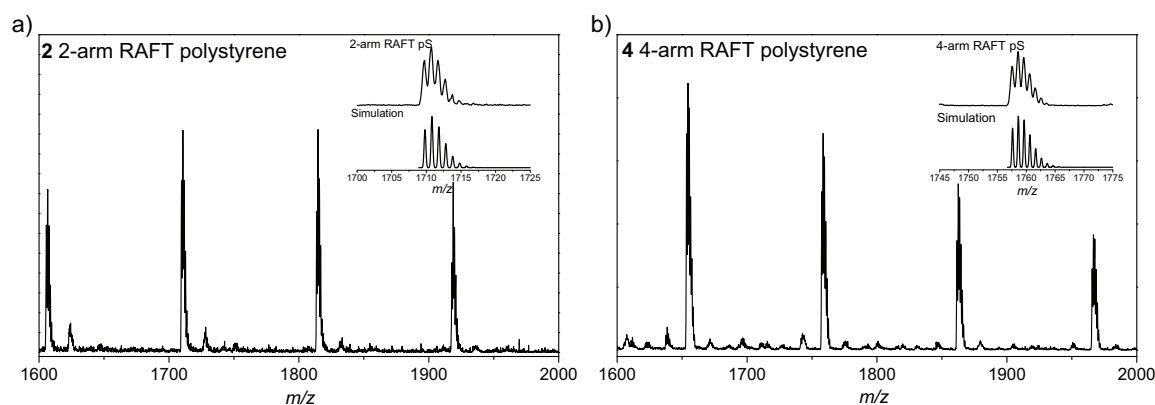


Figure 6.1. SEC/ESI-MS of RAFT polymers of styrene with a 2-arm (a) and a 4-arm (b) RAFT agent (non-rate retardant, R-approach) and the according simulations with 9 and 12 repeat units respectively. The spectra were measured via SEC/ESI-MS and only the range of single charged species is displayed in the figures. The counter ion in the main distribution is sodium. In the left hand spectra, a second less intense distribution with potassium as counter ion can be identified.

In the following step, the dithioester end-groups are converted to OH functionalities as shown in Scheme 6.2. Depending on the macroRAFT agent used, poly(styrene)s with two or more hydroxyl end-groups are obtained. For the details of the employed transformation mechanism the reader is referred to Chapter 4 and the references^[274–276]. The end-group conversion from the thiocarbonyl thio end-groups to hydroxyl groups can be assessed via MALDI mass spectra and SEC traces of the converted polymers. A typical MALDI-TOF mass spectrum of a dihydroxyl functional RAFT polymer is shown in Figure 6.2b, alongside a comparison of the theoretical and experimental isotopic pattern distributions. The four-armed star converted RAFT polymer was unfortunately unable to be imaged with reliable ionization via MALDI-TOF spectrometry. Thus, the number of obtained OH groups can only be indirectly accessed via the ROP process and the subsequent analysis (see below).

The OH converted poly(styrene) materials were employed as macro-initiators for the ROP of ϵ -caprolactone utilizing 1,5,7-triazabicyclo[4.4.0]dec-5-ene (TBD). Depending on the initial poly(styrene) either linear ABA or star-shaped block copolymers are obtained. The reaction conditions are collated in Table 6.3. The SEC traces of

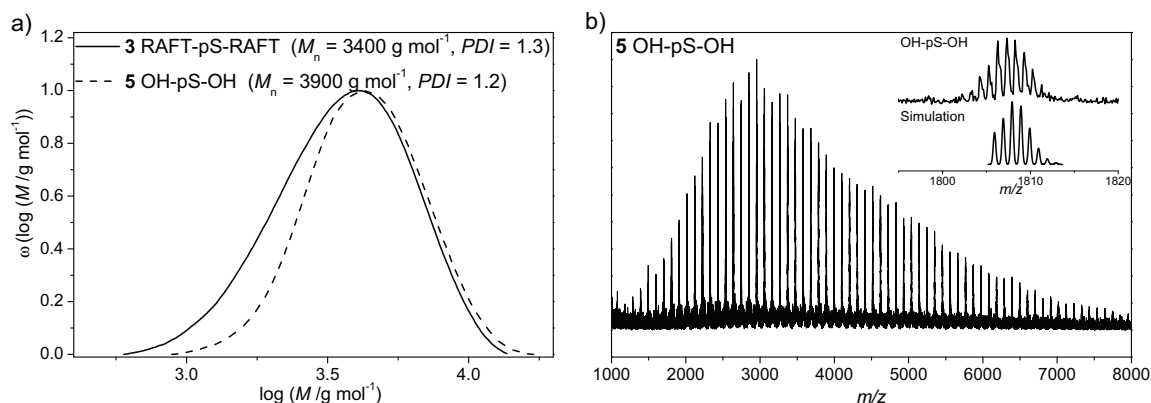


Figure 6.2. a) SEC traces of poly(styrene) possessing two OH end-group functions in comparison with the initial RAFT polymer and b) MALDI-TOF mass spectrum of OH-pS-OH and the corresponding isotopic pattern simulation (inset).

obtained block copolymers are depicted in Figure 6.3 and the associated average molar mass and polydispersity indices (*PDI*s) are given in Table 6.5.

Table 6.5. Collation of the number-average molar mass, M_n , and the *PDI* of the precursor polymers **5** and **6**, as well as of the ROP generated ABA (star) block copolymers **7a,b** and **8**.

Structure	Polymer	M_n / g mol^{-1}	<i>PDI</i>
5	OH-pS-OH	3 900	1.2
6	star pS-OH	4 400	1.1
7a	pCL- <i>b</i> -pS- <i>b</i> -pCL	12 500	1.5
7a	pCL- <i>b</i> -pS- <i>b</i> -pCL	33 000	1.3
8	star pS- <i>b</i> -pCL	36 000	1.4

Inspection of Figure 6.3a demonstrates that the linear ABA block copolymers **7a** and **7b** exhibit different molar masses, which is achieved by varying the monomer to macro-initiator ratio. Halving the macro-initiator concentrations of **7a** leads to a doubling of the number-average molar mass. To confirm the obtained results, the procedure leading to **7b** has been repeated (sample **7c**) and the corresponding data are depicted in Figure A.1 in the Appendix. The shift of the chromatograms towards lower retention volume of the ABA block copolymers compared with the macro-initiator hints at a successful chain extension. The chromatogram of **7b** does not reveal any low molar mass material, whereas the SEC chromatogram of **7a** exhibits a tailing in the lower molar mass range as well as a small shoulder. This may be due to incomplete chain extension of the macro-initiator pS or other side reactions such as initiation of ϵ -caprolactone with water residues or transesterification during the polymerization, which is typically observed at high catalyst content or at high

conversion.^[146,148] Clearly, further very detailed investigations are warranted and are provided below. Figure 6.3b displays the chromatogram of the chain extended star OH poly(styrene) to the possible star block copolymer **8**. Again, visual inspection suggests that nearly no hydroxyl star poly(styrene) initiator remained in the sample.

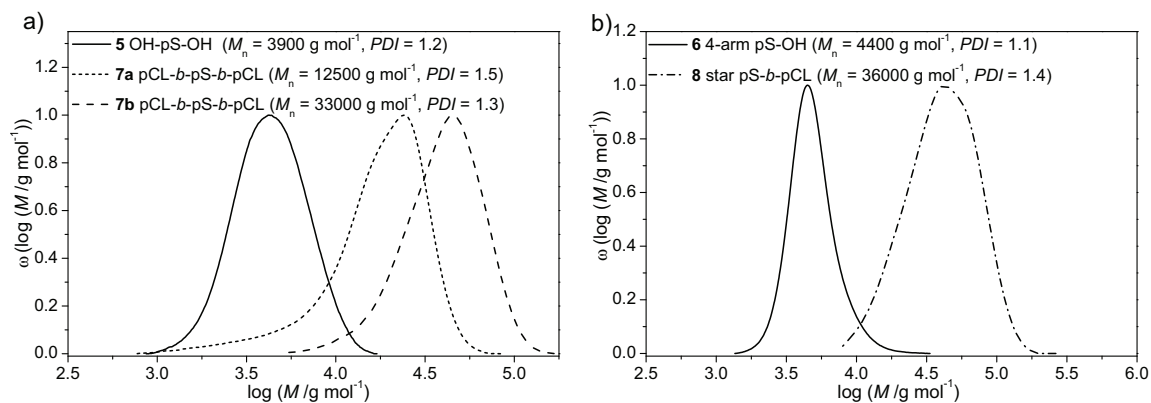


Figure 6.3. SEC traces of linear ABA block copolymers **7a** and **b** and the star block copolymer **8** synthesized via chain extension with ϵ -CL employing OH-pS-OH **5** and star pS-OH **6** respectively as macro-initiators. The associated average molar masses and the values of the polydispersity are depicted in the graphs.

After determining the molar masses of the ABA (star) block copolymers, a thorough investigation of the polymer structure is carried out. SEC traces can only provide limited evidence that a chain extension has occurred. For example, the SEC analysis does not indicate which number of OH groups attached to the poly(styrene) have initiated the ring-opening polymerization. With SEC, a block copolymer, an ABA block copolymer and a 4-arm star block copolymer are not distinguishable.

For the further characterization effort, $^1\text{H-NMR}$ spectra were subsequently collected. Figure 6.4 depicts the $^1\text{H-NMR}$ spectrum of the ABA block copolymer **7b**. The signals of the NMR spectrum correspond to the expected ^1H shifts of poly(styrene) and poly(ϵ -caprolactone). The signals a-c in Figure 6.4 can be assigned to the backbone of poly(styrene), the peaks d-h are associated with the backbone of poly(ϵ -caprolactone). The end-group of the polymer, $-\text{CH}_2\text{OH}$, is labeled with h'. Assuming that an ABA block copolymer is synthesized and thus two of the $-\text{CH}_2\text{OH}$ end-group h' exist – one on each side of the polymer chain – the molar masses of each block are calculated by integration of the significant signals (c for pS, h for pCL, h' as end-group). For the polymer **7b** a poly(styrene) block of 3900 g mol^{-1} is deduced and the two poly(ϵ -caprolactone) blocks together possess an M_n of 22000 g mol^{-1} . Alternatively, one may assume that only one end-group of the poly(styrene) initiated during the ring-opening polymerization resulting in a simple AB block copolymer. Hence, the block copolymer would feature only one $-\text{CH}_2\text{OH}$ end-group h'. Integrating the significant peaks under the 'AB block copolymer' assumption, a poly(styrene) block with a molar mass of

1900 g mol⁻¹ and a poly(ϵ -caprolactone) block of 11000 g mol⁻¹ is obtained. These results can consequently be compared with the results of the SEC traces (see Figure 6.3 and Table 6.4), where the poly(styrene) block exhibits a average molar mass of 3900 g mol⁻¹ and the chain extended system an average molar mass of 33000 g mol⁻¹ (with pS calibration). The molar mass of the poly(styrene) block under the hypothetical AB diblock copolymer assumption reads $M_n^{\text{pS-block}} = 1900 \text{ g mol}^{-1}$ (calculated via NMR signal integration) and does not correspond to the SEC analysis ($M_n^{\text{SEC,pS}} = 3900 \text{ g mol}^{-1}$); In contrast, the calculated molar mass of the poly(styrene) block for the deduced targeted ABA block copolymer ($M_n^{\text{NMR,pS}} = 3900 \text{ g mol}^{-1}$) matches perfectly with the SEC analysis. Based on the above calculations, the NMR analysis unambiguously supports an ABA block copolymer structure of polymer **7b**. Concerning the two poly(ϵ -caprolactone) blocks, it is very likely that the true molar mass is more realistically reflected by the integration of the NMR signals ($M_n^{\text{NMR,pCL}} = 22000 \text{ g mol}^{-1}$) than by the M_n values derived from the SEC traces, since the obtained data of the SEC are calibrated with linear poly(styrene) standards.

The ¹H-NMR spectra and the associated molar masses of the ABA (star) block copolymers **7a** and **8** are provided in Figure A.2 and Figure A.5 in the Appendix. The derivation of the number average of the molar mass via the integration of the signals in the NMR spectrum of sample **8** is of particular interest. Here, the integration procedure of the poly(styrene) backbone signal was based on the SEC deduced molar mass of the poly(styrene) macro-initiator and subsequently the end-group functionality $-CH_2OH$ was evaluated via the integration of the signal h'. The calculations reveal that not all four poly(styrene) chains were extended by ring-opening polymerization, yet the average value is close to 2.6 pCL end-groups, which signifies that approximately 65% of the pS-OH end-groups were activated as macroinitiators for the chain extension. As a possible reason the steric hindrance of the bulky star macroinitiator can be suggested. Additionally, the potential four -OH functions of the poly(styrene) macroinitiator are secondary alcohol termini. As soon as one chain is initiated by ring-opening of ϵ -CL, a primary-OH end function is formed. The primary-OH function of the pCL is more reactive to reinitiate the ROP compared to the secondary-OH end-group of the poly(styrene) macroinitiator. In addition, it may be possible that not all hydroperoxyl groups have been reduced to hydroxyl moieties. Due to simplicity, sample **8** will still be termed star block copolymer in further performed analysis. The NMR spectral analysis of sample **7a** reveals via an identical calculation that the average value of pCL end-groups is 2.1 (**7b**: 2.0). The only possible cause for the higher amount of end-groups in the formed ABA block copolymer than were present in the macroinitiator is the presence of a small additional poly(ϵ -caprolactone), formed during the polymerization process (see below for a detailed discussion).

For block copolymer analysis, ¹H-NMR spectroscopy and SEC analysis are not suf-

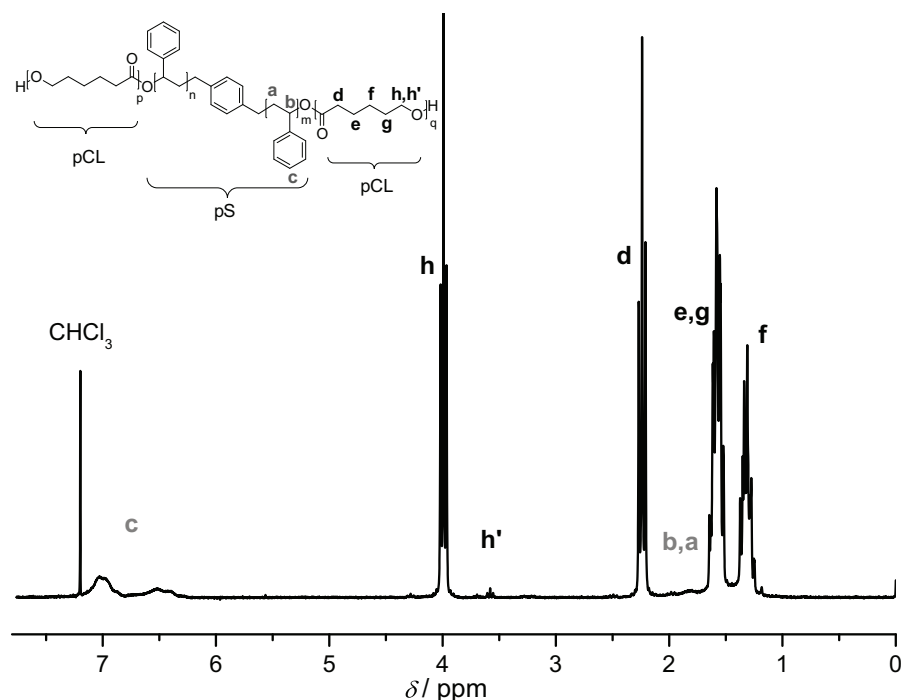


Figure 6.4. ^1H -NMR-spectrum of the pCL-*b*-pS-*b*-pCL block copolymer **7b**. The signals a-c correspond to the poly(styrene) block, the signals d-h to the poly(ϵ -caprolactone) block. The two end-groups are labeled with h'. The integration of the NMR signals, compared with the SEC analysis, supports the formation of an ABA block copolymer structure (for details see text).

ficient for obtaining information about their exact chemical composition and topology. In addition, evidence regarding the possible existence of homopolymer content in the samples remains circumstantial. Thus, a more in-depth analysis has been performed to obtain additional detailed and accurate information about the ABA (star) block copolymers. Two-dimensional chromatography (2D) is a reliable method to identify the occurrence of side reactions. To obtain a full 2D LAC-SEC analysis, a range of pre-analysis experiments have to be performed. Most importantly, the critical conditions of both block copolymer constituents have to be either known or separately established. The critical conditions for poly(styrene) are known from the previous Chapter 5 and are thus applied first. A 88.4 % (v/v) THF and 11.6 % (v/v) H_2O eluent mixture was employed on a reversed phase system (YMC-ODSA column). Firstly, the macroinitiator poly(styrene) samples with two (**5**) and more (**6**) end-groups respectively were measured under the critical conditions of poly(styrene) and compared with other poly(styrene) samples (*i.e.*, pS standard, pS RAFT **3** and pS-OH). The corresponding elugrams are displayed jointly with the elugrams of a poly(styrene) standard, the initial RAFT polymer **3** and a poly(styrene) with only one hydroxyl function (pS-OH) at the chain end in Figure 6.5. The pS RAFT polymer **3** contains two dithioacetate end-groups. For the synthesis of pS with one OH group the reader

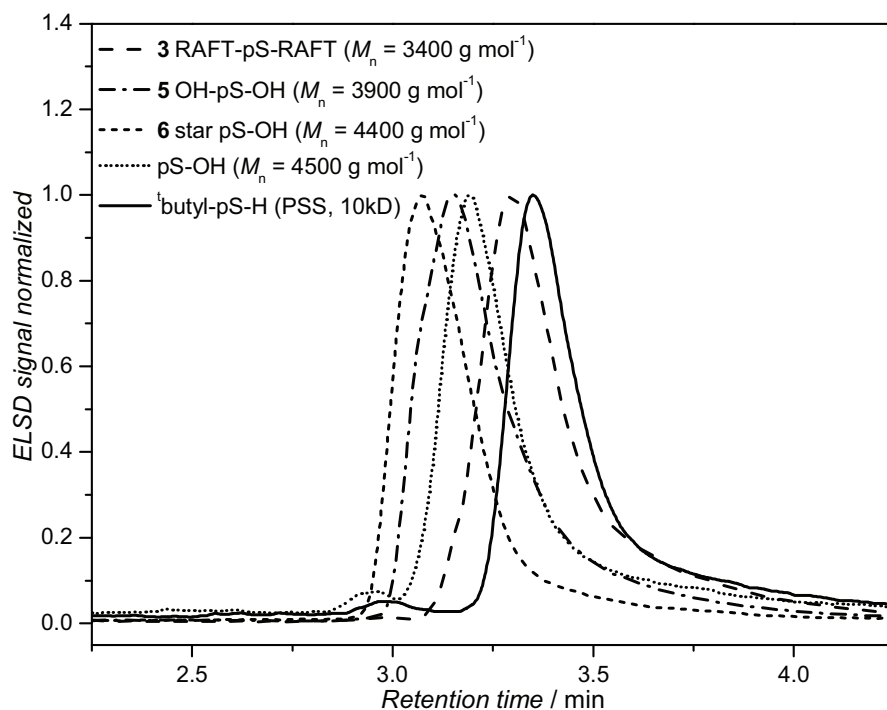


Figure 6.5. Elugrams of poly(styrene)s with different end-groups under critical conditions of poly(styrene) (reversed phase column, 88.4 % THF). Depending on the amount of hydrophobic end-groups, the elugram is shifted towards higher retention times.

is referred to the previous Chapter 5. The pS standard sample was purchased from PSS Standard Service and synthesized by anionic polymerization. The end-groups of the pS standard are consequently *t*butyl on one side and H on the other end. Thus, it represents a polymer with hydrophobic end-groups. All polymer samples possess average molar masses in the range between 3000-9000 g mol⁻¹. Under critical conditions of pS, pS samples with different molar masses elute at the same time, yet the elution time depends exclusively on the end-group functionality. On a reversed stationary phase the samples elute according to their hydrophobicity. The retention time increases with the amount of hydrophobic functions in the sample. The elugrams in Figure 6.5 reveal that on such a reversed system the pS samples with the hydrophobic end-groups elute later than the poly(styrene)s with hydrophilic end functionalities. Furthermore, it can clearly be observed that the polymer with the most hydrophilic end-groups (star pS-OH **6**, *i.e.*, the macro-initiator for the formation of star block copolymers) elutes earlier than the poly(styrene)s with two (OH-pS-OH) **5** or one OH-groups, respectively.

In the next step, the critical conditions of poly(styrene) were applied to ABA (star) block copolymers. Figure 6.6 depicts the elugrams of the samples compared with the poly(styrene) macro-initiator carrying two hydroxyl end-groups. Inspection of the ABA (star) block copolymers reveal that the star block copolymer **8** with an M_n

of 36000 g mol^{-1} elutes first while the ABA block copolymer **7a** with $M_n = 12500 \text{ g mol}^{-1}$ elutes last, which indicates that the different block copolymers elute under these conditions on a reversed phase system in the SEC mode. Further inspection of Figure 6.6 reveals that all elugrams exhibit a slight tailing. It is very likely that the tailing, which can be observed in all elugrams, is due to column interactions. Nevertheless, the tailing could also occur, for example, due to unreacted macro-initiator poly(styrene) homopolymer in the samples, since it is obvious that the tailing of the star **8** and triblock **7** copolymers overlaps with the elugram of the poly(styrene) homopolymer.

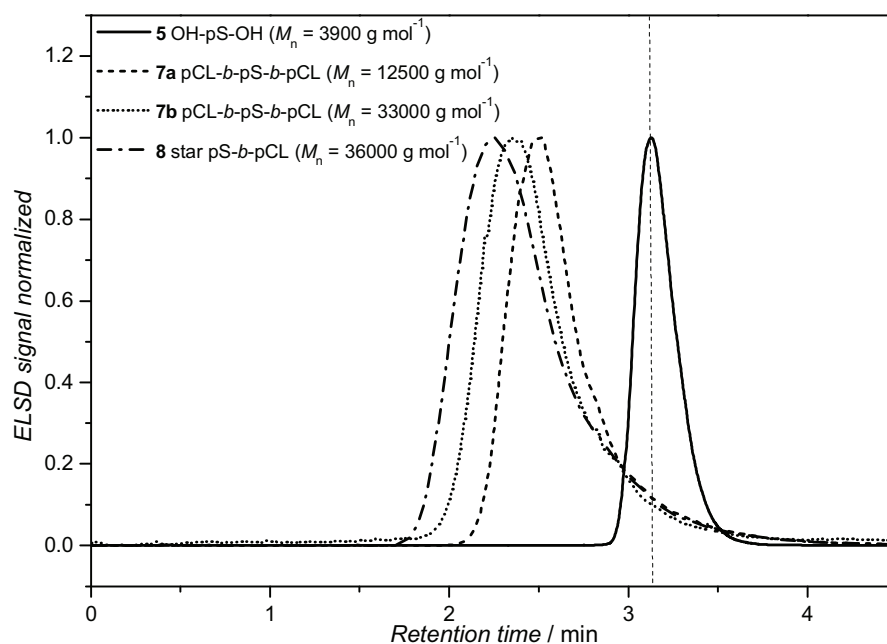


Figure 6.6. LCCC elugrams of ABA (star) block copolymers under critical conditions of poly(styrene) (88.4 % THF, 11.6 % H₂O). The elugrams reveal that the ABA (star) block copolymers elute in the SEC mode depending on the size of the pCL blocks in each sample.

Consequently, a method detecting the quantity of potentially remaining homopolymer poly(styrene) within the samples is required. For that reason two dimensional LCCC-SEC measurements of the samples **7** and **8** under critical conditions of pS were recorded. The corresponding LCCC-SEC chromatogram in combination with one dimensional elugrams of LCCC and SEC of the sample **7b** is presented in Figure 6.7. On the x-axis the recorded SEC elution volume and on the y-axis the LCCC elutions volume is indicated. The evaporative light scattering detector (ELSD) intensity in percentage (z-axis) is expressed by different colors. The ABA block copolymer appears diagonal in the 2D plot due to the fact that the sample elutes in the SEC modus. The dotted line in the chromatogram represents the LAC elution volume of the poly(styrene) macro-initiator under critical conditions of poly(styrene). Within

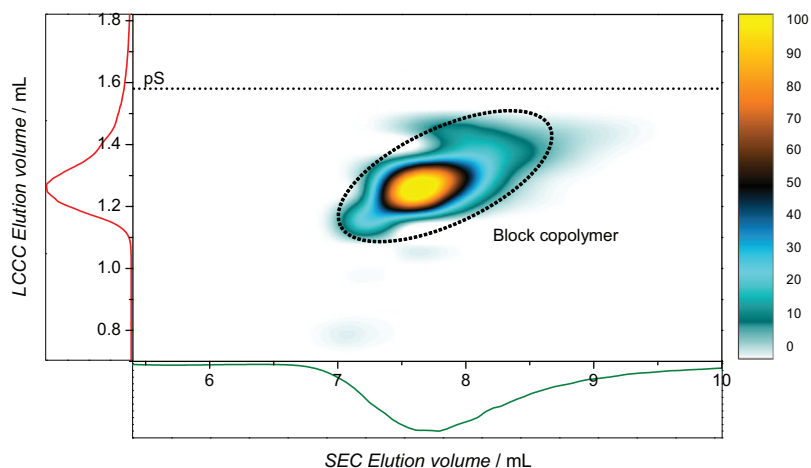


Figure 6.7. 2D LCCC-SEC plot of the pCL-*b*-pS-*b*-pCL block copolymer **7a**. The LCCC and the SEC traces are attached to the y-axis and the x-axis, respectively. The z-axis is given by the color scheme in percentage.

the detection limits of 2D LCCC-SEC chromatography, no residual macro-initiator (poly(styrene) homopolymer) is observed. The same conclusion can be drawn from the inspection of the LCCC-SEC chromatograms of **7a** and **8**, depicted in Figure A.3 and Figure A.4 in the Appendix.

As described above, the samples are chain extended via ring-opening polymerization. It is commonly known that side reactions can lead to pCL homopolymers in the block copolymer sample.^[336] Taking this into account, it is indispensable – beside the identification of residual macro-initiator poly(styrene) – to investigate the (potential) content of poly(ϵ -caprolactone) homopolymer in the ABA (star) block copolymer samples. An expedient method to separate pCL homopolymer from the ABA (star) block copolymers is the identification of the critical conditions of poly(ϵ -caprolactone) on an HPLC system. Critical conditions of pCL for the separation of block copolymers have been applied before.^[336,337] However, these conditions were utilized for the block copolymers poly(*n*-butyl acrylate)-*n*-poly(ϵ -caprolactone) and poly(ethylene glycol)-*b*-poly(ϵ -caprolactone), respectively, in which the connected block is still less hydrophobic than the poly(styrene) block. Consequently, the required separation efficiency for poly(styrene)-*b*-poly(ϵ -caprolactone) block copolymers is not given. For the establishment of the CC of pCL, the elugrams of poly(ϵ -caprolactone) homopolymers with different molar masses were recorded (see Table 6.4). Employing a reversed phase column (PLRP-S column) the solvent mixture of THF and MeOH was varied

until the poly(ϵ -caprolactone) samples elute at the same retention time. The corresponding elugrams are depicted in Figure 6.8. A solvent composition of 30 % (v/v)

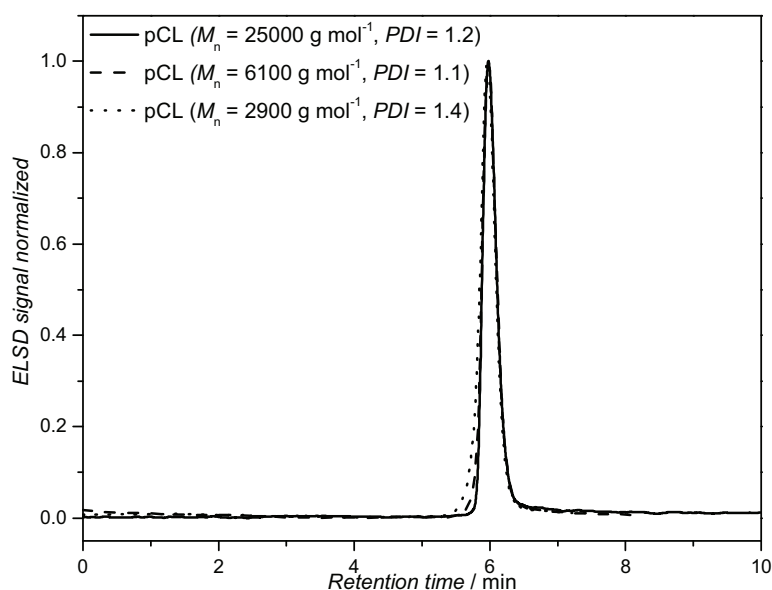


Figure 6.8. Elugrams of poly(ϵ -caprolactone) samples with different average molar masses. The measurement was conducted under critical conditions of pCL. Therefore a PLRP-S column with an eluent 30/70 % (v/v) THF/MeOH was employed.

THF and 70 % (v/v) MeOH was finally identified, where the retention times of the variable M_n poly(ϵ -caprolactone) samples are identical (5.97 min), which indicates the appropriate critical solvent composition is found.

Interestingly – under these conditions – the ABA (star) block copolymers are completely adsorbed onto the column. For a preferably complete recovery of the samples, the critical conditions of poly(ϵ -caprolactone) were combined with a solvent gradient (LCCC \times GELC), to ensure that the block copolymers are desorbed completely. To obtain information regarding the effectiveness of the separation, poly(styrene) homopolymer was measured via a LCCC-GELC system. In Figure 6.9 the elugrams of pCL homopolymer (dotted line, $M_n = 6100 \text{ g mol}^{-1}$, $PDI = 1.1$) and pS homopolymer (dashed line, $M_n = 8650 \text{ g mol}^{-1}$, $PDI = 1.03$) are displayed. On the left y-axis the % (v/v) of THF is indicated. The full line represents the THF content of the solvent mixture at a specific retention time. The measurement commences with a solvent mixture of 30 % THF and 70 % MeOH (CC of pCL) and concludes with 80 % of THF and 20 % of MeOH. The peak retention time of the pCL homopolymer is according to the critical point of pCL at around 6.0 min, whereas the poly(styrene) homopolymer elutes after the solvent gradient at 17.5 min. Via such an approach the two homopolymers pCL and pS are completely separated.

The new hybrid LCCC \times GELC method for separating poly(ϵ -caprolactone) and poly(styrene) was subsequently applied to the ABA (star) block copolymers. Due to

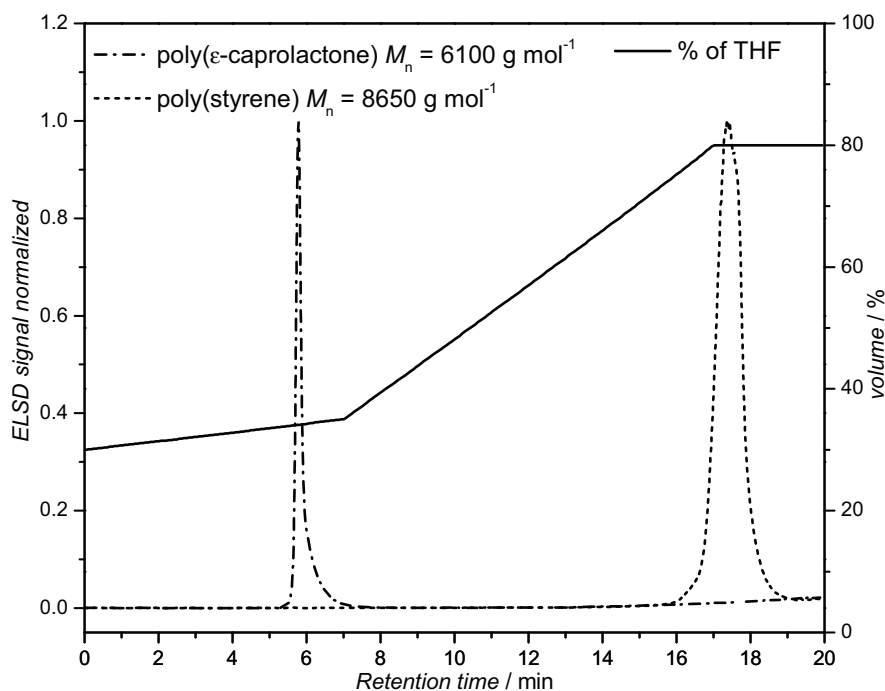


Figure 6.9. Slight gradient near critical conditions of poly(ϵ -caprolactone) combined with a gradient as a tool to separate pCL from pS homopolymers.

the CC of pCL the possible existence of the pCL homopolymer in the block copolymer can now be detected and a complete desorption of the sample from the column is provided by the subsequent solvent gradient. Initially, the elugram of the ABA block copolymer **7a** analyzed with the new CC-gradient system is discussed (presented in Figure 6.10), as that the elugram differs slightly from the samples **7b** and **8**, *i.e.*, **7b** and **8** represent the pure block copolymer structure. Two main signals can be observed. At the elution time of 6.00 min the first signal is visible. It corresponds to the time at which the pCL homopolymer elutes under critical conditions of poly(ϵ -caprolactone). The second signal has its peak maximum at 14.7 min retention time. Clearly – compared to Figure 6.9 – the first signal corresponds to the pCL homopolymer in the sample and the second signal corresponds to the block copolymer. Additionally, the pCL signal at 6 min retention time shows a shoulder at higher retention times. This implies that two different structures elute between 5.5 and 8 min retention time. Since the HPLC is performed on a reversed phase system, it is very likely that the first part of the signal possesses more hydrophilic end-groups than the subsequent shoulder. In the range of around 17.5 min retention time, at which poly(styrene) homopolymer elutes, no signal is observed. This observation corresponds well with the 2D plot measured under critical conditions of poly(styrene) (see Figure 6.7) and confirms that the macro-initiator poly(styrene) is completely consumed.

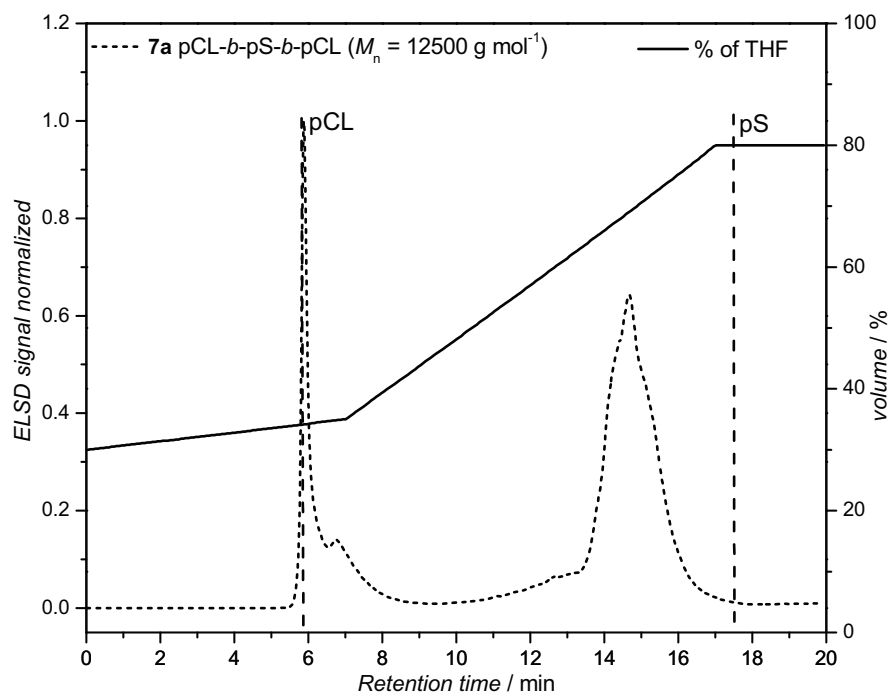


Figure 6.10. Gradient elution liquid chromatogram of the ABA block copolymer **7a**, conducted under critical conditions of pCL combined with a gradient.

In principle, a separation of a block copolymer AB from the homopolymer B may not be expected in a gradient system when block B is the adsorbing unit. However, since the average molar mass of the macro-initiator pS is fixed at 3900 g mol^{-1} and thus no smaller average molar masses of poly(styrene) were expected, the LCCC \times GELC system can also be applied for imaging potential residual poly(styrene) homopolymers, as the differences of masses between homo- and copolymer are sufficiently high. The GELC conditions were optimized concerning sample solvent, injection volume, column temperature and polymer sample concentration, so that a ‘breakthrough’ effect^[338] of copolymer respectively homopolymer poly(styrene) can be excluded, as evidenced by FT-IR and MALDI-TOF-MS measurements (see below). In addition, a GELC chromatogram of an pS-*b*-pCL diblock copolymer is depicted in Figure 6.11. For the synthesis and the characterization of the diblock copolymer the reader is referred to Chapter 5. This specific AB block copolymer possesses a small amount of macro-initiator poly(styrene) beside the block copolymer structure. In the chromatogram in Figure 6.11 a small shoulder is found at 17.5 min retention time beside the intense signal of the block copolymer at 15.2 min retention time. Thus, the chromatogram of the AB block copolymer is an excellent example to prove that poly(styrene) can be separated block copolymer via the LCCC-GELC system.

One possible option to identify the peaks in Figure 6.10 is to collect fractions of the sample at specific time intervals and to analyze these fractions via IR spectroscopy.

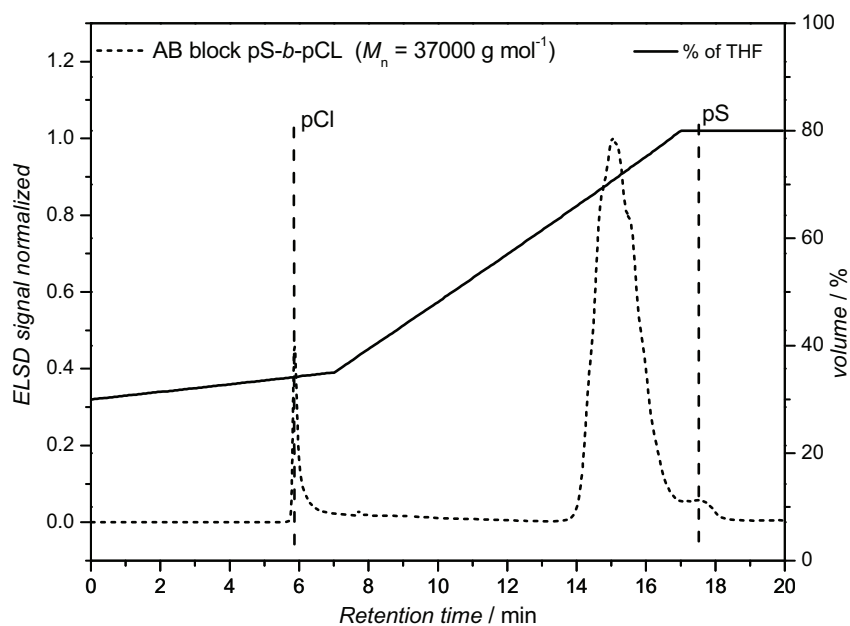


Figure 6.11. GELC chromatogram of an AB block copolymer pS-*b*-pCL ($M_n = 37000 \text{ g mol}^{-1}$, $PDI = 1.1$) in which macro-initiator pS residues are visible at 17.5 min retention time (shoulder) beside a small amount of homopolymer pCL (6 min retention time) and a high amount of block copolymer (15.2 min retention time). The synthesis and a detailed characterization of the AB block copolymer can be found in the Chapter 5.

Figure 6.12a displays the elugram of the ABA block copolymer **7a** including the division of the elugram in 4 fractions. Fraction 1 was collected between 5.5 and 5.8 min retention time, fraction 2 between 7.5 and 8.5 min, fraction 3 ranging from 11 to 12 min and the fraction 4 between 14.2 and 15 min. The fractions were selected in such a way that an overlap of two eluted structures is avoided. In Figure 6.12b, the IR spectrum of each fraction is displayed in the range of 500 to 3500 cm^{-1} . In all fractions the strong C=O stretching signal at 1724 cm^{-1} appears due to the pCL backbone ester groups. The IR spectra of fraction 3 and 4 additionally feature a signal at 700 cm^{-1} . This signal corresponds to the C-H stretching vibration of aromatic structures and thus signifies the presence of poly(styrene). The presence of both signals in fraction 3 and 4 – one corresponding to the backbone pCL and one corresponding to the repeat unit of poly(styrene) – proves the existence of block copolymer in sample **7a**. The signal strength of the C-H_{Ar} stretching is more pronounced in fraction 4; in fraction 3 the signal is rather weak, implying that the block copolymer part with longer pCL block length elutes at lower retention times whereas the block copolymer with shorter pCL block length elutes at higher retention times. No signal at 700 cm^{-1} is visible in fraction 1 and 2. Consequently, both fraction contain exclusively poly(ϵ -caprolactone). At first glance both fractions (1 and 2) exhibit the same IR spectrum.

A closer survey, however, reveals that in fraction 1 an additional signal at 1558 cm^{-1} appears which cannot be observed in fraction 2. Most likely the signal at 1558 cm^{-1} corresponds to a carboxylate stretching vibration. A possible explanation is that the material in fraction 1 possesses carboxylate end-groups, yet fraction 2 does not.

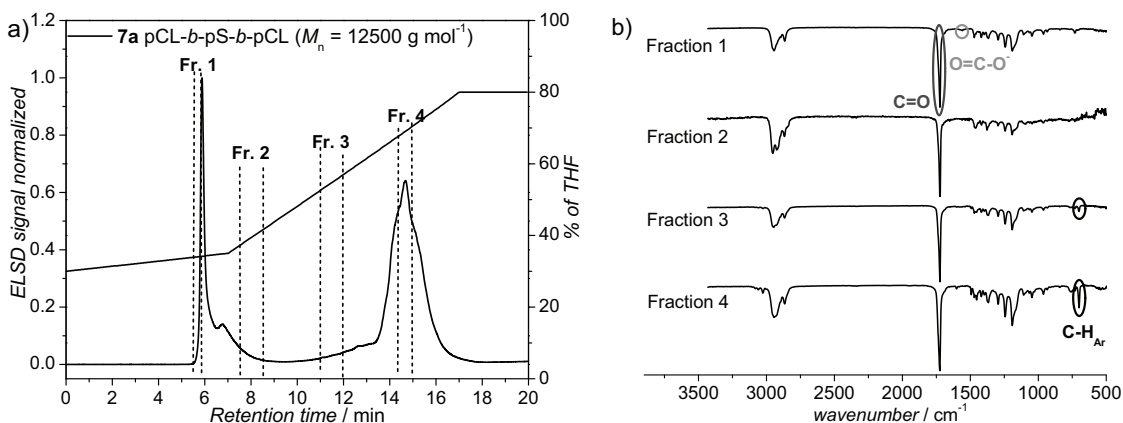


Figure 6.12. a) Fractionation of the sample **7a** according to the GELC-run for IR spectroscopic measurements; in b) the IR spectra of each fraction are presented. In the IR spectra of fraction 1 and 2 only the signals associated with the stretching vibration of poly(ϵ -caprolactone) can be identified, whereas in the spectra of fraction 3 and 4 the characteristic peaks for the stretching from the aromatic ring of poly(styrene) occurs in variable intensities.

The IR spectra of the fractions confirm that different functional groups (*i.e.*, carbonyl, carboxylate and aromatic moieties) are present in the different fractions. However, IR spectroscopy cannot identify the exact structure of the polymer, eluting at a specific retention time. For an unambiguous identification of the possible minor components of sample **7a**, the GELC system was coupled to MALDI-TOF mass spectrometry by means of an electrospray deposition device. A series of MALDI mass spectra recorded at retention times between 5.5 and 8.0 min (see chromatogram, Figure 6.10) is displayed in Figure 6.13. The peak-to-peak difference (*i.e.*, mass of repeat unit) of all distributions was m/z 114, which corresponds to pCL. In Figure 6.13a, a distribution can be identified that is attributed to linear pCL structures. Mass distributions that are characteristic for pCL possessing OH/carboxyl end-groups were found, which are formed by water residue initiated ϵ -CL (see Table 6.6). As shown in Figure 6.14 the measured isotope distribution of a linear pCL matches well with the simulated isotopic pattern (in addition see Table 6.6).

A minor distribution is found in the spectra, which corresponds to masses where the catalyst TBD is still attached to the linear chains. Figure 6.13b displays an additional series of peaks shifted by -18 Da from the previous peaks of the main distribution, which can be identified with minor intensity. These peaks correspond to macrocycles (see also overlay of theoretical and measured isotope pattern given in Figure 6.15).

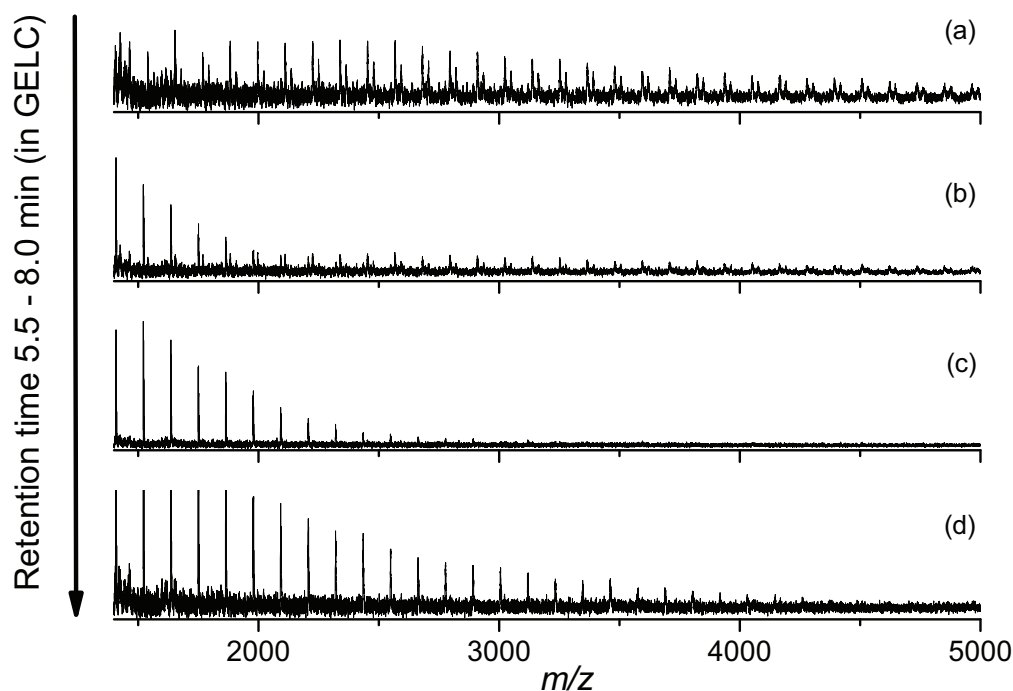


Figure 6.13. Series of MALDI-TOF mass spectra of sample **7a** recorded between 5.5 and 8.0 min of the GELC chromatogram (see Figure 6.10).

Table 6.6. Theoretical and measured m/z ratios of one peak in each distribution given in the Figure 6.14 and Figure 6.15.

Structure	$[M + Na]^+$		
	m/z^{theo}	m/z^{exp}	$\Delta m/z$
Linear pCL	2338.34	2338.06	0.28
Macrocycles	1407.78	1407.92	0.14

The formation of cyclic structures can occur by backbiting of the hydroxyl end-group to an ester group within the chain during the synthetic process.^[336] In Figure 6.13c these new series can be exclusively found. Its molar mass distribution increases from Figure 6.13b to d, *i.e.*, with increasing retention times. This correlates well with the assumed adsorption mode where small molecules elute first, whereas higher masses are longer retained on the column.

As shown in the chromatogram of sample **7a** (see Figure 6.10) a second intensive peak between 10-17 min retention time is observed. The MALDI-TOF mass spectra recorded in this range are depicted in Figure 6.16a. Only relatively noisy spectra with rather low resolution could be obtained, due to comparatively high average molar masses of the copolymers and the block copolymer structure itself. The repeat unit

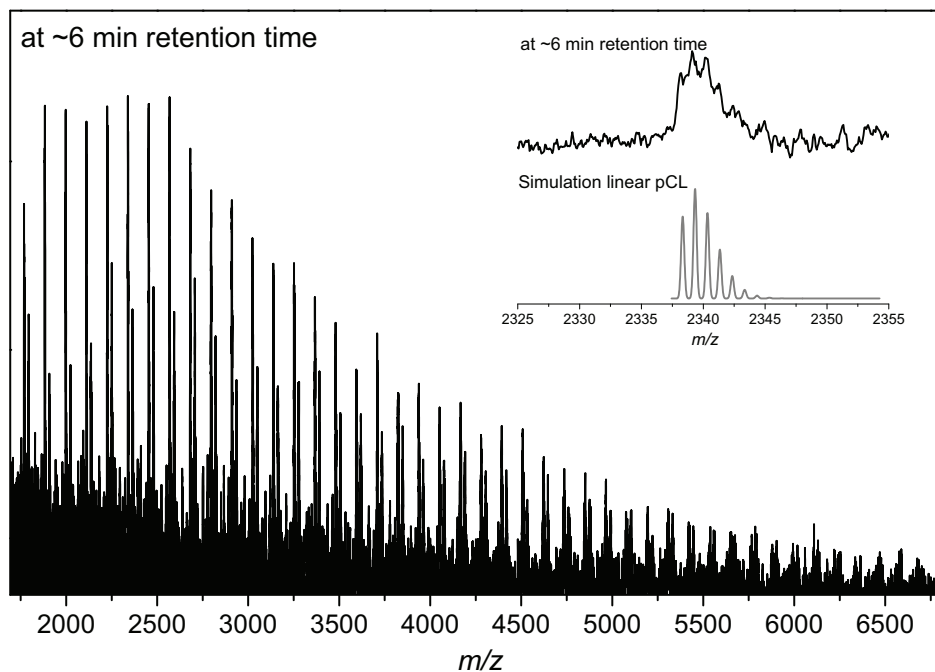


Figure 6.14. MALDI-TOF mass spectrum after approximately 6 min of the GELC run (Figure 6.13a) included in the series of spectra recorded by coupling an HPLC system to MALDI-TOF mass spectrometry. The inset shows the simulated isotopic pattern of water initiated linear homopolymer pCL in comparison with the MALDI measurement. The m/z ratios are given in Table 6.6.

of poly(styrene) is m/z 104, whereas pCL features a repeat unit of m/z 114. As a consequence, mass peaks with distances of m/z 10 were found, as shown in detail in Figure 6.16b. Figure 6.16b also reveals a successive shift of -10 Da of the measured peak distributions with increasing retention time (shown by the red lines). Such a shift can be readily explained by molecules having one of the ϵ -caprolactone units replaced by a styrene unit. Combined with the IR spectroscopy results of fractions 3 and 4 (see Figure 6.12), the MALDI data confirm our previous assumption that the amount of pCL units in the ABA block copolymer decreases with increasing retention time.

Finally, the 2D GELC-SEC analysis under critical conditions of pCL in combination with a gradient was performed. Figure 6.17 displays the obtained 2D plot. Due to the studies performed with IR spectroscopy and MALDI-TOF mass spectrometry, the spots in the 2D GELC-SEC plot can now be clearly identified. The narrow spot with the high intensity is associated with linear pCL homopolymer in the sample, the light and slight diagonal spot is identified as macrocyclic pCL in the sample. The broad and most intense spot is the ABA block copolymer. More importantly, the 2D plot reveals the molar masses of each spot. Following the SEC elution volume, the block copolymer possesses the highest and the macrocycles the lowest molar mass.

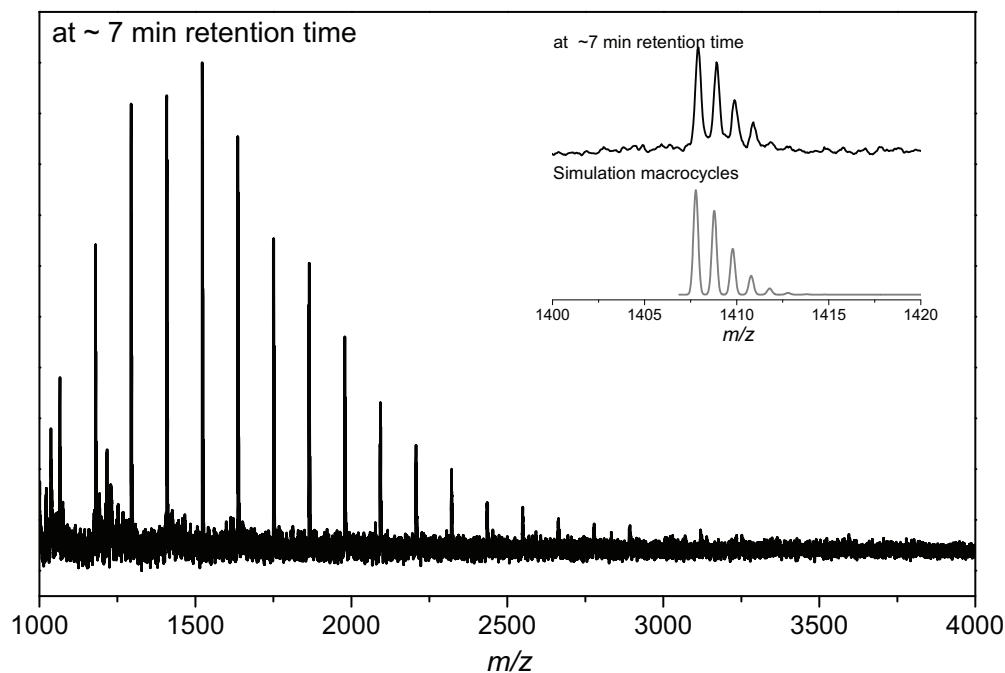


Figure 6.15. MALDI mass spectrum of the GELC coupled to online spray MALDI plate after approximately 7 min. The inset shows a comparison of the simulated and experimental isotopic pattern proving that the sample contains macrocycles. The m/z ratios are given in Table 6.6.

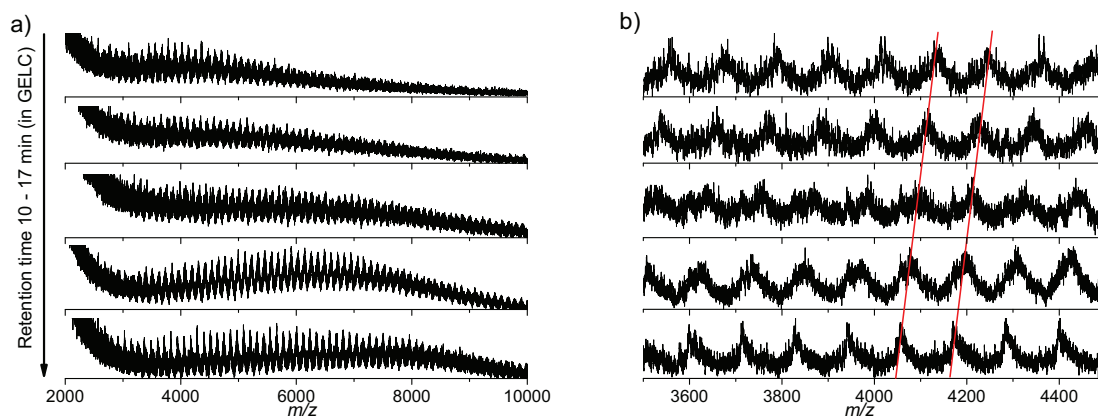


Figure 6.16. MALDI-TOF spectra of fractions 1, 3, 5, 7 and 9 of sample 7a in the range of 10 - 17 min of the GELC elugram; a) shows the complete detected distribution, whereas b) is a zoom-in of the spectra in the range of $m/z = 3500-4500$.

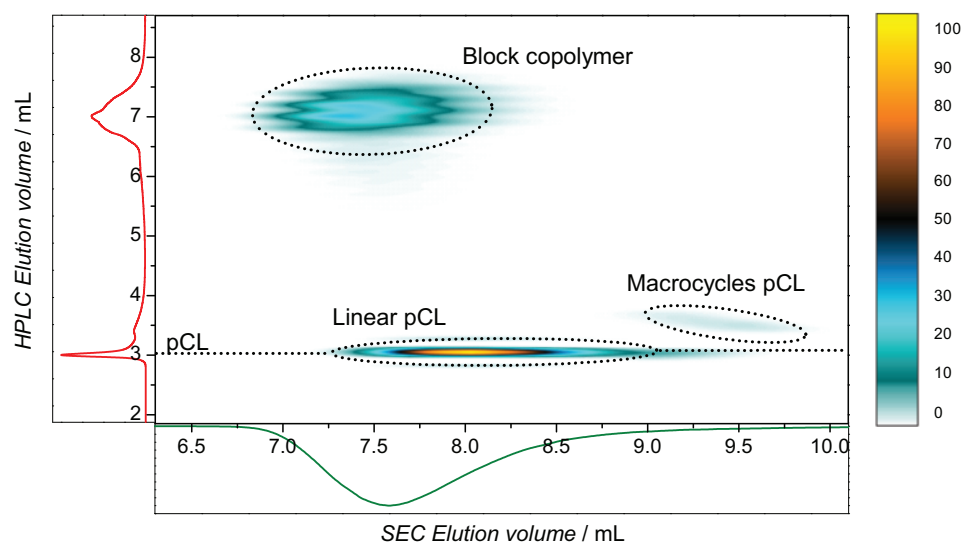


Figure 6.17. 2D LCCC-GELC-SEC chromatogram of the pCL-*b*-pS-*b*-pCL block copolymer **7a**. The GELC is conducted under CC of pCL combined with a solvent gradient. The chromatogram reveals the different molar masses of minor component linear and macrocyclic poly(ϵ -caprolactone).

As previously indicated, the chromatogram of the ABA block copolymer **7b** and the star block copolymer **8** under CC of pCL combined with the solvent gradient is discussed separately from sample **7a**. Employing the new CC-gradient system, the elugrams of the ABA (star) block copolymers **7b** (dotted line) and **8** (dashed line) are recorded (see Figure 6.18). The maximum of the elugram is located at 14.0 min retention time for sample **8** and 14.2 min retention time for sample **7b**. Both elugrams possess only a slight increase of the baseline at and after the critical point of pCL, implying that the samples contain only a very small amount of pCL homopolymer. A reason for the high content of pCL homopolymer in the sample **7a** compared to the samples **7b** and **8** is most likely associated with a higher ratio of catalyst in the reaction solution compared with the macro-initiator content (see Table 6.3). Similar to sample **7a** - in the range around 17.5 min retention time at which poly(styrene) homopolymer elutes - no signals are observed in either one of the elugrams. Thus, sample **7b** and **8** are relatively pure block copolymer structures.

Subsequently, the 2D GELC-SEC analyses of the ABA (star) block copolymers were performed. Figure 6.19 shows the 2D GELC-SEC plot of the star block copolymer **8**.

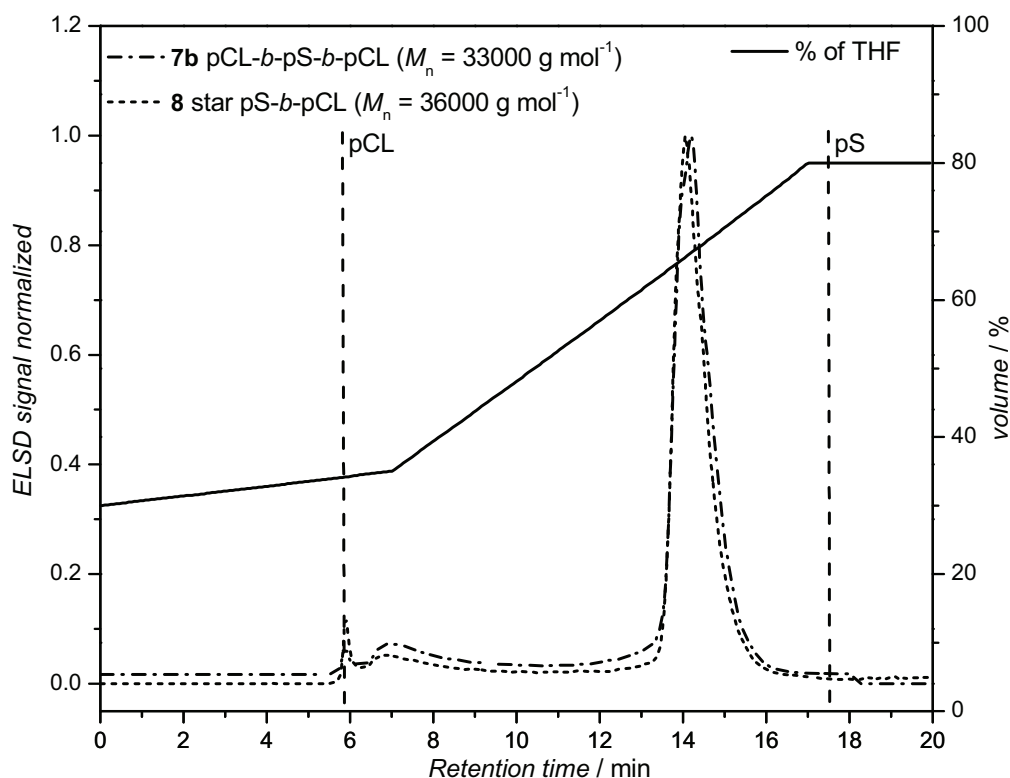


Figure 6.18. ABA block copolymer **7b** and star block copolymer **8** under the conditions presented in Figure 6.8. Clearly, the macro-initiator poly(styrene)-OH is completely consumed, in agreement with the chromatograms measured under CC of pS. Only a very low amount of pCL homopolymer can be identified analyzing the sample via the LCCC-GELC system starting from the critical conditions of pCL (30/70 % (v/v) THF/MeOH) and continuing with a solvent gradient.

The 2D plot of **7b** is presented in Figure A.6 in the Appendix. The LCCC-GELC was carried out under critical conditions of pCL (30/70 % (v/v) THF/MeOH) combined with the subsequent solvent gradient up to 80/20 % (v/v) THF/MeOH. The GELC and the SEC which correspond to the 2D plot are plotted along the vertical and horizontal axis. Two spots are visible in the LCCC-SEC chromatogram. The spot that elutes on the GELC at 3 mL retention volume corresponds to the critical point of pCL. Thus, this spot can be assigned to linear pCL homopolymer. In the 2D plots of the samples **7b** and **8** no macrocyclic pCL can be observed. The second spot at higher retention volume of the GELC run corresponds to the block copolymer in the sample. Following the SEC retention volume, the first spot of the sample elutes later than the second spot. Thus, the pCL homopolymer possesses a lower molar mass than the star block copolymer. The content of the pCL homopolymer in the sample **8** cannot be evaluated with full quantitative certainty, however a semi-quantitative statement can be made from the height and the broadness of the spot. According to the z-axis, which is illustrated by a color scheme, the intensity of the pCL homopolymer spot is

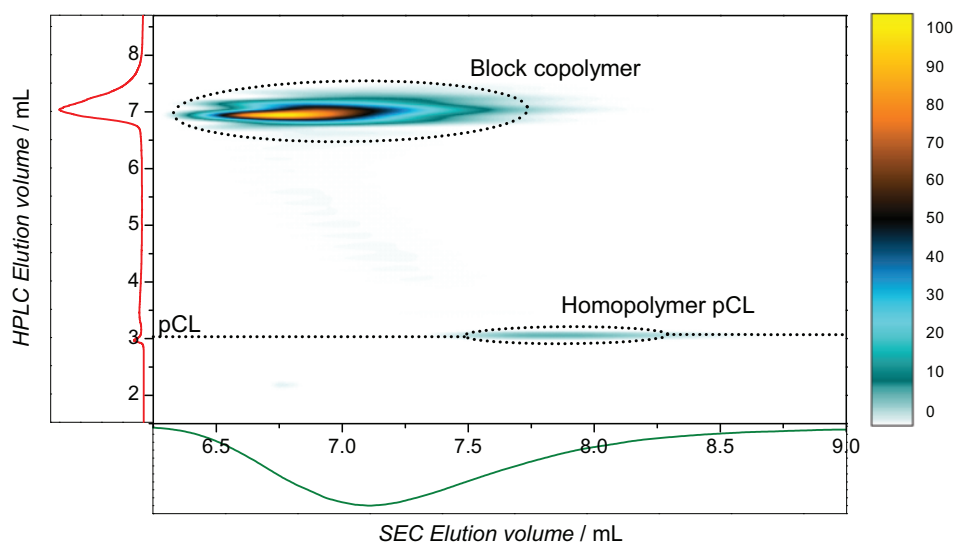


Figure 6.19. 2D LCCC-GELC-SEC chromatogram of the pS-*b*-pCL star block copolymer **8**. A very small amount of pCL homopolymer is detected.

in the range of 10% height. The spot of the block copolymer reaches 100 % and is in comparison to the first spot quite broad.

Thus, ABA (star) block copolymers with only very low amounts of impurities are synthesized via the newly introduced switch from RAFT to ROP. It is tempting to quantify the chromatographic data for all obtained polymers and to estimate the purities of the generated structures. The quantitative data are based on an integration of the ELSD signals and should be treated with some care as the correlation between ELSD signals of polymers of different structures is not necessarily strictly linear. For example, the quantitative evaluation of **7b** (by deconvoluting the individual ELSD signals) indicates that it contains 94 % of block copolymer, 0.5% of linear pCL, 5.5 % of macrocycles pCL and no homopolymer pS. Thus, it can be clearly seen that the in-depth characterization approach detailed in the current study is excellently applicable towards the characterization of pS-*b*-pCL block copolymers in general.

6.4. Conclusions

In the present chapter the procedure of switching from RAFT to ROP was successfully employed to synthesize ABA (star) block copolymers. For this purpose the end-

groups of 2-arm linear and 4-arm star R-approach RAFT polymers were modified and subsequently utilized as macro-initiators for ring-opening polymerization under organo-catalysis. The focus of the present study was on the characterization of the obtained materials by various analytical techniques, including two dimensional liquid chromatography. The separation of pCL homopolymer from the ABA (star) block copolymers was a particular focus and accomplished by the introduction of a new hybrid LCCC-GELC method – a system which combines the critical conditions of pCL with a solvent gradient – allowing for the first time the separation of pCL from pS. Thus, a new synthetic approach to ABA (star) block copolymer and – most importantly – a viable and powerful method for their complete characterization was demonstrated.

7

Multi-block Polyurethanes via RAFT End-group Switching

7.1. Introduction

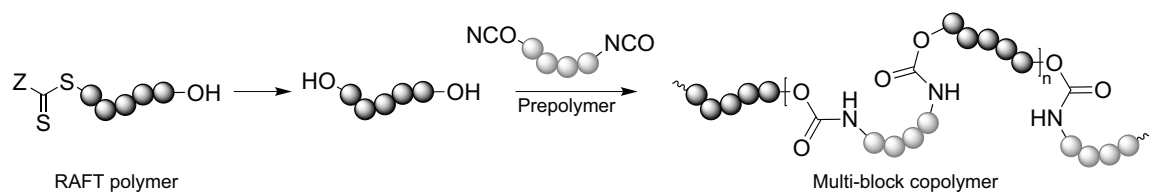
As described in Chapter 5, block copolymer formation can be performed either via a reaction of two polymer chains with specific end-functionalities (modular ligation) or via chain extension at their end functionality.^[306–308] For the formation of multi-block copolymers the same requirements hold as for diblock copolymers, however, the polymer chains should not only possess one, but two end functionalities. There exists a variety of multi-block copolymer synthetic strategies. A powerful approach proceeds via sequential anionic polymerization.^[339,340] An alternative route is via controlled/living radical polymerization such as ATRP and RAFT.^[341,342] Modular ligation concepts can be applied as an alternative method to synthesize well defined multi-block copolymers.^[343,344] Examples of combining different polymerization techniques to form multi-block copolymers can also be found in the literature. For example, Mahanthappa and coworkers synthesized multi-block copolymers via a combination of ring-opening metathesis polymerization (ROMP) and NMP.^[345] The sequential method of ring-opening polymerization and polycondensation also leads to multi-block copolymer formation as well.^[346]

Polyurethanes (pU) find – due to their flexible construction options – a wide variety of applications such as tissue engineering, coatings and adhesives.^[13,14] Linear

polyurethanes are commonly synthesized via polyaddition reactions of a diol and a diisocyanate.^[15] Due to the rigidity and H-bonding of the urethane linkages the polyurethane chains precipitate in many solvents and become insoluble with increasing chain length. Thus, macromolecular diols are often inserted in the polyaddition process to obtain a higher chain mobility and thus solubility of the polymer chains.^[16]

The combination of polyurethane chemistry and multi-block copolymer structures can result in new material properties and applications. Yin *et al.* reported that an improvement of the material properties, including mechanical properties and water resistance, is obtained by the insertion of vinyl polymers into the polyurethane structure.^[185] Potential shape memory materials were generated via a pU-multi-block synthesis by Lendlein and coworkers.^[347] A synthetic strategy of RAFT, ROP and polyurethane chemistry was realized by Webster and coworkers for coating films.^[348]

In Chapter 4 the procedure to modify the thiocarbonyl thio end-group of RAFT polymers into a hydroxyl moiety was presented,^[275,276] can open the unique possibility to employ RAFT-made polymers as building blocks – provided they feature two hydroxyl functionalities – for the construction of polyurethanes as macromonomers. In previous chapters the thiocarbonyl thio to hydroxyl-function switch was employed for the preparation of block copolymers structures prepared via RAFT and ring-opening polymerization. In Scheme 7.1 the general synthetic strategy followed in the current chapter is depicted.



Scheme 7.1 Schematic overview of the mechanistic switch from RAFT polymerization via end-group modification into dihydroxyl terminated polymers which enables a polyaddition to isocyanate-based prepolymers for the formation of multi-block copolymers.

The molar mass and the structure of linear polyurethanes and multi-block copolymers are conventionally characterized via NMR, FT-IR and SEC, presuming the material is soluble in suitable solvents.^[349,350] The determination of the molar masses of multi-block copolymers featuring building blocks which vary highly in their chemical composition, is inaccurate with conventional SEC due to the absence of accurate calibration methods. For obtaining more exact molar mass values of the copolymers, size exclusion chromatography coupled to triple detection can be applied.^[351] With triple detection – a sequence of differential refractive index detector, differential viscometer and especially multi-angle light scattering detector – the absolute M_w of homopolymers can be determined .

A very elegant way to obtain information of the chemical structure of a sample as a function of its molar mass is size-exclusion chromatography coupled online to electrospray ionization mass spectrometry (ESI-MS) and nuclear magnetic resonance detectors.^[352,353] However, ESI-MS is limited to relatively small macromolecules ($m/z \leq 2000$) while nuclear magnetic resonance detectors are cost-intensive and the SEC coupling is – due to solvent issues – not straight forward. On the other hand SEC coupled to Fourier transform infrared spectroscopy in general proceeds off-line as described in Chapter 6. The eluent of the SEC system is sprayed on an interface and the solvent is evaporated. Subsequently, the germanium circle plate – serving as target – is positioned in an FT-IR device for detection.^[253] Off-line SEC/FT-IR assembly requires a high sample mass or long scanning times to obtain spectra with a good resolution, which results in elongation of the analysis time. Furthermore, quantification of individual components can be challenging due to crystallization or oxidation of the analyte during the deposition process.^[254] Existing on-flow systems are for several reasons restricted to high temperature SEC for polyolefines in trichlorobenzene^[259] or by the use of deuterated water as eluent in protein analysis.^[262] They are not transferable to conventional SEC solvents and conditions used for general polymer characterization. In here, a new SEC/FT-IR coupling method is utilized for the detection of the multi-block copolymers circumventing the above mentioned problems with the aid of specialized mathematical solvent suppression techniques. This coupled measuring technique is being currently developed; basic ideas and first results have been reported by Beskers *et al.*^[263] In the current chapter the synthesis of multi-block RAFT based copolymers via urethane linkages and the subsequent characterization with state-of-the-art hyphenated methods are demonstrated.

7.2. Synthesis

The materials used in this section are collated in Chapter 3.

The synthesis of the RAFT agent 3-Hydroxypropyl-2-(((dodecylthio)carbonothioyl)-thio) propanoate **1**), see Scheme 7.2 can be found in the synthetic section of Chapter 4.

Preparation of the Thiocarbonyl Thio Terminal Polystyrene **2**

A solution of RAFT agent **1** (0.89 g, 37.1 mmol L⁻¹) and 2,2'-azobis(isobutyronitrile) (40 mg, 2.4 mmol L⁻¹) in 100 mL styrene was freed from oxygen by purging with nitrogen for 20 min. The solution was heated to 60 °C for 240 min. The reaction was stopped by cooling with liquid nitrogen and the polymer was precipitated in cold methanol. The average molar mass and the polydispersity was determined via SEC,

calibrated with pS standards. ($M_n = 3900 \text{ g mol}^{-1}$, $PDI = 1.2$).

End-Group Switching (Synthesis of Species **3**)

A solution of 2,2'-azobis(isobutyronitrile) (50 mmol L^{-1}) and the RAFT-polymer (**2**) (1.5 mmol L^{-1} based on its M_n) in THF was heated to $60 \text{ }^\circ\text{C}$ under vigorous stirring. After 40 min, the temperature was reduced to $40 \text{ }^\circ\text{C}$ and 3 equiv. triphenylphosphine were added. After 20 min the solution was concentrated under reduced pressure with subsequent precipitation of the polymer in cold methanol. The molar mass was determined with SEC, calibrated with pS standards ($M_n = 3700 \text{ g mol}^{-1}$, $PDI = 1.1$). The MALDI-TOF spectrum of **3** can be found in Figure 7.5.

Table 7.1. Assignment of the theoretical and measured m/z ratios of OH-pS-OH with 24 repeat units (see the Figure 7.1).

Structure	[M + Na] ⁺		
	m/z^{theo}	m/z^{exp}	$\Delta m/z$
OH-pS-OH	2648.41	2648.66	0.25

Synthesis of the Prepolymer (Synthesis of Species **4**, similar to^[354])

0.28 g of pTHF ($\sim 1000 \text{ g mol}^{-1}$), dissolved in dry DMAc, were added to a solution of 0.089 g TMDI (0.4 mmol) and 0.02 g of DBTDL (0.03 mmol) in DMAc at $80 \text{ }^\circ\text{C}$ under a nitrogen atmosphere. The mixture was stirred for 3 h. The prepolymer was dried for 5 h under reduced pressure at $100 \text{ }^\circ\text{C}$. The SEC traces of pTHF and the prepolymer can be found in Figure 7.2. However, due to the inaccuracy of the SEC results, for the molar masses of the prepolymer a value of close to 2500 g mol^{-1} is assumed, given by the addition of 3 isocyanate molecules and 2 pTHF chains.

Synthesis of the Multi-Block Copolymers Poly(styrene)-*b*-Poly(tetrahydrofuran) (Synthesis of Species **5-9**)

The obtained prepolymer (pp) **4**, dissolved in 1 mL DMAc, was heated to $80 \text{ }^\circ\text{C}$ under a nitrogen atmosphere. A solution of dihydroxy-terminated polystyrene **3** in DMAc (1.5 mL) was added together with 0.02 g of di-*n*-butyltindilaurate (0.03 mmol). The mixture was stirred for 48 h. The solution was cooled to stop the reaction and precipitated in methanol. The amount of pS was varied according to the required equivalents (see Table 7.2).

Table 7.2. Reaction conditions for the polyaddition as well as number average molar masses, M_n , and polydispersity indices (PDI s) of the poly(styrene)-*b*-poly(tetrahydrofuran) multi-block polyurethanes.

Structure	Equivalents prepolymer:pS	$m(pp)$ / g	$m(pS)$ / g	M_n / g mol ⁻¹	PDI
5	1:1.5	0.14	0.31	10 300	2.1
6	1:1	0.28	0.41	14 000	2.5
7	1.5:1	0.08	0.08	23 000	2.9
8	2:1	0.12	0.08	30 500	3.0
9	2:1	0.12	0.08	27 800	2.6

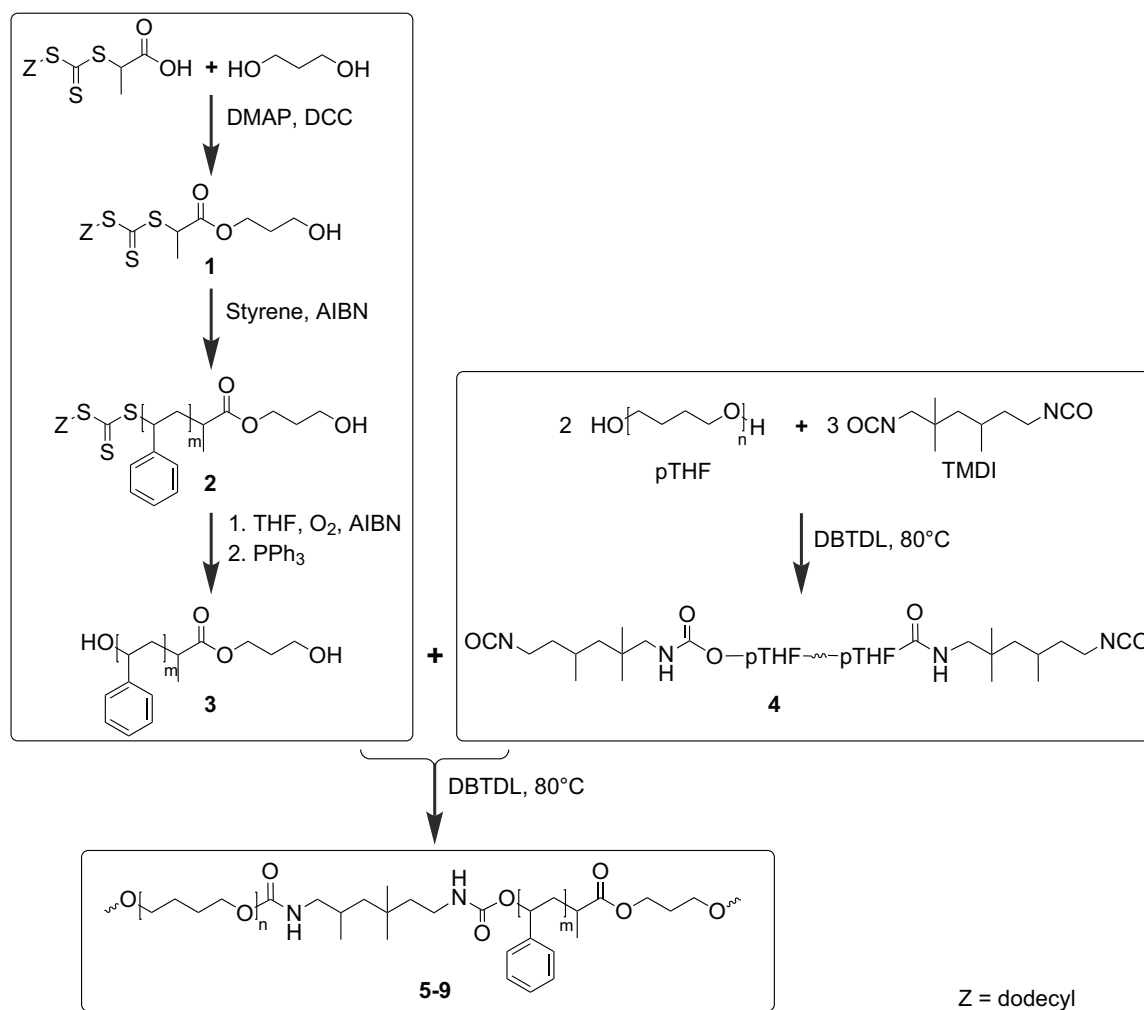
7.3. Results and Discussion

In the previous chapters the synthesis and the advanced characterization of pS-*b*-pCL di-, tri- (and star) block copolymers based on a mechanistic switch from RAFT to ROP via a modification of the thiocarbonyl thio group to an OH end functionality was presented. In here, the modification of the thiocarbonyl thio moiety to an OH group is carried out to connect poly(styrene) chains to a diisocyanate terminated prepolymer, thus to afford multi-block copolymers consisting of poly(styrene) and poly(tetrahydrofuran) units via urethane linkages. To obtain multi-block copolymers, difunctional building blocks are required. For this purpose, the RAFT agent 2[(dodecylsulfanyl) carbonothioyl]sulfanyl propanoic acid (DoPAT) was esterified in the first step with 1,3-propanediol (see Scheme 7.1, **1**) via a Steglich esterification employing *N,N'*-dicyclohexylcarbodiimide (DCC) as a coupling agent. After the polymerization of styrene **2** via the RAFT process in the presence of the new RAFT agent, the thiocarbonyl thio moiety was modified to form the dihydroxy-terminated polymer **3**.

The multi-block copolymers **5-9** are subsequently obtained by a polyaddition of the diisocyanate end-group containing prepolymer **4**, which was synthesized from poly(tetrahydrofuran) and 2,2,4-trimethylhexane-1,6-diisocyanate and the dihydroxy terminated polystyrene.

The diol end-functionalized polystyrene was characterized via SEC and MALDI-TOF MS. In Figure 7.1, the MALDI-TOF mass spectrum of the polystyrene with the two hydroxyl end moieties **3** is depicted. The inset shows the simulated isotopic pattern of OH-pS-OH in comparison to the measured data, which match perfectly. No starting material and no additional distributions were detected. The MALDI mass spectrum confirms that no other end-groups are attached to the polymer chain and a quantitative conversion of the reaction is obtained.

The formation of multi-block copolymers via urethane linkages requires – beside the



Scheme 7.2 Reaction sequence and conditions for the synthesis of the multi-block copolymers poly(styrene)-*b*-poly(tetrahydrofuran).

dihydroxy terminated polymer – a second polymer type featuring two isocyanate end-groups. Due to solubility issues, poly(tetrahydrofuran) was chosen as a soft segment within the multi-block copolymer. The exact molar mass ($M_n = 990 \text{ g mol}^{-1}$) of pTHF was determined by adding trichloro acetyl isocyanate to the NMR tube and subsequently integrating and comparing the signals of the converted end-group with the signals of the polymer backbone. The pTHF was equipped with isocyanate end-groups via a prepolymer synthesis. A pTHF to diisocyanate ratio of 2 to 3 was chosen to obtain a doubling in molar mass.^[354] The prepolymer was analyzed via SEC and the isocyanate content was determined via titration. The SEC trace of the prepolymer, confirming the increase in molar mass, is presented in Figure 7.2 and is compared with the SEC elugram of the initial pTHF.

In the last synthetic step the prepolymer and the diol terminated polystyrene were combined with the catalyst, *i.e.*, di-*n*-butyltindilaurate (DBTDL) and dissolved in DMAc. In this addition process, high molar masses can only be obtained, if exact

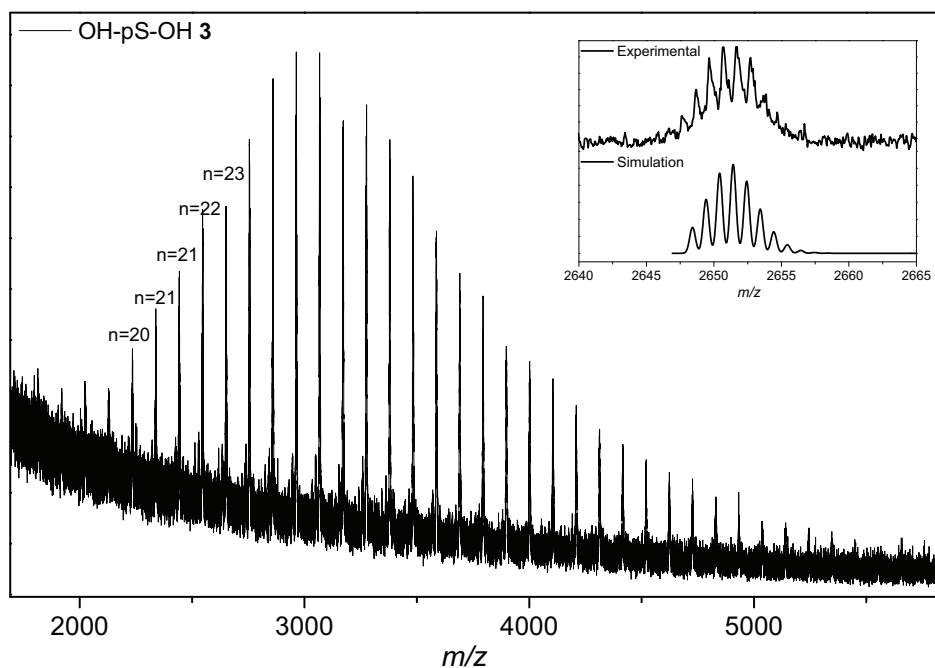


Figure 7.1. MALDI TOF mass spectrum of the dihydroxy-terminated poly(styrene) obtained via modification of the RAFT end-group. The inset depicts the comparison of the measured spectra with the simulated isotopic pattern (Gaussian profile with 0.5 Dalton resolution of $[M + Ag]^+$).

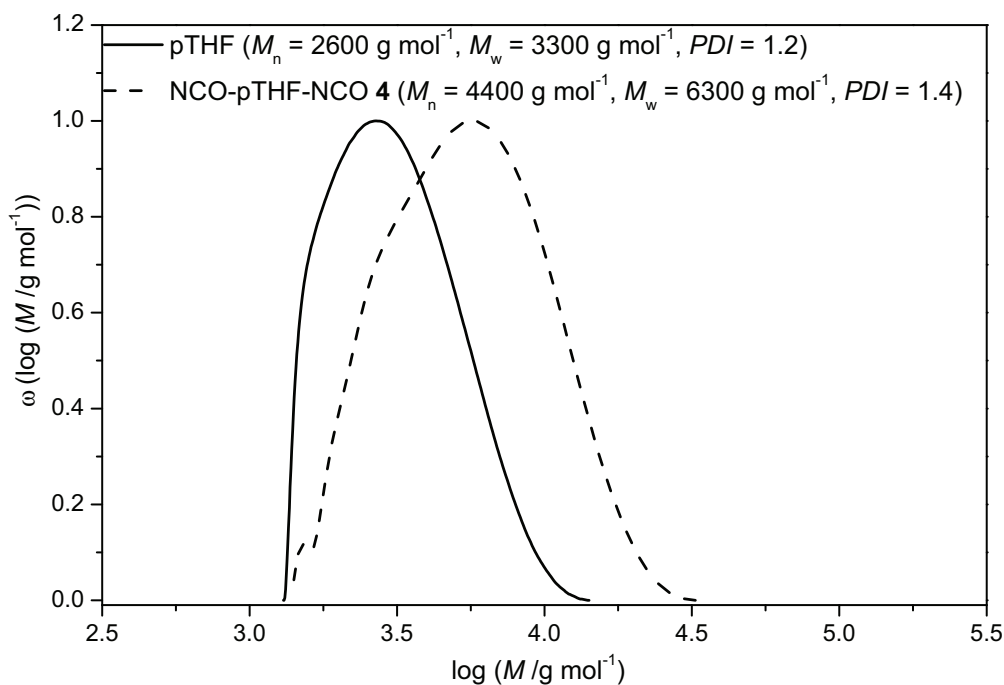


Figure 7.2. SEC traces of the prepolymer and the initial poly(tetrahydrofuran). A clear shift is visible; according to the SEC data obtained with pS calibration, a doubling in molar mass is observed during the prepolymer synthesis.

stoichiometry of the components is provided. By employing macromolecules in the polyaddition process accurate stoichiometry is hampered due to the nature of macromolecules possessing a certain dispersity. Consequently, the equivalents of the prepolymer NCO-pTHF-NCO compared to the OH-pS-OH were varied to gain multi-block copolymers with high molar masses and with only minor amounts of residual starting material. The multi-block copolymers were formed at a temperature of 80 °C. After the synthesis, the pS-*b*-pTHF copolymers **5-8** were precipitated in cold methanol, dried and characterized in first instance via conventional SEC (pS calibration). The ratios and the molar masses obtained in this way are depicted in Table 7.2. The SEC trace of the multi-block copolymer pS-*b*-pTHF **5-8** in comparison with the elugrams of the starting material poly(styrene) is presented in Figure 7.3. In the elugrams a

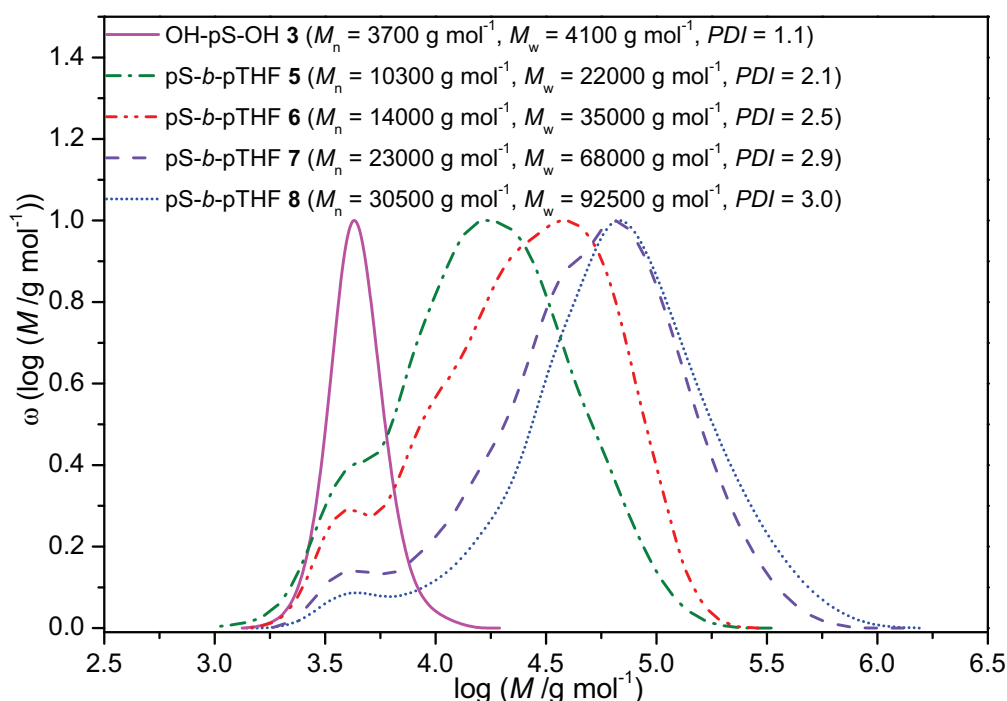


Figure 7.3. SEC traces of the multi-block copolymer samples **5-8** generated via urethane linkages. In addition, the SEC elugram of the initial homopolymer poly(styrene) is depicted. All molar mass data given in the plot are based on a linear poly(styrene) calibration.

clear shift of the starting material to the generated multi-block copolymer is observed. The polydispersity of the obtained polymers are relatively high (between 2 and 3), as expected for the polyaddition process. It should be noted that the pTHF prepolymer already possesses a relatively high PDI of 1.4 (see Figure 7.2). Also, a small fraction in the SEC traces at lower molar masses is visible, which indicates that a low amount of starting material did not react, increasing the overall PDI . At this stage, it was very likely to suppose that the small amount of low molar mass material is polystyrene homopolymer, based on the fact that the multi-block copolymer was precipitated in

methanol, in which pTHF with a low molar mass does not precipitate well (*vide infra*). Due to the broad mass distribution of the prepolymer and an unavoidable SEC error in the pS molar mass determination, the complete disappearance of the starting material pS in the SEC traces of the copolymer was not achieved. It is noted that less starting material is left when increasing the pTHF : pS ratio. It is expected that a slightly higher and optimal pTHF to pS ratio would eventually afford a copolymer without any residual pS left. Nevertheless, as a high molar mass copolymer containing only a small portion of residual pS could be obtained with 2 equivalents of pTHF relative to pS (sample **8**, Table 7.2), the molar ratio of pTHF to pS was not further increased.

Via liquid chromatography under critical conditions, starting materials such as homopolymer residues in the multi-block copolymer samples can be identified. The critical conditions for polystyrene can be found in Chapter 3 (YMC-ODSA column, 88.4 % THF / 11.6 % H₂O (v/v)). Under the same conditions, the block copolymer samples have been analyzed. Figure 7.4 depicts the elugrams of the multi-block copolymers compared with an elugram of the ps homopolymer. The multi-block copolymers elute in the SEC modus. In addition it is observed that the detected signal of the block copolymers are very broad. One explanation for this circumstance is the alternating structure of the multi-block copolymers and the broad polydispersity of the polymer samples. Furthermore, the block copolymers display signals at the elution volume, at which the pure pS homopolymer elutes. Consequently residues of pS homopolymer are present in the copolymer samples.

In addition, Figure 7.5 displays the elugram of the multi-block copolymer sample **6** measured not only with the ELSD detector, yet also with UV detection with two different wavelengths at 254 nm and 230 nm. Polystyrene can absorb UV light readily and shows strong signals, whereas pTHF absorbs almost no UV light in THF. Furthermore, the molar absorptivity of polystyrene is higher in the region of shorter wavelengths. This circumstance was exploited to clearly identify the homopolymer pS in the LCCC setup. The elugrams in Figure 7.5 show that the small peak, which is visible by ELSD detection, is much more pronounced with UV detection with a wavelength at 254 nm and even more prominent at a wavelength detection of 230 nm. This verifies the assumption made from the SEC traces that pS homopolymer residues are present in the multi-block copolymer samples.

Conventional SEC is sufficient to obtain a first indication whether the multi-block copolymer synthesis was successful. However, it cannot determine the exact molar masses of the multi-block copolymers. Due to the very significant difference in polymer structure of poly(tetrahydrofuran) and poly(styrene), the molar masses determined via conventional SEC – which is calibrated via poly(styrene) standards – are beset with a substantial error.

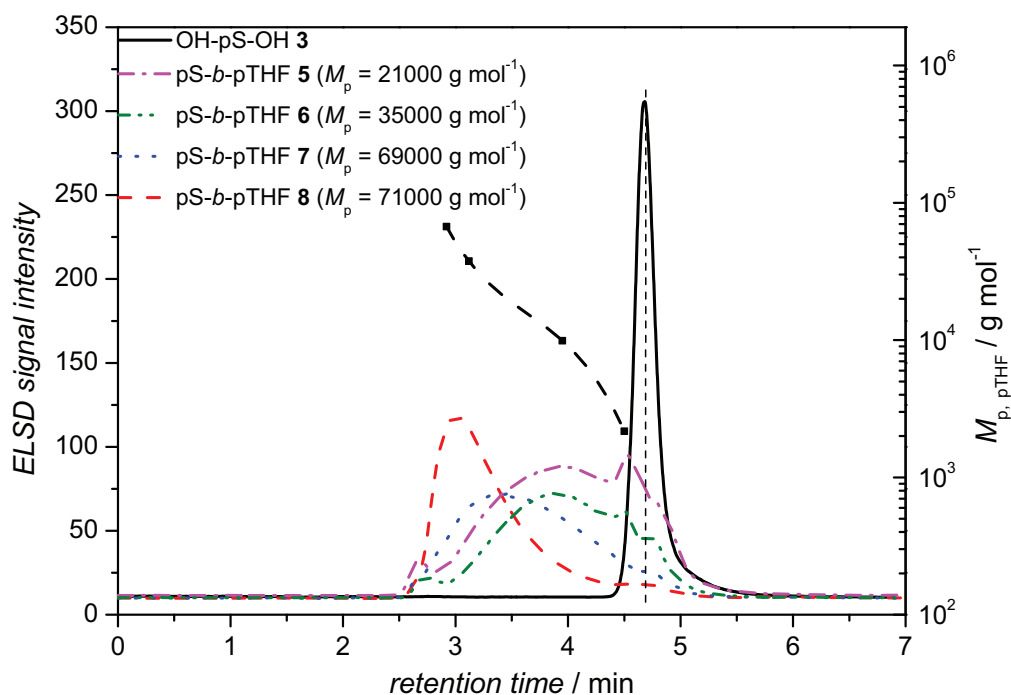


Figure 7.4. Elugrams of the multi-block copolymer samples **5-8** compared with polystyrene precursor at the critical conditions of polystyrene (YMC-ODSA column, 88.4 % THF / 11.6 % H₂O (v/v)).

One way to determine accurate weight-average molar masses of a polymer structure is by measuring the samples on a SEC system equipped with triple detection. The detection system combines viscosimetry, light-scattering and refractive index detectors. Taking advantage of the fact that the excess Rayleigh ratio is directly proportional to the product of the concentration and the weight-average molar mass M_w , the molar mass can be determined directly by the combination of a concentration sensitive detector and the light scattering detector.^[198]

For an accurate detection of the molar masses of the multi-block copolymers it is required that no homopolymer is present in the sample. One possibility would be to perform dialysis with an appropriate membrane. Yet, in here fractionation of the samples via a SEC system coupled to a fraction collector was employed. The conditions at which the separation was carried out can be found in Chapter 3.

After drying the fractionated samples, SEC with triple detection was performed. In Figure 7.6 the elugrams of the multi-block copolymer samples, obtained via SEC with triple detection, are presented. The molar masses and the *PDI*'s, which are obtained by a light-scattering detector, are included in the graphs. The elugrams reveal that the fractionation was successful as no shoulder or additional signal is detected

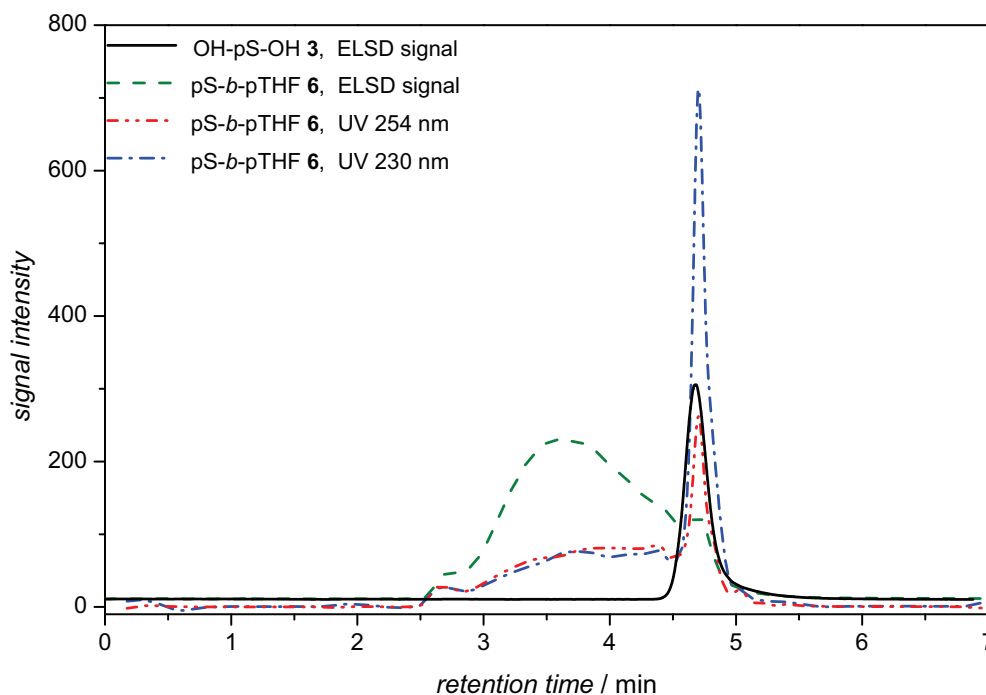


Figure 7.5. Elugrams of the multi-block copolymer sample **6** and the polystyrene precursor at the critical conditions of polystyrene (YMC-ODSA column, 88.4 % THF / 11.6 % H₂O (v/v)). The detection with UV at 254 nm and 230 nm is applied to reveal the polystyrene homopolymer content.

in the lower molar mass regions. Depending on the conditions used for the block copolymer synthesis, M_w varies between 26300 and 85700 g mol^{-1} . Because of the fractionation process, the polydispersity indices decrease to values lower than two. If the dn/dc value of homopolymers or polymers with homogeneous composition would be determined before, the triple detection should allow to obtain accurate weight-average molar mass.^[355] For multi-block copolymers, however, the dn/dc varies with the composition of the two blocks in the polymer. Thus, the dn/dc values are unemployable for multi-block copolymer samples with varying individual block content. Alternatively, the method ‘factor multiplied with concentration’ can be applied for weight-average molar mass determination as described in Chapter 3 giving the values shown in Figure 7.6.

One very important issue for potential future use is the accurate reproducibility of the polymerization process. Consequently, the synthesis accompanied with the characterization steps of the multi-block copolymer sample **8** was repeated, affording sample **9**. The SEC elugram, obtained via triple detection of the samples **8** and **9**, are compared in Figure 7.7. The determined weight-average molar mass and the dispersities are again included within the figure. Although the molar mass of sample **9** ($M_w = 82400 \text{ g mol}^{-1}$) does not match absolute exactly with the one of sample **8**

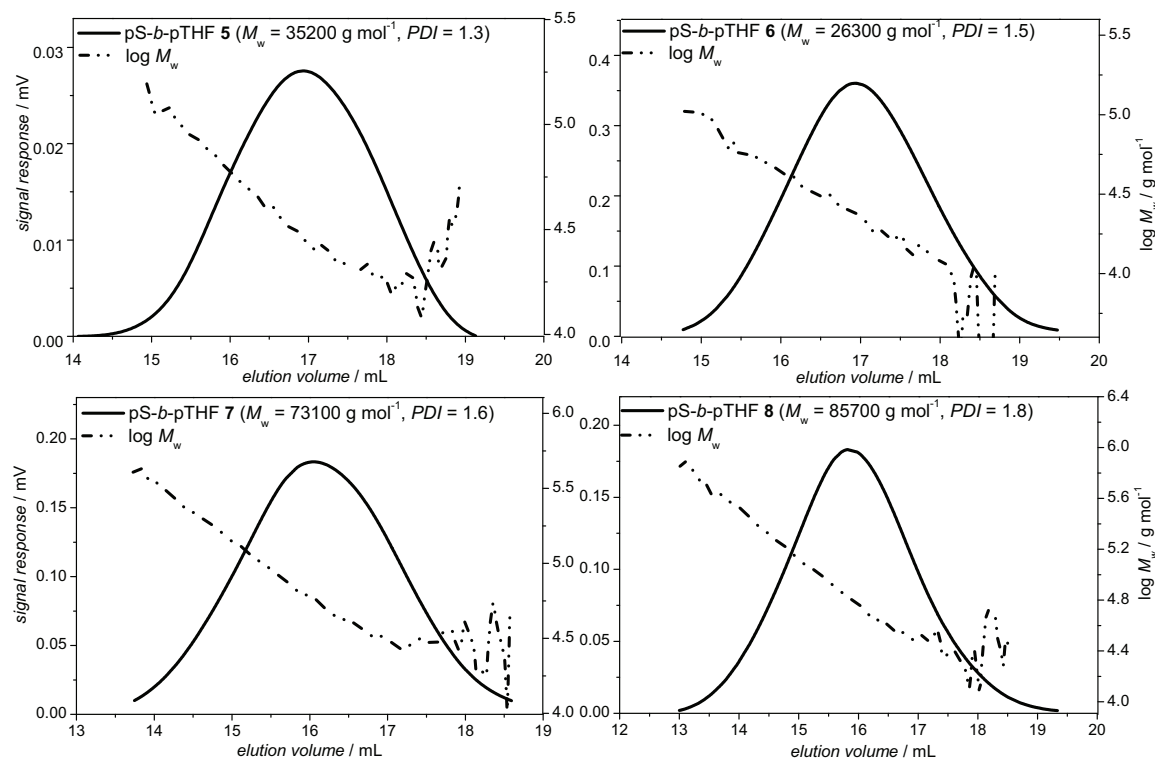


Figure 7.6. Molar mass determination of the multi-block copolymers **5-8** after fractionation via SEC equipped with triple detection. Due to the fractionation, the PDI is smaller than the values expected for a polyaddition process. From 18 mL elution volume onwards, the data are no longer considered due to the higher error.

($M_w = 85700$ g mol⁻¹), the slight deviation is still in an acceptable reproducibility range.

While absolute SEC measurements provide the molar masses of the samples, no information about the chemical composition is obtained. Due to the precipitation after the multi-block copolymer synthesis and the fractionation of the samples, it is very likely that the composition departs from the initial applied ratio between poly(styrene) and poly(tetrahydrofuran) in the synthesis. Therefore ¹H-NMR spectra of the samples **5-8** were recorded with a 400 MHz spectrometer in CDCl₃. The NMR spectrum of sample **7** is depicted in Figure 7.8. Further NMR spectra of samples **5**, **6** and **8** can be found in Figure A.7 in the Appendix. All signals are assigned to the multi-block copolymer structure, which is included within Figure 7.8. Additional signals – not belonging to the copolymer – can be assigned to the stabilizer used in commercial THF, *i.e.*, butylhydroxytoluene (BHT). After the fractionation, the multi-block copolymer samples were enriched with BHT due to the utilized eluent THF in the SEC system. Determination of the block ratio of pS and pTHF requires integration of the corresponding polymer backbone signals and the subsequent calculation of the ratio percentage. For poly(styrene), the signal associated with $-C_6H_5$, m (5H), and

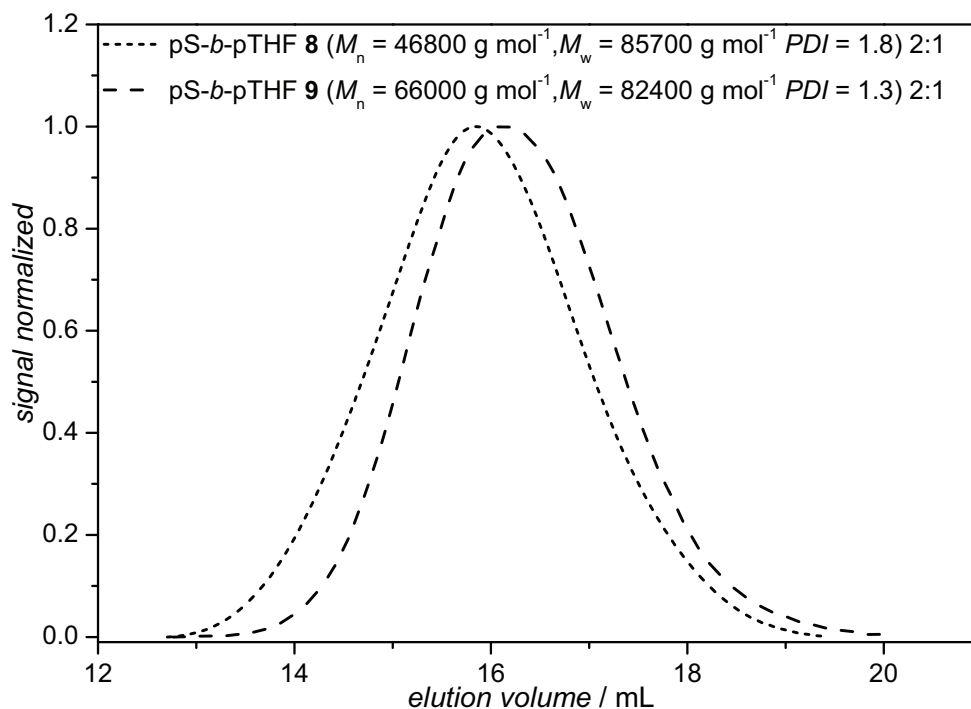


Figure 7.7. Multi-block copolymer synthesis was tested with regard to reproducibility by repeating the synthesis for sample **9** under the identical conditions as for sample **8**. The elugrams in the figure - obtained via SEC coupled to triple detection - depict that the weight-average molar mass of the reproduced sample **9** is in good agreement with the one of sample **8**.

for poly(tetrahydrofuran) the $-OCH_2$ signal, a (4H), were chosen for the integration. At the chemical shift of the pS backbone signal m, the aromatic protons of BHT are detected as well. Thus - initially - the BHT signal part had to be eliminated from calculations, before deducing the pS : pTHF ratio. The calculated ratios of each multi-block copolymer **5-8** are collated in Table 7.3 and compared to the theoretical values. The theoretical fractions in percentage of pTHF and pS are calculated from the initially employed equivalents (which are based on the pS and the prepolymer chains) and referred to the repeating units of styrene and THF within the polymer. Although the values determined via NMR differ from the theoretical values due to the fractionation process, it can be observed that an increasing amount of pTHF during the synthesis results also in higher pTHF content in the copolymer structure. In ideal cases, due to the polyaddition process, the ratio of prepolymer to polystyrene diol should not deviate from an equimolar ratio because of the alternating polymer structure. However, in the polymerization process of polyurethanes it is commonly known that the highly reactive isocyanate groups of the prepolymer can undergo side reactions, *e.g.*, they undergo dimerization or - if traces of water are present in the reaction flask - two isocyanate groups can form an urea bond, liberating carbon dioxide.^[161] In case of sample **5**, in which a lower pTHF content than 50% is calculated

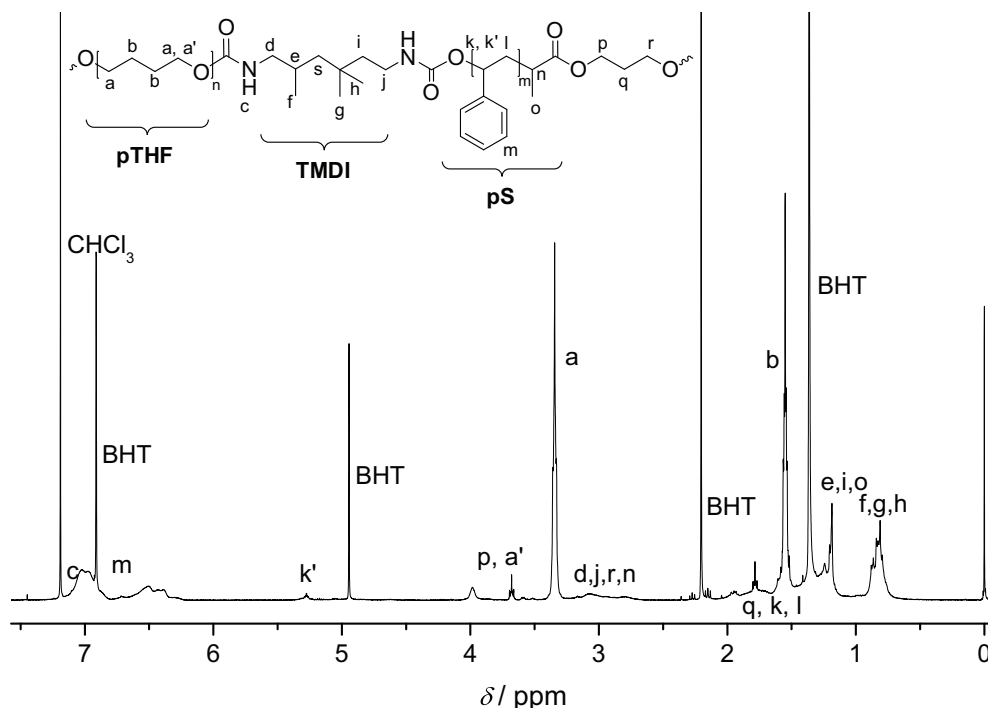


Figure 7.8. ^1H -NMR spectrum of the multi-block copolymer pS-*b*-pTHF **7** after fractionation. Due to the fact that the SEC eluent used for the fractionation contained BHT, the inhibitor is visible in the NMR spectrum. However, the BHT content can be quantified and the integral of the signal m can be corrected.

via NMR, it is certain that the copolymer structure possesses polystyrene on both chain termini.

Table 7.3. Collation of the results concerning the fractions in molar percentage of the individual blocks in the multi-block copolymer samples obtained via NMR (fraction NMR). The results are compared to the initially employed content based on the repeating units of the homopolymers pS and pTHF in the reaction flask (fraction theoretical).

Sample	pS fraction theoretical	pTHF fraction theoretical	pS fraction NMR	pTHF fraction NMR
5	74 %	26 %	60.6 %	39.4 %
6	65 %	35 %	46.9 %	53.1 %
7	56 %	44 %	47.8 %	52.2 %
8	48 %	52 %	34.1 %	65.9 %

In addition to NMR spectroscopy, FT-IR ATR measurements of the multi-block copolymers were conducted to confirm the molecular structure of the block copolymers. Figure 7.9 depicts the infrared absorbance of the multi-block copolymer molecule **8** after fractionation. The very similar IR spectra of the samples **5**, **6** and **7** are shown in Figure A.8 in the Appendix. The signal at 1724 cm^{-1} is associated with the ure-

thane moiety linking the pTHF and pS blocks. The IR absorbance at 1110 cm^{-1} correlates with the $-CO-$ stretching vibration of the pTHF backbone while the signals at 1493 cm^{-1} as well as at 700 cm^{-1} and 749 cm^{-1} are associated with the pS polymer structure. Again – as described in the context of the NMR spectra – BHT is included in the samples, which explains for example the strong absorbance at 700 cm^{-1} due to the overlapping of absorbance intensity resulting from pS and BHT.

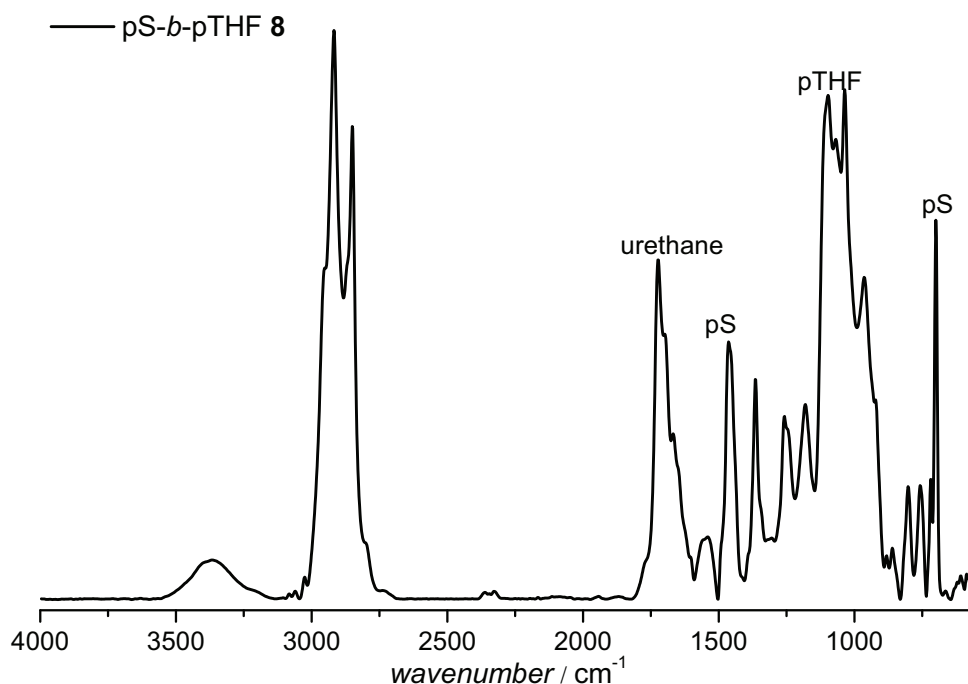


Figure 7.9. FT-IR spectrum of the multi-block copolymer **8**, after fractionation, determined via ATR. The significant bands and signals derived from the vibrations of the urethane linkage, the pTHF and the pS backbone are labeled in the figure.

Even more details of the multi-block copolymer structure can be obtained by SEC on-line coupled to infrared spectroscopy. With this system, 12 complete infrared spectra (each 50 scans) per minute are collected with a resolution of 4 cm^{-1} . Because of the low concentrations in SEC the IR spectra mainly show solvent signals and only small changes during the elution results from polymer signals. To suppress the constant solvent signals a second order polynomial is fitted for every wavenumber to reference data taken before and after the chromatogram, in a region where the RI detector displayed that no polymer was present, to determine exclusively the solvent signals and the drift. This second order polynomial is then subtracted from the time evolution at this wavenumber. After this baseline correction and smoothing a 2D spectral chromatogram is obtained, from which each chromatogram for each component can be extracted. For a more detailed description of the SEC/FT-IR setup, the reader is referred to reference.^[263]

In Figure 7.10, the SEC elugrams of the multi-block copolymers **5-8** detected via the absorbance intensity at the specimen wave numbers 1493 cm^{-1} (aromatic ring of pS) and 1110 cm^{-1} (CO in pTHF), respectively, are illustrated. The wavenumbers were chosen after measuring pTHF and pS homopolymers with the online SEC/FT-IR system. pTHF does not show any absorbance at 1493 cm^{-1} , where the signal of the phenyl ring of the pS polymer is detected, whereas pS does not show any absorbance at 1110 cm^{-1} , at which pTHF shows strong absorbance due to the CO ether stretching vibration in its polymer backbone (see Figure A.9). Thus, an ideal situation for the individual integration of each signal is given. The elugrams in Figure 7.10 show the signal intensities derived from the pS and the pTHF content, respectively, as a function of the elution volume, from which molar mass can be derived. The elugrams are overlapping very well, which signifies that at all molar masses, poly(styrene) and poly(tetrahydrofuran), are incorporated and thus blend of two homopolymers was produced.

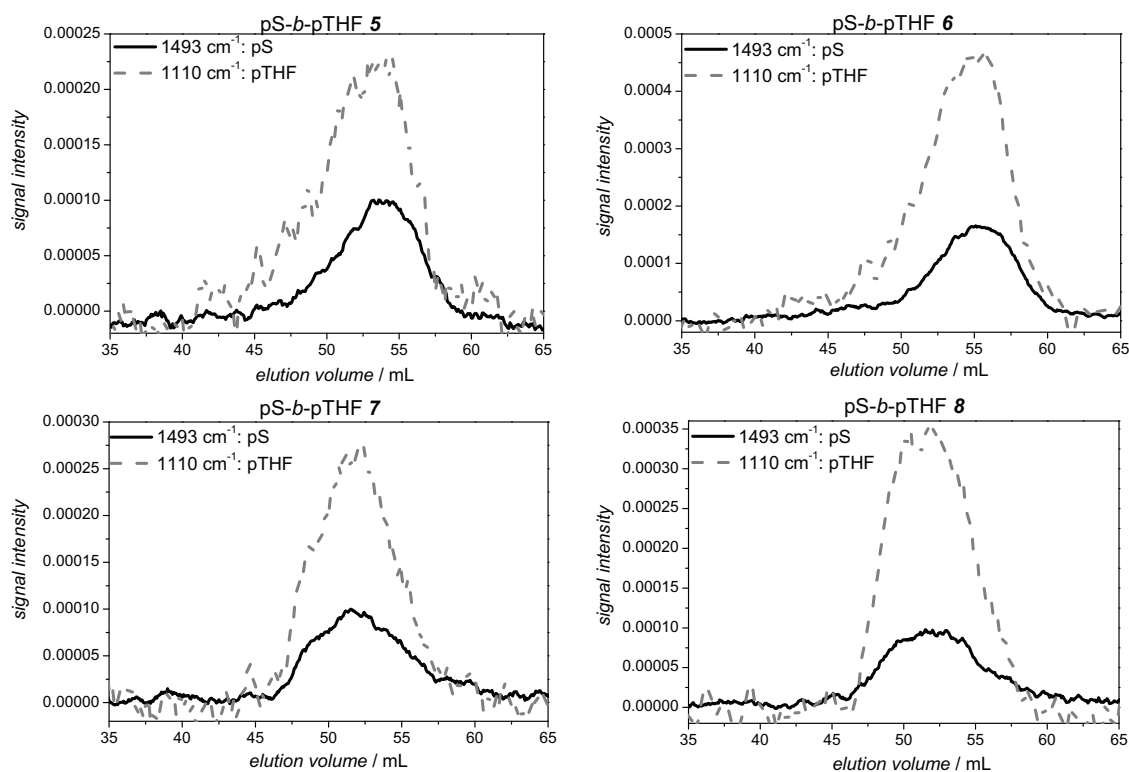


Figure 7.10. Elugrams of the multi-block copolymer samples **5-8** measured via SEC/FT-IR. Two wavenumbers are depicted at 1493 cm^{-1} and 1110 cm^{-1} , which correspond to the vibration of the aromatic ring in poly(styrene) and the CO stretching of the poly(tetrahydrofuran), respectively.

Determining the content of one block in the multi-block copolymer structure at a certain molar mass, however, requires a calibration of the signal intensities. For this purpose polymer blend solutions with known concentrations were injected into the

SEC/FT-IR system and the signal intensity was detected. All information about the calibration of the SEC/FT-IR system can be found in the Chapter 3 (see Figure 3.1). By plotting the signal intensity against the amount of absorbing units and a subsequent linear regression the slope was calculated. The value of the slope was applied to the absorbing intensities of the SEC-IR elugrams. In Figure 7.11, the SEC-IR elugrams of the multi-block copolymers **5** and **8** after application of the calibration correction are depicted. These elugrams correlate with the amounts of pS and pTHF

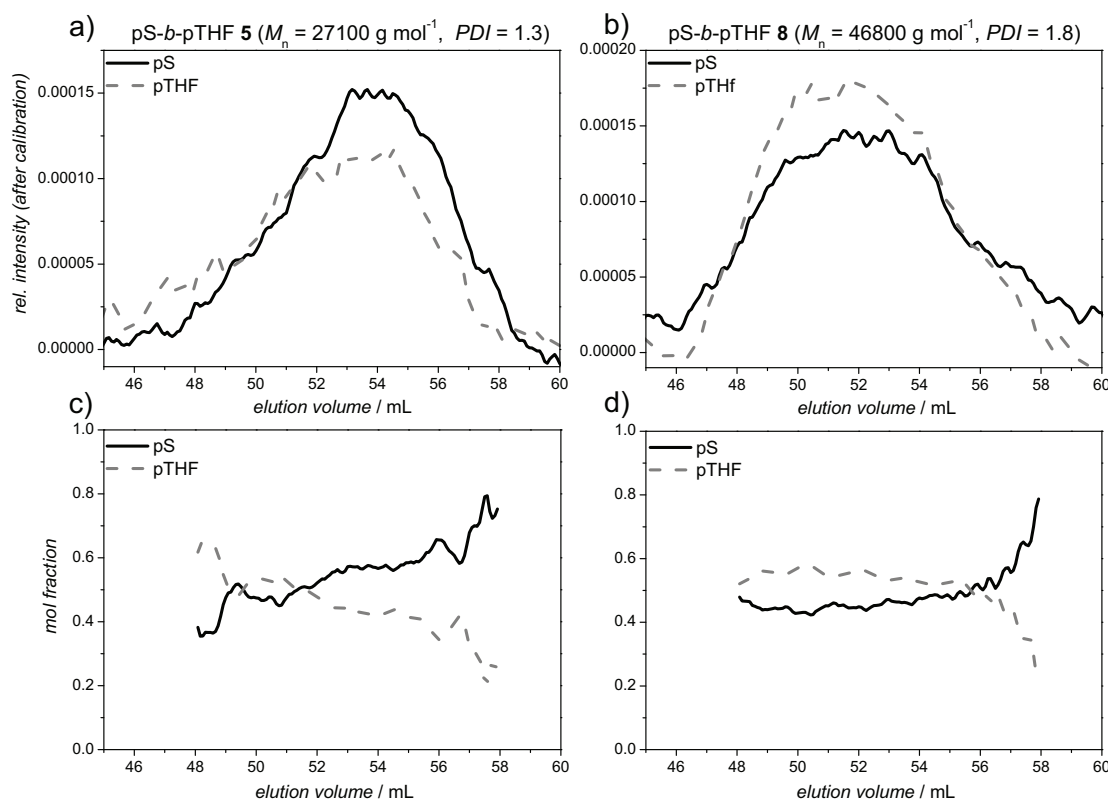


Figure 7.11. a) and b) Calibrated online SEC/FT-IR measurements of the multi-block copolymer samples **5** and **8**. Figure 7.11 c) and d) show the block poly(styrene) and the block poly(tetrahydrofuran) fractions, respectively, in the multi-block copolymer as a function of the elution volume of the SEC system and thus on the molar masses of the multi-block copolymer samples.

present in the sample. In the lower half of Figure 7.11 the ratio of the pS and the pTHF content in the multi-block copolymer sample is illustrated as a function of the elution volume. Ratios are only calculated for values larger than $> 5 \%$ of the peak maximum in the chromatogram, because noise dominates the regions beyond. It can be observed that the two samples exhibit differences in their copolymer structure. The pS content of sample **5** is increasing from 30 % to 70 % with increasing elution time, whereas the pS content of sample **8** is not changing during the elution process. Thus, the multi-block copolymer sample **5** possesses a gradient in its constitution, whereas the relative composition in sample **8** is independent of the molar mass. The

elugrams and ratios as a function of the elution volume for sample **6** and **7** are given in Figure A.10 in the Appendix. Both samples, **6** and **7**, show only a very slight increase in the pS content as a function of the elution volume. From the initial SEC elugrams it is known that sample **5** has a rather low molar mass, compared to sample **8**. Furthermore, the pS content in sample **5** was chosen much higher than the pS content in sample **8** in the synthetic process. Consequently, the chain ends of sample **5** are very likely pS terminated. For an ABA triblock copolymer the ratio of pS to the prepolymer is 2:1, it shifts to a 3:2 ratio for an ABABA pentablock copolymer. Following the reasoning, the ratio becomes closer to 1:1 at higher molar masses. As a result, the pS content in sample **5** increases with increasing elution volume.

By integrating the calibrated elugrams, the overall amount of pS and pTHF present in the multi-block copolymer sample can be calculated. Ideally, if the sensitivity of this newly developed SEC/FT-IR method is sufficiently high, the values should be in-line with the ratios obtained via NMR. In Table 7.4 a summary of the data obtained via the different analytical methods is provided. Figure 7.12 visualizes the same data in a graph. The amount of pTHF (in mol-percent) obtained via NMR integration and SEC/FT-IR measurements, is directly compared. The pTHF content calculated on the basis of the NMR spectra correlates very well with one obtained via integration of the calibrated SEC/FT-IR elugram. The molar masses obtained with conventional SEC and with triple detection differ as a result of the different detection method and of the fractionation process that was performed before the data of the SEC with triple detection were measured. However, the fractionation process was necessary to obtain absolute molar masses of the pure multi-block copolymers. The data obtained with the conventional SEC are clearly not that accurate for the multi-block copolymer size due to residues of pS homopolymer producing peak broadening or shoulders in the elugram. Moreover, in conventional SEC the data are obtained with pS calibration, which results in very imprecise values for the multi-block copolymers. A possible explanation for the observed increase in average molar mass of the multi-block copolymers with increasing amounts of pTHF, is the formation of a urea bond additionally to the urethane bond, which occurs in the presence of water residues with two isocyanate groups. Via such an additional reaction, more pTHF can be incorporated into the multi-block copolymer and thus, also the molar masses increase.

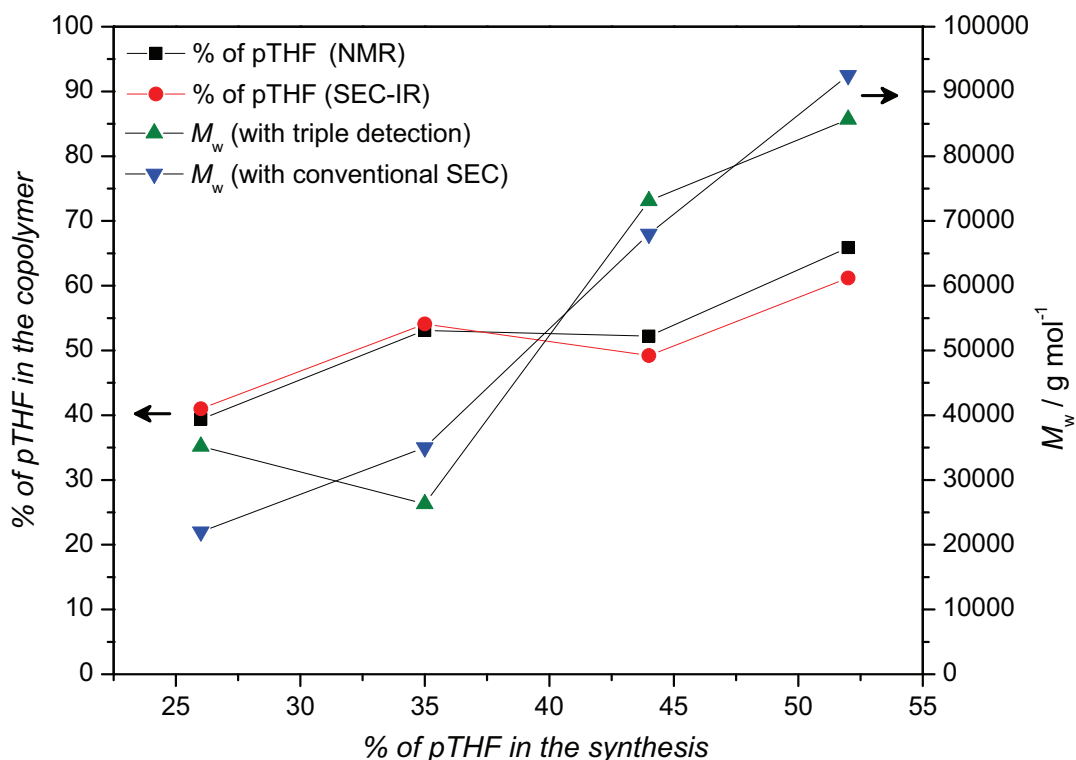


Figure 7.12. Correlation between pTHF mole fraction in percentage in the feed mixture and the pTHF content in the resulting multi-block copolymers **5-8** obtained via two analytical methods, *i.e.*, online SEC-IR and NMR. In addition, the obtained weight-average molar masses as a function of the initial pTHF fraction are depicted.

Table 7.4. Collated data of the molecular specifications of the synthesized multi-block copolymers.

Sample	Equivalents prepolymer:pS	M_w (LS) / g mol^{-1}	M_w (RI) / g mol^{-1}	pTHF fraction	pTHF fraction	pTHF fraction
				theoretical	NMR	FT-IR
5	1:1.5	35 200	22 000	26 %	39.4 %	41 %
6	1:1	26 300	35 000	35 %	53.1 %	54.1 %
7	1.5:1	73 100	68 000	44 %	52.2 %	49.2 %
8	2:1	85 700	92 500	52 %	65.9 %	61.2 %

7.4. Conclusions

In the current chapter the procedure of switching the RAFT end-group of a polymer chain to a hydroxyl function was successfully employed to synthesize diol terminated poly(styrene). The macro-diol was subsequently reacted with a diisocyanate end-functional poly(tetrahydrofuran) to obtain high molar mass multi-block polyurethanes. The multi-block copolymer structure and its size were determined by a variety of

analytical methods such as SEC with triple detection, NMR and SEC coupled on-line to FT-IR. It was demonstrated that the NMR and SEC/FT-IR measurement show highly comparable results for the quantification of the exact composition of each polymer structure, evidencing the power and the sensitivity of the newly introduced on-line SEC/FT-IR coupling technique for elucidating polymer structures. The current contribution has thus evidenced that high molar mass polyurethanes ($M_n = 46800 \text{ g mol}^{-1}$, $M_w = 85700 \text{ g mol}^{-1}$) based on polymer chains made by RAFT can be accessed in a reproducible fashion. The presented general synthetic approach can be readily applied to other ω -functional hydroxyl polymers that are accessible via the RAFT processes and the thiocarbonyl thio to hydroxyl switch protocol.

8

Concluding Remarks and Outlook

8.1. Concluding Remarks

In the current thesis, the full establishment of the novel switching technique from RAFT to sulfur-free hydroxyl functional polymers for a range of thiocarbonyl thio end caps as well as polymer backbones was demonstrated. Subsequently employing the OH terminal macromolecules, the generation of di-, tri-, and star block copolymers via ROP as well as the generation of multi-block polyurethanes and their in-depth characterization with hyphenated techniques was achieved.

A variety of monomers were polymerized in the presence of a selection of chain transfer agents via the RAFT process. The end-group conversion reactions were carried out for the synthesized RAFT polymers, employing AIBN and THF at 60 °C at ambient conditions and were tracked by SEC/ESI-MS (Chapter 4) and MALDI-MS, respectively. Additionally, modifications have been investigated to expand the variability of the end-group conversion process, including the use of alternative azo-initiators and other reducing agents as well as the substitution of thermal energy with UV irradiation.

Subsequently, hydroxyl terminal polystyrenes were utilized as macroinitiators for the ring-opening polymerization of ϵ -CL (Chapter 5) employing TBD as catalyst. The obtained block copolymers pS-*b*-pCL (with $26000 \leq M_n/\text{g mol}^{-1} < 45000$) were characterized in detail via liquid chromatography at the critical conditions of pS and two dimensional chromatography (LCCC-SEC) to confirm the purity of the products

and to evidence that the RAFT process serves as a methodology for the generation of sulfur-free block copolymers via an efficient end-group switch. Furthermore, pA-*b*-pCL and pMMA-*b*-pCL block copolymers were synthesized via chain extension of hydroxyl functional poly(acrylate)s as well as poly(methacrylate)s with ϵ -CL under metal- and organo-catalysis. Poly(methyl acrylate), poly(isobornyl acrylate), and poly(methyl methacrylate) were used as the acrylic block parts. Via chain extension of poly(methyl methacrylate) the tertiary OH functionality was also successfully employed as initiator for the ring-opening polymerization of ϵ -CL.

An alternative approach for the generation of block copolymers starting from RAFT polymers – which were hydrolyzed to form thiol end-capped polymers – was investigated. In a collaboration with Dr. Catherine Lefay (Université de Provence, Lyon) it was successfully demonstrated that the thiol terminated polymers can be employed as macroinitiators for the polymerization of pLA. The obtained pS-*b*-pLA block copolymers were characterized via multiple detector SEC and liquid chromatography under critical conditions substantiating the block copolymer formation alongside with homopolymer residues in small quantities.

The block copolymer formation strategy – switching from RAFT to ROP via generation of hydroxyl terminal polymers – was expanded for the generation of ABA (star) block copolymers, involving the end-group conversion of polystyrene synthesized via a 2-arm linear and 4-arm star R-approach (Chapter 6) generating polymers with more than one OH end-functionality. For the characterization liquid chromatography at the critical conditions of pCL were combined with a solvent gradient – LCCC with concomitant GELC – enabling for the first time the separation of the pCL-*b*-pS-*b*-pCL block copolymers from pCL as well as from pS homopolymers. The structures separated via the new hybrid technique LCCC-GELC were determined by coupling off-line FT-IR and MALDI-MS to the chromatographic system.

In the final chapter of the thesis it was demonstrated that high molar mass multi-block polyurethanes ($17800 \text{ g mol}^{-1} \leq M_n \leq 46800 \text{ g mol}^{-1}$) can be generated based on the procedure of switching RAFT end capped polymers to hydroxyl functional polymers (Chapter 7). The multi-block copolymers were formed by the reaction of a diisocyanate terminal prepolymer with the macro-diol which was synthesized via the end-group conversion of thiocarbonyl thio terminal polymers. Via characterization with a variety of analytical techniques – including SEC with triple detection, LCCC, NMR, and SEC coupled on-line to FT-IR – the molar masses and the composition of the block copolymers were identified. By comparing the quantification results with NMR spectroscopy, the sensitivity of the new on-line SEC/FT-IR technique was demonstrated. The generated multi-block polyurethanes exhibit high molar masses ($M_n = 46800 \text{ g mol}^{-1}$, $M_w = 85700 \text{ g mol}^{-1}$) when the content of the prepolymer is high in the feed mixture.

Thus – in summary – the thiocarbonyl thio to hydroxyl switch protocol was demonstrated to be applicable to a wide range of polymer backbones as well as a diverse RAFT agents. Switching from RAFT to hydroxyl functional polymers served as a versatile base for the subsequent formation of sulfur-free complex polymer architectures. The combination of advanced hyphenated techniques with the newly developed analytical methods proved to be efficient in providing a very detailed characterization of the synthesized block copolymer structures.

8.2. Outlook

The end-group conversion of RAFT polymers to hydroxyl functional materials and their subsequent employment for block copolymer formation has been extensively investigated within the current thesis. However, based on the end-group switch it would be very interesting to exploit further synthetic approaches. For instance, it should be feasible to utilize the end-group switch for the synthesis of polymers bearing specific end-functionalities, since the so introduced OH moiety on the polymer chain end is a versatile chemical anchor. The OH functionality could be modified to a variety of end-functionalities including precursors for light-triggered pericyclic reaction chemistry. The new end-functionalities could be attached to a core-molecule via simply triggering the reaction with UV light. With this new approach it would be possible to generate well-defined star polymer structures, including variation in number and length of the arms. Liquid chromatography at critical conditions would be the ideal analytical method for characterization the complex polymer architectures. Even of higher interest – due to their well-defined structure and the specific end-groups attached to the arms – the star polymers with different numbers of arms could be employed as model compounds for the LCCC.

An alternative approach to continue the current thesis in the future would be the investigation of the physical properties of the various synthesized block copolymers for potential applications. Promising structures are for instance the multi-block polyurethanes pS-*b*-pTHF. Due to the different transition temperatures of the connected polymer types they could be investigated for the application as shape-memory materials. The material could be improved by modifying the polymer backbones – for example by substituting poly(styrene) with different poly(acrylate)s – to alter the transition temperatures.

In conclusion, future work can address new synthetic fields, starting from the end-group switch, as well as engaging application areas of the complex block structures by investigation of their physical properties.

Bibliography

- [1] Barner-Kowollik, C. *Handbook of RAFT Polymerization*; Wiley-VCH, Weinheim, Germany, **2008**.
- [2] Barner, L.; Perrier, S. *Handbook of RAFT polymerization*; Barner-Kowollik, C., Ed.; Wiley-VCH, Weinheim, Germany; Chapter 12: Polymers with Well-Defined End Groups Via RAFT – Synthesis, Application and *Postmodifications*; **2008**, 455-478.
- [3] Stridsberg, K. M.; Ryner, M.; Albertsson, A.-C. *Advances in Polymer Science* **2002**, *157*, 41–65.
- [4] You, Y.; Hong, C.; Wang, W.; Lu, W.; Pan, C. *Macromolecules* **2004**, *37*, 9761–9767.
- [5] Hales, M.; Barner-Kowollik, C.; Davis, T. P.; Stenzel, M. H. *Langmuir* **2004**, *20*, 10809–10817.
- [6] Glaied, O.; Delaite, C.; Dumas, P. *Journal of Polymer Science Part A: Polymer Chemistry* **2006**, *44*, 1796–1806.
- [7] Han, D.-H.; Pan, C.-Y. *Journal of Polymer Science Part A: Polymer Chemistry* **2007**, *45*, 789–799.
- [8] Xu, X.; Huang, J. *Journal of Polymer Science Part A: Polymer Chemistry* **2004**, *42*, 5523–5529.
- [9] Xu, J.; He, J.; Fan, D.; Wang, X.; Yang, Y. *Macromolecules* **2006**, *39*, 8616–8624.
- [10] Xu, X.; Huang, J. *Journal of Polymer Science Part A: Polymer Chemistry* **2006**, *44*, 467–476.
- [11] Villarroya, S.; Zhou, J.; Thurecht, K. J.; Howdle, S. M. *Macromolecules* **2006**, *39*, 9080–9086.

- [12] Luan, B.; Zhang, B.-Q.; Pan, C.-Y. *Journal of Polymer Science Part A: Polymer Chemistry* **2006**, *44*, 549–560.
- [13] Chattopadhyay, D. K.; Raju, K. V. S. N. *Progress in Polymer Science* **2007**, *32*, 352–418.
- [14] Santerre, J. P.; Woodhouse, K.; Laroche, G.; Labow, R. S. *Biomaterials* **2005**, *26*, 7457–7470.
- [15] Lyman, D. J. *Journal of Macromolecular Science, Part C: Polymer Reviews* **1966**, *1*, 191–237.
- [16] Krol, P. *Progress in Materials Science* **2007**, *52*, 915–1015.
- [17] Mishra, A. K.; Patel, V. K.; Vishwakarma, N. K.; Biswas, C. S.; Raula, M.; Misra, A.; Mandal, T. K.; Ray, B. *Macromolecules* **2011**, *44*, 2465–2473.
- [18] Kipping, M.; Krahl, F.; Döring, A.; Adler, H.-J. P.; Kuckling, D. *European Polymer Journal* **2010**, *46*, 313–323.
- [19] Wolf, F. F.; Friedemann, N.; Frey, H. *Macromolecules* **2009**, *42*, 5622–5628.
- [20] Müller, A. H.; Matyjaszewski, K. *Controlled and Living Polymerization*; Wiley-VCH, **2009**.
- [21] Odian, G. *Principles of Polymerization*; Odian, G., Ed.; Wiley-Interscience, **2004**.
- [22] Szwarc, M. *Nature* **1956**, *178*, 1168–9.
- [23] Hawker, C. J.; Bosman, A. W.; Harth, E. *Chemical Reviews* **2001**, *101*, 3661–3688.
- [24] Kato, M.; Kamigaito, M.; Sawamoto, M.; Higashimura, T. *Macromolecules* **1995**, *28*, 1721–3.
- [25] Wang, J.-S.; Matyjaszewski, K. *Journal of the American Chemical Society* **1995**, *117*, 5614–15.
- [26] Chiefari, J.; Chong, Y. K.; Ercole, F.; Krstina, J.; Jeffery, J.; Le, T. P. T.; Mayadunne, R. T. A.; Meijs, G. F.; Moad, C. L.; Moad, G.; Rizzardo, E.; Thang, S. H. *Macromolecules* **1998**, *31*, 5559–5562.
- [27] Le, T. P.; Moad, G.; Rizzardo, E.; Thang, S. H.; *Polymerization with living characteristics with controlled dispersity, polymers prepared thereby, and chain-transfer agents used in the same*; WO 9801478 (A1); **1998**.

- [28] Georges, M. K.; Veregin, R. P. N.; Kazmaier, P. M.; Hamer, G. K. *Macromolecules* **1993**, *26*, 2987–2988.
- [29] Hawker, C. J. *Handbook of Radical Polymerization*; Matyjaszewski, K.; David, T. P., Eds.; John Wiley and Sons, **2002**.
- [30] Bertin, D.; Gimes, D.; Marque, S. R. A.; Tordo, P. *Chemical Society Reviews* **2011**, *40*, 2189–2198.
- [31] Brinks, M. K.; Studer, A. *Macromolecular Rapid Communications* **2009**, *30*, 1043–1057.
- [32] Gimes, D.; Marque, S. R. A. *Encyclopedia of Radicals in Chemistry, Biology and Materials*; Chatgililoglu, C.; Studer, A., Eds.; John Wiley & Sons, Ltd; Chapter : Nitroxide-Mediated Polymerization and its Applications; **2012**.
- [33] Grubbs, R. B. *Polymer Reviews* **2011**, *51*, 104–137.
- [34] Matyjaszewski, K.; Xia, J. *Chemical Reviews* **2001**, *101*, 2921–2990.
- [35] di Lena, F.; Matyjaszewski, K. *Progress in Polymer Science* **2010**, *35*, 959–1021.
- [36] Pintauer, T.; Matyjaszewski, K. *Chemical Society Reviews* **2008**, *37*, 1087–1097.
- [37] Wang, J.-S.; Matyjaszewski, K. *Macromolecules* **1995**, *28*, 7572–7573.
- [38] Jakubowski, W.; Matyjaszewski, K. *Macromolecules* **2005**, *38*, 4139–4146.
- [39] Min, K.; Gao, H.; Matyjaszewski, K. *Journal of the American Chemical Society* **2005**, *127*, 3825–3830.
- [40] Oh, J. K.; Tang, C.; Gao, H.; Tsarevsky, N. V.; Matyjaszewski, K. *Journal of the American Chemical Society* **2006**, *128*, 5578–5584.
- [41] Jakubowski, W.; Matyjaszewski, K. *Angewandte Chemie, International Edition* **2006**, *45*, 4482–4486.
- [42] Min, K.; Gao, H.; Matyjaszewski, K. *Macromolecules* **2007**, *40*, 1789–1791.
- [43] Matyjaszewski, K.; Jakubowski, W.; Min, K.; Tang, W.; Huang, J.; Braunecker, W. A.; Tsarevsky, N. V. *Proceedings of the National Academy of Sciences of the United States of America* **2006**, *103*, 15309–15314.
- [44] Matyjaszewski, K. *Macromolecules* **2012**, *45*, 4015–4039.
- [45] Corpart, P.; Charmot, D.; Biadatti, T.; Zard, S.; Michelet, D.; *Block polymer synthesis by controlled radical polymerization*; WO 9858974 (A1); **1998**.

- [46] Rizzardo, E.; Chen, M.; Chong, B.; Moad, G.; Skidmore, M.; Thang, S. H. *Macromolecular Symposia* **2007**, *248*, 104–116.
- [47] Vana, P.; Albertin, L.; Barner, L.; Davis, T. P.; Barner-Kowollik, C. *Journal of Polymer Science Part A: Polymer Chemistry* **2002**, *40*, 4032–4037.
- [48] Barner-Kowollik, C.; Buback, M.; Charleux, B.; Coote, M. L.; Drache, M.; Fukuda, T.; Goto, A.; Klumperman, B.; Lowe, A. B.; McLeary, J. B.; Moad, G.; Monteiro, M. J.; Sanderson, R. D.; Tonge, M. P.; Vana, P. *Journal of Polymer Science Part A: Polymer Chemistry* **2006**, *44*, 5809–5831.
- [49] Barner-Kowollik, C.; Davis, T. P.; Heuts, J. P. A.; Stenzel, M. H.; Vana, P.; Whittaker, M. *Journal of Polymer Science Part A: Polymer Chemistry* **2003**, *41*, 365–375.
- [50] Moad, G.; Rizzardo, E.; Thang, S. H. *Polymer International* **2011**, *60*, 9–25.
- [51] Pissuwan, D.; Boyer, C.; Gunasekaran, K.; Davis, T. P.; Bulmus, V. *Biomacromolecules* **2010**, *11*, 412–420.
- [52] Chang, C.-W.; Bays, E.; Tao, L.; Alconcel, S. N. S.; Maynard, H. D. *Chemical Communications* **2009**, 3580–3582.
- [53] Gibson, M. I.; Froehlich, E.; Klok, H.-A. *Journal of Polymer Science Part A: Polymer Chemistry* **2009**, *47*, 4332–4345.
- [54] Zhu, J.-L.; Cheng, H.; Jin, Y.; Cheng, S.-X.; Zhang, X.-Z.; Zhuo, R.-X. *Journal of Materials Chemistry* **2008**, *18*, 4433–4441.
- [55] Sinnwell, S.; Inglis, A. J.; Stenzel, M. H.; Barner-Kowollik, C. *Macromolecular Rapid Communications* **2008**, *29*, 1090–1096.
- [56] Chan, J. W.; Yu, B.; Hoyle, C. E.; Lowe, A. B. *Chemical Communications* **2008**, 4959–4961.
- [57] Kim, B. J.; Given-Beck, S.; Bang, J.; Hawker, C. J.; Kramer, E. J. *Macromolecules* **2007**, *40*, 1796–1798.
- [58] Spruell, J. M.; Levy, B. A.; Sutherland, A.; Dichtel, W. R.; Cheng, J. Y.; Stoddart, J. F.; Nelson, A. *Journal of Polymer Science Part A: Polymer Chemistry* **2009**, *47*, 346–356.
- [59] Li, H.; Yu, B.; Matsushima, H.; Hoyle, C. E.; Lowe, A. B. *Macromolecules* **2009**, *42*, 6537–6542.

- [60] Harvison, M. A.; Roth, P. J.; Davis, T. P.; Lowe, A. B. *Australian Journal of Chemistry* **2011**, *64*, 992–1006.
- [61] Willcock, H.; O'Reilly, R. K. *Polymer Chemistry* **2010**, *1*, 149–157.
- [62] Moad, G.; Chong, Y. K.; Postma, A.; Rizzardo, E.; Thang, S. H. *Polymer* **2005**, *46*, 8458–8468.
- [63] Postma, A.; Davis, T. P.; Li, G.; Moad, G.; O'Shea, M. S. *Macromolecules* **2006**, *39*, 5307–5318.
- [64] Postma, A.; Davis, T. P.; Evans, R. A.; Li, G.; Moad, G.; O'Shea, M. S. *Macromolecules* **2006**, *39*, 5293–5306.
- [65] Postma, A.; Davis, T. P.; Moad, G.; O'Shea, M. S. *Macromolecules* **2005**, *38*, 5371–5374.
- [66] Chong, B.; Moad, G.; Rizzardo, E.; Skidmore, M.; Thang, S. H. *Australian Journal of Chemistry* **2006**, *59*, 755–762.
- [67] Lehrle, R. S.; Place, E. J. *Polymer Degradation and Stability* **1997**, *56*, 215–219.
- [68] Lehrle, R. S.; Place, E. J. *Polymer Degradation and Stability* **1997**, *56*, 221–226.
- [69] Liu, Y.; He, J.; Xu, J.; Fan, D.; Tang, W.; Yang, Y. *Macromolecules* **2005**, *38*, 10332–10335.
- [70] Tschugaeff, L. *Berichte der deutschen chemischen Gesellschaft* **1899**, *32*, 3332–3335.
- [71] DePuy, C. H.; King, R. W. *Chemical Reviews* **1960**, *60*, 431–457.
- [72] Lima, V.; Jiang, X.; Brokken-Zijp, J.; Schoenmakers, P. J.; Klumperman, B.; Van Der Linde, R. *Journal of Polymer Science Part A: Polymer Chemistry* **2005**, *43*, 959–973.
- [73] Patton, D. L.; Mullings, M.; Fulghum, T.; Advincula, R. C. *Macromolecules* **2005**, *38*, 8597–8602.
- [74] Legge, T. M.; Slark, A. T.; Perrier, S. *Journal of Polymer Science Part A: Polymer Chemistry* **2006**, *44*, 6980–6987.
- [75] Mayadunne, R. T. A.; Jeffery, J.; Moad, G.; Rizzardo, E. *Macromolecules* **2003**, *36*, 1505–1513.
- [76] Harrison, S. *Macromolecules* **2009**, *42*, 897–898.

- [77] Sumerlin, B. S.; Lowe, A. B.; Stroud, P. A.; Zhang, P.; Urban, M. W.; McCormick, C. L. *Langmuir* **2003**, *19*, 5559–5562.
- [78] Scales, C. W.; Convertine, A. J.; McCormick, C. L. *Biomacromolecules* **2006**, *7*, 1389–1392.
- [79] Hruby, M.; Korostyatynets, V.; Benes, M. J.; Matejka, Z. *Collection of Czechoslovak Chemical Communications* **2003**, *68*, 2159–2170.
- [80] Thomas, D. B.; Convertine, A. J.; Hester, R. D.; Lowe, A. B.; McCormick, C. L. *Macromolecules* **2004**, *37*, 1735–1741.
- [81] Stenzel, M. H.; Davis, T. P.; Barner-Kowollik, C. *Chemical Communications* **2004**, 1546–1547.
- [82] Llauro, M.-F.; Loiseau, J.; Boisson, F.; Delolme, F.; Ladavière, C.; Claverie, J. *Journal of Polymer Science Part A: Polymer Chemistry* **2004**, *42*, 5439–5462.
- [83] Schilli, C.; Lanzendoerfer, M. G.; Müller, A. H. E. *Macromolecules* **2002**, *35*, 6819–6827.
- [84] Mayadunne, R. T. A.; Rizzardo, E.; Chiefari, J.; Krstina, J.; Moad, G.; Postma, A.; Thang, S. H. *Macromolecules* **2000**, *33*, 243–245.
- [85] Whittaker, M. R.; Goh, Y.-K.; Gemici, H.; Legge, T. M.; Perrier, S.; Monteiro, M. J. *Macromolecules* **2006**, *39*, 9028–9034.
- [86] Wang, Z.; He, J.; Tao, Y.; Yang, L.; Jiang, H.; Yang, Y. *Macromolecules* **2003**, *36*, 7446–7452.
- [87] Lowe, A. B.; Sumerlin, B. S.; Donovan, M. S.; McCormick, C. L. *Journal of the American Chemical Society* **2002**, *124*, 11562–11563.
- [88] Shen, W.; Qiu, Q.; Wang, Y.; Miao, M.; Li, B.; Zhang, T.; Cao, A.; An, Z. *Macromolecular Rapid Communications* **2010**, *31*, 1444–1448.
- [89] Zelikin, A. N.; Such, G. K.; Postma, A.; Caruso, F. *Biomacromolecules* **2007**, *8*, 2950–2953.
- [90] Spain, S. G.; Albertin, L.; Cameron, N. R. *Chemical Communications* **2006**, 4198–4200.
- [91] Boyer, C.; Bulmus, V.; Davis, T. P. *Macromolecular Rapid Communications* **2009**, *30*, 493–497.

- [92] Xu, J.; Tao, L.; Boyer, C.; Lowe, A. B.; Davis, T. P. *Macromolecules* **2009**, *43*, 20–24.
- [93] Koo, S. P. S.; Stamenovic, M. M.; Prasath, R. A.; Inglis, A. J.; Du Prez, F. E.; Barner-Kowollik, C.; Van Camp, W.; Junkers, T. *Journal of Polymer Science Part A: Polymer Chemistry* **2010**, *48*, 1699–1713.
- [94] Chen, M.; Ghiggino, K. P.; Rizzardo, E.; Thang, S. H.; Wilson, G. J. *Chemical Communications* **2008**, 1112–1114.
- [95] Chong, Y. K.; Moad, G.; Rizzardo, E.; Thang, S. H. *Macromolecules* **2007**, *40*, 4446–4455.
- [96] Perrier, S.; Takolpuckdee, P.; Mars, C. A. *Macromolecules* **2005**, *38*, 2033–2036.
- [97] Chen, M.; Moad, G.; Rizzardo, E. *Journal of Polymer Science Part A: Polymer Chemistry* **2009**, *47*, 6704–6714.
- [98] Quiclet-Sire, B.; Zard, S. Z. *Bulletin of the Korean Chemical Society* **2010**, *31*, 543–544.
- [99] Pfukwa, R.; Pound, G.; Klumperman, B. In *236th National Meeting of the American-Chemical-Society, Philadelphia, PA, August 17-21*; **2008**.
- [100] Cerreta, F.; Lenoche, A. M.; Leriverend, C.; Metzner, P.; Pham, T. N. *Bulletin De La Societe Chimique De France* **1995**, *132*, 67–74.
- [101] Metzner, P. *Pure and Applied Chemistry* **1996**, *68*, 863–868.
- [102] De Brouwer, H.; Schellekens, M. A. J.; Klumperman, B.; Monteiro, M. J.; German, A. L. *Journal of Polymer Science Part A: Polymer Chemistry* **2000**, *38*, 3596–3603.
- [103] Quinn, J. F.; Barner, L.; Barner-Kowollik, C.; Rizzardo, E.; Davis, T. P. *Macromolecules* **2002**, *35*, 7620–7627.
- [104] Lu, L.; Zhang, H.; Yang, N.; Cai, Y. *Macromolecules* **2006**, *39*, 3770–3776.
- [105] Lu, L.; Yang, N.; Cai, Y. *Chemical Communications* **2005**, 5287–5288.
- [106] Dubois, P. *Handbook of Ring-Opening Polymerization*; Dubois, P.; Coulombier, O.; Raquez, J.-M., Eds.; Wiley-VCH, **2009**.
- [107] Dainton, F. S.; Ivin, K. J. *Quarterly Reviews, Chemical Society* **1958**, *12*, 61–92.

- [108] Finke, H. L.; Scott, D. W.; Gross, M. E.; Messerly, J. F.; Waddington, G. *Journal of the American Chemical Society* **1956**, *78*, 5469–5476.
- [109] Sanda, F.; Endo, T. *Journal of Polymer Science Part A: Polymer Chemistry* **2000**, *39*, 265–276.
- [110] Biela, T.; Kowalski, A.; Libiszowski, J.; Duda, A.; Penczek, S. *Macromolecular Symposia* **2006**, *240*, 47–55.
- [111] Penczek, S. *Journal of Polymer Science Part A: Polymer Chemistry* **2000**, *38*, 1919–1933.
- [112] Penczek, S.; Cypriak, M.; Duda, A.; Kubisa, P.; Slomkowski, S. *Progress in Polymer Science* **2007**, *32*, 247–282.
- [113] Hashimoto, K. *Progress in Polymer Science* **2000**, *25*, 1411–1462.
- [114] Kricheldorf, H. R.; Kreiser-Saunders, I.; Stricker, A. *Macromolecules* **2000**, *33*, 702–709.
- [115] Kowalski, A.; Duda, A.; Penczek, S. *Macromolecules* **2000**, *33*, 689–695.
- [116] Nijenhuis, A. J.; Grijpma, D. W.; Pennings, A. J. *Macromolecules* **1992**, *25*, 6419–6424.
- [117] Du, Y. J.; Lemstra, P. J.; Nijenhuis, A. J.; Van, A. H. A. M.; Bastiaansen, C. *Macromolecules* **1995**, *28*, 2124–2132.
- [118] In't, V. P. J. A.; Velner, E. M.; Van, D. W. P.; Hamhuis, J.; Dijkstra, P. J.; Feijen, J. *Journal of Polymer Science Part A: Polymer Chemistry* **1997**, *35*, 219–226.
- [119] Degee, P.; Dubois, P.; Jerome, R.; Jacobsen, S.; Fritz, H.-G. *Macromolecular Symposia* **1999**, *144*, 289–302.
- [120] Kricheldorf, H. R.; Damrau, D. O. *Macromolecular Chemistry and Physics* **1997**, *198*, 1767–1774.
- [121] Kreiser-Saunders, I.; Kricheldorf, H. R. *Macromolecular Chemistry and Physics* **1998**, *199*, 1081–1087.
- [122] Dittrich, W.; Schulz, R. C. *Angewandte Makromolekulare Chemie* **1971**, *15*, 109–126.
- [123] Kricheldorf, H. R.; Berl, M.; Scharnagl, N. *Macromolecules* **1988**, *21*, 286–293.

- [124] Dubois, P.; Jacobs, C.; Jerome, R.; Teyssie, P. *Macromolecules* **1991**, *24*, 2266–2270.
- [125] Dechy-Cabaret, O.; Martin-Vaca, B.; Bourissou, D. *Chemical Reviews* **2004**, *104*, 6147–6176.
- [126] Baran, J.; Duda, A.; Kowalski, A.; Szymanski, R.; Penczek, S. *Macromolecular Symposia* **1997**, *123*, 93–101.
- [127] Penczek, S.; Duda, A.; Szymanski, R. *Macromolecular Symposia* **1998**, *132*, 441–449.
- [128] Albertsson, A.-C.; Varma, I. K. *Biomacromolecules* **2003**, *4*, 1466–1486.
- [129] Knani, D.; Gutman, A. L.; Kohn, D. H. *Journal of Polymer Science Part A: Polymer Chemistry* **1993**, *31*, 1221–1232.
- [130] Uyama, H.; Kobayashi, S. *Chemistry Letters* **1993**, 1149–1150.
- [131] Uyama, H.; Takeya, K.; Kobayashi, S. *Proceedings of the Japan Academy, Series B* **1993**, *69*, 203–207.
- [132] Fujioka, M.; Hosoda, N.; Nishiyama, S.; Noguchi, H.; Shoji, A.; Kumar, D. S.; Katsuraya, K.; Ishii, S.; Yoshida, Y. *Senrsquoi Gakkaishi* **2006**, *62*, 63–65.
- [133] Bourissou, D.; Moebs-Sanchez, S.; Martín-Vaca, B. *Comptes Rendus Chimie* **2007**, *10*, 775–794.
- [134] Varma, I. K.; Albertsson, A.-C.; Rajkhowa, R.; Srivastava, R. K. *Progress in Polymer Science* **2005**, *30*, 949–981.
- [135] Kobayashi, S. *Macromolecular Symposia* **2006**, *240*, 178–185.
- [136] Kobayashi, S.; Uyama, H.; Kimura, S. *Chemical Reviews* **2001**, *101*, 3793–3818.
- [137] Nederberg, F.; Connor, E. F.; Moeller, M.; Glauser, T.; Hedrick, J. L. *Angewandte Chemie, International Edition* **2001**, *40*, 2712–2715.
- [138] Steglich, W.; Hoeffle, G. *Angewandte Chemie, International Edition* **1969**, *8*, 981.
- [139] Spivey, A. C.; Arseniyadis, S. *Angewandte Chemie, International Edition* **2004**, *43*, 5436–5441.
- [140] Connor, E. F.; Nyce, G. W.; Myers, M.; Möck, A.; Hedrick, J. L. *Journal of the American Chemical Society* **2002**, *124*, 914–915.

- [141] Dove, A. P.; Pratt, R. C.; Lohmeijer, B. G. G.; Culkin, D. A.; Hagberg, E. C.; Nyce, G. W.; Waymouth, R. M.; Hedrick, J. L. *Polymer* **2006**, *47*, 4018–4025.
- [142] Nyce, G. W.; Glauser, T.; Connor, E. F.; Möck, A.; Waymouth, R. M.; Hedrick, J. L. *Journal of the American Chemical Society* **2003**, *125*, 3046–3056.
- [143] Culkin, D. A.; Jeong, W.; Csihony, S.; Gomez, E. D.; Balsara, N. P.; Hedrick, J. L.; Waymouth, R. M. *Angewandte Chemie, International Edition* **2007**, *46*, 2627–2630.
- [144] Kamber, N. E.; Jeong, W.; Waymouth, R. M.; Pratt, R. C.; Lohmeijer, B. G. G.; Hedrick, J. L. *Chemical Reviews* **2007**, *107*, 5813–5840.
- [145] Schuchardt, U.; Vargas, R. M.; Gelbard, G. *Journal of Molecular Catalysis A: Chemical* **1995**, *99*, 65–70.
- [146] Pratt, R. C.; Lohmeijer, B. G. G.; Long, D. A.; Waymouth, R. M.; Hedrick, J. L. *Journal of the American Chemical Society* **2006**, *128*, 4556–4557.
- [147] Murayama, M.; Sanda, F.; Endo, T. *Macromolecules* **1998**, *31*, 919–923.
- [148] Lohmeijer, B. G. G.; Pratt, R. C.; Leibfarth, F.; Logan, J. W.; Long, D. A.; Dove, A. P.; Nederberg, F.; Choi, J.; Wade, C.; Waymouth, R. M.; Hedrick, J. L. *Macromolecules* **2006**, *39*, 8574–8583.
- [149] Corey, E. J.; Grogan, M. J. *Organic Letters* **1999**, *1*, 157–160.
- [150] Simón, L.; Goodman, J. M. *The Journal of Organic Chemistry* **2007**, *72*, 9656–9662.
- [151] Leibfarth, F. A.; Lohmeijer, B. G. G.; Nederberg, F.; Pratt, R. C.; Logan, J. W.; Waymouth, R. M.; Hedrick, J. L. In *Abstracts of Papers, 233rd ACS National Meeting, Chicago, IL, United States, March 25-29; 2007*.
- [152] Kaljurand, I.; Kütt, A.; Sooväli, L.; Rodima, T.; Mäemets, V.; Leito, I.; Koppel, I. A. *The Journal of Organic Chemistry* **2005**, *70*, 1019–1028.
- [153] Bayer, O. *Angewandte Chemie* **1947**, *59*, 257–272.
- [154] Biskup, K.; Keggenhoff, B.; *Manufacture of toluene diisocyanate (TDI), special mixtures from toluenediamine and water and their use for the manufacture of TDI*; EP 757034 (A1); **1997**.
- [155] Wehman, P.; Dol, G. C.; Moorman, E. R.; Kamer, P. C. J.; van Leeuwen, P. W. N. M.; Fraanje, J.; Goubitz, K. *Organometallics* **1994**, *13*, 4856–4869.

- [156] Bolzacchini, E.; Meinardi, S.; Orlandi, M.; Rindone, B. *Journal of Molecular Catalysis A: Chemical* **1996**, *111*, 281–287.
- [157] Fukuoka, S.; Chono, M.; Kohno, M. *Chemtech* **1984**, *14*, 670–676.
- [158] Farkas, A.; Strohm, P. F. *Industrial & Engineering Chemistry Fundamentals* **1965**, *4*, 32–38.
- [159] Burkhart, G.; Kollmeier, H. J.; Schloens, H. H. *Journal of Cellular Plastics* **1984**, *20*, 37–41.
- [160] Baker, J. W.; Holdsworth, J. B. *Journal of the Chemical Society* **1947**, 713–726.
- [161] Frisch, K. C.; Rumao, L. P. *Journal of Macromolecular Science - Reviews in Macromolecular Chemistry* **1970**, *5*, 103–149.
- [162] Oertel, G. *Polyurethane handbook (2nd ed.)*; Hanser Publishers, Munich, **1993**.
- [163] Kusan, J.; Keul, H.; Hoecker, H. *e-Polymers* **2001**, *10*, 11–14.
- [164] Neffgen, S.; Keul, H.; Hocker, H. *Macromolecular Rapid Communications* **1999**, *20*, 194–199.
- [165] Morgan, P. W. *Journal of Polymer Science* **1964**, *4*, 1075–1096.
- [166] Rokicki, G.; Piotrowska, A. *Polymer* **2002**, *43*, 2927–2935.
- [167] Grozos, S. J.; Drechsel, E. K.; *Polyurethans*; US 2802022; **1957**.
- [168] Figovsky, O. L.; *Hybrid nonisocyanate polyurethane network polymers and composites formed therefrom*; WO 9965969 (A1); **1999**.
- [169] Tomita, H.; Sanda, F.; Endo, T. *Journal of Polymer Science Part A: Polymer Chemistry* **2001**, *39*, 851–859.
- [170] Whelan, J., John M.; Samuels, J., Wm P.; *Multiple cyclic carbonate polymers from erythritol dicarbonate*; US 2935494; **1960**.
- [171] Mikheev, V. V.; Svetlakov, N. V.; Sysoev, V. A.; *Manufacture of crosslinked polyurethane coatings from multifunctional cyclic carbonate group-containing compounds and hexamethylenediamine or diethylenetriamine*; SU 970856 (A1); **1996**.
- [172] Mikheev, V.; Ivanova, R. *Russian Journal of Applied Chemistry* **2006**, *79*, 310–313.

- [173] Figovsky, O. L.; Shapovalov, L.; Axenov, O. *Surface Coatings International Part B* **2004**, *87*, 83–90.
- [174] Figovsky, O. L.; Shapovalov, L. In *Advances in Coatings Technology, International Conference, 6th, Warsaw, Poland, November 23-26; 2004*, 1–10.
- [175] Desai, S.; Thakore, I. M.; Sarawade, B. D.; Devi, S. *Polymer Engineering & Science* **2000**, *40*, 1200–1210.
- [176] Kendagannaswamy, B. K.; Annadurai, V.; Siddaramaiah, V.; Somashekar, R. *Journal of Macromolecular Science, Part A* **2000**, *37*, 1617–1625.
- [177] Paul, C. J.; Gopinathan Nair, M. R.; Neelakantan, N. R.; Koshy, P.; Idage, B. B.; Bhelhekar, A. A. *Polymer* **1998**, *39*, 6861–6874.
- [178] Chevali, V.; Fuqua, M.; Ulven, C. A. *Handbook of Bioplastics and Biocomposites Engineering Applications*; Srikanth, P., Ed.; Scrivener Publishing; Chapter Vegetable oil based rigid foam composites; **2011**, 269-284.
- [179] Desroches, M.; Escouvois, M.; Auvergne, R.; Caillol, S.; Boutevin, B. *Polymer Reviews* **2012**, *52*, 38–79.
- [180] Lu, Y.; Larock, R. C. *ACS Symposium Series* **2010**, *1043*, 87–102.
- [181] Pfister, D. P.; Xia, Y.; Larock, R. C. *ChemSusChem* **2011**, *4*, 703–717.
- [182] Spychaj, T.; Wilpiszewska, K.; Spychaj, S. *Handbook of Engineering Biopolymers*; Fakirov, S.; Bhattacharyya, D., Eds.; Carl Hanser Verlag; Chapter : Starch-urethane polymers: physicochemical aspects, properties, application; **2007**, 155-191.
- [183] Zagar, E.; Zigon, M. *Polymer* **1999**, *40*, 2727–2735.
- [184] Perez-Liminana, M. A.; Aran-Ais, F.; Torro-Palau, A. M.; Cesar Orgiles-Barcelo, A.; Miguel Martin-Martinez, J. *International Journal of Adhesion and Adhesives* **2005**, *25*, 507–517.
- [185] Jin, Y.-Z.; Hahn, Y. B.; Nahm, K. S.; Lee, Y.-S. *Polymer* **2005**, *46*, 11294–11300.
- [186] Potoczek, M.; Heneczowski, M.; Oleksy, M. *Ceramics International* **2003**, *29*, 259–264.
- [187] Lai, Y.-C.; Baccei, L. J. *Journal of Applied Polymer Science* **1991**, *42*, 3173–3179.

- [188] Keskin, S.; Usanmaz, A. *Journal of Applied Polymer Science* **2010**, *117*, 458–466.
- [189] Tsvett, M. *Berichte der Deutschen Botanischen Gesellschaft* **1906**, *24*, 316–323.
- [190] Ettre, L. S. *Analytical Chemistry* **1971**, *43*, 20–31A.
- [191] Snyder, L. R.; Kirkland, J. J. *Introduction to Modern Liquid Chromatography*. 2nd Ed; Wiley-Interscience, **1979**.
- [192] Desty, D. H. *LC-GC – Magazine of Separation Science* **1991**, *9*, 414–418.
- [193] Berek, D. *Progress in Polymer Science* **2000**, *25*, 873–908.
- [194] Trathnigg, B. *Progress in Polymer Science* **1995**, *20*, 615–650.
- [195] Chang, T. *Advances in Polymer Science* **2003**, *163*, 231–245.
- [196] Porath, J.; Flodin, P. *Nature* **1959**, *183*, 1657–1659.
- [197] Moore, J. C. *Journal of Polymer Science* **1964**, *2*, 835–843.
- [198] Striegel, A. *Modern Size-Exclusion Liquid Chromatography*, 2nd ed.; Wiley: New Jersey, **2009**.
- [199] Du, Y.; Xue, Y.; Frisch, H. L. *Physical Properties of Polymers Handbook*, 2nd ed.; Mark, J. E., Ed.; Springer; Chapter : Mark-Houwink-Staudinger-Sakurada constants [of polymers]; **1996**, 241-248.
- [200] Bareiss, R. E. *Chemiker-Zeitung* **1981**, *105*, 97–103.
- [201] Gallot-Grubisic, Z.; Rempp, P.; Benoit, H. *Journal of Polymer Science - Polymer Letters Edition* **1967**, *5*, 753–759.
- [202] Greene, S. V. *Encyclopedia of Chromatography*, 3rd ed.; Cazes, J., Ed.; CRC Press, Taylor and Francis Group; Chapter : SEC with on-line triple detection: light scattering, viscometry, and refractive index; **2010**, 2120-2123.
- [203] Heinzmann, G.; Tartsch, B. *BioTec* **2007**, *18*, 24–25.
- [204] Rubinstein, M. *Polymer Physics*; Oxford University Press, **2003**.
- [205] Falkenhagen, J.; Much, H.; Stauf, W.; Müller, A. H. E. *Macromolecules* **2000**, *33*, 3687–3693.
- [206] Falkenhagen, J.; Much, H.; Stauf, W.; Muller, A. H. E. *Polymer Preprints* **1999**, *40*, 984–985.

- [207] Belenky, B. G.; Gankina, E. S.; Tennikov, M. B.; Vilenchik, L. Z. *Journal of Chromatography A* **1978**, *147*, 99–110.
- [208] Pasch, H. *Advances in Polymer Science* **1997**, *128*, 1–45.
- [209] Macko, T.; Hunkeler, D. *Advances in Polymer Science* **2003**, *163*, 161–216.
- [210] Lee, W.; Park, S.; Chang, T. *Analytical Chemistry* **2001**, *73*, 3884–3889.
- [211] Trathnigg, B.; Kollroser, M.; Rappel, C. *Journal of Chromatography A* **2001**, *922*, 193–205.
- [212] Lepoittevin, B.; Dourges, M.-A.; Masure, M.; Hemery, P.; Baran, K.; Cramail, H. *Macromolecules* **2000**, *33*, 8218–8224.
- [213] Jiang, X.; van der Horst, A.; Lima, V.; Schoenmakers, P. J. *Journal of Chromatography A* **2005**, *1076*, 51–61.
- [214] Porath, J. *Nature* **1962**, *196*, 47–48.
- [215] Belenkii, B. G.; Gankina, E. S. *Journal of Chromatography A* **1970**, *53*, 3–25.
- [216] Inagaki, H.; Matsuda, H.; Kamiyama, F. *Macromolecules* **1968**, *1*, 520–525.
- [217] Teramachi, S.; Hasegawa, A.; Matsumoto, T. *Journal of Chromatography A* **1991**, *547*, 429–433.
- [218] Kilz, P.; Krüger, R. P.; Much, H.; Schulz, G. In *Chromatographic Characterization of Polymers*; Advances in Chemistry, Vol. 247; American Chemical Society, 1995; pp 223–241.
- [219] Kilz, P.; Krüger, R. P.; Much, H.; Schulz, G. *Polymeric Materials: Science and Engineering* **1993**, *69*, 114–115.
- [220] Berek, D. *Analytical and Bioanalytical Chemistry* **2010**, *396*, 421–441.
- [221] Pasch, H.; Gallot, Y.; Trathnigg, B. *Polymer* **1993**, *34*, 4986–4989.
- [222] Dugo, P.; Cacciola, F.; Kumm, T.; Dugo, G.; Mondello, L. *Journal of Chromatography A* **2008**, *1184*, 353–368.
- [223] van der Horst, A.; Schoenmakers, P. J. *Journal of Chromatography A* **2003**, *1000*, 693–709.
- [224] Knecht, D.; Rittig, F.; Lange, R. F. M.; Pasch, H. *Journal of Chromatography A* **2006**, *1130*, 43–53.

- [225] Glockner, G.; Van Den Berg, J. H. M. *Journal of Chromatography A* **1991**, *550*, 629–638.
- [226] Dole, M.; Mack, L. L.; Hines, R. L.; Mobley, R. C.; Ferguson, L. D.; Alice, M. B. *The Journal of Chemical Physics* **1968**, *49*, 2240–2249.
- [227] Yamashita, M.; Fenn, J. B. *The Journal of Physical Chemistry* **1984**, *88*, 4671–4675.
- [228] Yamashita, M.; Fenn, J. B. *The Journal of Physical Chemistry* **1984**, *88*, 4451–4459.
- [229] Fenn, J. B.; Mann, M.; Meng, C. K.; Wong, S. F.; Whitehouse, C. M. *Mass Spectrometry Reviews* **1990**, *9*, 37–70.
- [230] Whitehouse, C. M.; Dreyer, R. N.; Yamashita, M.; Fenn, J. B. *Analytical Chemistry* **1985**, *57*, 675–679.
- [231] Iribarne, J. V.; Thomson, B. A. *The Journal of Chemical Physics* **1976**, *64*, 2287–2294.
- [232] Thomson, B. A.; Iribarne, J. V. *The Journal of Chemical Physics* **1979**, *71*, 4451–4463.
- [233] Kebarle, P.; Verkerk, U. H. *Electrospray and MALDI Mass Spectrometry: Fundamentals, Instrumentation, Practicalities, and Biological Applications, 2nd Edition*; Cole, R. B., Ed.; John Wiley and Sons, **2010**.
- [234] Bier, M. E. *ES and MALDI Coupling to Mass Spectrometry Instrumentation*; Cole, R. B., Ed.; John Wiley and Sons, **2010**.
- [235] Prokai, L.; Simonsick, W. J. *Rapid Communications in Mass Spectrometry* **1993**, *7*, 853–856.
- [236] Simonsick William, J.; Prokai, L. *Chromatographic Characterization of Polymers*; Provder, T.; Barth, H. G.; Urban, M. W., Eds.; American Chemical Society; Chapter : Size-Exclusion Chromatography with Electrospray Mass Spectrometric Detection; **1995**, 41-56.
- [237] Nielen, M. W. F. *Rapid Communications in Mass Spectrometry* **1996**, *10*, 1652–1660.
- [238] Nielen, M. W. F.; Buijtenhuijs, F. A. *Analytical Chemistry* **1999**, *71*, 1809–1814.
- [239] Gründling, T.; Guilhaus, M.; Barner-Kowollik, C. *Macromolecules* **2009**, *42*, 6366–6374.

- [240] Gründling, T.; Guilhaus, M.; Barner-Kowollik, C. *Analytical Chemistry* **2008**, *80*, 6915–6927.
- [241] Falkenhagen, J.; Weidner, S. *Analytical Chemistry* **2009**, *81*, 282–287.
- [242] Vastola, F. J.; Mumma, R. O.; Pirone, A. J. *Organic Mass Spectrometry* **1970**, *3*, 101–104.
- [243] Fenner, N. C.; Daly, N. R. *Review of Scientific Instruments* **1966**, *37*, 1068–1070.
- [244] Karas, M.; Bachmann, D.; Hillenkamp, F. *Analytical Chemistry* **1985**, *57*, 2935–2939.
- [245] Karas, M.; Bachmann, D.; Bahr, U.; Hillenkamp, F. *International Journal of Mass Spectrometry and Ion Processes* **1987**, *78*, 53–68.
- [246] Tanaka, K.; Waki, H.; Ido, Y.; Akita, S.; Yoshida, Y.; Yoshida, T.; Matsuo, T. *Rapid Communications in Mass Spectrometry* **1988**, *2*, 151–153.
- [247] Nielen, M. W. F. *Mass Spectrometry Reviews* **1999**, *18*, 309–344.
- [248] Cotter, R. J. *Analytical Chemistry* **1992**, *64*, 1027A–1039A.
- [249] Esser, E.; Keil, C.; Braun, D.; Montag, P.; Pasch, H. *Polymer* **2000**, *41*, 4039–4046.
- [250] Montaudo, G.; Garozzo, D.; Montaudo, M. S.; Puglisi, C.; Samperi, F. *Macromolecules* **1995**, *28*, 7983–7989.
- [251] Weidner, S. M.; Falkenhagen, J. *Maldi Mass Spectrometry for Synthetic Polymer Analysis*; Liang, L., Ed.; John Wiley & Sons; Chapter 11 : LC-MALDI MS for polymer characterization; **2011**, 247-265.
- [252] Hanton, S. D.; Liu, X. M. *Analytical Chemistry* **2000**, *72*, 4550–4554.
- [253] Willis James, N.; Dwyer James, L.; Liu, X.; Dark William, A. *Chromatography of Polymers*; Provde, T., Ed.; ACS Symposium Series, Vol. 731; ACS Publications; Chapter 16: Size Exclusion Chromatography FTIR Analysis of Polyethylene; **1999**, 226-231.
- [254] Kok, S. J.; Wold, C. A.; Hankemeier, T.; Schoenmakers, P. J. *Journal of Chromatography A* **2003**, *1017*, 83–96.
- [255] Kok, S. J.; Arentsen, N. C.; Cools, P. J. C. H.; Hankemeier, T.; Schoenmakers, P. J. *Journal of Chromatography A* **2002**, *948*, 257–265.

- [256] Sabo, M.; Gross, J.; Wang, J. S.; Rosenberg, I. E. *Analytical Chemistry* **1985**, *57*, 1822–1826.
- [257] Louden, D.; Handley, A.; Taylor, S.; Lenz, E.; Miller, S.; Wilson, I. D.; Sage, A. *Analytical Chemistry* **2000**, *72*, 3922–3926.
- [258] Eichhorn, K.-J.; Voigt, D.; Komber, H.; Pospiech, D. *Macromolecular Symposia* **1997**, *119*, 325–338.
- [259] Zhang, L.; Wang, Q.; Lei, P.; Wang, X.; Wang, C.; Cai, L. *Journal of Polymer Science Part A: Polymer Chemistry* **2007**, *45*, 2617–2623.
- [260] Boelens, H. F. M.; Eilers, P. H. C.; Hankemeier, T. *Analytical Chemistry* **2005**, *77*, 7998–8007.
- [261] Tribe, K.; Saunders, G.; Meißner, R. *Macromolecular Symposia* **2006**, *236*, 228–234.
- [262] Remsen, E. E.; Freeman, J. J. *Applied Spectroscopy* **1991**, *45*, 868–873.
- [263] Beskers, T. F.; Hofe, T.; Wilhelm, M. *Macromolecular Rapid Communications* **2012**, DOI: 10.1002/marc.201200403.
- [264] Aoyagi, N.; Endo, T. *Journal of Polymer Science Part A: Polymer Chemistry* **2009**, *47*, 3702–3709.
- [265] Bivigou-Koumba, A. M.; Kristen, J.; Laschewsky, A.; Müller-Buschbaum, P.; Papadakis, C. M. *Macromolecular Chemistry and Physics* **2009**, *210*, 565–578.
- [266] Perrier, S.; Barner-Kowollik, C.; Quinn, J. F.; Vana, P.; Davis, T. P. *Macromolecules* **2002**, *35*, 8300–8306.
- [267] Chaffey-Millar, H.; Stenzel, M. H.; Davis, T. P.; Coote, M. L.; Barner-Kowollik, C. *Macromolecules* **2006**, *39*, 6406–6419.
- [268] Schindler, A.; Hibionada, Y. M.; Pitt, C. G. *Journal of Polymer Science: Polymer Chemistry Edition* **1982**, *20*, 319–326.
- [269] Dervaux, B.; Junkers, T.; Schneider-Baumann, M.; Du Prez, F. E.; Barner-Kowollik, C. *Journal of Polymer Science Part A: Polymer Chemistry* **2009**, *47*, 6641–6654.
- [270] Buback, M.; Kurz, C. H.; Schmaltz, C. *Macromolecular Chemistry and Physics* **1998**, *199*, 1721–1727.

- [271] Beuermann, S.; Paquet, D. A.; McMinn, J. H.; Hutchinson, R. A. *Macromolecules* **1996**, *29*, 4206–4215.
- [272] Chen, Y.-J.; Li, J.; Hadjichristidis, N.; Mays, J. W. *Polymer Bulletin* **1993**, *30*, 575–578.
- [273] Strazielle, C.; Benoit, H.; Vogl, O. *European Polymer Journal* **1978**, *14*, 331–334.
- [274] Gründling, T.; Pickford, R.; Guilhaus, M.; Barner-Kowollik, C. *Journal of Polymer Science Part A: Polymer Chemistry* **2008**, *46*, 7447–7461.
- [275] Gründling, T.; Dietrich, M.; Barner-Kowollik, C. *Australian Journal of Chemistry* **2009**, *62*, 806–812.
- [276] Dietrich, M.; Glassner, M.; Gruending, T.; Schmid, C.; Falkenhagen, J.; Barner-Kowollik, C. *Polymer Chemistry* **2010**, *1*, 634–644.
- [277] Joralemon, M. J.; McRae, S.; Emrick, T. *Chemical Communications* **2010**, *46*, 1377–1393.
- [278] Hirai, T.; Leolukman, M.; Jin, S.; Goseki, R.; Ishida, Y.; Kakimoto, M.; Hayakawa, T.; Ree, M.; Gopalan, P. *Macromolecules* **2009**, *42*, 8835–8843.
- [279] Zeng, F.; Yang, M.; Zhang, J.; Varshney, S. K. *Journal of Polymer Science Part A: Polymer Chemistry* **2002**, *40*, 4387–4397.
- [280] Vlcek, P.; Otoupalová, J.; Janata, M.; Látalová, P.; Kurková, D.; Toman, L.; Masar, B. *Macromolecules* **2003**, *37*, 344–351.
- [281] Pitsikalis, M.; Siakali-Kioulafa, E.; Hadjichristidis, N. *Macromolecules* **2000**, *33*, 5460–5469.
- [282] Pitsikalis, M.; Siakali-Kioulafa, E.; Hadjichristidis, N. *Journal of Polymer Science Part A: Polymer Chemistry* **2004**, *42*, 4177–4188.
- [283] Sciannamea, V.; Jerome, R.; Detrembleur, C. *Chemical Reviews* **2008**, *108*, 1104–1126.
- [284] Ouchi, M.; Terashima, T.; Sawamoto, M. *Chemical Reviews* **2009**, *109*, 4963–5050.
- [285] Braunecker, W. A.; Matyjaszewski, K. *Progress in Polymer Science* **2007**, *32*, 93–146.

- [286] Perrier, S.; Takolpuckdee, P. *Journal of Polymer Science Part A: Polymer Chemistry* **2005**, *43*, 5347–5393.
- [287] Moad, G.; Rizzardo, E.; Thang, S. H. *Australian Journal of Chemistry* **2005**, *58*, 379–410.
- [288] Moad, G.; Rizzardo, E.; Thang, S. H. *Australian Journal of Chemistry* **2006**, *59*, 669–692.
- [289] Moad, G.; Rizzardo, E.; Thang, S. H. *Australian Journal of Chemistry* **2009**, *62*, 1402–1472.
- [290] Barner-Kowollik, C.; Perrier, S. *Journal of Polymer Science Part A: Polymer Chemistry* **2008**, *46*, 5715–5723.
- [291] Ren, T.; Lei, X.; Yuan, W. *Materials Letters* **2012**, *67*, 383–386.
- [292] Tian, H.-Y.; Yan, J.-J.; Wang, D.; Gu, C.; You, Y.-Z.; Chen, X.-S. *Macromolecular Rapid Communications* **2011**, *32*, 660–664.
- [293] Kataoka, K.; Harada, A.; Nagasaki, Y. *Advanced Drug Delivery Reviews* **2001**, *47*, 113–131.
- [294] de Lambert, B.; Charreyre, M.-T.; Chaix, C.; Pichot, C. *Polymer* **2007**, *48*, 437–447.
- [295] Öztürk, T.; Göktas, M.; Hazer, B. *Journal of Applied Polymer Science* **2010**, *117*, 1638–1645.
- [296] Saeed, A. O.; Dey, S.; Howdle, S. M.; Thurecht, K. J.; Alexander, C. *Journal of Materials Chemistry* **2009**, *19*, 4529–4535.
- [297] Li, J.; Ren, J.; Cao, Y.; Yuan, W. *Polymer* **2010**, *51*, 1301–1310.
- [298] Zhang, W.; Wang, S.; Li, X.; Yuan, J.; Wang, S. *European Polymer Journal* **2012**, *48*, 720–729.
- [299] Glaied, O.; Delaite, C.; Riess, G. *Polymer Bulletin* **2012**, *68*, 607–621.
- [300] Bian, Q.; Xiao, Y.; Lang, M. *Polymer* **2012**, *53*, 1684–1693.
- [301] Kakwere, H.; Perrier, S. *Journal of Polymer Science Part A: Polymer Chemistry* **2009**, *47*, 6396–6408.
- [302] Le Hellaye, M.; Lefay, C.; Davis, T. P.; Stenzel, M. H.; Barner-Kowollik, C. *Journal of Polymer Science Part A: Polymer Chemistry* **2008**, *46*, 3058–3067.

- [303] Kolb, H. C.; Finn, M. G.; Sharpless, K. B. *Angewandte Chemie* **2001**, *113*, 2056–2075.
- [304] Kolb, H. C.; Finn, M. G.; Sharpless, K. B. *Angewandte Chemie, International Edition* **2001**, *40*, 2004–2021.
- [305] Barner-Kowollik, C.; Du Prez, F. E.; Espeel, P.; Hawker, C. J.; Junkers, T.; Schlaad, H.; Van Camp, W. *Angewandte Chemie, International Edition* **2011**, *50*, 60–62.
- [306] Gründling, T.; Oehlenschlaeger, K. K.; Frick, E.; Glassner, M.; Schmid, C.; Barner-Kowollik, C. *Macromolecular Rapid Communications* **2011**, *32*, 807–812.
- [307] Altintas, O.; Hizal, G.; Tunca, U. *Journal of Polymer Science Part A: Polymer Chemistry* **2008**, *46*, 1218–1228.
- [308] Quemener, D.; Davis, T. P.; Barner-Kowollik, C.; Stenzel, M. H. *Chemical Communications* **2006**, 5051–5053.
- [309] Tao, L.; Luan, B.; Pan, C.-y. *Polymer* **2003**, *44*, 1013–1020.
- [310] Hiller, W.; Pasch, H.; Sinha, P.; Wagner, T.; Thiel, J.; Wagner, M.; Müllen, K. *Macromolecules* **2010**, *43*, 4853–4863.
- [311] Albert, K. *Journal of Chromatography A* **1995**, *703*, 123–147.
- [312] Gründling, T.; Weidner, S.; Falkenhagen, J.; Barner-Kowollik, C. *Polymer Chemistry* **2010**, *1*, 599–617.
- [313] Falkenhagen, J. *ChemMedChem* **2008**, *3*, 502.
- [314] Malik, M. I.; Trathnigg, B.; Saf, R. *Journal of Chromatography A* **2009**, *1216*, 6627–6635.
- [315] Gao, H.; Min, K.; Matyjaszewski, K. *Macromolecular Chemistry and Physics* **2006**, *207*, 1709–1717.
- [316] Song, C. X.; Sun, H. F.; Feng, X. D. *Polymer Journal* **1987**, *19*, 485–491.
- [317] Jung, J. H.; Ree, M.; Kim, H. *Catalysis Today* **2006**, *115*, 283–287.
- [318] Philipsen, H. J. A.; Klumperman, B.; van Herk, A. M.; German, A. L. *Journal of Chromatography A* **1996**, *727*, 13–25.

- [319] Beaudoin, E.; Dufils, P. E.; Gimes, D.; Marque, S.; Petit, C.; Tordo, P.; Bertin, D. *Polymer* **2006**, *47*, 98–106.
- [320] Uhrich, K. E.; Cannizzaro, S. M.; Langer, R. S.; Shakesheff, K. M. *Chemical Reviews* **1999**, *99*, 3181–3198.
- [321] Puppi, D.; Chiellini, F.; Piras, A. M.; Chiellini, E. *Progress in Polymer Science* **2010**, *35*, 403–440.
- [322] Nair, L. S.; Laurencin, C. T. *Progress in Polymer Science* **2007**, *32*, 762–798.
- [323] Gupta, A. P.; Kumar, V. *European Polymer Journal* **2007**, *43*, 4053–4074.
- [324] Anderson, K. S.; Schreck, K. M.; Hillmyer, M. A. *Polymer Reviews* **2008**, *48*, 85–108.
- [325] Rasal, R. M.; Janorkar, A. V.; Hirt, D. E. *Progress in Polymer Science* **2010**, *35*, 338–356.
- [326] Kamigaito, M.; Ando, T.; Sawamoto, M. *Chemical Reviews* **2001**, *101*, 3689–3746.
- [327] Favier, A.; Charreyre, M.-T. *Macromolecular Rapid Communications* **2006**, *27*, 653–692.
- [328] Zhang, X.; Odon, M.; Giani, O.; Monge, S.; Robin, J.-J. *Macromolecules* **2010**, *43*, 2654–2656.
- [329] Chernikova, E.; Terpugova, P.; Garina, E.; Golubev, V. *Polymer Science Series A* **2007**, *49*, 108–119.
- [330] Petit, C.; Luneau, B.; Beaudoin, E.; Gimes, D.; Bertin, D. *Journal of Chromatography A* **2007**, *1163*, 128–137.
- [331] Guillaneuf, Y.; Dufils, P.-E.; Autissier, L.; Rollet, M.; Gimes, D.; Bertin, D. *Macromolecules* **2009**, *43*, 91–100.
- [332] Macko, T.; Hunkeler, D.; Berek, D. *Macromolecules* **2002**, *35*, 1797–1804.
- [333] Chang, T. *Journal of Polymer Science Part B: Polymer Physics* **2005**, *43*, 1591–1607.
- [334] Srbek, J.; Coufal, P.; Bosáková, Z.; Tesarová, E. *Journal of Separation Science* **2005**, *28*, 1263–1270.

- [335] Barner-Kowollik, C.; Davis, T. P.; Stenzel, M. H. *Australian Journal of Chemistry* **2006**, *59*, 719–727.
- [336] Ahmed, H.; Trathnigg, B. *Journal of Separation Science* **2009**, *32*, 1390–1400.
- [337] Chagneux, N.; Trimaille, T.; Rollet, M.; Beaudoin, E.; Gérard, P.; Bertin, D.; Gimes, D. *Macromolecules* **2009**, *42*, 9435–9442.
- [338] Jiang, X.; van der Horst, A.; Schoenmakers, P. J. *Journal of Chromatography A* **2002**, *982*, 55–68.
- [339] Fleury, G.; Bates, F. S. *Macromolecules* **2009**, *42*, 3598–3610.
- [340] Alfonzo, C. G.; Fleury, G.; Chaffin, K. A.; Bates, F. S. *Macromolecules* **2010**, *43*, 5295–5305.
- [341] Ramakrishnan, A.; Dhamodharan, R. *Macromolecules* **2003**, *36*, 1039–1046.
- [342] Boyer, C.; Soeriyadi, A. H.; Zetterlund, P. B.; Whittaker, M. R. *Macromolecules* **2011**, *44*, 8028–8033.
- [343] Hu, D.; Zheng, S. *European Polymer Journal* **2009**, *45*, 3326–3338.
- [344] Hu, J.; Ge, Z.; Zhou, Y.; Zhang, Y.; Liu, S. *Polymer Preprints* **2011**, *52*, 436–437.
- [345] Banik, S. M.; Monnot, B. L.; Weber, R. L.; Mahanthappa, M. K. *Macromolecules* **2011**, *44*, 7141–7148.
- [346] Na, K.; Lee, K. H.; Lee, D. H.; Bae, Y. H. *European Journal of Pharmaceutical Sciences* **2006**, *27*, 115–122.
- [347] Zotzmann, J.; Ziegler, H. J.; Behl, M.; Zierke, M.; Radke, W.; Lendlein, A. *Journal of Materials Science: Materials in Medicine* **2011**, *22*, 2147–2154.
- [348] Vora, A.; Nasrullah, M.; Webster, D. *Journal of Coatings Technology and Research* **2010**, *7*, 409–417.
- [349] Jaisankar, S. N.; Nelson, D. J.; Brammer, C. N. *Polymer* **2009**, *50*, 4775–4780.
- [350] Yamaguchi, I.; Tanaka, H.; Osakada, K.; Yamamoto, T. *Macromolecules* **1998**, *31*, 30–35.
- [351] Liu, X. M.; Maziarz, E. P.; Heiler, D. J. *Journal of Chromatography A* **2004**, *1034*, 125–131.

- [352] Liu, X. M.; Maziarz, E. P.; Heiler, D. J.; Grobe, G. L. *Journal of the American Society for Mass Spectrometry* **2003**, *14*, 195–202.
- [353] Hehn, M.; Hiller, W.; Wagner, T.; Thiel, J.; Pasch, H. *Macromolecular Chemistry and Physics* **2012**, *213*, 401–410.
- [354] Tang, D.; Noordover, B. A. J.; Sablong, R. J.; Koning, C. E. *Journal of Polymer Science Part A: Polymer Chemistry* **2011**, *49*, 2959–2968.
- [355] Mhatre, R.; Krull, I. S. *Analytical Chemistry* **1993**, *65*, 283–286.

A

Appendix

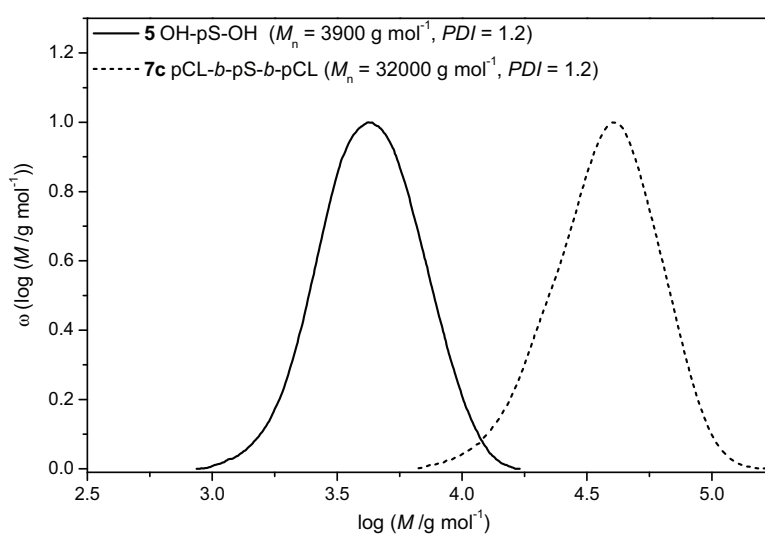


Figure A.1. SEC trace of the chain extension of **5** to the ABA block copolymer **7c** as a repetition of **7b**.

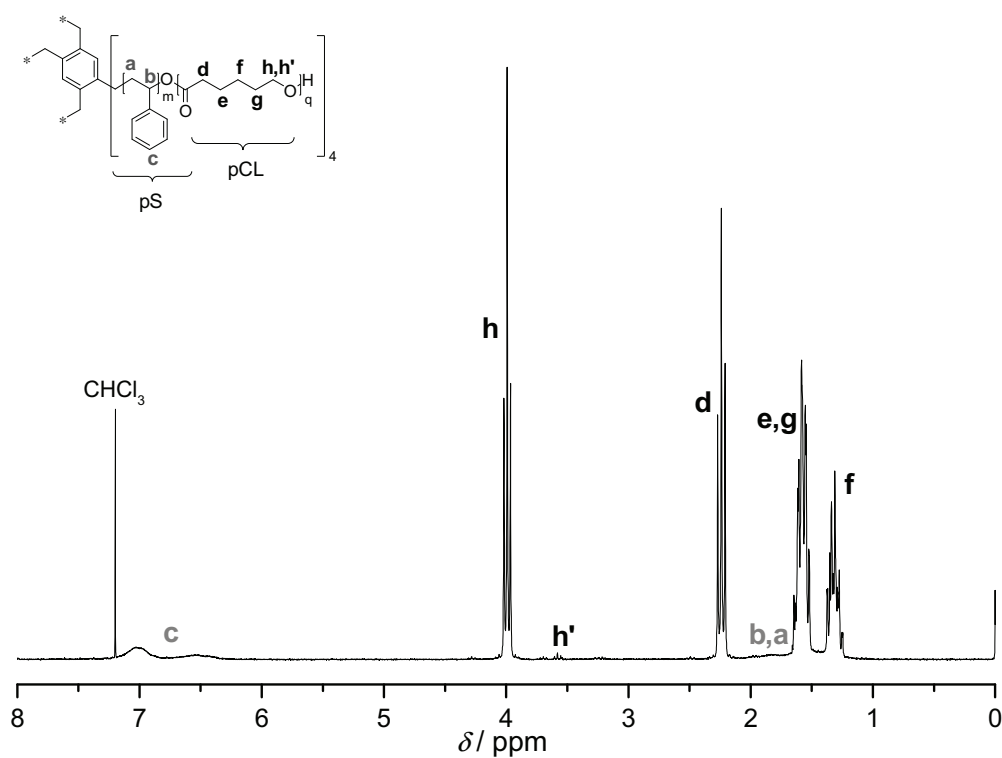


Figure A.2. ¹H-NMR spectrum of the star block copolymer **8** ($M_n^{\text{GPC}} = 36000 \text{ g mol}^{-1}$, $PDI = 1.4$). The integration of the pS backbone is based on the SEC chromatogram of the macro-initiator **6** ($M_n^{\text{GPC}} = 4400 \text{ g mol}^{-1}$) and subsequently the end-group functionality is evaluated via the integration of the signal h'. The calculation revealed that only 65 % of the pS OH endgroups were activated as macroinitiators for the chain extension.

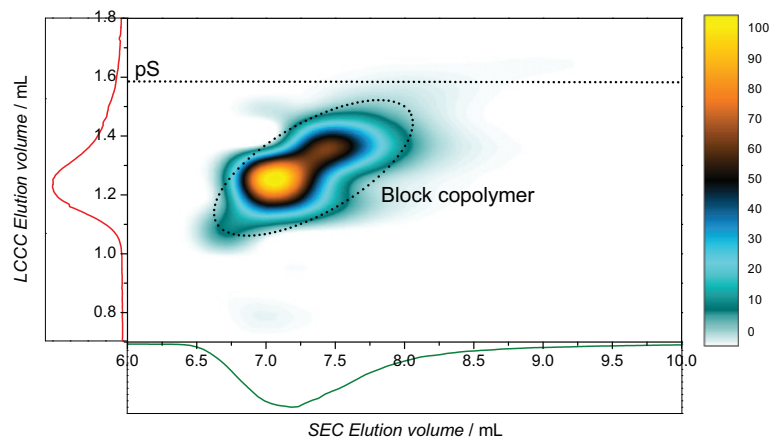


Figure A.3. 2D LCCC-SEC plot of 2D LCCC-SEC chromatogram of **7b**. The LCCC run was conducted under critical conditions of pS (88.4/11.6 % (v/v) THF/Water on a reversed phase system). The exact conditions can be found in Chapter 3.

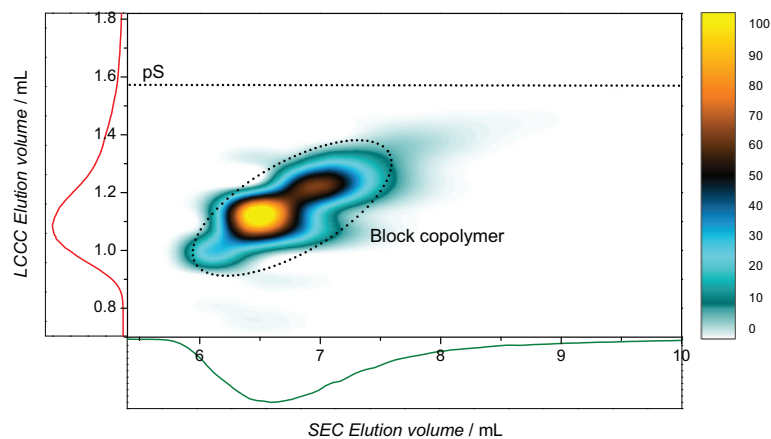


Figure A.4. 2D LCCC-SEC chromatogram of the star block copolymer **8**. For the generation of the plot, critical conditions of poly(styrene) were applied on an HPLC system.

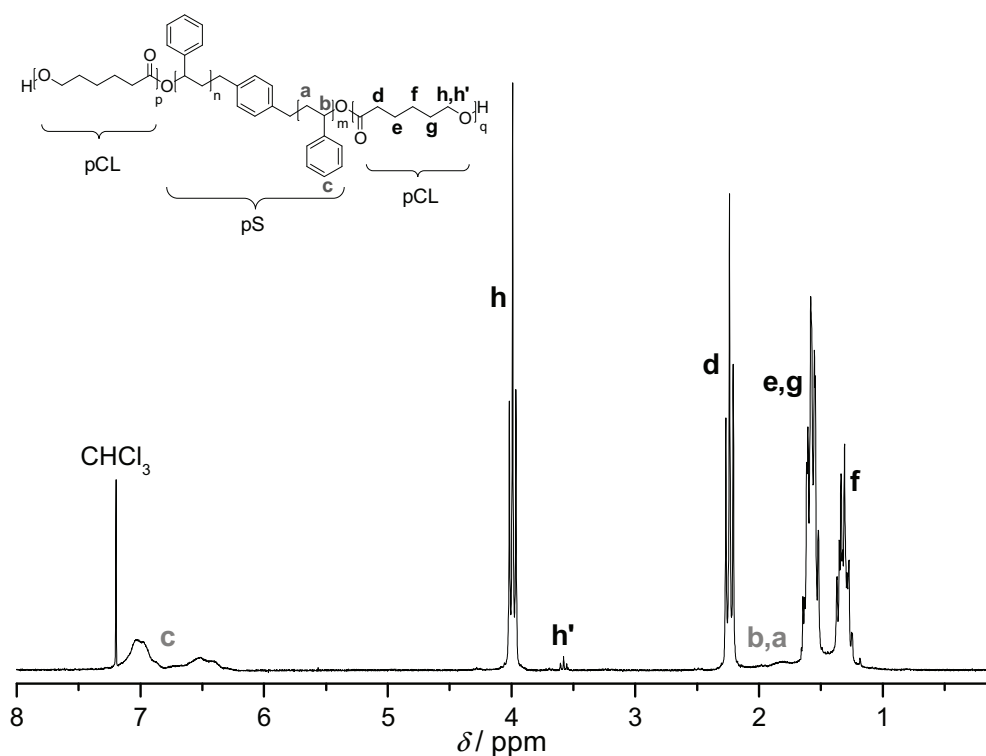


Figure A.5. ^1H -NMR spectrum of the ABA type block copolymer **7a** ($M_n^{\text{GPC}} = 12500 \text{ g mol}^{-1}$, $PDI = 1.5$). Similar to the procedure employed for the data evaluation in Figure A.2, the integration of the pS is based on the SEC traces of the macro-initiator **5** ($M_n^{\text{GPC}} = 3900 \text{ g mol}^{-1}$) and the value of the pCL end-groups is obtained by subsequent integration of the signal h' . According to the calculation the value is 2.1 and thus higher than the end-group functionality of the macro-initiator (2.0), which can only be explained by additional small amounts homopolymer pCL in the sample formed during the polymerization process.

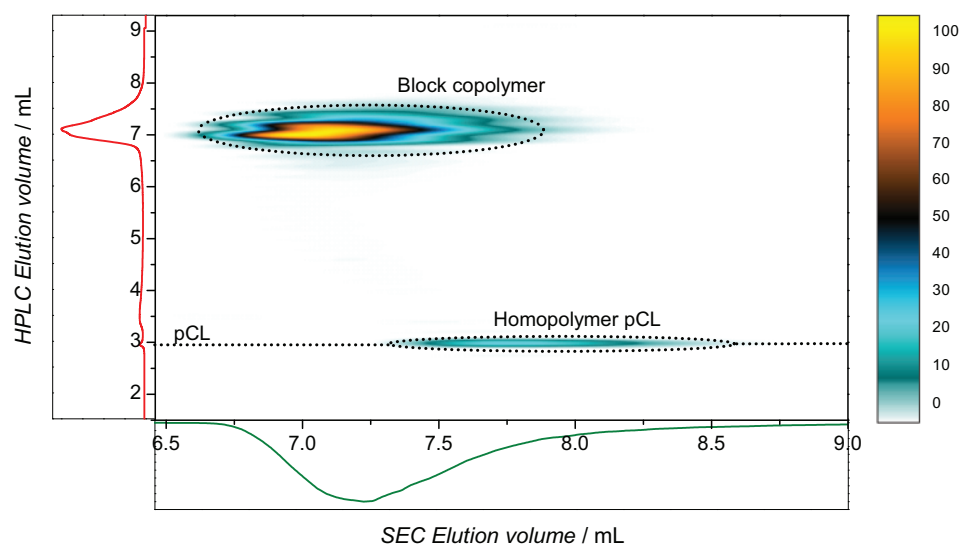


Figure A.6. 2D LCCC-GELC-SEC chromatogram of **7b**. On the HPLC system the critical conditions of pCL were combined with a solvent gradient (LCCC-GELC) to separate potential homopolymer pCl and pS from block copolymer. The exact conditions can be found in Chapter 3.

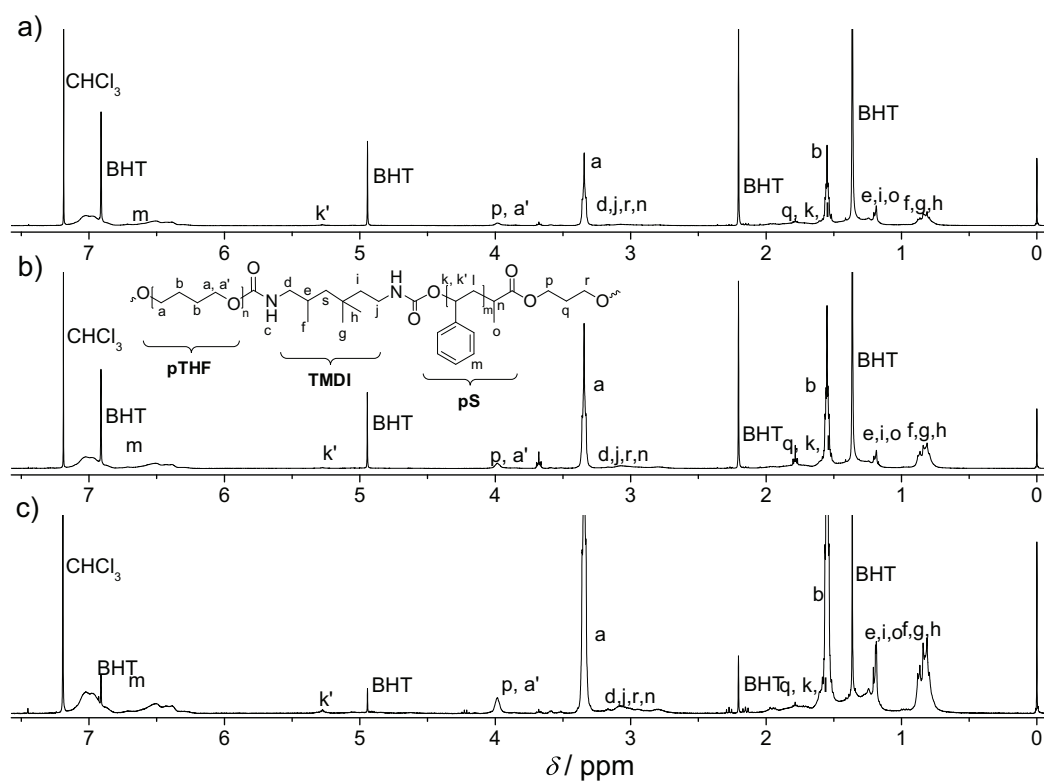


Figure A.7. $^1\text{H-NMR}$ spectra with assigned resonances of the multi-block copolymers **5** (Figure a)), **6** (Figure b)) and **8** (Figure c)). By integrating the backbone signals of pS and pTHF the fraction of each block in the block copolymer structure is obtained, which can be found in Table 7.2.

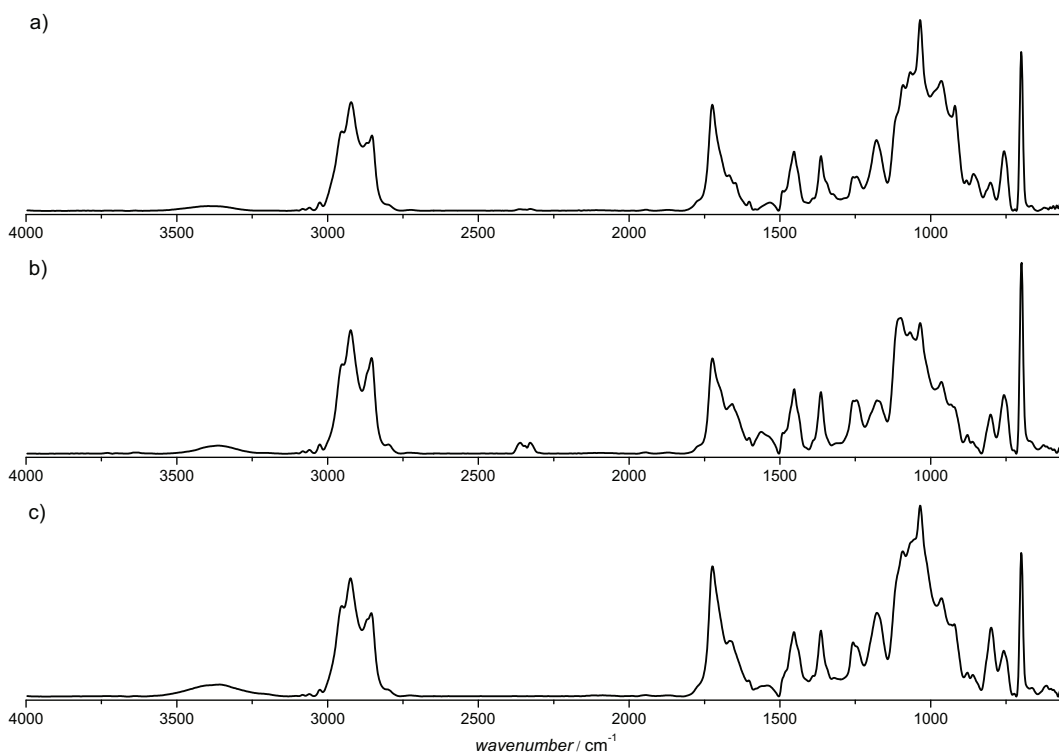


Figure A.8. FT-IR ATR spectra of the multi-block copolymer samples pS-*b*-pTHF. Figure a) shows sample **5**, b) sample **6** and c) sample **7**.

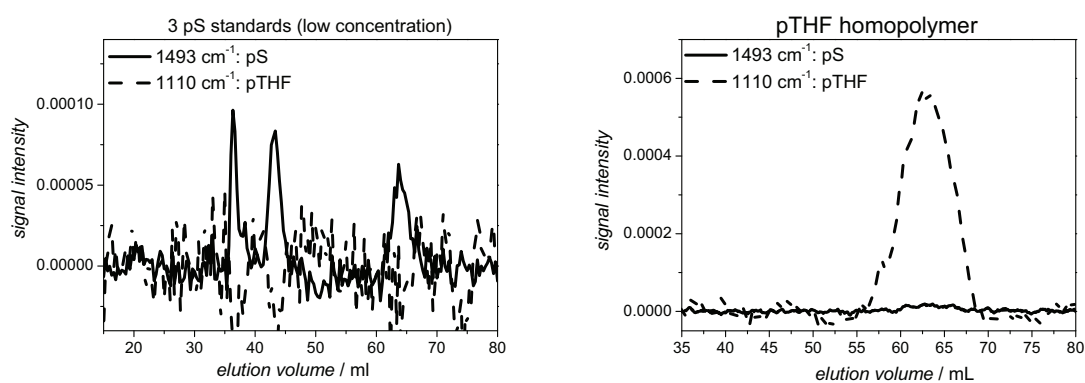


Figure A.9. Elugrams of pTHF homopolymer, which does not show any absorbance at 1493 cm^{-1} , where the signal of the phenyl ring of the pS polymer is detected, and pS homopolymer standards, which do not show any absorbance at 1110 cm^{-1} , at which pTHF shows strong absorbance due to the -CO ether stretching vibration in its polymer backbone.

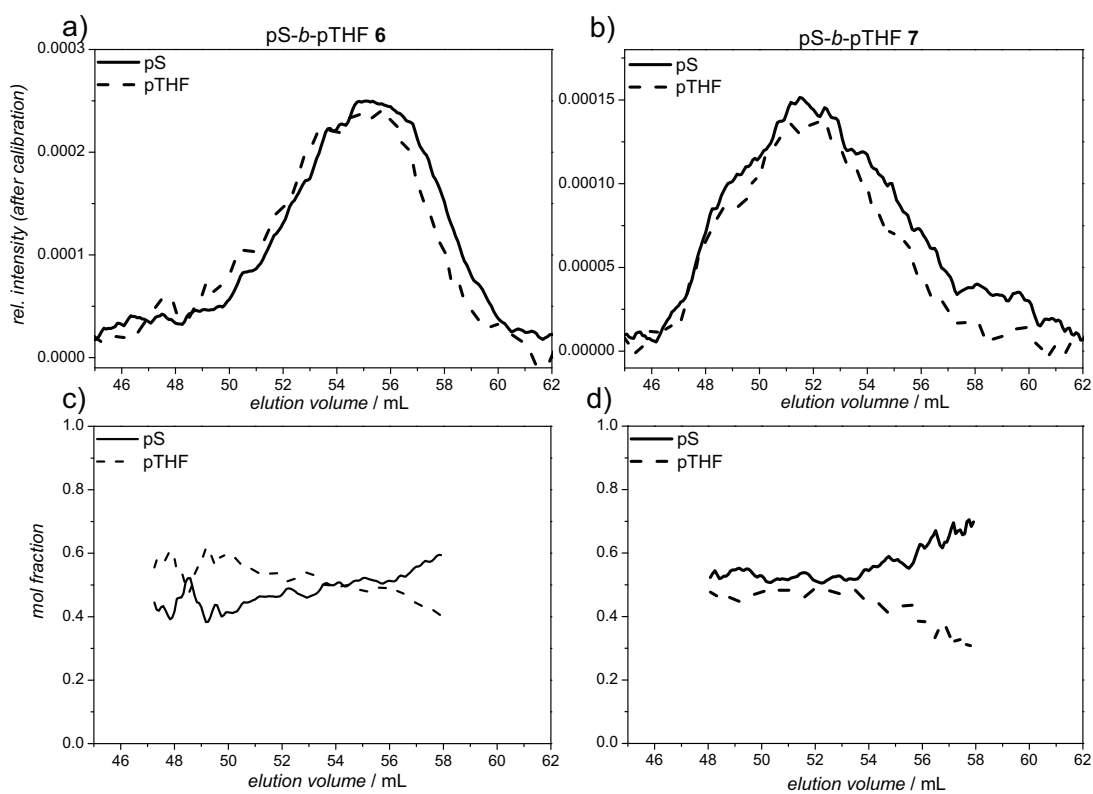


Figure A.10. a) and b) SEC/FT-IR elugrams after calibration of the multi-block copolymer samples **6** and **7**. Figure A.10 c) and d) show the block fraction of pS and pTHF in the block copolymer samples **6** and **6** dependent on the elution volume.

List of Abbreviations

AIBN	2,2'-azobis(2-methylpropionitrile)
ARGET	activators regenerated by electron transfer
ATR-IR	attenuated total reflection - infrared
ATRP	atom transfer radical polymerization
BPDF	benzyl pyridin-2-ylthioformate
CID	collision induced dissociation
CRP	controlled radical polymerization
CTA	chain transfer agent
CBDB	cyanoisopropyl dithiobenzoate
DBTC	dibenzyl trithiocarbonate
DBU	1,8-diazabicyclo[5.4.0]undec-7-ene
DCC	dicyclohexylcarbodiimide
DMF	dimethylformamide
DMAc	dimethylacetamide
DMAP	4-(dimethylamino)pyridine
DP_n	degree of polymerization
<i>e.g.</i> ,	exempli gratia
ELSD	evaporative light scattering detector
equiv.	equivalents
ESI-MS	electrospray ionization mass spectrometry
<i>et al.</i>	et alii / et aliae
FRP	free radical polymerization
FT-IR	Fourier transform infrared
GELC	gradient elution liquid chromatography
GPC	gel permeation chromatography
HPLC	high performance liquid chromatography
<i>iBoA</i>	isobornyl acrylate
<i>i.e.</i> ,	id est
k'	retention factor
k_a	rate coefficient of activation

k_{add}	rate coefficient of addition
k_{β}	rate coefficient of fragmentation
k_{d}	rate coefficient of dissociation
k_{da}	rate coefficient of deactivation
k_{i}	rate coefficient of initiation
k_{p}	rate coefficient of propagation
k_{t}	rate coefficient of termination
λ	wavelength
LC	liquid chromatography
LCCC	liquid chromatography at critical conditions
LC-MS	Liquid Chromatography - Mass Spectrometry
MALDI	matrix-assisted laser desorption/ionization
M_{n}	number-average molar mass
M_{w}	weight-average molar mass
MS	mass spectrometry
MMD	molar mass distribution
NIPAM	<i>N</i> -isopropylacrylamide
NMP	nitroxide mediated polymerization
NMR	nuclear magnetic resonance
ΔP	differential pressure
pBA	poly(butyl acrylate)
pCL	poly(ϵ -caprolactone)
<i>PDI</i>	polydispersity index
pEO	poly(ethylene oxide)
p <i>i</i> BoA	poly(isobornyl acrylate)
pLA	poly(lactic acid)
pMA	poly(methyl acrylate)
pMMA	poly(methyl methacrylate)
PNIPAM	poly(<i>N</i> -isopropylacrylamide)
pS	poly(styrene)
pU	polyurethane
RAFT	reversible addition fragmentation chain transfer
RI	refractive index
ROP	ring-opening polymerization
SEC	size-exclusion chromatography
TBD	1,4,7-triazabicyclodecene
THF	tetrahydrofuran
ToF	time-of-flight
UV	ultra-violet

UV/Vis	ultra-violet/visible
V_I	volume in the interstitial space
V_M	volume of the mobile phase
V_P	volume in the internal pore volume
V_R	retention volume
V_S	volume of stationary phase

Curriculum Vitae

Date of Birth 21.March 1983
Place of Birth Würzburg, Germany
Nationality German

Education

2009 – Present **Doctoral Studies in Chemistry**
Under the supervision of Prof. Dr. Christopher Barner-Kowollik
Karlsruhe Institute of Technology (KIT), Germany

2008 **Diploma in Chemistry**
*Synthesis of Epoxypropylphosphonates and their Polymerization
to Polyol Formation for Flame-Retardant Polyurethanes*
Under the supervision of Prof. Dr. Manfred Wilhelm
Universität Karlsruhe (TH) / Fraunhofer Institute for Chemical
Technology (ICT), Germany

2003 – 2008 **Studies of Chemistry**
Universität Karlsruhe (TH), Karlsruhe, Germany

2002 **High School Certificate**
Schweinfurt, Germany

Employment History

March 2009 – Present **Institute of Chemical Technology and Polymer
Chemistry**
Karlsruhe Institute of Technology (KIT), Karlsruhe, Germany
Scientific Co-worker

2008 – February 2009 **Environmental Engineering**
Fraunhofer Institute for Chemical Technology (ICT), Germany
Scientific Co-worker

List of Publications and Conference Contributions

Refereed Journal Publications

- [6] *Multi-Block Polyurethanes via RAFT End-group Switching and their Characterization by Advanced Hyphenated Techniques*
Schmid, C.; Falkenhagen, J.; Beskers, T. F.; Nguyen, L.-T. T.; Wilhelm, M.; Du Prez, F. E.; Barner-Kowollik, C. **Macromolecules** **2012**, DOI: 10.1021/ma301117k.
- [5] *In-Depth LCCC-(GELC)-SEC Characterization of ABA Block Copolymers Generated by a Mechanistic Switch from RAFT to ROP*
Schmid, C.; Weidner, S.; Falkenhagen, J.; Barner-Kowollik, C. **Macromolecules** **2012**, *45*, 87–99.
- [4] *UV Light-Triggered Macromolecular Click Conjugations via the Use of o-Quinodimethanes*
Gruendling, T.; Oehlschlaeger, K. K.; Frick, E.; Glassner, M.; Schmid, C.; Barner-Kowollik, C. **Macromol. Rapid Comm.** **2011**, *32*, 807–812.
- [3] *Block Copolymers via Macromercaptan Initiated Ring Opening Polymerization*
Lefay, C.; Glé, D.; Rollet, M.; Mazzolini, J.; Bertin, D.; Viel, S.; Schmid, C.; Boisson, C.; D'Agosto, F.; Gigmès, G.; Barner-Kowollik, C. **J. Polym. Sci., Part A: Polym. Chem.** **2011**, *49*, 551–819.
- [2] *An Efficient Avenue to Poly(styrene)-block-(ϵ -Caprolactone) Polymers via Switching from RAFT to Hydroxyl Functionality: Synthesis and Characterization*
Schmid, C.; Falkenhagen, J.; Barner-Kowollik, C. **J. Polym. Sci., Part A: Polym. Chem.** **2011**, *49*, 1–10.

- [1] *Facile Conversion of RAFT Polymers into Hydroxyl Functional Polymers: A Detailed Investigation of Variable Monomer and RAFT Agent Combinations*
Dietrich, M.; Glassner, M.; Gruendling, T.; Schmid, C.; Falkenhagen, J.; Barner-Kowollik, C. ***Polym. Chem.*** **2010**, *1*, 634–644.

Conference Contributions

- [6] *Block Copolymers via Macromercaptan Initiated Ring Opening Polymerization*
Glé, D.; Lefay, C.; Rollet, M.; Gimes, D.; Bertin, D.; Schmid, C.; Barner-Kowollik, C. ***32nd Australasian Polymer Symposium***, 12th to 15th February 2012, Hobart, Australia (Oral presentation).
- [5] *Block Copolymers via Macromercaptan Initiated Ring Opening Polymerization*
Glé, D.; Lefay, C.; Rollet, M.; Gimes, D.; Bertin, D.; Schmid, C.; Barner-Kowollik, C. ***European Polymer Federation Congress*** 26th of June to 1st of July 2011, Granada, Spain (Oral presentation).
- [4] *Switching From RAFT to ROP: A Facile Route to Complex and Sulfur-Free Macromolecular Architectures*
Schmid, C.; Falkenhagen, J.; Barner-Kowollik, C. ***11th Annual UNESCO/IUPAC Conference on Functional Polymeric Materials and Composites***, 27th to 29th of April 2011, Stellenbosch, South Africa (Poster Presentation, Poster Prize Winner).
- [3] *Copolymer Characterization by Coupled LC - MS/MS Techniques*
Falkenhagen, J.; Weidner, S.; Schmid, C.; Barner-Kowollik, C. ***PacifiChem 2010***, 16th to 20th of December 2010 Honolulu, Hawaii (Oral Presentation).
- [2] *Rapid Bonding/Debonding on Demand Systems and A Mechanistic Switch*
Barner-Kowollik, C. 17th of September 2010, Universität Jena, Jena, Germany (Oral Presentation).
- [1] *Facile Conversion of RAFT Polymers into Hydroxyl Functional Polymers: A Detailed Investigation of Variable Monomer and RAFT Agent Combinations*
Dietrich, M.; Glassner, M.; Gruendling, T.; Schmid, C.; Falkenhagen, J.; Barner-Kowollik, C. ***CRP meeting***, 17th to 18th of September 2009, Houffalize, Belgium (Poster Presentation).

Acknowledgements

Firstly, I would like to express my deep and sincere gratitude to my thesis advisor Prof. Dr. Christopher Barner-Kowollik for offering me the opportunity to work on exciting projects regarding polymer synthesis and analytics as well as for his constant support during the entire time of the thesis. Moreover I want to thank him for his motivation and encouragement as well as the confidence he placed in me.

Very special thanks I want to give to Dr. Jana Falkenhagen for supervising the analytical approaches and aspects of my thesis as well as for her essential view of critical examining data, but also many thanks for her cordiality and care during my stays in Berlin.

Prof. Dr. Filip Du Prez is highly thanked for the part-time supervision during my research stay in Gent (Belgium) as well as for the subsequent insightful scientific discussions. In this context I also want to acknowledge the *Karlsruhe House of Young Scientists* for financial support.

Dr. Catherine Lefay is thanked for the prosperous collaboration on thiol-based block copolymers.

Of course, I warmly thank the entire *macroarc* group for the pleasant atmosphere, the helpful environment, and enjoyable time with all of you.

Highly appreciative thanks go to Dr. Steffen Weidner and Rosemarie Laging for all the measured MALDI mass spectra, to Pia Lang and Tanja Ohmer for performing NMR measurements and to Timo Beskers for conducting SEC/FT-IR of my samples.

I would like to say special thanks to Dr. Maria Schneider for helping me getting started with the 2D system by teaching me the basics in handling chromatographic systems. For giving advises and introducing me to the analytical methods, SEC/ESI-MS and FT-IR, I want to thank Dr. Anna-Marie Zorn, Michael Kaupp, Dr. Till Gründling, Dr. Mathias Dietrich and Thomas Tischer.

Dr. Till Gründling, Mathias Dietrich and Mathias Glassner are thanked for discussions dealing with end-group conversion difficulties. Furthermore, Bernhard Schmidt and Kim Öhlenschläger are thanked for synthetic discussions and fruitful hints.

I would like to say many, many thanks to Dr. Sandy Koo, Dr. Guillaume Delaittre, Dr. Anja Goldmann and Dr. Andrew Vogt for proof-reading. For final trouble shooting I thank Dr. Anna-Marie Zorn, Bernhard Schmidt, Nicolas Zydziak, Tanja Wolfer and Gesa Lüdemann.

I also thank Sihuai Chen, Katharina Rebel and Paul Lederhose for assisting me as ‘Vertiefer’ and ‘HiWi’ students.

Gabriele Herrmann and Evelyn Stüring are thanked for their the organization and administrative work.

In addition, I thank the *Polymer Analysis* team at the BAM who made the stays in Berlin a nice and enjoyable time.

Further, I want to thank the whole *PCR* group for making me feel welcome during the stay in Gent. In particular I thank Tugba Dispinar and Catheline Colard for their company during the stay, Le-Thu Nguyen for scientific discussions and the subsequent collaboration and Bart Dervaux for sharing insights concerning the MALDI-MS setup in Gent.

I’m grateful to Anja, Alex, Massimo and André for the interesting time at the conference in Stellenbosch as well as exciting moments during the subsequent short trip through South Africa.

To Tanja and Ina: thanks for the afternoon coffee breaks. I will miss the time sitting on the AC terrace with you on a sunny summer day.

Finally, I want to thank my whole family, my friends and especially David for constant support and appreciation during the past and more recent years of my life.